

The University of Nottingham

UNITED KINGDOM · CHINA · MALAYSIA

Innovation of Louver Daylighting System via Using Parametric Design Approach to Enhance Daylight Uniformity and Stability in Deep-plan Buildings

PhD thesis in Building Technology contains nine chapters, investigating innovative daylighting louvre system by using Parametric control, to achieve daylight uniformity and stability inside the buildings, for visual comfort and energy saving.

UoN User
Building Technology;Department of Architecture and Built Environment



The Department of Architecture and Built Environment

Innovation of Louvre Daylighting System via Using Parametric Design Approach to Enhance the Daylight Uniformity and Stability in the Deep-plan Buildings

by

Ahmad Eltaweel, BSc, MSc (Hons)

Thesis submitted to The University of Nottingham
for the degree of Doctor of Philosophy

October 2019

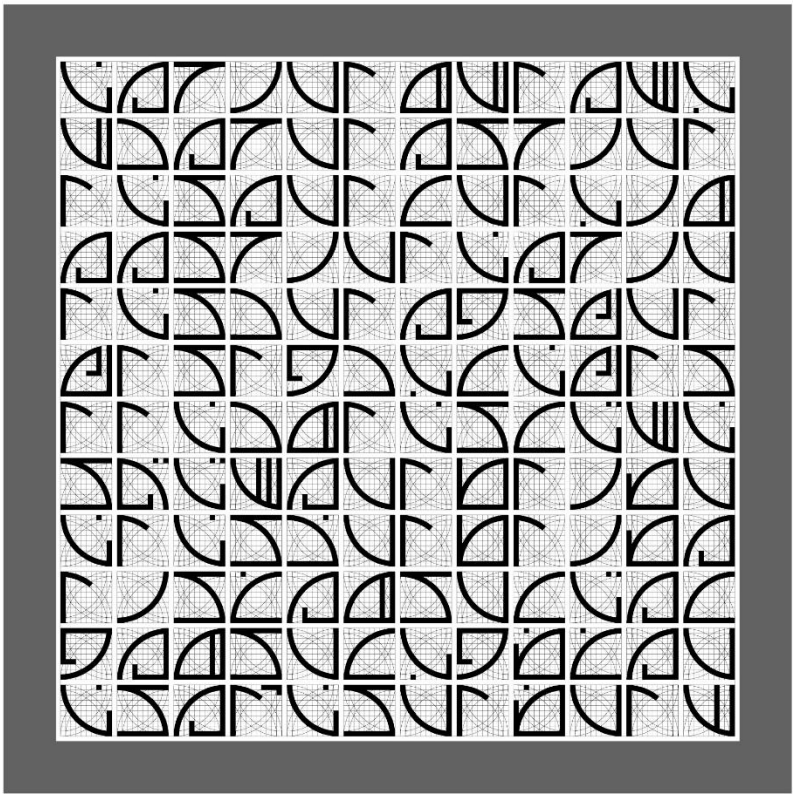
Abstract

For daylighting optimisation, shading devices are increasingly operated automatically to overcome the limitations of manual operation. Automated daylighting systems need to be controlled to maximise the benefits of daylight on the aspects of redirecting sunlight, occupant comfort and energy consumption. However, the conventional control methods focused on minimising adverse impacts of daylight, but they might fail to maximise the positive impacts of daylight. They may often inaccurately predict the position or angle of slats of louvre or blinds, resulting in the undesirable blockage of useful daylight needed.

This PhD thesis puts forward an innovative control method for automated louvres to optimise the utilisation of daylight. The proposed control method can not only protect occupants from sunlight glare but also maximise daylight penetration into deep-plan office rooms based on algorithmic methods. The proposed control method is designed to reflect the incident sunlight onto the ceiling, where the reflected light acts as a source of light for illumination. The reflective mirrored slats are individually angled but rotated with the same angle, i.e., they respond to the sun altitude angles parametrically in individual heliotropic response so that they can reflect sunlight to the corresponding positions on a ceiling. Accordingly, this process can exploit the optimal use of natural daylight and provide shading simultaneously.In addition to the louvres, windows are the most common architectural elements widely used in office buildings to protect them from climate changes. Advanced glazing and other fenestration systems can further improve daylighting performance.

This PhD study proposes an advanced integrated daylighting system combining the automated louvre of parametrically-angled mirrored slats with electrochromic and thermochromic glazing, which can respond to the sun movement and solar intensity simultaneously, based on parametric control. The criterion is to keep a relatively uniform daylight distribution in the range of 300~500 lx over the whole desktop area, aiming to provide sufficient daylight to achieve visual comfort and save energy for a maximised period of a day. Simulation studies have been held in the locations of New-Cairo in Egypt and Birmingham in the UK, while, a field study has been held in an example office room at the University of Nottingham in the UK.

To my Grandfather



Acknowledgements

This research was conducted under the supervision of Dr Yuehong Su, to whom I sincerely express my gratitude for his guidance, support, patience, assistance and inspiration throughout my study at the University of Nottingham. Thanks also to my previous supervisor Professor M. Alaa Mandour, at Helwan University in Egypt for his support and encouragement to gain this scholarship from Cultural Affairs and Missions Sector.

I would also like to thank my brother Waleed Eltaweel, my friend Mohammed Magdy and my colleague Jan-Frederik Flor for giving expert advice and technical support in this project. Special thanks go to my friends and colleagues at the SRB at the University of Nottingham, for their advice, help, support and encouragement during my study in the SRB, which was like a second home for me. Thanks, must also go to my close friend Cagri Cutlu who helped and gave me lots of support in the experimental stage.

Finally, I would like to thank my lovely wife Mariam for her constant support, understanding, sacrificing and encouragement during this course of study and many before even during her own extremely difficult time. And big thanks to my grandmother, my parents, my brothers and my lovely sister for their moral support and prayers. Special thanks to my lovely daughters Noor and Sama who mitigated my hard-times.

*Firstly, and lastly, thanks and gratitude to **ALLAH** who supported me in my whole life!*

Declaration

The work described in this thesis was conducted at the University of Nottingham, The Department of Architecture and Built Environment, Faculty of Engineering, between December 2015 and October 2019. I declare that the work is my own and has not been submitted for a degree for another university.

Contents

Chapter 1 Introduction *1*

1.1 Background **1**

1.2 Research questions and gaps **4**

1.3 The aim and objectives **6**

1.4 Structure of the thesis **7**

Chapter 2 Literature review of daylighting and parametric design *9*

2.1 Introduction **9**

2.2 The light **9**

2.2.1 Light behaviour 10

2.2.2 Light metrics 12

2.3 Daylighting and solar radiation **13**

2.3.1 Daylighting influence factors 14

2.3.2 Solar radiation 19

2.3.3 Daylighting metrics 20

2.3.4 Climate-based daylight modelling 22

2.3.5 Daylighting requirements in Architecture 22

2.4 Daylighting systems **24**

2.4.1 Light Guiding Systems 26

2.4.2 Light Transporting Systems 28

2.4.3 Fenestration systems 33

2.5 Parametric design **41**

2.5.1 The origins of parametric design 43

2.5.2 The principle of parametric design 44

2.5.3 Parametric design as a software 45

2.6 Implementations of parametric design in general fields 47

2.6.1 In urban planning 47

2.6.2 In architecture 48

2.6.3 In decoration 48

2.6.4 In fashion 48

2.6.5 In acoustics 49

2.6.6 In structure study 49

2.6.7 In environmental study 49

2.7 Daylighting systems control via parametric design 52

2.7.1 Louvres design 52

2.7.2 Skylight design 55

2.7.3 Mass and shadows study 60

2.7.4 Fenestration design 64

2.7.5 Windows design 66

2.7.6 Façade design 67

2.7.7 Prototypes design 70

2.7.8 Photovoltaics design 73

2.8 Summary 74

Chapter 3 Parametric Control of a Rotating Louvre Consisting of Parametrically-angled Mirrored Slats, Methodological study 76

3.1 Introduction 76

3.2 Methodology description of the parametric daylighting louvre 77

3.2.1 Parametric daylighting louvre software control 78

3.2.2 Parametric daylighting louvre main components: 82

3.2.3 Parametric daylighting louvre control mechanism 84

3.3 Case Study description of the Parametric Louvre _____ 88

3.4 Examining the Parametric Louvre in an example office room in New Cairo in three different seasons, to evaluate the daylight performance _____ 90

3.4.1 Case 1: clear sky with the sun on the 21st of December _____ 90

3.4.2 Case 2: clear sky with the sun on the 21st of September _____ 93

3.4.3 Case 3: clear sky with the sun on the 21st of June _____ 94

3.5 Cases study comparison and analysis _____ 95

3.6 Summary _____ 99

Chapter 4 Prototyping and Validation of the Parametric Louvre _____ 100

4.1 Introduction _____ 100

4.2 Prototyping the Parametric Louvre _____ 101

4.2.1 The physical part of the prototype _____ 102

4.2.2 The digital part of the prototype _____ 103

4.2.3 The measurement part _____ 104

4.2.4 Limitations of the experimental design _____ 105

4.2.5 Sky conditions _____ 107

4.3 Monitoring results of the Parametric Louvre at different times and dates 108

4.4 Validation of the Parametric Louvre _____ 110

4.5 Summary _____ 113

Chapter 5 Combining the Parametric Louvre with Advanced Glazing and Chamfered Ceiling for Better Daylighting Uniformity _____ 115

5.1 Introduction _____ 115

5.2 Modelling method of the proposed system in an example office room by using Grasshopper _____ 116

5.3 Evolution phases of the integration between the Parametric Louvre with the advanced glazing and the chamfered ceiling by using parametric design _____ 117

5.3.1 Phase 1; using conventional louvre _____ 118

5.3.2 Phase 2; applying parametric control to the rotating louvre with the addition of fixed slats shade _____ 119

5.3.3 Phase 3; reversing the slats' targeting of the rotating louvre, parametrically __ 120

5.3.4 Phase 4; Adding Electrochromic and Thermochromic windows to the Parametric Louvre 120

5.3.5 Phase 5; adding a chamfered ceiling to the Parametric Louvre _____ 122

5.4 Comparison study between the phases of the Integrated Parametric Louvre on the 21st of September at noontime _____ 123

5.5 Comparison study for the Integrated Parametric Louvre during the working hours on the 21st of each month from June to December _____ 126

5.6 Analysis discussion for the Integrated Parametric Louvre _____ 130

5.7 Summary _____ 132

Chapter 6 Evaluating the Integrated Parametric Louvre in different orientations and throughout the year _____ 134

6.1 Introduction _____ 134

6.2 Model description of the Integrated Parametric Louvre and Conventional Static Louvre for a comparison study _____ 135

6.3 Comparison criteria between the Integrated Parametric Louvre and the Conventional Static Louvre in different orientations _____ 136

6.3.1 Daylight coverage percentage analysis for the IPL and CSL on the 21st of June, 21st of September and 21st of December _____ 138

6.3.2 Daylight coverage percentage analysis on the 21st of June, 21st of September, and 21st of December for the CSL in different orientations during the working hours _____ 140

6.3.3 Daylight coverage percentage on the 21st of June, 21st of September and 21st of December for the IPL in different orientations 142

6.4 Potential energy saving throughout the year for the IPL 145

6.5 Summary 151

Chapter 7 Proposing an Innovative Control Method to Increase the Daylighting Stability, via using Dual-axis and Double-layer Parametric Louvre 152

7.1 Introduction 152

7.2 Hypothesis control development mechanism of the Integrated Parametric louvre (IPL) 153

7.2.1 Integrated Parametric Louvre based on One-axis rotation control (the original system) 154

7.2.2 Integrated Parametric Louvre based on Dual-axis rotation control (the new proposed system – 1st alternative) 156

7.2.3 Integrated Parametric Louvre based on Double-layer rotation control with a combination of horizontal and vertical louvre (the new proposed system – 2nd alternative) 158

7.2.4 Addition of a Thermochromic (TC) glass 160

7.3 A comparison study between the one-axis, dual-axis and double-layer Integrated Parametric Louvre 160

7.4 Results and discussion between the one-axis, dual-axis and double layer Parametric Louvre 167

7.5 Summary 172

Chapter 8 Adaption of the Parametric Louvre to slim and curved slats to increase its feasibility 174

8.1 Introduction 174

8.2 Reducing the slat's size of the Parametric Louvre 175

8.2.1 Simulation of reducing the slat's width of the Parametric Louvre in seven intervals 175

8.2.2 Prototyping the reduced size of the Parametric Louvre via using 1:1 mock-up (2.5 cm slat width) 177

8.2.3 Validating the reduced slats' size of the Parametric Louvre via using 1:1 mock-up (2.5 cm slat width) 178

8.3 Modifying the slat's shape of the Parametric Louvre 182

8.3.1 Simulation of reducing the concave slats' width of the Parametric Louvre at seven intervals 183

8.3.2 Simulation of reducing the convex slats' width on the Parametric Louvre at seven intervals 183

8.4 Examining the Parametric Louvre performance with the reduced slat width and the modified slat's shape on the 21st of June, 23rd of September and 21st of December during the working hours at the New Cairo location 186

8.5 Results and discussion about the performance of reducing the size and modifying the shape of the Parametric Louver 190

8.5.1 The influence of reducing the size and modifying the shape of the Parametric Louver performance 191

8.5.2 The outcome of the reduced size and the modified shapes of the Parametric Louver at different times and dates 192

8.5.3 Discussion about the reflection behaviour of the Flat, Concave and Convex–Parametric Louver 194

8.6 Summary 197

Chapter 9 Conclusion 199

9.1 Conclusion 199

9.2 Discussion 200

9.3 Recommendations _____ **201**

9.4 Potential outcome _____ **202**

9.5 Limitations of the system _____ **202**

9.6 Future work _____ **203**

References _____ ***204***

Appendix _____ ***220***

Appendix A: List of journal publications _____ **220**

Appendix B: Submitted for Review _____ **220**

Appendix C: Grasshopper's formula _____ **220**

List of Figures

FIGURE 1-1: CIRCADIAN RHYTHM FOR HUMAN IN 24 HOURS, BIOLOGICAL CLOCK [5]. 2

FIGURE 1-2: STRUCTURE OF THE PHD THESIS 8

FIGURE 2-1: LIGHT WAVELENGTH AND VISIBILITY RANGE [16] 9

FIGURE 2-2: TWO RAYS REFLECTED ON A METAL SURFACE WITH EQUAL ANGLES TO THE PERPENDICULAR LINE (LEFT) GEOMETRIC REFLECTION BEHAVIOUR BASED ON THE SURFACE TYPE (RIGHT) [17] 10

FIGURE 2-3: REFRACTION OF LIGHT RAY [19] 11

FIGURE 2-4: GEOMETRIC TRANSMISSION BEHAVIOUR BASED ON THE SURFACE TYPE. 11

FIGURE 2-5: SAMPLE SKETCH OF LIGHT MEASUREMENTS 12

FIGURE 2-6: FOUR SEASON'S DIAGRAM [22] 16

FIGURE 2-7: EARTH POSITIONS AND MOVEMENT AROUND THE SUN, FOR DAYLIGHT ILLUSTRATION. 17

FIGURE 2-8: SOLAR COVERAGE ON EARTH [22] 19

FIGURE 2-9: (TOP) THE ANNUAL NUMBER OF PUBLICATIONS BETWEEN 1983 AND 2018, AND (BOTTOM) THE COUNT OF PUBLICATIONS EACH TYPE ABOUT USING AUTOMATION CONTROL WITH THE DAYLIGHTING SYSTEM [3, 8, 12, 49, 52, 56-134] 25

FIGURE 2-10: OPTICAL LOUVRE DAYLIGHTING SYSTEM [132] 27

FIGURE 2-11: SIDE VIEW – LIGHT SHELF PERFORMANCE [142] 27

FIGURE 2-12: SUNCENTRAL [135] 28

FIGURE 2-13: SUN PIPES 29

FIGURE 2-14: FIBRE OPTICS; SHAPE (LEFT), REFLECTION PROCESS (RIGHT) [146] 29

FIGURE 2-15: PARABOLIC TROUGH [148] 30

FIGURE 2-16: HIMAWARI SYSTEM (LEFT), FRESNEL LENS (RIGHT) 31

FIGURE 2-17: PARANS SYSTEM LIGHT COLLECTOR [135] 32

FIGURE 2-18: EFFECT OF SUNDOLIER INDOOR (LEFT), SUNDOLIER SHAPE (RIGHT) [135] 32

FIGURE 2-19: HELIOSTAT SYSTEM [135] 33

FIGURE 2-20: SUNPORTAL SYSTEM [75] 33

FIGURE 2-21: SKYLIGHT SHAPES 34

FIGURE 2-22: LIGHTWELL SHAPES 34

FIGURE 2-23: GLASS BRICKS SHAPES 35
FIGURE 2-24: PRISMATIC PANEL 35
FIGURE 2-25: SHAPES OF PERFORATED SHEETS AND MASHRABIA 36
FIGURE 2-26: EXAMPLES OF DOUBLE SKIN FACADES [157]. 36
FIGURE 2-27: SELF-CLEANING PROCESS, (A) A SMOOTH SURFACE, WHERE PARTICLES ARE JUST REDISTRIBUTE BY WATER DROPLETS, (B) A ROUGH SURFACE, WHERE PARTICLES STICK TO THE WATER DROPLETS AND REMOVED FROM THE SURFACE [164]. 38
FIGURE 2-28: VENETIAN BLINDS AND ROLLER SHADES 39
FIGURE 2-29: LOUVRES TYPES AND SHAPES 39
FIGURE 2-30: PHOTO-BIOREACTORS SHAPES 40
FIGURE 2-31: SHOWING BIOMIMETIC SYSTEM; INSPIRATION FROM NATURE FOR DAYLIGHTING PURPOSE [21]. 41
FIGURE 2-32: COMPARISON DIAGRAM BETWEEN PARAMETRIC DESIGN PROCESS, AND CONVENTIONAL ONES, SHOWING THE DIFFERENCE IN TIME-CONSUMING. 42
FIGURE 2-33: A MODEL OF THE STADIUM BY LUIGI MORETTI, EXHIBITED AT THE 1960 PARAMETRIC ARCHITECTURE EXHIBITION AT THE TWELFTH MILAN TRIENNIAL. THE STADIUM DERIVES FROM A PARAMETRIC MODEL CONSISTING OF NINETEEN PARAMETERS (LEFT). THE PLANS OF THE STADIUM (RIGHT) [178]. 44
FIGURE 2-34: DOMINATION OFFICE BUILDING (LEFT), LONDON AQUATICS CENTRE, 2005 (RIGHT) 45
FIGURE 2-35: THE SHORTEST SOLUTION FOR THE PEDESTRIAN PATHWAY VIA USING OPTIMISATION METHOD (GALAPAGOS) IN GRASSHOPPER [188] 48
FIGURE 2-36: ARCHITECTURAL MODELS CREATED BASED ON PARAMETRIC DESIGN [197], (BOTTOM RIGHT DESIGNED BY AHMAD ELTAWEEL). 50
FIGURE 2-37: FIG. 1. IDEAS OF PARAMETRIC DESIGN IN DECORATION [198] 50
FIGURE 2-38: IDEAS OF PARAMETRIC DESIGN IN FASHION, INSPIRED BY NATURE [199-201] 50
FIGURE 2-39: REFLECTED RAYS CALCULATED IN "SONIC", A PLUGIN BASED ON GRASSHOPPER [192] 50
FIGURE 2-40: STRUCTURE STUDY USING ALGORITHMIC CALCULATIONS IN GRASSHOPPER [202, 203] 51
FIGURE 2-41: STRUCTURAL DESIGN ANALYSIS [193] 51
FIGURE 2-42: SUN PATH AND DAYLIGHT ANALYSIS, GRASSHOPPER. 51
FIGURE 2-43: THE LOUVRE PARAMETERS. A= SCREEN TILT ANGLE, WWR= WINDOW TO WALL RATIO [195] 53
FIGURE 2-44: THE CONTROLLING PROCESS USING GRASSHOPPER [21]. 55

FIGURE 2-45: THE TETRA-SCRIPT PAVILION CONCEPT, CONTROLLED PARAMETRICALLY [21]. 56
FIGURE 2-46: THE PARAGEN PLUGIN CYCLE [205]. 57
FIGURE 2-47: DIFFERENT TYPES OF REFLECTIVE SYSTEM DESIGN [218]. 59
FIGURE 2-48: DAYLIGHTING REDIRECTING STRATEGIES AT UNIVERSITY CROSSING [218]. 59
FIGURE 2-49: CONFIGURATION OF ADAPTIVE FAÇADE COMPONENTS. 60
FIGURE 2-50: OVERSHADOW OF NEIGHBOURING BUILDINGS [171]. 61
FIGURE 2-51: ANALYSIS OF OVERSHADOWING AREA [171]. 61
FIGURE 2-52: BUILDING A MASS STUDY WITH SOLAR RADIATION [171]. 62
FIGURE 2-53: THE FOUR SOLUTIONS FOR THE SYSTEM'S GEOMETRY AND THE ENVIRONMENTAL ANALYSIS FOR EACH SOLUTION [222]. 63
FIGURE 2-54: GRID ANALYSIS BY ECOTECT (LEFT), GALAPAGOS INTERFACE (RIGHT) [112] 64
FIGURE 2-55: EXAMPLES OF PARAMETRIC MODELS CONCEPTS AND VARIABLES [226]. 66
FIGURE 2-56: TRANSFORMATION OF THE HEXAGONAL SHAPE IN THE FAÇADE [228]. 67
FIGURE 2-57: FAÇADE GEOMETRY GENERATION [230]. 68
FIGURE 2-58: PATTERNS OF THE ROTATION MOTION FOR THE KINETIC FAÇADE [232]. 69
FIGURE 2-59: ORIGAMI FORMS BASED ON GEOMETRICAL RULES [234]. 70
FIGURE 2-60: THE KINEMATIC BEHAVIOUR USING THE CURVED LINE ADAPTIVE [239]. 71
FIGURE 2-61: THE THREE CHOSEN PATTERNS IN THREE MODELLING TYPES [241]. 72
FIGURE 3-1: HELIOTROPE PLANT (A), SUPERPOSITION COMPOUNDS EYE (B) AND SADDLE JOINT (C) 78
FIGURE 3-2: GRASSHOPPER INTERFACE SHOWING THE CANVAS OF SLIDERS AND CONNECTIONS (TOP). RHINOCEROS 3D INTERFACE SHOWING THE MODEL VIEWPORT (BOTTOM) 79
FIGURE 3-3: LINKS BETWEEN RHINOCEROS, GRASSHOPPER, HONEYBEE AND LADYBUG TO GENERATE AN ENVIRONMENTALLY CONSCIOUS MODEL [262-264]. 80
FIGURE 3-4: SAMPLE DAYLIGHT SIMULATION ANALYSIS FOR AN EXAMPLE OFFICE ROOM 81
FIGURE 3-5: REAL MAP PERSPECTIVE VIEW FROM 3D MAX SHOWING THE ELEMENTS OF THE PROPOSED DAYLIGHTING LOUVRE SYSTEM (LEFT), FISHEYE MAP FROM RADIANCE SHOWING THE REFLECTED LIGHT ON THE CEILING (RIGHT). 82
FIGURE 3-6: CROSS-SECTIONAL VIEW OF THE ROOM SHOWING THE INCIDENT SUNLIGHT REFLECTED BY THE ROTATING MIRRORED SLATS TO A FIXED TARGET, RESULTING IN DIFFUSE LIGHT TO THE OCCUPANTS. EVERY SINGLE SLAT HAS A SPECIFIC ROTATION ANGLE ACCORDING TO THE TARGET POSITION, WHICH IS RELATED TO THE SLAT. 85

FIGURE 3-7: CROSS-SECTIONAL VIEW OF THE SLATS SHOWING SUN ALTITUDE OUTSIDE IS CHANGING DURING DAYTIME, AND THE SLATS ARE ROTATING RESPONDING TO SUN MOVEMENT IN ORDER TO KEEP THE REFLECTED LIGHT TOWARDS THE FIXED TARGET POINTS ON THE CEILING, AND THIS PROCESS CONDUCTED VIA KEEPING THE OPPOSING ANGLES (Ω) EQUAL WHEREVER THE SUN POSITION. 85

FIGURE 3-8: A COMPARISON SHOWING THE INFLUENCE OF THE DISTANCE BETWEEN SLATS ON THE LIGHT REFLECTED; (A) BIG DISTANCE, (B) SMALL DISTANCE, AND (C) IS THE CRITICAL DISTANCE WHICH IS ACCEPTABLE ACCORDING TO THE BALANCE ACHIEVED WITH THE CUT-OFF ANGLE B* (REQUIRED B). 86

FIGURE 3-9: IT CAN BE NOTICED THE 1° ROTATION DIFFERENCE BETWEEN CASE (A) AND CASE (B); MEANWHILE, EACH SALT HAS ITS UNIQUE ROTATION ANGLE. 87

FIGURE 3-10: RADIANCE MAPS INSIDE THE ROOM SHOWING THE PARALLEL REFLECTION ON THE CEILING DURING THE DAYTIME FROM 9 A.M.: 5 P.M. 87

FIGURE 3-11: CROSS-SECTIONAL FOR THE OFFICE SHOWING THE CONTROLLED PARAMETERS; X: SLATS DISTANCE FROM THE WINDOW, Y: THE DISTANCE BETWEEN SLATS, L: THE DISTANCE BETWEEN TARGETS, H: SLATS' THRESHOLD FROM THE FINISH FLOOR. 88

FIGURE 3-12: SUN PATH EXPORTED FORM RHINOCEROS 3D, ON JUNE 21ST, SEPTEMBER 21ST, AND DECEMBER 21ST AND SUN ALTITUDES 83.3°, 60.2°, AND 36.4° RESPECTIVELY AT ZENITH TIME. 89

FIGURE 3-13: CROSS-SECTION IN THE WORKSTATION SHOWING THE COVERED AREA BY REFLECTED LIGHT 90

FIGURE 3-14: TOP VIEW OF THE OFFICE ROOM SHOWING HOURLY ILLUMINATED COVERAGE AREA (83.2% COVERAGE) FROM 8 A.M. TO 5 P.M. ON THE 21ST OF DECEMBER (LEFT), SUN PATH (RIGHT) 91

FIGURE 3-15: (LEFT); CROSS-SECTIONAL VIEW ON THE WORKSTATION SHOWING SUN RAYS AT ZENITH TIME WITH 36.4° ALTITUDE ON DECEMBER 21ST, USING A HIGH NUMBER OF SLATS [35 SLATS], (RIGHT); DETAILED SECTION FOR THE SLATS 91

FIGURE 3-16: SOLAR RADIATION IN CAIRO ON THE 21ST OF JUNE, 21ST OF SEPTEMBER AND 21ST OF DECEMBER FROM 8 A.M. TO 5 P.M. 92

FIGURE 3-17: TOP VIEW OF THE OFFICE ROOM SHOWING HOURLY ILLUMINATED COVERAGE AREA (22.7% COVERAGE) FROM 8 A.M. TO 5 P.M. ON THE 21ST OF SEPTEMBER (LEFT), CROSS-SECTIONAL VIEW FOR THE WORKSTATION SHOWING SUN RAYS AT ZENITH TIME 60.2° ALTITUDE, USING LOW NUMBER OF SLATS [16 SLATS]. (RIGHT)..... 94

FIGURE 3-18: TOP VIEW OF THE OFFICE ROOM SHOWING HOURLY ILLUMINATED COVERAGE AREA (3.7% COVERAGE) FROM 8 A.M. TO 5 P.M. ON THE 21ST OF DECEMBER (LEFT), CROSS-SECTIONAL VIEW FOR THE WORKSTATION SHOWING SUN RAYS AT ZENITH TIME WITH 83.3° ALTITUDE, USING TILTED BLINDS [16 SLATS]. (RIGHT) 94
FIGURE 3-19: RADIANCE MAPS FOR THE OFFICE ROOM AT 8 A.M. ON 21ST OF DECEMBER, 21ST OF SEPTEMBER AND 21ST OF JUNE, FROM LEFT TO RIGHT (TOP), RAYTRACING AND SOLAR ALTITUDES (BOTTOM) 96
FIGURE 3-20: RADIANCE MAPS FOR THE OFFICE ROOM AT 10 A.M. ON 21ST OF DECEMBER, 21ST OF SEPTEMBER AND 21ST OF JUNE, FROM LEFT TO RIGHT (TOP), RAYTRACING AND SOLAR ALTITUDES (BOTTOM) 97
FIGURE 3-21: RADIANCE MAPS FOR THE OFFICE ROOM AT 12 P.M. ON 21ST OF DECEMBER, 21ST OF SEPTEMBER AND 21ST OF JUNE, FROM LEFT TO RIGHT (TOP), RAYTRACING AND SOLAR ALTITUDES (BOTTOM) 98
FIGURE 4-1: CONCEPTUAL DIAGRAM SHOWING THE RELATION BETWEEN SOFTWARE, HARDWARE, SENSORS AND ACTUATORS 101
FIGURE 4-2: 1:20 SCALED PROTOTYPE FOR DAYLIGHTING SYSTEM VALIDATION 102
FIGURE 4-3: THE EXPANSION SHIELD ON THE LEFT SIDE IS ATTACHED TO THE ARDUINO MEGA 2560 BOARD IN THE MIDDLE TO FORM THE FINAL SHAPE OF THE BOARD ON THE RIGHT SIDE 103
FIGURE 4-4: CONNECTION PROCESS FROM THE COMPUTER TO ARDUINO VIA FIREFLY FIRMATA PROTOCOL 104
FIGURE 4-5: THE SENSORS POSITIONS INSIDE THE PROTOTYPE 105
FIGURE 4-6: A SINGLE SHADING PLATE ADJACENT TO THE PARAMETRIC LOUVRE SYSTEM 105
FIGURE 4-7: THE INITIAL SETTING OF THE PROTOTYPE WITH TEN MIRRORED SLATS 106
FIGURE 4-8: DAYLIGHT COVERAGE FOR 10 AND 3 MIRRORED SLATS, RESPECTIVELY 107
FIGURE 4-9: DAYLIGHT HOURLY MONITORING IN MAY ON RANDOM DAYS BETWEEN 11 A.M. AND 3 P.M. 109
FIGURE 4-10: DAYLIGHT HOURLY MONITORING IN JULY ON RANDOM DAYS BETWEEN 10 A.M. AND 3 P.M. 109
FIGURE 4-11: DAYLIGHT HOURLY MONITORING IN AUGUST ON RANDOM DAYS BETWEEN 1 P.M. AND 3 P.M. 109
FIGURE 5-1: THE TEST POINTS DISTRIBUTION, TOP VIEW EXPORTED FROM RHINOCEROS 3D (LEFT), PERSPECTIVE VIEW (RIGHT) 117
FIGURE 5-2: DETAILED CROSS-SECTION FOR THE FIXED SLATS SHADE 119
FIGURE 5-3: SIDE VIEW OF THE REVERSED TARGETING SEQUENCE. 120
FIGURE 5-4: COMPARISON BETWEEN THE CURVED AND CHAMFERED CEILING, USING RAYTRACING AND TEST POINTS. THE CURVED CEILING RESULTS IN 86% AREA BETWEEN 300~500 LX (TOP), WHILE THE CHAMFERED CEILING RESULTS IN 88.6% BETWEEN 300~500 LX (BOTTOM) 123

FIGURE 5-5: SIDE VIEW, ILLUSTRATING RAYTRACING STUDY; STARTING FROM THE TOP WITH CONVENTIONAL SLATS, AND ENDING WITH THE PARAMETRIC SEQUENCE-REVERSED LOUVRE WITH EC WINDOW AND CHAMFERED CEILING, RESPECTIVELY (LEFT). THE PERCENTAGE COVERAGE AREA FOR THE DAYLIGHT ILLUMINANCE RANGE BETWEEN 300 - 500 LX (RIGHT). 124
FIGURE 5-6: CONVENTIONAL SLATS WITH 45° TILT ANGLE (LEFT) SIDE VIEW, (RIGHT) TOP VIEW. 125
FIGURE 5-7: BAR GRAPH SHOWING THE COVERAGE PERCENTAGE BETWEEN 300 ~ 500 LX FOR THE FIVE PHASES ON SEPTEMBER 21ST AT NOONTIME 126
FIGURE 5-8: COVERAGE PERCENTAGE FOR THE DAYLIGHT ILLUMINANCE RANGE OF 300 - 500 LX DURING WORKING HOURS ON 21ST OF JUNE 127
FIGURE 5-9: COVERAGE PERCENTAGE FOR THE DAYLIGHT ILLUMINANCE RANGE OF 300 - 500 LX DURING WORKING HOURS ON 21ST OF JULY 127
FIGURE 5-10: COVERAGE PERCENTAGE FOR THE DAYLIGHT ILLUMINANCE RANGE OF 300 - 500 LX DURING WORKING HOURS ON 21ST OF AUGUST 127
FIGURE 5-11: COVERAGE PERCENTAGE FOR THE DAYLIGHT ILLUMINANCE RANGE OF 300 - 500 LX DURING WORKING HOURS ON 21ST OF SEPTEMBER 128
FIGURE 5-12: COVERAGE PERCENTAGE FOR THE DAYLIGHT ILLUMINANCE RANGE OF 300 - 500 LX DURING WORKING HOURS ON 21ST OF OCTOBER 128
FIGURE 5-13: COVERAGE PERCENTAGE FOR THE DAYLIGHT ILLUMINANCE RANGE OF 300 - 500 LX DURING WORKING HOURS ON 21ST OF NOVEMBER 128
FIGURE 5-14: COVERAGE PERCENTAGE FOR THE DAYLIGHT ILLUMINANCE RANGE OF 300 - 500 LX DURING WORKING HOURS ON 21ST OF DECEMBER 129
FIGURE 5-15: FALSE-COLOUR FISHEYE MAPS EXPORTED FROM HONEYBEE PLUGIN; SHOWING THE REFLECTED LIGHT DISTRIBUTION ON THE CEILING. PHASE 2 (LEFT), PHASE 3 (RIGHT). 131
FIGURE 6-1: THE PROPOSED INTEGRATED PARAMETRIC LOUVRE, SHOWING THE THREE MAIN TOOLS (RENDERED IN V-RAY FOR 3D MAX). 136
FIGURE 6-2: THE FIVE DIFFERENT ORIENTATIONS OF THE OFFICE ROOM. 137
FIGURE 6-3: DAYLIGHT COVERAGE PERCENTAGE ANALYSIS DURING THE WORKING HOURS USING THE CSL FOR A SOUTH-ORIENTED OFFICE ROOM ON 21ST OF JUNE (A), 21ST OF SEPTEMBER (B), AND 21ST OF DECEMBER (C). 138

FIGURE 6-4: DAYLIGHT COVERAGE PERCENTAGE ANALYSIS DURING THE WORKING HOURS USING THE IPL FOR A SOUTH-ORIENTED OFFICE ROOM ON 21ST OF JUNE (A), 21ST OF SEPTEMBER (B), AND 21ST OF DECEMBER (C). 139
FIGURE 6-5: COVERAGE PERCENTAGE BETWEEN 300~500 LX DURING THE WORKING HOURS IN 21ST OF JUNE, 21ST OF SEPTEMBER, AND 21ST OF DECEMBER BY USING THE CSLS FOR THE SOUTH ORIENTED ROOM. 140
FIGURE 6-6: COVERAGE PERCENTAGE BETWEEN 300~500 LX DURING THE WORKING HOURS IN THE 21ST OF JUNE, 21ST OF SEPTEMBER, AND 21ST OF DECEMBER BY USING THE INTEGRATED PARAMETRIC LOUVRE FOR THE SOUTH ORIENTED ROOM. 140
FIGURE 6-7: COVERAGE PERCENTAGE BETWEEN 300~500 LX DURING THE WORKING HOURS FOR THE OFFICE ROOM THROUGH FIVE ORIENTATIONS ON THE 21ST OF JUNE, USING THE CSL. 141
FIGURE 6-8: COVERAGE PERCENTAGE BETWEEN 300~500 LX DURING THE WORKING HOURS FOR THE OFFICE ROOM THROUGH FIVE ORIENTATIONS ON THE 21ST OF SEPTEMBER, USING THE CSL. 141
FIGURE 6-9: COVERAGE PERCENTAGE BETWEEN 300~500 LX DURING THE WORKING HOURS FOR THE OFFICE ROOM THROUGH FIVE ORIENTATIONS ON THE 21ST OF DECEMBER, USING THE CSL. 142
FIGURE 6-10: DAYLIGHT AVERAGE COVERAGE PERCENTAGE IN THE 21ST OF JUNE (A), 21ST OF SEPTEMBER (B), AND 21ST OF DECEMBER (C) BY USING THE CSL ON THE FIVE ORIENTATIONS. 142
FIGURE 6-11: COVERAGE PERCENTAGE DURING THE WORKING HOURS FOR THE OFFICE ROOM THROUGH THE FIVE ORIENTATIONS ON THE 21ST OF JUNE, USING THE IPL. 143
FIGURE 6-12: COVERAGE PERCENTAGE DURING THE WORKING HOURS FOR THE OFFICE ROOM THROUGH THE FIVE ORIENTATIONS ON THE 21ST OF SEPTEMBER, USING THE IPL. 144
FIGURE 6-13: COVERAGE PERCENTAGE DURING THE WORKING HOURS FOR THE OFFICE ROOM THROUGH THE FIVE ORIENTATIONS ON THE 21ST OF DECEMBER, USING THE IPL. 144
FIGURE 6-14: DAYLIGHT AVERAGE COVERAGE PERCENTAGE IN THE 21ST OF JUNE (A), 21ST OF SEPTEMBER (B), AND 21ST OF DECEMBER (C) BY USING THE IPL ON THE FIVE ORIENTATIONS. 144
FIGURE 6-15: MONTHLY CONSUMED ELECTRICAL LIGHTING IN THE OFFICE ROOM BY USING THE IPL SYSTEM. 148
FIGURE 6-16: MONTHLY AVERAGED DAYLIGHT COVERAGE PERCENTAGE IN THE OFFICE ROOM FOR THE DAYLIGHT ILLUMINANCE RANGE OF 300 ~ 500 LX BY USING THE INTEGRATED SYSTEM. 149
FIGURE 6-17: DAYLIGHT ANALYSIS BY USING DIFFERENT ACCURACY SETTINGS FOR THE SAME TIME AND DATE, SHOWING 79%, 77% AND 72% OF DAYLIGHT COVERAGE FOR HIGH, MEDIUM AND LOW SETTINGS, RESPECTIVELY. 150
FIGURE 7-1: ONE-AXIS ROTATION CONTROL SYSTEM 155

FIGURE 7-2. RADIANCE ILLUMINANCE MAPS SHOWING THE ILLUMINATED PATH IS MOVING OVER THE CEILING FROM 9 A.M. TO 5 P.M. ON THE 21ST OF SEPTEMBER. 155
FIGURE 7-3. HOURS OF DAYLIGHT AUTONOMY FOR THE RANGE OF 300-500 LX AT THE DESKTOP LEVEL ON THE 21ST OF SEPTEMBER. 156
FIGURE 7-4: DUAL-AXIS PARAMETRIC LOUVRE – RAYTRACING STUDY 156
FIGURE 7-5: DUAL-AXIS ROTATION MOVEMENTS 157
FIGURE 7-6: DUAL-AXIS ROTATION CONTROL 157
FIGURE 7-7: GRASSHOPPER FORMULA TO CONTROL THE ROTATION ANGLES 158
FIGURE 7-8: RADIANCE ILLUMINANCE MAPS FOR THE DUAL-AXIS ROTATION CONTROL FROM 9 A.M. TO 5 P.M. ON THE 21ST OF SEPTEMBER. 158
FIGURE 7-9: DOUBLE-LAYER ROTATION CONTROL 159
FIGURE 7-10: PERSPECTIVE VIEW SHOWING THE RAY-TRACING DIRECTIONS FOR THE ONE-AXIS, DUAL-AXIS AND DOUBLE-LAYER ROTATION CONTROL SYSTEMS RESPECTIVELY, AT 9 A.M., 12 P.M. AND 3 P.M. ON THE 21ST OF SEPTEMBER. 161
FIGURE 7-11: TOP VIEW FOR THE OFFICE ROOM SHOWING THE RAY-TRACING DIRECTIONS FOR THE ONE-AXIS, DUAL-AXIS AND DOUBLE-LAYER SYSTEMS RESPECTIVELY, AT 9 A.M., 12 P.M. AND 3 P.M. ON THE 21ST OF SEPTEMBER..... 162
FIGURE 7-12: DAYLIGHT COVERAGE FOR THE ONE-AXIS, DUAL-AXIS AND DOUBLE-LAYER IPL SYSTEMS, RESPECTIVELY ON THE 22ND OF MARCH 163
FIGURE 7-13: DAYLIGHT COVERAGE FOR THE ONE-AXIS, DUAL-AXIS AND DOUBLE-LAYER ROTATION CONTROL SYSTEMS, RESPECTIVELY ON THE 21ST OF JUNE 164
FIGURE 7-14: DAYLIGHT COVERAGE FOR THE ONE-AXIS, DUAL-AXIS AND DOUBLE-LAYER IPL SYSTEMS, RESPECTIVELY ON THE 21ST OF SEPTEMBER 165
FIGURE 7-15: DAYLIGHT COVERAGE FOR THE ONE-AXIS, DUAL-AXIS AND DOUBLE-LAYER IPL SYSTEMS, RESPECTIVELY ON THE 21ST OF DECEMBER 166
FIGURE 7-16: THE INFLUENCE OF SOLAR RADIATION ON THE WINDOW SURFACE. 168
FIGURE 7-17: PERCENTAGE DAYLIGHT COVERAGE DURING WORKING HOURS ON THE 21ST OF MARCH OF THE ONE-AXIS, DUAL-AXIS AND DOUBLE-LAYER SYSTEMS 169
FIGURE 7-18: PERCENTAGE DAYLIGHT COVERAGE DURING WORKING HOURS ON THE 21ST OF JUNE OF THE ONE-AXIS, DUAL-AXIS AND DOUBLE-LAYER SYSTEMS 169

FIGURE 7-19: PERCENTAGE DAYLIGHT COVERAGE DURING WORKING HOURS ON THE 21ST OF SEPTEMBER OF THE ONE-AXIS, DUAL-AXIS AND DOUBLE-LAYER SYSTEMS 170
FIGURE 7-20: PERCENTAGE DAYLIGHT COVERAGE DURING WORKING HOURS ON THE 21ST OF DECEMBER OF THE ONE-AXIS, DUAL-AXIS AND DOUBLE-LAYER SYSTEMS 170
FIGURE 7-21: A DIAGRAM SHOWING THE PROCESS IN GRASSHOPPER TO CONTROL THE WINDOW TRANSMISSION 170
FIGURE 7-22: DAYLIGHT COVERAGE BEFORE AND AFTER MOVING THE TARGETS AT 4 P.M. ON THE 21STOF SEPTEMBER.171
FIGURE 7-23: PERCENTAGE DAYLIGHT COVERAGE OF THE THREE SYSTEMS AFTER APPLYING THE SHIFTED TARGETS, ON THE 21ST OF SEPTEMBER 172
FIGURE 8-1: FLAT PARAMETRIC LOUVRE SHAPE – APPLIED IN AN EXAMPLE OFFICE ROOM IN NEW CAIRO ON THE 22ND OF MARCH AT NOONTIME, SHOWING; TOP VIEW – DAYLIGHT ANALYSIS PERCENTAGE, SIDE VIEW – RAYTRACING STUDY AND DGP MAP, RESPECTIVELY. 176
FIGURE 8-2: 1:1 MOCK-UP FOR THE PARAMETRIC LOUVRE MADE OF LASER CUT ACRYLIC AND ALUMINIUM SLATS 177
FIGURE 8-3: THE TWO IMAGES SHOWING THE DIFFERENCE BETWEEN OPENED AND CLOSED STATE (OFF/ON) OF THE PARAMETRIC LOUVRE MOCK-UP 178
FIGURE 8-4: VARIOUS SLAT SHAPES (WIDTH IN CENTIMETRE), HEIGHT IS 0.1 CM 183
FIGURE 8-5: CONCAVE PARAMETRIC LOUVRE SHAPE – APPLIED IN AN EXAMPLE OFFICE ROOM IN NEW CAIRO ON 22ND OF MARCH AT NOONTIME, SHOWING; TOP VIEW – DAYLIGHT ANALYSIS PERCENTAGE(LEFT), SIDE VIEW – RAYTRACING STUDY (MIDDLE) AND DGP MAP (RIGHT), RESPECTIVELY 184
FIGURE 8-6: CONVEX PARAMETRIC LOUVRE SHAPE – APPLIED IN AN EXAMPLE OFFICE ROOM IN NEW CAIRO ON 22ND OF MARCH AT NOONTIME, SHOWING; TOP VIEW – DAYLIGHT ANALYSIS PERCENTAGE (LEFT), SIDE VIEW – RAYTRACING STUDY (MIDDLE) AND DGP MAP (RIGHT), RESPECTIVELY 185
FIGURE 8-7: DAYLIGHT COVERAGE PERCENTAGE DURING THE DAYTIME ON JUNE 21ST AT NEW CAIRO LOCATION FOR THE SF-PL, SCC-PL AND SCV-PL 187
FIGURE 8-8: DAYLIGHT COVERAGE PERCENTAGE DURING THE DAYTIME ON SEPTEMBER 23RD AT NEW CAIRO LOCATION FOR THE SF-PL, SCC-PL AND SCV-PL 188
FIGURE 8-9: DAYLIGHT COVERAGE PERCENTAGE DURING THE DAYTIME ON DECEMBER 21ST AT NEW CAIRO LOCATION FOR THE SF-PL, SCC-PL AND SCV-PL 189
FIGURE 8-10: DAYLIGHT COVERAGE PERCENTAGE COMPARISON RESULTS 191

FIGURE 8-11: DAYLIGHT GLARE PROBABILITY COMPARISON RESULTS OF THE REDUCED SLATS' SIZE OF THE SF-PL, CCS-PL AND CVS-PL 191

FIGURE 8-12: 21ST OF JUNE DAYLIGHT COVERAGE PERCENTAGE GRAPH FOR THE SF-PL, SCC-PL AND SCV-PL FROM 9 A.M. TO 5 P.M. 193

FIGURE 8-13: 23RD OF SEPTEMBER DAYLIGHT COVERAGE PERCENTAGE GRAPH FOR THE SF-PL, SCC-PL AND SCV-PL FROM 9 A.M. TO 5 P.M. 193

FIGURE 8-14: 21ST OF DECEMBER DAYLIGHT COVERAGE PERCENTAGE GRAPH FOR THE SF-PL, SCC-PL AND SCV-PL FROM 9 A.M. TO 5 P.M. 194

FIGURE 8-15: SIDE VIEW SHOWING THE SHAPE OF THE REFLECTED LIGHT WITH A 5 CM CONCAVE SLAT IN DIFFERENT INCLINATION ANGLES, THE RED CIRCLES INDICATE THE FOCAL POINTS WHICH MAY OCCUR A RISK FOR A HEAT CONCENTRATION SPOTS 195

FIGURE 8-16: SIDE VIEW SHOWING THE SHAPE OF THE REFLECTED LIGHT WITH A 5 CM CONVEX SLAT IN DIFFERENT INCLINATION ANGLES 195

FIGURE 8-17: HDMI FALSE COLOUR MAPS FOR THE CASES (1), (4) AND (7) OF THE FLAT, CONCAVE AND CONVEX-PARAMETRIC LOUVRE, RESPECTIVELY. 196

List of Tables

TABLE 2-1: DAYLIGHT PERFORMANCE AND ENERGY SAVED WITHIN PARAMETRIC DESIGN 74

TABLE 3-1: SLATS SETTINGS 92

TABLE 4-1: SKY TYPES 107

TABLE 4-2: A COMPARISON BETWEEN THE HDRI MAPS IN THE PROTOTYPE AND THE SIMULATION AS A VALIDATION STUDY, IN ADDITION TO THE DAYLIGHT ANALYSIS MAP TO INDICATE THE ILLUMINANCE VALUES..... 111

TABLE 5-1. LIST OF MODELLING PHASES (CHANGES BETWEEN THE PHASES APPEAR IN RED ITALIC)..... 118

TABLE 6-1: DAILY AVERAGE OF ELECTRICAL LIGHTING ENERGY CONSUMPTION WH/M² AT THE DESK LEVEL IN BIRMINGHAM, UK BY USING THE IPL. 146

TABLE 6-2: DAILY DAYLIGHT COVERAGE PERCENTAGE FOR THE DAYLIGHT ILLUMINANCE RANGE OF 300~500 LX AT THE DESK LEVEL IN BIRMINGHAM, UK BY USING THE INTEGRATED PARAMETRIC LOUVRE. 149

TABLE 7-1: DEFINITIONS OF SKY TYPES 154

TABLE 7-2: SOLAR RADIATIONS ON SEPTEMBER 21ST FROM 9 A.M. TO 5 P.M. IN NEW CAIRO BY USING ONE-AXIS ROTATION CONTROL IN NEW CAIRO LOCATION 168

TABLE 8-1: COMPARISON BETWEEN OFF/ON STATES USING THREE DIFFERENT SENSORS IN A MEETING ROOM AT THE UNIVERSITY OF NOTTINGHAM, FROM MAY TO AUGUST IN SELECTED SUNNY DAYS WITH CLEAR SKY CONDITION . 179

TABLE 8-2: COMPARISON RESULTS BETWEEN SLATS COUNT, DAYLIGHT COVERAGE PERCENTAGE, DGP AND GLARE EFFECT OF THE PARAMETRIC LOUVRE VIA USING FLAT SLATS 190

TABLE 8-3: COMPARISON RESULTS BETWEEN SLATS COUNT, DAYLIGHT COVERAGE PERCENTAGE, DGP AND GLARE EFFECT OF THE PARAMETRIC LOUVRE VIA USING CONCAVE SLATS..... 190

TABLE 8-4: COMPARISON RESULTS BETWEEN SLATS COUNT, DAYLIGHT COVERAGE PERCENTAGE, DGP AND GLARE EFFECT OF THE PARAMETRIC LOUVRE VIA USING CONVEX SLATS..... 190

Chapter 1 Introduction

1.1 Background

It is necessary to observe the significant increase of conventional energy consumption that leads to global warming and carbon emissions, which therefore encouraged many countries to implement new energy policies and promote renewable energy applications [1]. A study revealed that lighting energy consumption of the global is approximately 19% of total electricity consumption, which expected to increase to 40% by 2030 if no practical solution policy is considered [2]. Usually, half of electricity consumption in commercial and office buildings is for lighting. This could be significantly reduced with sufficient use of daylighting, which is one of the fundamental measures in sustainable buildings development. However, only within 3 meters from windows, daylighting can provide sufficient illuminance and its distribution is highly non-uniform. This has largely limited the energy saving potential of daylighting in deep-plan buildings.

Therefore, buildings are dramatically moving towards bioclimatic design and particularly passive natural cooling technologies or passive solar building, which is a necessary step towards energy-efficient building and fully sustainable Zero Energy approach. This step can be improved via exchange the conventional energy sources with renewable energy sources (RES). This trade-off can be achieved by optimising the use of free natural resources such as daylight and solar energy.

From another aspect, inside our bodies, the exploitation of natural daylight is one of the vital approaches to our health. Based on photometric, medical, psychological, and physiological criteria; these various human

needs should be taken into consideration. Besides, these criteria have many aspects like visibility, activity, health, safety, comfort, social contact, communication, aesthetic appreciation, and so forth [3]. Light influences our bodies in two ways. Firstly, through our eyes' retina, then go to our vision system to stimulate our metabolism, endocrine and hormone system. Secondly, it interacts with our skin by way of photosynthesis and produces vitamin D [4].

The hypothalamus, a part of the brain beneath the thalamus, can control most of our body's life-sustaining functions. The hypothalamus is responsible for several metabolic processes and autonomic activities such as energy, growth, maturation, circulation, breathing, emotional balance, fluid balance, reproduction, heat regulation and circadian cycle, Figure 1-1.

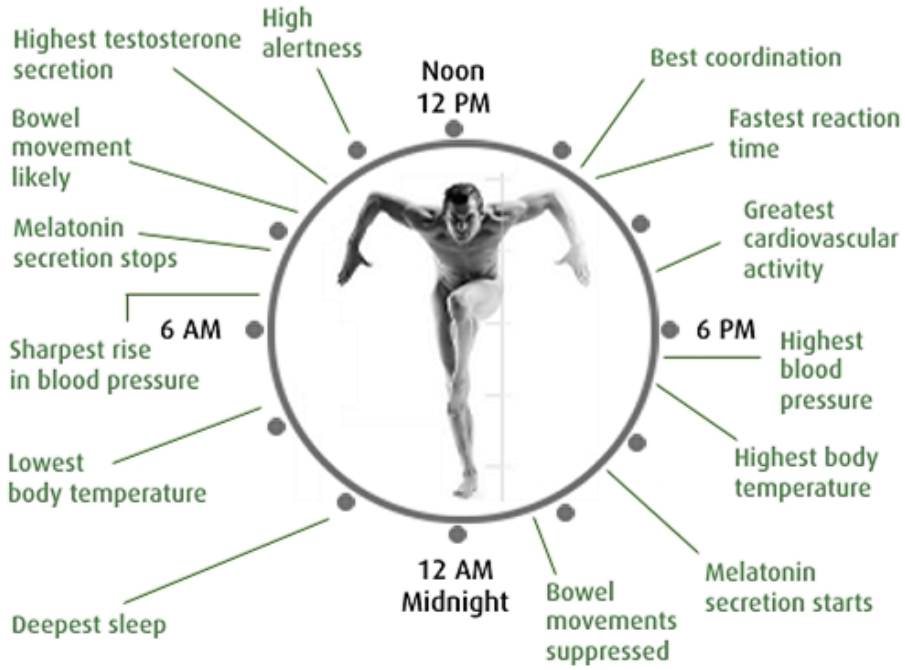


Figure 1-1: Circadian rhythm for human in 24 hours, biological clock [5].

Our daily activities and night sleeping are regulated by a control centre in the hypothalamus called the suprachiasmatic nucleus (SCN), which also known as "body clock". The body clock receives signals from SCN to control these activities. The day-night cycle of the 24-hour solar day is the primary

natural signal that stimulates our body-clock rhythms. Our body must receive these signals with the right amount of light at the right time and frequency. When it doesn't, the internal clock may disturb, which affect our bodily functions. The most powerful signal is the bright light, such as sunshine. The SCN serves as a timer or a pacemaker for our internal body clock or circadian rhythm, as shown in *Figure 1-1* and is directly influenced by the daylight. Daylight catalyses the secretion of hormones in our brains. At low light levels, our brains give a signal to occur the drowsiness. People who live and work in windowless environments or places lacking adequate daylight can be at risk of having their internal clock continually disturbed [4], which can adversely affect their bodies' functions and activities.

Accordingly, natural daylight should be available regularly inside the building envelope and controlled efficiently, to meet human convenience and improve their activities. The excessive use of artificial systems for aesthetic aim instead of their functional purpose could be a disadvantage. In such cases, architecture works 'worse than climate', and therefore, these systems should be functionally exploited for better building performance and energy-saving [6].

At the building envelope, glazing interactive with several physical phenomena and processes. For instance, at the outdoor ambient, there are many changeable factors such as air temperature, humidity, wind velocity, solar radiation and other outer electromagnetic fields. All these factors are permanently changeable, which have a significant influence on the spectral distribution of the daylight and solar intensity. The most of approaches currently in use, even in the most developed fenestration technologies are daylight and solar heat gains. To control the amount of light and the

intensity of solar radiation inside the building envelope, daylighting tools such as louvre systems can play a crucial role for such aim [7].

Louvre systems are a common type of shading devices and are increasingly operated automatically to overcome the limitations of using manual operation [8]. Automated louvre systems need to be controlled to optimise the benefits of daylight on the aspect of redirecting sunlight, for occupants' comfort and energy consumption. Meanwhile, the common control methods are focused on minimising the adverse impacts of daylight, rather than maximising their positive impacts. They may often inaccurately predict the slats' position, resulting in undesirable blockage of useful daylight needed. The current thesis therefore puts forward an innovative parametrically controlled daylighting louvre system, which can redirect sunlight to illuminate the ceiling and hence provide more uniform and steadier daylight in a room of up to 8 meters deep with more than 90% coverage, during most of the daytime. Hence, this system can maximise use of daylighting in deep-plan buildings and thereby significantly reduce lighting energy consumption.

1.2 Research questions and gaps

Several factors influence the amount of daylight inside space, such as seasonal fluctuations, climate changes, geographical conditions, sun positions, building orientation and fenestration system. These parameters can determine illuminance quality and energy performance inside a building. In order to improve the illuminance quality and reduce energy consumption at the same time, a balance between these parameters should be considered via using advanced architectural skins and innovative designs, in addition to occupants' comfort [9].

Studies revealed that 20-30% of the total energy, used in commercial buildings [10]; while, 35% of electrical energy goes to office buildings [11]. Recent studies found that using daylighting systems in office buildings can save up to 50% of the total energy consumption [12]. Although, various daylighting systems are introduced to the market and available in the building industry, however, their usage still limited due to their cost, maintenance and performance limitations. Most of these daylighting system is based on a tailor-made, required specific design and only used in some high profile projects due to their high cost [13]. For instance, some daylighting systems such as light pipes can provide up to seven hours of illuminance inside the space at maximum level 200 lx, compared to four hours achieved by light shelves [14]. However, light pipes are more expensive, requiring more maintenance, and their performance can be affected by sky conditions and solar fluctuations [15]. On the other hand, light pipes are effectively beneficial for daylighting in windowless spaces comparing to other daylighting systems.

Generally, daylighting systems have benefits and drawbacks; this can be specified based on the quality and the quantity of the light provided in addition to their primary function. A pilot study has been made over the general daylighting system to figure out these issues and to fill in these gaps. To summarise, there are two main issues, the external conditions such as solar fluctuations, seasonal and climate changes, and internal conditions such as the type of daylighting system, cost, maintenance, accessibility and the purpose of this system. In order to achieve the required quality and quantity of daylighting illuminance inside the space, it is essential to consider a compromise between all those mentioned

parameters simultaneously. So, how long during a day can a daylighting system achieve the required illumination level inside the space (as a quantity criterion)? Furthermore, how far inside the space can a daylighting system achieve more uniformly distributed illumination (as a quality criterion)?

1.3 The aim and objectives

Aim: The aim of this study is to improve the daylight distribution inside the buildings via using movable reflective louvre which can redirect the incident sunlight deep into the building. The louvre can rotate parametrically by responding to the sun movement – wherever the sun moves – to collect as much as possible of daylight. Then, the daylight is reflected into specific targets on the ceiling; then the ceiling works as a source light to the room. Primarily, the study focuses on exploiting the benefits of parametric design as a control method to increase the steadiness and distribution of the daylight inside the building during the daytime, which, contributes to achieving visual comfort for the occupants, whereas, they can use the daylight instead of artificial lights.

Objectives:

1. *Investigate daylighting and parametric design, via pilot study about daylight, and literature review about parametric design facilities and its applications. Highlight previous studies that used the parametric approach to optimise the benefits of daylight.*
2. *Develop an innovative daylighting optimisation method, via using "mirrored louvre system", based on parametric control.*
3. *Examine and validate the daylight reflection process in a deep-plan room using the proposed daylighting system.*
4. *Investigate the steadiness and distribution of the daylight inside the room via integrating the proposed daylighting system with advanced windows and chamfered ceiling.*
5. *Measure the long-term performance of the integrated daylighting system at different times and orientations.*
6. *Increase the feasibility of the proposed daylighting system by using a smaller size and different shapes.*

1.4 Structure of the thesis

The current PhD thesis studies an innovative daylighting louvre system to improve the daylight in a typical office room via using Grasshopper as a parametric control. The PhD thesis consists of nine chapters, starts with the thesis introduction in Chapter 1, literature review and background about daylighting and parametric design in chapter 2. The proposed louvre system has been investigated in chapter 3. A validation study has performed in chapter 4. The louvre system has been integrated with advanced glazing and chamfered ceiling in chapter 5. Then the integrated system has been evaluated throughout the year in different orientation in chapter 6. An innovative controlling method has been investigated in chapter 7, then the system has been improved to be more practical in chapter 8, and finally, the conclusion and recommendation in chapter 9, see Figure 1-2.

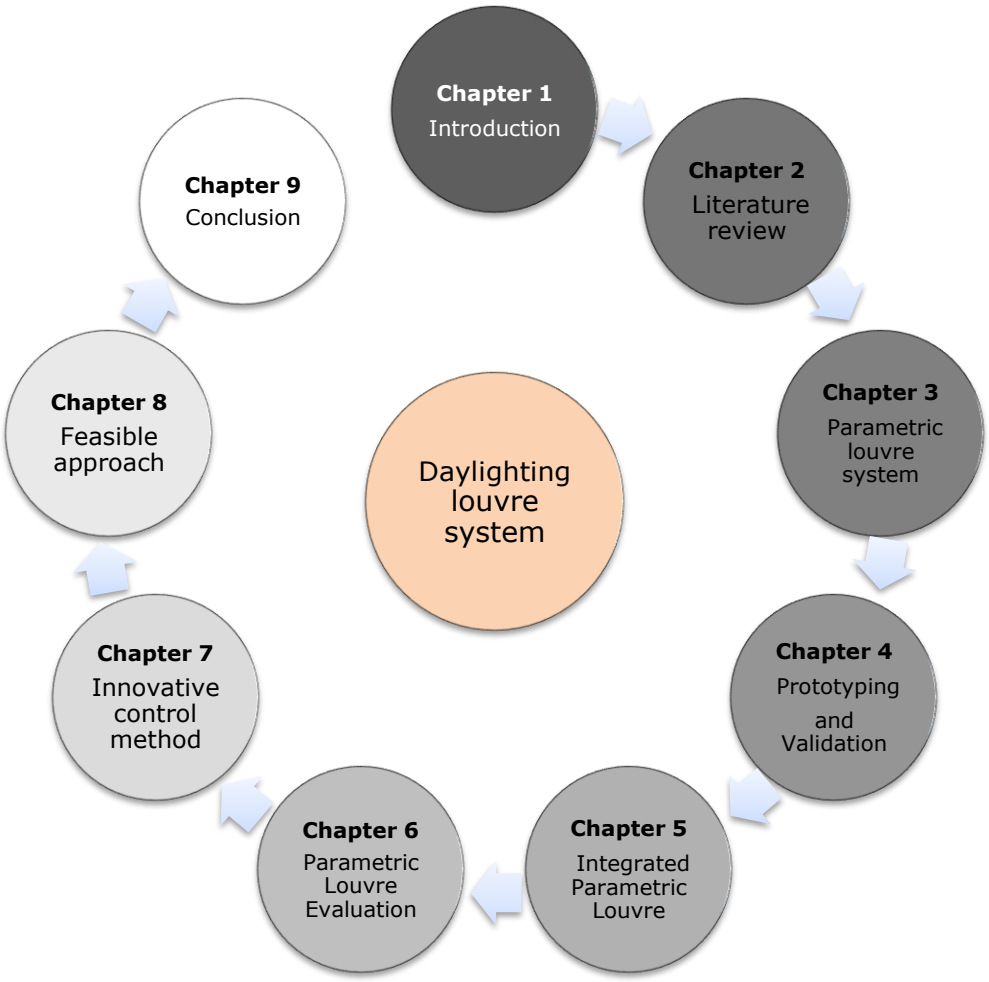


Figure 1-2: Structure of the PhD thesis

Chapter 2 Literature review of daylighting and parametric design

2.1 Introduction

This chapter consists of a literature review about daylighting and parametric design. The chapter went through a general background about the daylight in addition to its related definitions, metrics and classifications, described in sections *2.2* - *2.4*. Then the following sections went through a pilot study about parametric design, its origin, principals, software and its applications. The final section is literature about previous researches who investigated parametric design concerning daylighting and how to utilise the capability of parametric design tools to optimise the use of daylight via case studies and applications.

2.2 The light

Light is that part of the electromagnetic spectrum that is perceived by naked eyes. The wavelength range of light can be recognised between 380 and 780 nm. The visible parts for us are between ultraviolet and infrared, see Figure 2-1. We can see colours at the daytime, while at night we can only see shades of grey [16, 17]. Light may vary on its trajectory and colour based on the physical property of a receiver surface as listed below.

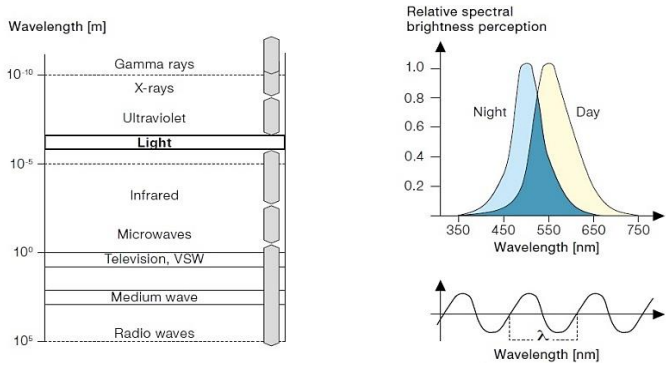


Figure 2-1: Light wavelength and visibility range [16]

2.2.1 Light behaviour

1. Reflected light

As the wavelength of light radiation is tiny, light does not pass through opaque surfaces, but it is reflected over them. Initially, reflection involves two rays, an incoming ray and an outgoing or reflected ray. Also, the reflected ray varies in its state based on the reflection surface. The law of reflection requires that the two rays are at identical angles but located on opposite sides, where, the two rays' angles are equal with the normal line on the reflector surface. In architecture, the character of most surfaces have diffused reflection [17]; thus, this behaviour tends to distribute natural light more uniformly inside the interior spaces. Only high polished surfaces and those with an ordered internal molecular structure can display regular behaviour with reflection; however, all other irregular and matt surfaces can behave in diffuse and irregular reflection, see Figure 2-2 [17].

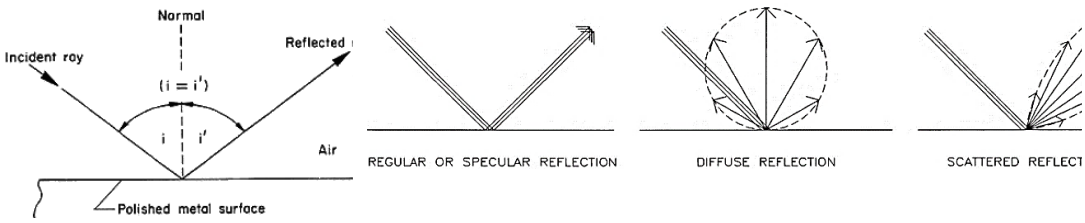


Figure 2-2: two rays reflected on a metal surface with equal angles to the perpendicular line (left) geometric reflection behaviour based on the surface type (right) [17]

2. Refracted light

Refraction is a natural phenomenon of a light wave that bends its path when it enters from one medium to other with different speed. When the light passes from a fast medium such as air to a slower medium such as water, as shown in Figure 2-3, the light ray bends towards the perpendicular line to the boundary between the two medium. The amount of refraction inside the slower medium can be identified with a metrics

known as Index of refraction (IOR), while, each media has its unique IOR. Thomas Young was the first who invented and used the term "IOR" [18].

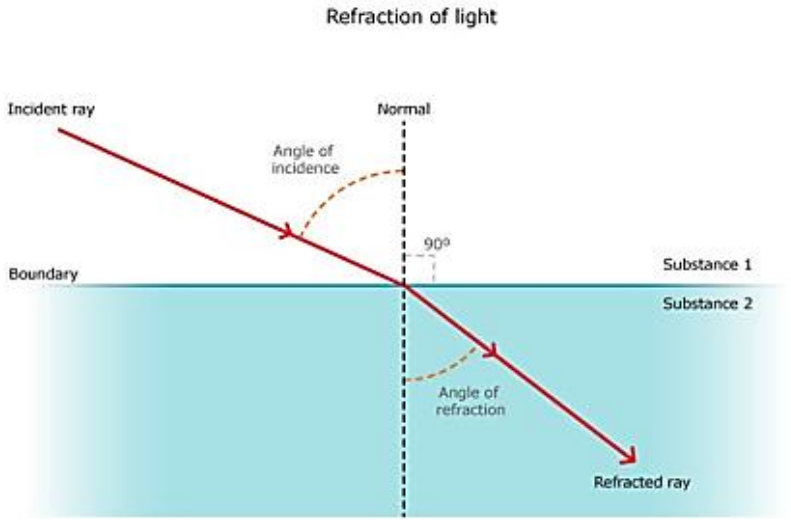


Figure 2-3: refraction of light ray [19]

3. Transmitted light

Light can be transmitted through transparent, semi-transparent and translucent materials; moreover, it can be refracted into spectrum light through these materials based on their colour, Index of Refraction (IOR) and geometries. From the geometric point of view, the finish and the internal structure of the material can affect the type of transmission. As long as the material or the vacuumed medium is irregular, the transmitted light will be diffused. Meanwhile, if these irregularities are dramatically smaller, regular transmission will occur with no modification of the geometry of the transmitted light, see *Figure 2-4* [17].

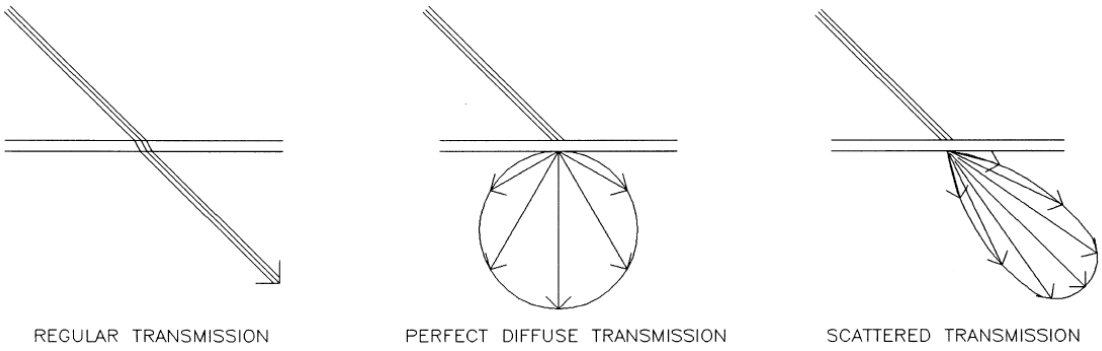


Figure 2-4: geometric transmission behaviour based on the surface type.

4. Absorption of light

Light absorption occurs when light strikes a material, where, the energy in the light is absorbed by the atoms of the material then converted into thermal energy. For instance, white light consists of different frequencies of the spectrum; red, orange, yellow, green, blue, indigo and violet. When an object reflects all these lights, it appears in white. However, when an object absorbs all these colours of light, it appears black. On the other hand, an object that appears with a particular colour means that the object absorbs most of the frequencies and only reflects the colour of the object. For instance, the human eye can see the leaf in green because it absorbs all the frequencies of light except for *green* [17].

2.2.2 Light metrics

1. Luminous flux (Unit: lumen or lm)

The luminous flux is the measure of the perceived power of light. It describes the quantity of light emitted by the source of light [16], see Figure 2-5.

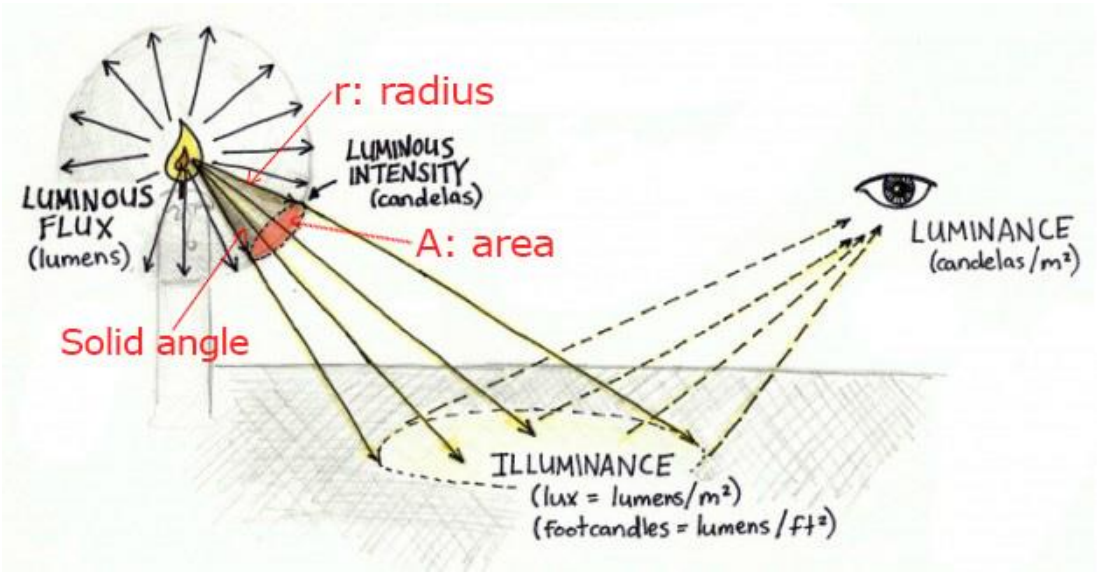


Figure 2-5: Sample sketch of light measurements

2. Luminous intensity (Unit: candela or cd)

The wavelength emitted from a light source in a particular direction on a unit solid angle and the human eye is the standard model of the luminous intensity [20]. A solid angle is a two-dimensional angle with units called Steradians, it can be imagined as a beginning of a point that encompassing through an area (A) on a sphere with specific radius (r), where the magnitude of a solid angle is: A/r^2, see Figure 2-5.

3. Illuminance (Unit: lux or lx)

The quantity of luminous flux distributed on a surface. Illuminance is the most common metric for daylight measurement in architecture [16]. Illuminance: $\mathrm{E(lx)} = \frac{\text{luminous flux (lm)}}{\text{area } (m^2)}$, see Figure 2-5.

4. Luminance (Unit: cd/m^2) Candela per meter square

Luminance is the primary lighting parameter that is perceived by human eye. Luminance specifies the brightness of any surface and dependents on its physical property (finish and colour) [16], see Figure 2-5.

2.3 Daylighting and solar radiation

On our planet, sunlight is the primary source of light, energy, photosynthesis and other biological processes. Without sunlight, the human being can be under risk of diseases and health problems; therefore, the existence of sunlight is vital for well-being, while it controls the biological clock and activates of the body functions [4] and it provides us photochemical ingredients necessary for our lives. Sunlight serves as a link to the outside world when we are indoors, facilitates our essential connection with nature and giving a sense of time and our position in that

daily cycle. Buildings that are made to cover ourselves from the harsh environment, create filters between us and nature. We do not feel delighted when we are away from the natural environment. Therefore, sunlight needs to be controlled and balanced in terms of "sufficiency versus excess" in order to suit the occupant comfort requirements. Latitude location influence on the intensity of sunlight, which decreases gradually from the equator to the poles based on the penetration distance of the sunbeam through the atmosphere [21, 22]. Daylight in buildings is influenced by four main factors; geographical location, weather conditions, seasons of the year and sun attitudes.

2.3.1 Daylighting influence factors

1. Geographical location

The geographical location depends on latitude and longitude of the site, to assign a specific location [23], which intuitively influences the territory nature of this location. Recently, the GPS (Global Positioning System) is used as a satellite navigation system to determine a specific geographical location. GPS technology was first invented and used by the US military in the 1960s, then expanded to civilian use in a few decades [24].

2. Weather conditions

Weather condition refers to the atmospheric state in terms of temperature, wind, clouds and precipitation. New technologies within specific environmental tools are used to predict the weather forecast up to 10 days, and in some advanced technologies can achieve 14 days as an ultimate limit. This predictability is studied by professionals and experts in Meteorologies such as European Centre of Medium-Range Weather

Forecasts (ECMWF) and Next-Generation Global Prediction System (NGGPS) in the U.S.[25]. Generally, weather condition can be specified by the availability of the; sun, clouds, fog, rains, snow and ice which characterises the climate type of any location, for instance; 'hot territory, cold territory, Mediterranean, tropical', etcetera. Weather condition often depends on the latitude location of the territory. For computer simulation, a morphing method has been investigated by Belcher, Hacker and Powell to produce design weather data for building simulation that accounted for future changes to climate [26]; meanwhile, Q-Sin method has been developed by Chow and Levermore to project future weather data [27]. Jentsch, James, Bourikas and Bahaj [28] investigated a "climate change" weather file tool, to allow the end-user to generate future weather data via using "Typical Meteorological Year" (TMY) and "EnergyPlus/ESP-r Weather (EPW) file formats, as a Microsoft Excel output [29]. For daylight simulation, Climate-based Daylight Modelling (CBDM) is commonly used to predict the amount of daylight in a space-based weather file data for a specific location [30]. However, a study found that the accuracy of these predictions can vary, especially when studying daylighting levels [31].

3. Seasons of the year

Changing between seasons related to solar fluctuations, which influence on the variation of daytime and night length. Throughout the year the earth rotates around the sun one full rotation. However, the earth's spine is tilted at an angle of 23.5° with its orbital path, which accordingly occurs two solstices and two equinoxes represented in the four-season. In spring and autumn on 21st of March and 23rd of September respectively, the daytime and night-time are approximately equal to 12 hours, this phenomenon is

known as "equinox" which in Latin means "equal nights" where the sun rays are aligned with the equator at this time. On these days, the earth's latitude is equal in light and darkness; thus, every half of the earth receives equal daytime and night 12 hours for each. In summer and winter on 21st of June and 21st of December, the ancient Greek observed the movement of the sun and specified the points at which the stops occurred solstices meaning "sun stand still", and we still use their word. At this time in summer, the daytime is the longest in a year, and the round starts to revers where the night begins to become longer and the day becomes shorter going to winter passing through the equinox, as the equinox is the mid-time between summer and winter solstice. This phenomenon can be noticed well in the northern and southern hemisphere, where the dates are reversed [22], see Figure 2-6.

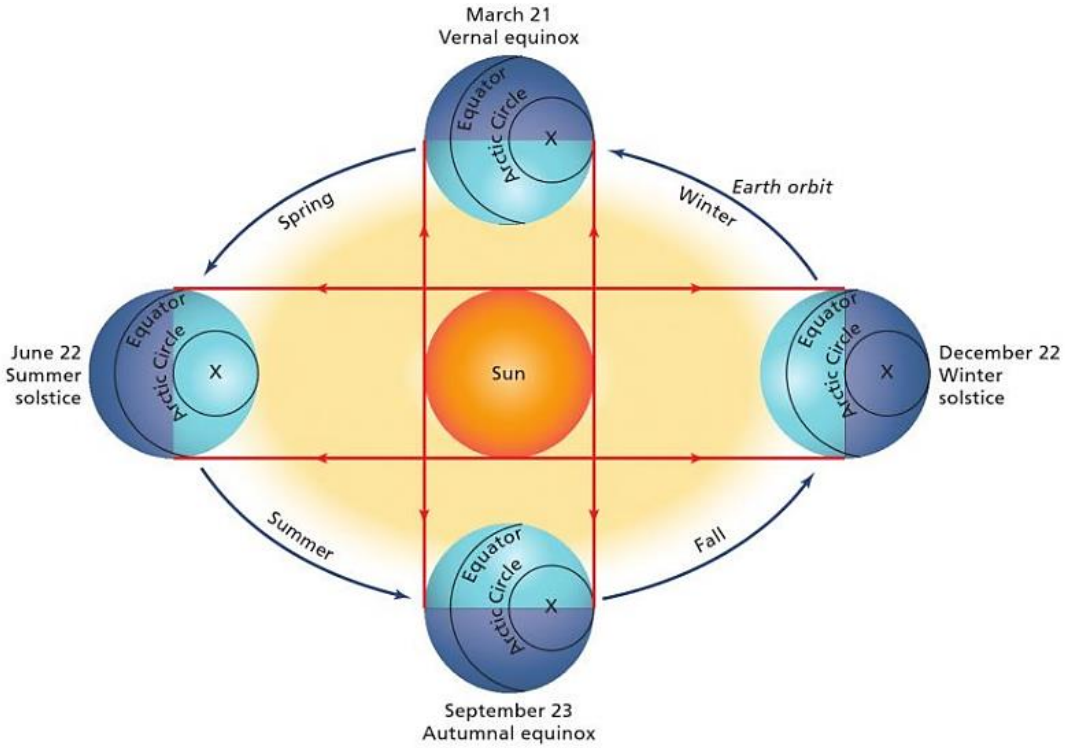


Figure 2-6: four season's diagram [22]

To have a clear idea about the season's causes, we may imagine that we are looking down at the Earth's orbit around the sun from a point high

above the solar system, as shown in *Figure 2-6*. The North Pole always points to the right. When it is the summer solstice, the Arctic Circle receives sunlight during the entire daily rotating of earth, and the northern hemisphere receives more than 12 hours of daylight. This area receives a larger amount of solar radiation in the summer season. On the other hand, when the winter solstice occurs, the area inside the Arctic Circle becomes dark, where, the adjacent parts of the northern hemisphere receive fewer than 12 hours of sunlight, and solar energy levels become very low [22], see for more illustration, see Figure 2-7.

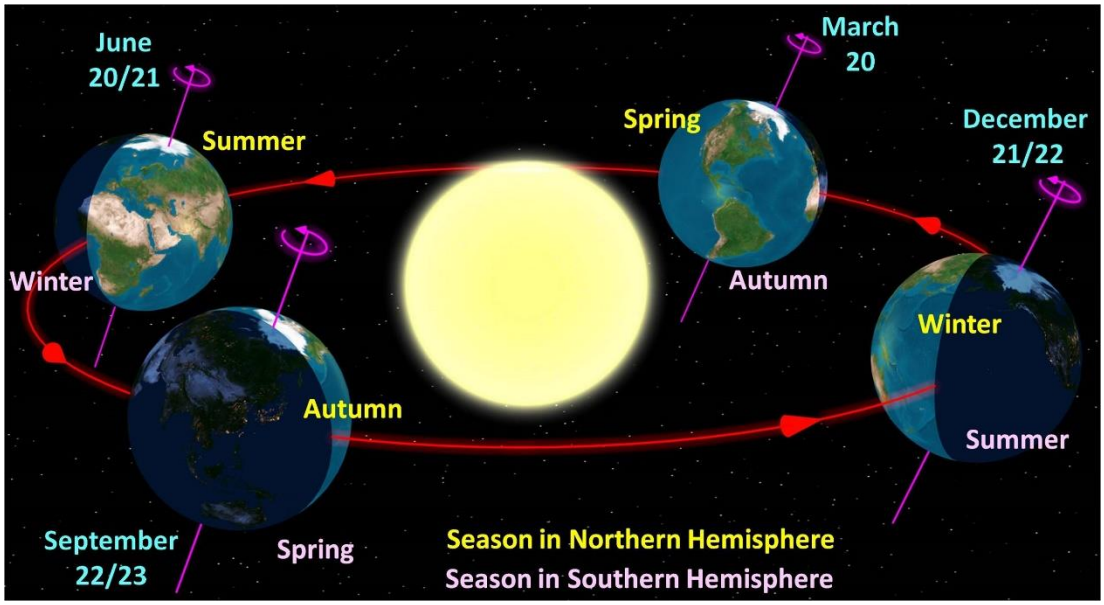


Figure 2-7: Earth positions and movement around the sun, for daylight illustration.

4. Sun altitudes

The relationships between the Earth and Sun leads us to understand why the intensity of the sun's rays varies from place to another throughout the year and how the seasonal changes occur on Earth. The directed solar radiation to the earth is known as "insolation", and it is the primary source of energy on our planet. The fluctuations in insolation are the primary cause of the seasonal variations in temperature which we feel. The real

factors that cause variations in insolation lie under two significant phenomena that vary regularly due to the Earth position while our planet rotates on its axis and revolves around the sun, which accordingly leads to the duration of daylight and angles of the solar rays. The amount of daylight influenced by the duration of solar radiation and the sun rays angles directly affect the intensity of the solar radiation received over a surface. The intensity and the duration of solar radiation together are the major factors that influence the amount of solar insolation available at any location on the Earth.

Therefore, the solar intensity at any location on the Earth can be determined based on the sun angle with this location. The intensity of the sun varies from one place to another on Earth due to its spherical surface. Hence, only the area at the equator can receive right angle radiation, while the other parts on the Earth should receive oblique angles. Accordingly, solar energy that strikes Earth surface at a nearly vertical angle receives more intense energy but covers a smaller area than an equal amount of solar beam striking earth at a sharp angle [17, 22, 32], see Figure 2-8. Besides, the oblique rays must pass through a greater distance of atmosphere than vertical rays; more insolation will be lost on this process. Lambert's law is used to determine the intensity of insolation received at any given latitude, which named for a German scientist Johann Lambert. On the other hand, the natural phenomenon of light is to expand through space when originating from its emitting source. Consequently, the illuminance it produces on a surface decrease by the square of distance [17]. Therefore, if the surface is not perpendicular to the incident light, the solar intensity decreased by the cosine of the angle of deviation.

$$E = (I/d^2) * \cos a$$

In the relation between the Earth and Sun, due to the great distance of the emitting source, variation is negligible on the Earth's surface, and the light beams are considered parallel, which means that:

$$E = (I) * \cos a$$

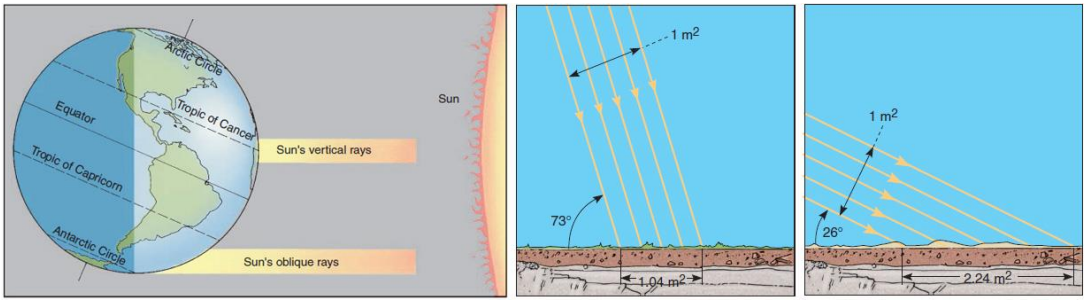


Figure 2-8: solar coverage on Earth [22]

2.3.2 Solar radiation

1. *Direct Normal Irradiance (DNI)*

Also known as vertical illuminance, it can be determined by calculating the intensity of direct sunlight perpendicularly over a unit surface (Wh/m^2). It is the visible light which comes from the sun directly, and it comes in a straight line from its current position in the sky [17]. When Direct normal irradiance is more than 200% of diffuse horizontal light, the sky type classified as "clear sky" [33].

2. *Diffuse Horizontal Irradiance (DIF)*

Also known as horizontal illuminance, it can be determined by calculating the indirect light from the skydome when the sky is clear or from the overcast/uniform sky (Wh/m^2). It is solar radiation that does not arrive on a direct path from the sun, but it has been scattered by particles and molecules in the atmosphere from the skydome, at this case. When direct normal irradiance is less than 5% of diffuse horizontal irradiance,

the sky is associated as "overcast sky", where, the light comes equally from all directions [17, 33].

3. Global Horizontal Radiation

The total amount of direct normal irradiance and diffuse horizontal irradiance, measured by (Wh/m^2).

4. Near-Infrared (NIR)

Infrared is an electromagnetic radiation (EMR) with wavelengths longer that those visible light, therefore, it is invisible for human eye. Infrared radiation is used in industrial, scientific, military and medical applications. Night-vision devices using active near-infrared illumination that allow the observer to see any living creature in a total dark conditions. It is also used to offer accurate information about the composition of materials that can be used for material identification, quality control, process monitoring, and many medical applications. NIR is ranging between the wavelength 900-2500 nm, i.e. just beyond the visible light for human eye.

2.3.3 Daylighting metrics

1. Daylight factor (DF),

It is the ratio between the quantity of daylight inside a room and the total daylight available outside the room, and this ratio is measured in percentage (%) [32]. DF can be calculated in the next equation:

$$DF = \frac{\text{Indoor illuminance from daylight}}{\text{Horizontal unobstructed outdoor illuminance}} \; X \; 100\%$$

Daylight factor used as an indicator to measure the penetrated light level inside a room related to the light level outside the room. As long as the outdoor daylight is always changeable, the interior illuminance will also

change according to the outdoor illumination, for that reason, daylight factor will remain constant for such interior [34]. According to Danish Building Regulations, for working spaces, the window area should be at least 10% of the floor area and 7% for skylights, it can be calculated as at least 2% of daylight factor should be provided at the working place [35]. In general, the analysis found that the satisfaction of occupants increased as the daylight factor increased, which means higher ratings of the daylight levels. However, a high DF more than a proper level i.e. 5%, can be a disadvantage which may produce unpleasant glare at the work-surfaces. DF considered the most widely used measure among the metrics standards to characterise daylight quality and quantity [31].

2. *Daylight autonomy (DA),*

DA is used to measure the illuminance level at a certain point maintained by the use of daylight alone, and can be expressed as a percentage of the occupied time, either annually or on a month-by-month basis [31, 36].

3. *Daylight glare probability (DGP)*

Glare is defined as the notable difference effect of the light within a visual field due to the presence of bright light sources [37]. Daylight Glare Probability is the most recent index used to evaluate glare from daylight [38], and it was conducted by experimental data in private office spaces involving human test subjects. DGP is considered as a part of the main climate-based daylighting metrics to assess daylight quality [39] and establishing adaptive zones [40]. Based on human visual comfort survey

[37, 41], DG level below 0.35 supposed to be an acceptable level and will not cause glare to the occupants.

2.3.4 Climate-based daylight modelling

Climate-based daylight modelling is the prediction of various radiant or luminous quantities such as irradiance, illuminance, radiance and luminance of the sun and sky conditions, via using a weather data of meteorological datasets. For instance, Climate-based modelling can predict the absolute illuminance quantities of a specified building location with a specific orientation, in addition to the building's geometry parameters and material properties [42]. The term climate-based daylight modelling does not have a formally accepted definition, where, it was first named in a paper research by Mardaljevic [43].

2.3.5 Daylighting requirements in Architecture

Daylighting is the source of light which comes from both sun and sky, where the skydome produces diffuse light, which results from the scattering and reflection by clouds and air humidity in the sky and depends on the atmospheric conditions [17]. Natural daylight illumination can vary from 5000 lx in the heavily overcast sky to over 80,000 lx in direct sunlight. These values are significantly higher than adequate indoor lighting demands [44]. Typical indoor illumination requires an illuminance level of threshold 500 lx for workspaces [45], according to the European Standard.

Regarding our thesis study, which focuses on office spaces, *Illuminating Engineering Society of North America* (IESNA) [20] recommends 500 lx of illuminance level or below [34] at the desk level 0.75 m [16]. Likewise, the *Chartered Institution of Building Services Engineers* (CIBSE) [46]

recommends the illuminance level to remain at range 300~500 lx as well. A pilot study investigated 73 office workers and found that illuminance level can be lower than 300 lx when the task dramatically depends on screen-based. When the task involves working on both paper and screen in an equal base, illuminance higher than 300 lx is appreciable [47]. The study indicated an average preferred horizontal illuminance of around 325 lx for work on a computer screen, while 425-500 lx was preferred for other tasks (reading, writing, forth). For all tasks other than the computer screen, 500 lx at least is recommended as an average illuminance at the reading task and 300 lx at least at the desk level. Furthermore, the overall lighting shall not be less than 100 lx at any point, 0.5 m away from the inner walls at the level of 0.75 m from the floor [34]. On the other hand, a previous study claims that lighting level between 100~2000 lx can meet the visual comfort based on occupants' survey [45].

It should bear in mind that some studies indicated that some users might not accept the minimum illuminance level required by most standards. A review by IESNA [20] revealed that superior illuminance levels increased based on age and task contrast. Most users preferred 1000 lx with high contrast and 1800 lx with low contrast. On average contrast levels, the younger users less than 50 years old preferred 2000 lx, while the older users preferred 5000 lx. Another study by Begemann [48] revealed that the average preferred illuminance at the desk level varied between 1100 – 3000 lx based on outdoor daylight condition and sky type. To summarise, most lighting standards require an illuminance level 500 lx at least at the desk level in offices for most tasks, including computer-

based within the range 300 – 500 lx. In any case, the work plane illuminance should never be lower than 100 lx.

In addition to the previous point, orientation, as well as a significant influence on the building's, envelop which determined by the positioning of the building concerning the sun path. Orientation has a substantial effect on façade's design and fenestration treatments [3, 32, 49]. Exquisite orientation can enhance the users' comfort, improve the building performance and increase the energy efficiency of the building.

2.4 Daylighting systems

Daylighting systems refer to innovative appliances and technologies which have been developed to bring sunlight more profound into the building envelope, while, reducing glare problems and excessive sunlight. Meanwhile, daylighting systems can be used as a solar shading and glare protection. Solar shading and glare protection are different functions that require special design consideration. For instance, solar shading is used to high intensity and heat gain against direct sunlight, and glare protection is used as a visual comfort against specular surfaces and high contrast illuminance [50]. Daylighting systems have been dramatically investigated in combination with automatic control in order to improve their performance [15, 51]. The number and kinds of worldwide publications about the automated daylighting system in the last 30 years are shown as a statistical survey in Figure 2-9. The statistical survey was done by using the keywords "daylighting systems" and "automatic control" in different research engines. Meanwhile, 80% of these automated daylighting systems are "blinds" basis, due to their feasibility and ease of use. Furthermore, it has been found that up to 50% of electrical energy saving

can be achieved by using such automated blinds systems in general buildings [52]. Accordingly, such systems have been improved in order to enhance the daylight in the deep interior of buildings [53]. Generally, Daylighting systems consist of static [51, 54] and dynamic elements [55] allocated onto or near a building's façade to collect and redirect daylight into the building [12] to improve daylighting performance, increase visual comfort and save energy.

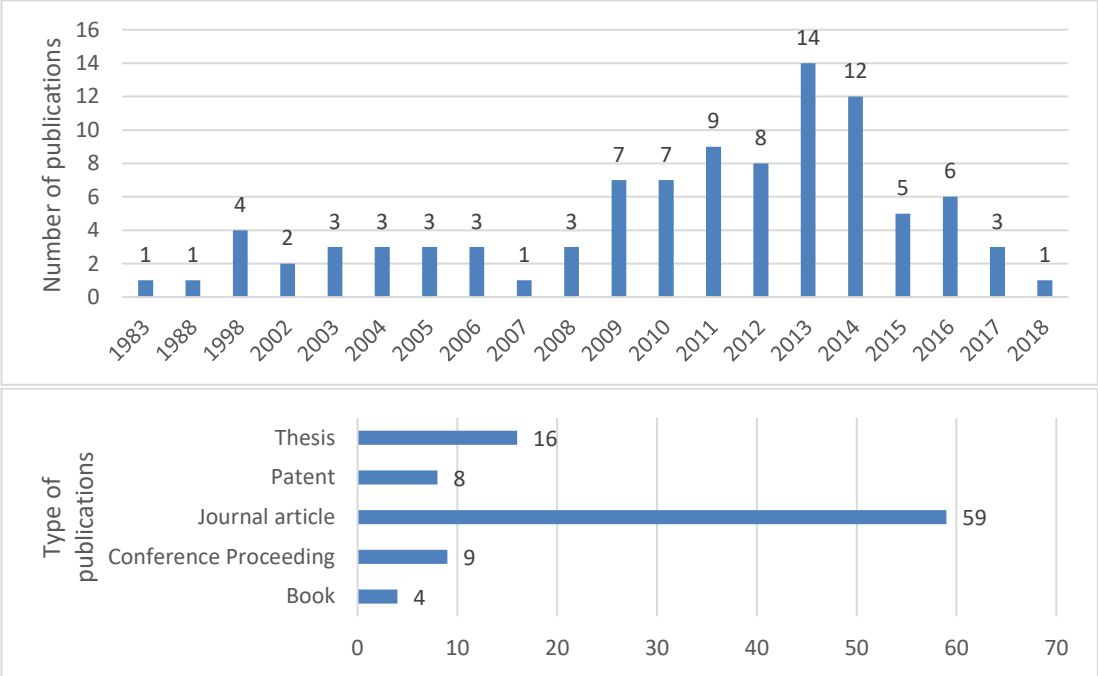


Figure 2-9: (top) the annual number of publications between 1983 and 2018, and (bottom) the count of publications each type about using automation control with the daylighting system [3, 8, 12, 49, 52, 56-134]

Previous studies by Littlefair [54] and Mayhoub [75] investigated more than 30 types of innovative daylighting systems, which can be divided into three main categories: Light Guiding System (LGS), Light Transporting System (LTS) [32, 135] and fenestration system (FS). LGS is based on mirrored surfaces which can reflect and redirect sunlight to the back of the room, where, daylight is probably dim, and sunlight cannot reach this deep area with only typical windows. However, LTS is based on reflective optics which can collect, transport and distribute sunlight to inner, isolated and

windowless zones, with no access through windows or skylights. FS is used to protect from outer climate fluctuations such as wind, rain, temperature, direct sunlight and simultaneously, keep the visual connection between the indoor and the outer envelope. Furthermore, they can control the penetration of daylight and heat gain inside the building. These types of daylighting systems can be used to enhance the performance of daylight in the building envelope and to control the intensity of direct sunlight. The following are a list of Light guiding system, Light transporting system and fenestration system as daylighting systems.

2.4.1 Light Guiding Systems

Light guiding system is often mounted at the upper part of a typical window and uses static or dynamic devices such as light shelves, movable mirrors [136], optical louvre system, anidolic solar blinds, prismatic panel, etcetera. These well-known daylighting systems can directly reflect sunlight into a deep plan room.

1. Optical louvre system

Optical louvre system is a commercial product, also known as a light-louvre daylighting system, consists of 65 mm aluminium slats, vertically scattered, concave up, polished mirrored material (approximately 85% total visible light reflectance). The louvre designed to redirect incident sunlight onto the ceiling and simultaneously provide shade below head height and protect from potential glare. The system is static, required no adjustment and completely obstruct views to the outdoors. The system usually installed at the upper part of the window [137], see Figure 2-10.



Figure 2-10: Optical louvre daylighting system [132]

2. Light shelves [138]

A light shelf is a kind of louvre system utilised to redirect sunlight that hits its surface deep into the building space towards the ceiling [139, 140]. This light strikes the ceiling works as a source of diffuse light to the room. Light-shelves can be used as a flat shape and curve shape. However, the curve shape is capable of redirecting the sun rays in multitude angles, with any solar altitude or azimuth. Daylight near the windows depends more on the light coming from the skydome. However, the daylight level at the back of a room depends significantly on the internally reflected daylight [56, 141], see Figure 2-11.



Figure 2-11: side view – light shelf performance [142]

3. SunCentral

SunCentral is a Canadian system, which had been announced to the market in 2013. The system can deliver sunlight into the interior by using an array of slats mounted horizontally as a canopy at the roof level [135], consists of a set of lenses and mirrors which capable of tracking and

concentrating sunlight. The light is then deflected into a prismatic dual-function light guide spreading above the building interior [143]. The mirrored slats are used to reflect the sunlight into the luminaire and can distribute the light up to 15 m inside the building using highly reflective films, see *Figure 2-12*. SunCentral system can provide a maximum level 350 lx of light based on 1.5 m centre spacing and 100,000 lx reference input illuminance



Figure 2-12: SunCentral [135]

2.4.2 Light Transporting Systems

The light transporting system uses a different process, which is more complicated; a collector device to collect the sunlight, then transport it in specific reflectors, and finally distribute it inside the room [135].

1. *Sun pipes*

Sun pipes can deliver longer distance of light based on its diameter, the bigger diameter of sun pipe; the longer distance it can deliver. The inner core of the sun pipes consists of fibre optics or glass core tapers. Sun pipes can be used within most of LTS, see *Figure 2-13*. Sun pipes can provide illuminance levels between 80~600 lx based on several factors such as, the delivery length, reflectivity of the pipe, diameter, the quality of the fibre optics, solar intensity, sky conditions and other technical factors

[144]. This could be a drawback of such a system while its performance is entirely influenced by the sky conditions and solar fluctuations.

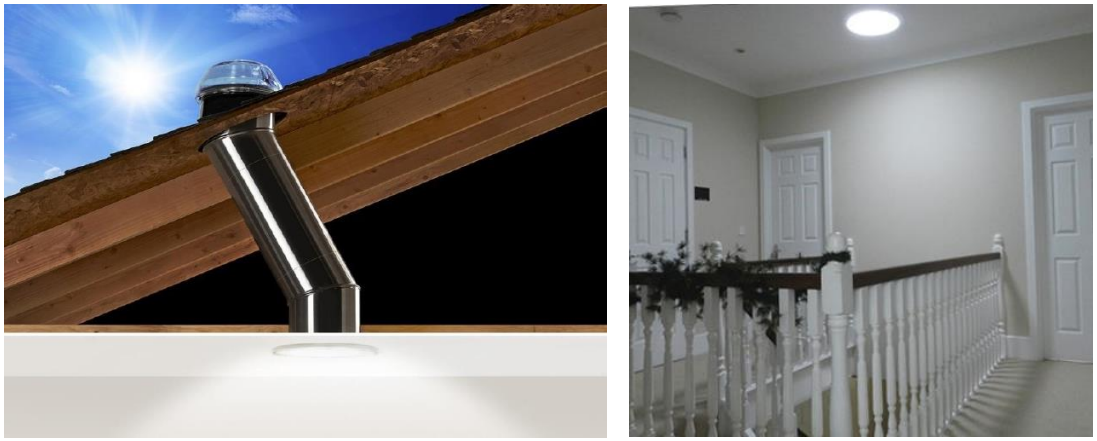


Figure 2-13: sun pipes

2. Fibre optics

Fibre optics or (optical fibre) is a flexible, transparent material made of silica or plastic, and its diameter is thicker than the human hair. Optical fibres are used in communications, while they can do longer distances and higher performance than electrical cables, with no electromagnetic interference. Optical fibres are also used as a means to transmit light between two ends of a fibre [145]. Therefore, they can be used for illumination and imaging, while, they are often wrapped in bundles so they can transmit a significant amount of light, see Figure 2-14. A transparent cladding material covers the fibre optics core with low IOR. Transmitted light is kept in their core by the characteristics of total internal reflection, which accordingly act as a waveguide [145].



Figure 2-14: Fibre optics; shape (left), reflection process (right) [146]

3. Parabolic trough

The parabolic trough is used as a way to collect sunlight and concentrate it into a single optical fibre through a flat mirror [147], see Figure 2-15. For the sake of light transmission, optical fibres were utilised. In the reflection process, most of the light potentially lost through the outer surface of the optical fibre. Therefore, most of the light will not be able to reach the parabolic reflector. The parabolic trough was used for solar thermal applications to produce energy rather than daylight because it requires a minimum number of concentrators to produce uniform illumination performance [148].

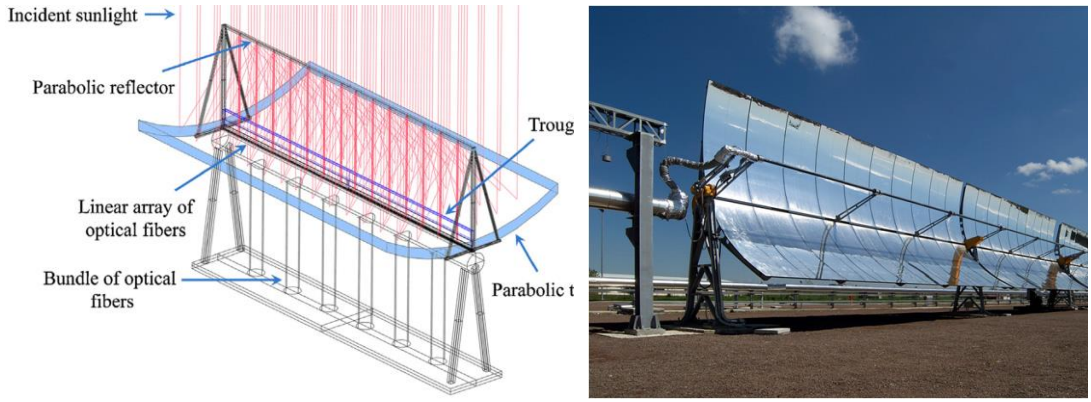


Figure 2-15: Parabolic trough [148]

4. Himawari solar lighting system

The Japanese Himawari system is considered to be the first commercial fibre optic daylighting system since the early of the 1970s. Himawari system consists of a sun-tracking device capable of reacting to the sun movement to capture direct sunlight during the daytime. The incident light is focused through a significant lens known as "Fresnel lens". The Fresnel lens is a reduced amount of material compared to a conventional lens, in which, its lens is divided into a set of concentric annular sections [149]. An ideal Fresnel lens would have infinitely many such sections. In each section, the overall thickness is decreased to be aligned at one level

compared to an equivalent simple lens, see Figure 2-16. The continuous surface of a standard lens is divided into a set of surfaces of the same curvature, with gradual discontinuities between them. The Fresnel lens capable of capturing more oblique light from a light source; thus, the light emitted from a lighthouse can be visible over greater distances [148].

The transmitted light through the Fresnel lens is only the visible light, which then concentrated into the optical fibres. Himawari system has two series of models with a different number of lenses and optical fibres, which exhibit low losses during light transmission [144, 148], see Figure 2-16. It can deliver luminous flux between 3840 lm to 63,360 lm according to the number of lenses under a direct sun with illuminance of 98,000 lux [75].

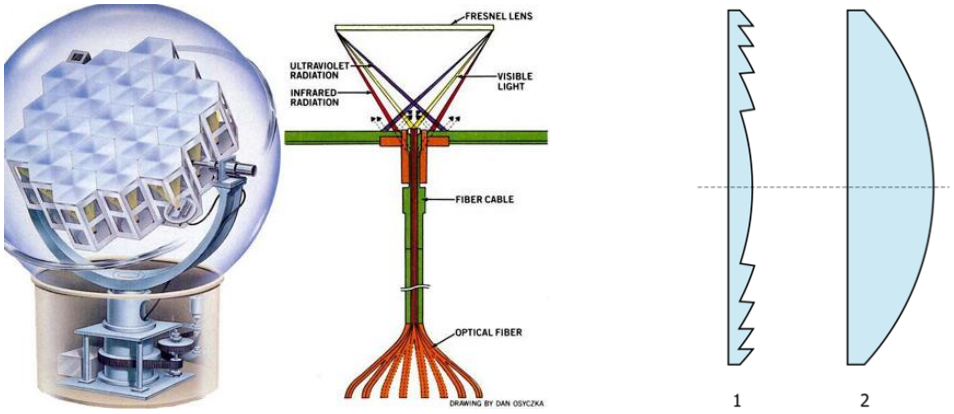


Figure 2-16: Himawari system (left), Fresnel lens (right)

5. Parans lighting

A similar concept is used by the Swedish Parans system that produced the first commercial product in 2004. After that time, three generations have been developed; all of them consist of an array of small Fresnel lenses, which can track and collect daylight, see Figure 2-17 [75]. The collected light is transmitted to a bundle of fibre optics up to 20 m length as a guide to be distributed inside the interiors by various types of custom-designed luminaries [150]. Total output flux of Parans system is around 4600 lm under direct sunlight of illuminance level 130,000 lx [75].

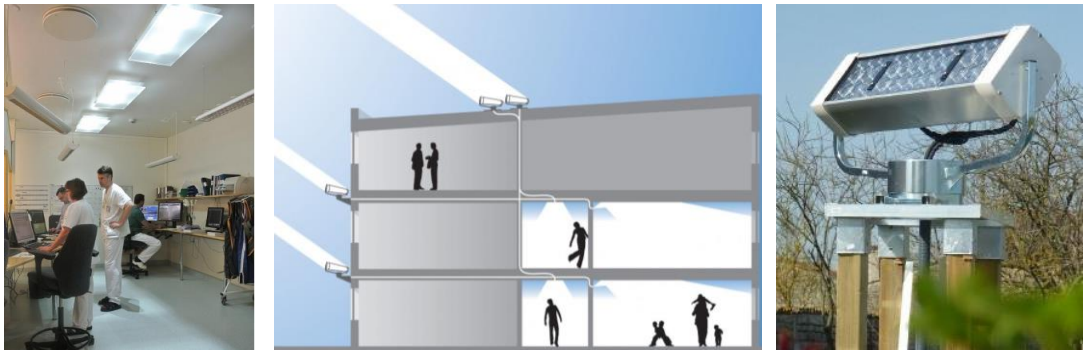


Figure 2-17: Parans system light collector [135]

6. Sundolier

Sundolier is an American manufactured daylighting system; it is a light collector of 0.6 m diameter, which collects daylight by using a set of mirrors that can track and concentrate sunlight, see Figure 2-18 [75]. The collected daylight is distributed to indoor areas using unique in-room fixtures. The system has been used in many building types since founded in 2004. The Sundolier can deliver up to 100,000 lm of light.



Figure 2-18: effect of sundolier indoor (left), sundolier shape (right) [135]

7. Heliostat

Heliostat is mainly produced to collect sunlight by using a set of reflectors and lenses, which accordingly sent into building core via vertical voids. A custom-designed set of mirrors can be used to distribute the light inside the building envelope, see Figure 2-19 [151].



Figure 2-19: Heliostat system [135]

8. Sunportal

Sunportal was developed by a South Korean team in 2012. It captures the sunlight by the aid of the Heliostat with a reflector and concentrator. The collected light travels through a series of optical lenses providing transmission rate up to 200 m length and it can deliver illuminance level between 80~500 lx of light. A transparent tube diffuser is used to illuminate underground spaces [75], see *Figure 2-20*.

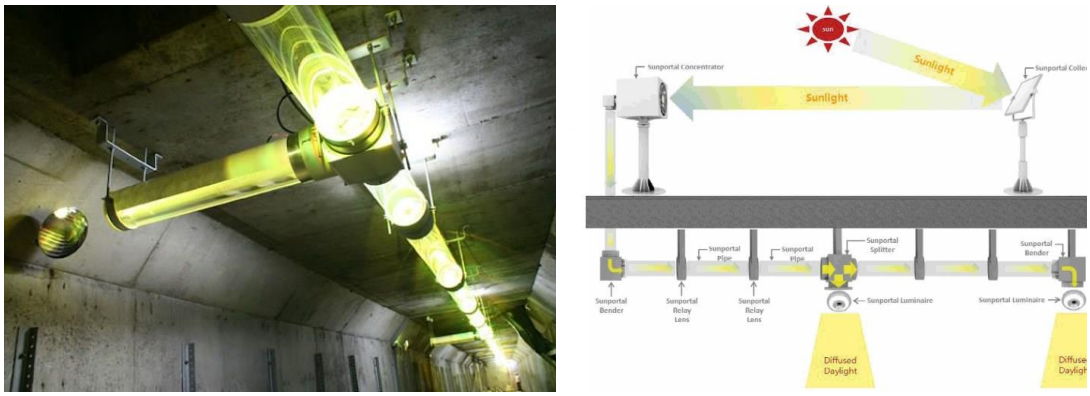


Figure 2-20: Sunportal system [75]

2.4.3 Fenestration systems

1. Skylights

Skylight refers to the apertures in the roof of the building, which can be fully covered with structural glazing or part of it as an orifice to the sky for daylighting purpose, see Figure 2-21. Skylights serve to reduce the necessity of electrical light inside the buildings; furthermore, they usually

employed for the sake of decoration as an architectural concept to emphasise a specific space such as entrances, domes and main halls.



Figure 2-21: skylight shapes

2. Lightwell

Lightwell is mainly used to provide a vertical or narrow volume of space with natural light. In some kinds of buildings, it is used to allow air and light to reach the buildings' envelope. Lightwell can be opened or covered with structural glazing, glass bricks or translucent glass to increase the reflections and provide diffuse light, see Figure 2-22. Studies found that lightwell is only efficient in the upper 2 floors of buildings to achieve the threshold of light level 300 lx of 93% of daily hours during the year [152].



Figure 2-22: lightwell shapes

3. Glass brick or Glass block

Glass block is a common element in architecture made of a customed shape of the glass. Its appearance can vary in colour, size, texture and form. Glass bricks have significant function while it can provide visual

obscuration while providing light. The origin of glass block was developed based on prism lighting principles since the 1900s, aiming to provide natural light to the buildings. Recently, glass blocks can be used in walls, partitions, skylights, and sidewalk lights.



Figure 2-23: glass bricks shapes

4. Prismatic panel

The prismatic panel consists of a bundle of small prisms placed side by side in a serrated shape revealed in one side [153], likewise the Fresnel lens [148], however, Fresnel lens capable of redirecting light to a specific target. The prismatic panel mainly used as a dispersing tool to provide diffuse light by its significant property of scattering the daylight. It has several shapes such as pyramid shape, leaner shape, plated film [154], and it has also been used as louvre shape [155], see Figure 2-24.

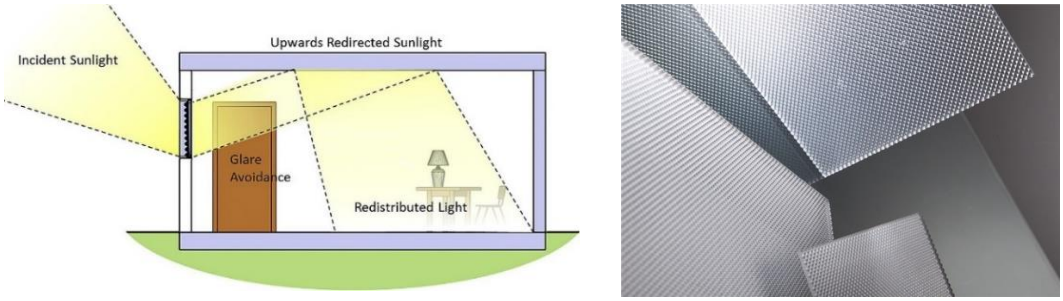


Figure 2-24: Prismatic panel

5. Perforated sheets and Mashrabia

Refer to any light-transmitting screen that incorporates semi-transparent material. They are patterned in variable materials, assembled

in a specific design or sculptured on its surface to create geometrical shapes of systematic apertures based on a specific design. These kinds of screens can allow limited penetration of incident sunlight due to its small orifices. Penumbra effect plays a vital role in such systems while it can provide an adequate amount of daylight [156], see Figure 2-25.

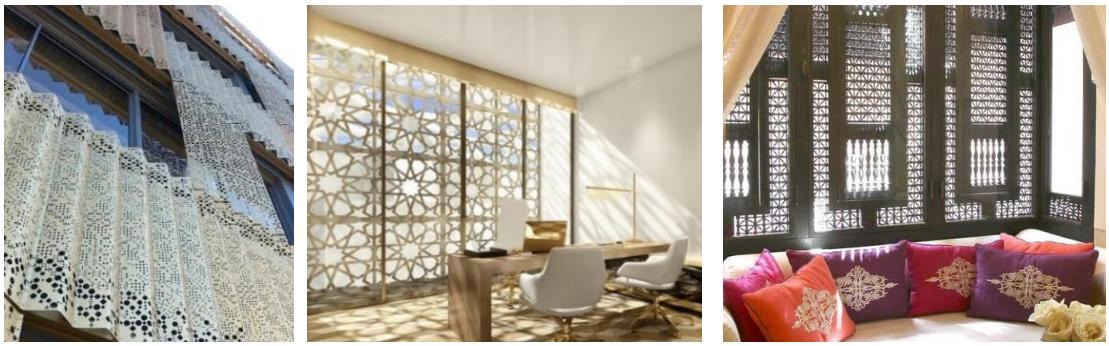


Figure 2-25: shapes of perforated sheets and Mashrabia

6. Double skin façade

DSF is an addition of an extra screen layer in front of the building's façade, used as a cavity to improve acoustic isolation, solar control, enhance daylighting performance, airflow path, façade maintenance and additional insulation in cold and hot climates. The cavity can be ventilated naturally or mechanically and can be coupled with a ventilation system. The double skin façade can also be used for several functions such as PV-sells, phase change materials to reduce thermal fluctuations or even as a design concept by using second screen pattern [157].



Figure 2-26: examples of double skin facades [157].

7. Advanced glazing

All types of windows which can change their phases to respond to the ambient fluctuations such as Electrochromic and Thermochromic windows [158]. These kinds of windows can control the transmission of solar radiation [159] and play a crucial role in improving daylight performance inside the buildings [76], besides, to reduce heating and save cooling energy [160]. They can also be used in the interiors for privacy and decoration sake.

8. Self-cleaning glazing

Self-cleaning glazing is a thin-film that can be attached to the outer layer of doors and windows products, therefore, they are adapted to afford the outdoor climate changes. It has the ability to withstand dirt and maintain clean overtime, accordingly, self-cleaning products require less maintenance compared to ordinary windows and doors. Hence, these products may lead to increase the solar energy utilisation and thus improve energy performance and users comfort [161]. The capability of self-cleaning can be achieved by photocatalytic reactions within a titanium dioxide (TiO_2) thin film coating. For the cleaning operation, the thin film must be activated, which occurs by exposure to daylight/UV radiation (for about one week for full activation), where the TiO_2 reacts with the oxygen and water molecules in the air and produces free radicals leading to oxidative species [162]. When dirt or dust sticks to the window surface, the UV radiation causes oxidative species that results in photo-generated electrons and holes, where, electrons will reduce oxygen in water and holes will oxidize the organic matter, thus remove the dirt and dust [163], see

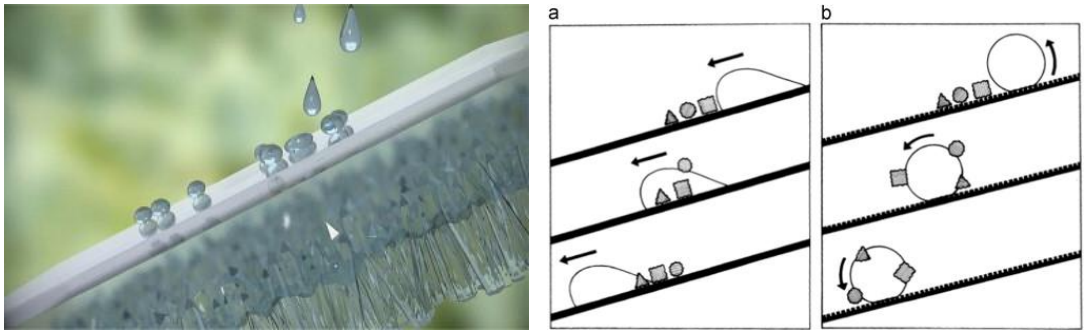


Figure 2-27: Self-cleaning process, (a) a smooth surface, where particles are just redistribute by water droplets, (b) a rough surface, where particles stick to the water droplets and removed from the surface [164].

9. Infrared (IR) and near-infrared (NIR) coating technology

Solar radiation that reaches the earth surface is divided into three parts, the ultraviolet (UV) of region 5%, visible light of region 46% and near-infrared (NIR) of region 49% [163]. Therefore, an efficient coating that can absorb the visible light range, and simultaneously, reflect the near-infrared range of solar radiation [165], in order to mitigate the heat gain inside the building. Generally, it is so-called, near-infrared reflective coating. The coating is created of metal oxide nanoparticles [166], and it can be optimised via manipulating the pigmented coating by controlling the size, volume concentration of pigmented particles and coating thickness, to increase its reflectivity, meanwhile, minimise its visibility [167].

10.Venetian blinds & roller shades

Venetian blinds consist of a bundle of slats deployed vertically in a parallel direction; likewise, the roller shades; however, the latter deployed in a plain shape. Both systems can be installed at the upper part of the window, over its frame or between double glazing. Venetian blinds and roller shades are the most common shading tools used as indoor blinds. They are primarily used to prevent the penetration of sunlight inside the indoor. They have many shapes, dimensions and materials; furthermore, they can be controlled manually or automatically, see Figure 2-28.



Figure 2-28: Venetian blinds and roller shades

11.Louvre

The Louvre is a bundle of slats usually installed over the buildings' skins in different scales, directions and dimensions. It consists of scattered slats in relatively bigger size and rigid material in order to afford environmental factors and climate fluctuations. They usually used to protect from direct sunlight and in other cases used for daylighting control, see Figure 2-29.



Figure 2-29: louvres types and shapes

12.Photo-bioreactors (PBR):

Photo-bioreactors are based on organic materials (algae). PBR system consists of transparent containers using the development of flat panel to uplift Bioreactor, in which air bubbles rise inside the cavity creating strong turbulence which helps the algae growth. The shading factor of this system depends on the density of cells. The system represents an adaptive and interactive shading system; during times of high solar radiation, the density of the cells increases, blocking the light and providing shade. In contrast, light transmission can be increased by an intensified harvesting process [3], see Figure 2-30.



Figure 2-30: photo-bioreactors shapes

The utilisation of biochemical process represents on Photosynthesis which generates biomass by absorbing daylight and CO_2. Therefore, trees and plants are used in landscaping as smart shading devices. Higher plants go through a relatively slow yearly cycle, but micro-organisms such as algae respond to changing conditions within hours. Hence, micro-organisms can be utilised to provide shading to the buildings [168].

13.Biomimetic system

Going to the same concept of exploiting daylight with bioreactor systems. A biomimetic system approaches bio-functional tuning, adaptability phenomena and bio-optimal control. Biomimetic dynamically responsive self-adaptive material (i.e. glazing) feature to the radiation spectra changes as a biological design search aimed to optimise solar radiation and daylighting. In architecture, biomimetic is a contemporary philosophy of architecture looking for natural, sustainable life, not only by iterating the natural forms but by understanding the rules governing those forms in order to adapt with the outer circumstances. It is an interdisciplinary approach to sustainable design that follows a set of principles rather than stylistic forms; in other words, "form follows function". It is part of new movement known as biomimicry, which is the

examination of nature, its morphology, systems, rules and process for the purpose of gaining inspiration from the nature for adaptation and responsiveness with climate fluctuations and sun movements in order to improve/increase the use of daylight [3, 169, 170], see Figure 2-31.

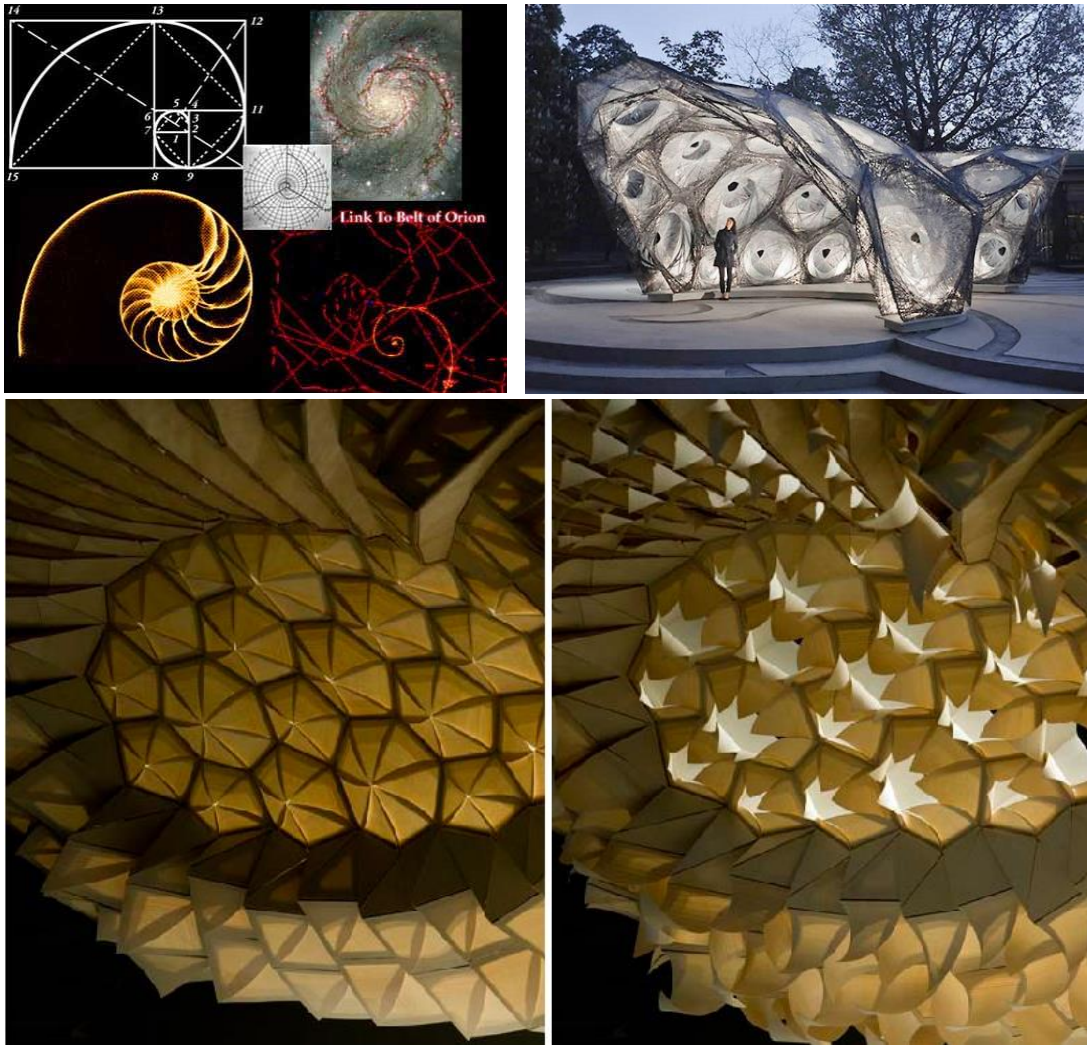


Figure 2-31: Showing Biomimetic system; inspiration from nature for daylighting purpose [21].

2.5 Parametric design

In architecture, all design aspects and their dimensions can be considered as parameters, such as location, orientation, shape, daylighting, solar radiation, and so forth. In the conventional way of design, once an initial model has been created, and if the designer wants to change any parameters, the whole process has to be repeated, which

considered time-consuming. In contrast, the parametric design can efficiently amend and improve the design process by integrating and coordinating design components simultaneously. Therefore, any change, modification, editing or developing will be automatically updated in the model. This parametric process works as a "short cut" to the final model [123]. A graphical comparison between the conventional approach and the parametric design is shown in Figure 2-32.

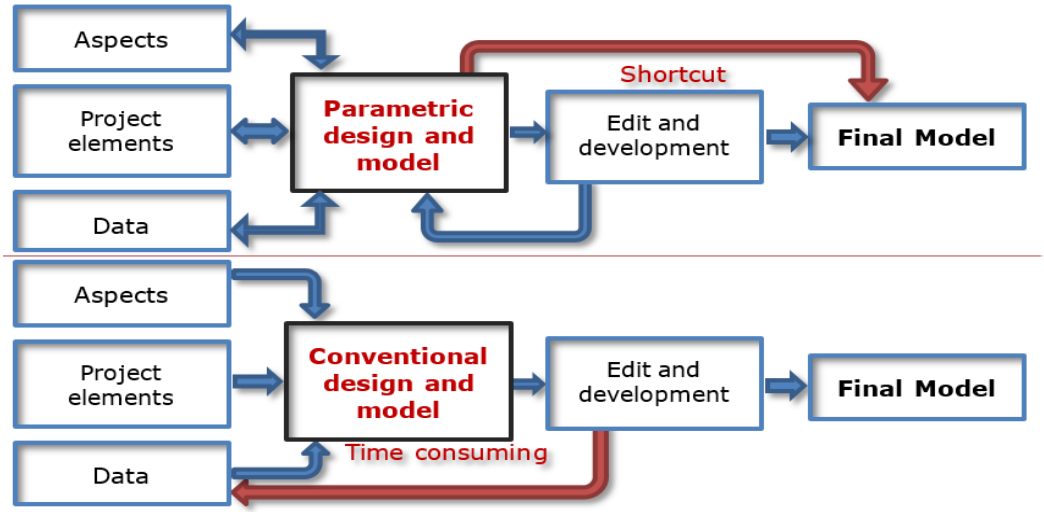


Figure 2-32: Comparison diagram between parametric design process, and conventional ones, showing the difference in time-consuming.

The process of any conventional design within a project goes through several stages, where changes, editing or developing are conventional processes, and these processes could be iterated till achieving the optimum design and best solution. However, for big and complex projects, these processes will be more sophisticated. Accordingly, dealing with these complicated relations will be money and time-consuming. Therefore, parametric design approach can be a vital solution for this kind of project which can work as a coordination tool, in order to facilitate the relationship between different disciplines, and deal with the modifications smoothly with no need to iterate the whole process of the project [171], because, all parameters and elements are connected parametrically.

2.5.1 The origins of parametric design

Daniel Davis, a researcher in the technology of the building industry, RMIT University, his PhD was about computational design; wrote a thesis about Parametric Origins titled as "A History of Parametric" [172]. He claimed that the term parametric originates from mathematics, and the first use of this word is not known. Another researcher, David Gerber [173], claimed that Maurice Ruiter, who is firstly used this term in his book in 1988, which titled as *Advances in Computer Graphics III* [174]. In the same year, mathematician Professor Samuel Geisberg founded the PTC (Parametric Technology Corporation) [175] and created the first parametric modelling software; Pro/ENGINEER, which is an integrated CAD.CAM/CAE solution, and was the first rule-based constraint applied software used nowadays in mechanical design in many companies [176]. In 1978, Hillyard and Braid [177] created a system that could combine two parameters simultaneously, such as dimensions and tolerances in order to design mechanical components, which could be considered as a parametric approach. On the other hand, Robert Stiles argued that the first appearance of parametric concept was earlier in 1940 by Luigi Moretti in his book *Writings of Architect* [178] who wrote extensively about parametric architecture. However, Daniel [179] found that there was also an earlier example; James Dana 1888 who was using the language of parameters, variables and ratios to define general steps to draw a range of crystals, which explained in his paper *On the Drawing of Figures of Crystals* [180].

Moretti defined parametric architecture as a study of architecture system which aims to define the relationships between the dimensions that

depend on various parameters. He used an example of a stadium to explain how the stadium's form can be divided into nineteen parameters, considering things such as viewing angles and economical cost of concrete as shown in Figure 2-33. His parametric stadium was presented in an exhibition at the Twelfth Milan Triennial in 1960, as part of his *Parametric Architecture work* [172, 179].

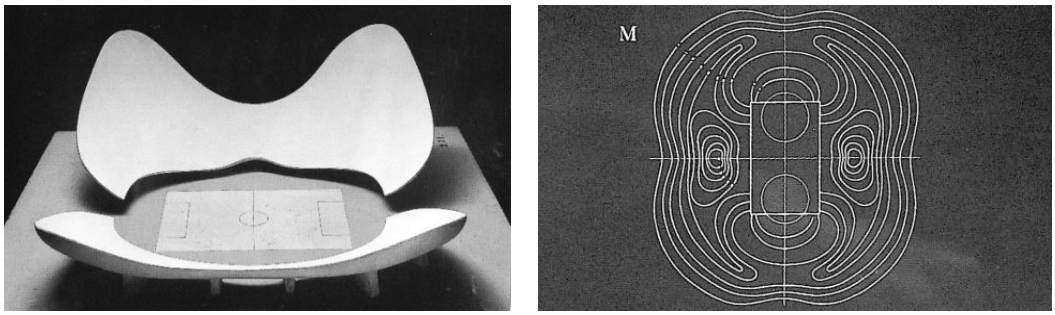


Figure 2-33: A model of the stadium by Luigi Moretti, exhibited at the 1960 Parametric Architecture exhibition at the Twelfth Milan Triennial. The stadium derives from a parametric model consisting of nineteen parameters (left). The plans of the stadium (right) [178].

2.5.2 The principle of parametric design

The term parametric refers to using specific parameters or variables and primarily originates from mathematics, and so, can manipulate with the equation results. Where the relationship between the design elements is shown as parameters which could be reformulated to generate complex geometries, these geometries are based on the elements' parameters, by changing these parameters; new shapes are created simultaneously.

A former Architect, Antoni Gaudi, investigated the design space using analogue models; then he used modern integrated systems in his designs [181]. As well, the modern Architecture of Zaha Hadid used integrated design systems and parametric approach to solve her complex curvilinearity and fluid forms, see *Figure 2-34* [182]. Recently, there is a clear relationship between the parametric term and Computer-Aided Design (CAD) [183], which, facilitate the ways to draw a geometrical model

with specified dimensions and parameters. However, if we need to modify a specific element in the model; it will change only the parameters of this element independently regardless of other design elements. For instance, when changing floor height of a building, we will modify the extrusion of the wall; however, other related parameters such as doors and windows will need to be modified as well in order to match the room height. Accordingly, this process will be iterative and time-consuming when dealing with a complicated model. On the other hand, these modifications process can be performed simultaneously, by connecting the model elements in an algorithmic relation known as "parametric design". Therefore, parametric design can be considered as an advanced version of the CAD system, based on "Generative Algorithms" that can explore design and algorithmic solutions through formulas rather than using standard geometries.



Figure 2-34: Domination office building (left), London Aquatics Centre, 2005 (right)

2.5.3 Parametric design as a software

Parametric design software are newly revealed in 2008 and developed by many software developers such as; Catia, 3D Maya, 3D MAX, Revit, Grasshopper based on Rhinoceros 3D, Dynamo, Generative Components, Marionette, and Modular. However, among all these software, Grasshopper, is the most common software used as a parametric design,

while it can involve different plugins in several fields; such as architecture, urban, structure, environment, mechanical/civil engineering, acoustics, medicine, fashion, decoration and many other disciplines. For instance, "ladybug and Honeybee" [184] are plugins in Grasshopper help to create comprehensive environmental data for any specific location [185], and these plugins can interact simultaneously. On the contrary, other software packages do not provide the necessary components and connections for the creation of a homogeneous workflow as smooth and fluid manner as Grasshopper [186]. Although Grasshopper can deal with many parameters by using a low-performance computer, however, it may take (2-5 min) longer time than 3D MAX in rendering complicated geometry.

Generally, Grasshopper can provide full control, easy manipulation and accurate results of the model's elements by defining form-generating components, which can be optimised through with simple scripting or the use of sliders and mathematical expressions [98]. Grasshopper interface consists of components known as capsules, and they are connected as a canvas in order to build the formula of Grasshopper, and this formula consists of sliders. Changing these sliders influence the whole functions and geometries simultaneously, which can be observed in the Rhinoceros window. Grasshopper has a significant characteristic in optimising the results; a component is known as "Galapagos" is used to optimise, filter and analyse between multiple parameters to achieve the optimum result, via finding the minimum or maximum solution based on the designer needs. Many researchers used the method of optimization to find better solutions, such as Pratt and Bosworth [187] in order to get the best performance of a shaded window in their building.

2.6 Implementations of parametric design in general fields

Nowadays, parametric design is used in many fields and disciplines, which consists of complex algorithmic relations, interdisciplinary work, creative forms, and multiprocessing treatments. It is not easy to control these operations using conventional tools or imagine them using our minds, so it is needed to use complex operating systems, parametric tools, and specific software. Due to this advancement in our life, we can find many implementations of parametric design in many fields like; decoration, fashion, architecture, urban planning, sonic study, structural analysis, medicine and so on.

2.6.1 In urban planning

Parametric design can provide several alternatives in a wide range of design, while it gives distinctive results in the iterative design process, and these results can hardly be obtained using conventional methods. The discrete method of problem-solving can deal with multiple layers in urban design case by saving time in writing the formula and coordinating between these layers. For example, the pedestrian pathway in a previous study [188] was chosen to determine the connections between the project's area, putting into consideration the smaller buildings which block the visual connection on the streets. The sliced landscape was used to divide the pedestrian circulation into patterns. The formula created in this study conducted by Grasshopper aimed to determine the shortest pedestrian pathway, as shown in Figure 2-35. Mohamed and Khalid [189] investigated using parametrical methods to achieve more responsive environmental and sustainable urban morphology concerning human comfort values, such as wind study, solar envelop and daylight availability.

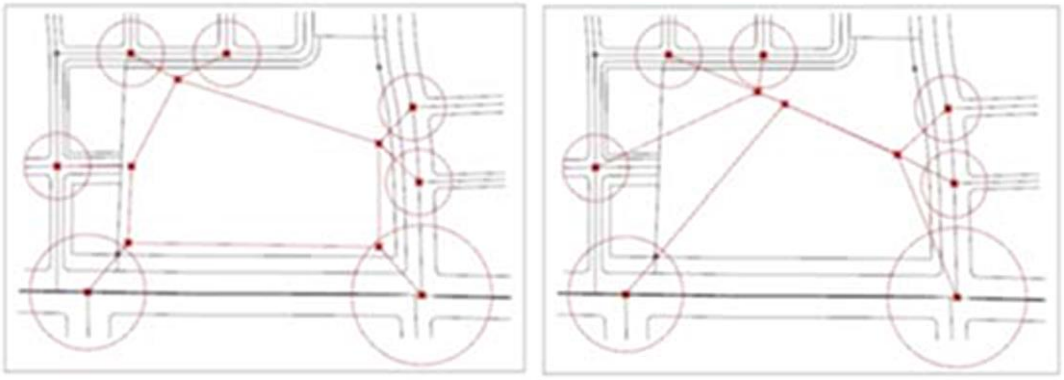


Figure 2-35: The shortest solution for the pedestrian pathway via using optimisation method (Galapagos) in Grasshopper [188]

2.6.2 In architecture

Parametric design can generate creative shapes, deal with sophisticated relations and control them parametrically, and it utilises parameters to set relations between design elements in order to define a range of formal alternatives. Moreover, the parametric design provides a comprehensive exploration of multiple solutions to general design issues using algorithmic methods. Therefore, the parametric design provides vast opportunities to utopian architects to generate creative solutions in the design process [190, 191], see Figure 2-36.

2.6.3 In decoration

Parametric design provides creative forms, iterative dynamic shapes which are inspired by nature, and depends on algorithmic connections. Moreover, it can create unlimited options of modular forms based on simple elements, via adding parametric modifiers, see Figure 2-37.

2.6.4 In fashion

Nowadays, parametric design is used in a wide range of design fields, because it provides new unpredictable ideas with future styles, as shown in Figure 2-38.

2.6.5 In acoustics

Parametric programs can be used in sonic studies to calculate bounces, cast multiple rays, calculate flow paths down a sloped surface like water runoff [192], see Figure 2-39.

2.6.6 In structure study

Parametric design can calculate algorithmic formulas and manipulate complex connections and create sophisticated relations with many kinds of materials, as shown in Figure 2-40. An example of a spiral building was investigated in previous research [193] to study the structural system design. Diagrid system was chosen for this building according to the advantages of this shape [194]. The parametric method was applied to this building to specify deflections and material behaviour. This study was done by analysing the algorithm, which concluded that spiral columns are no longer needed, and beam profiles can be smaller than slandered ones, additionally, they can be replaced by spring beam system, see Figure 2-41.

2.6.7 In environmental study

Parametric programs can study and analyse all climatic and environmental changes such as sun movement, date, location, intensity, humidity, illumination, radiation, wind, heat gain, shadows, shades, and control them parametrically. Also, it can make simulation in the 4^{th} dimension using the time aspect which can influence on the building in real-time, and how the time can change the performance of the building parametrically. So we can anticipate and solve many design issues at the early stages of design [21, 195, 196], see Figure 2-42.

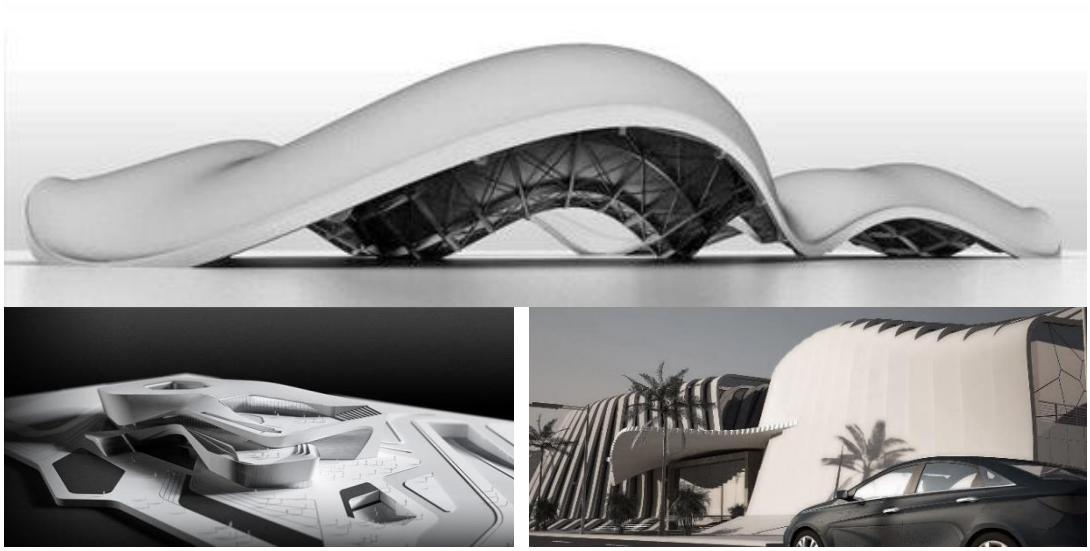


Figure 2-36: Architectural models created based on parametric design [197], (bottom right designed by Ahmad Eltaweel).



Figure 2-37: Fig. 1. Ideas of parametric design in decoration [198]



Figure 2-38: Ideas of parametric design in fashion, inspired by nature [199-201]

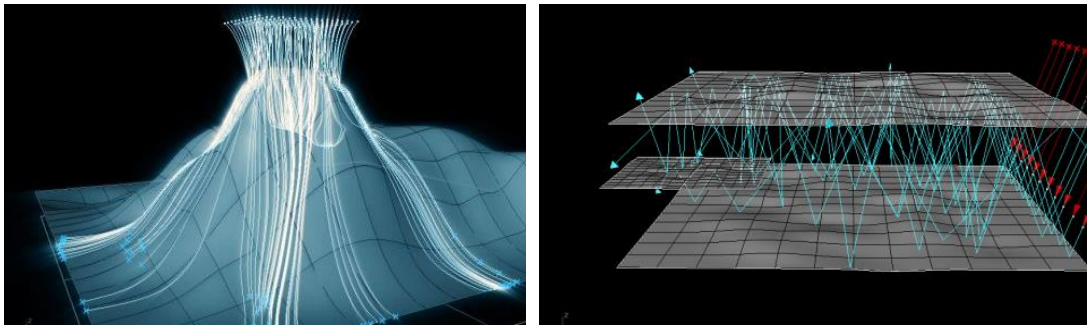


Figure 2-39: Reflected rays calculated in "Sonic", a plugin based on Grasshopper [192]



Figure 2-40: Structure study using algorithmic calculations in Grasshopper [202, 203]

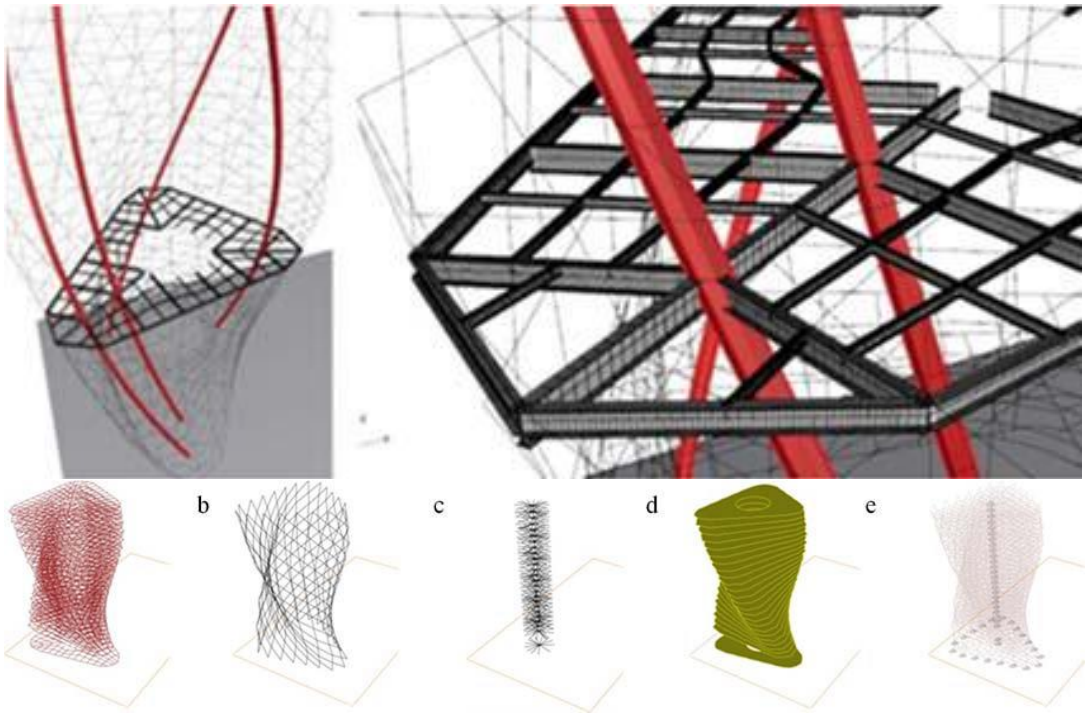


Figure 2-41: Structural design analysis [193]

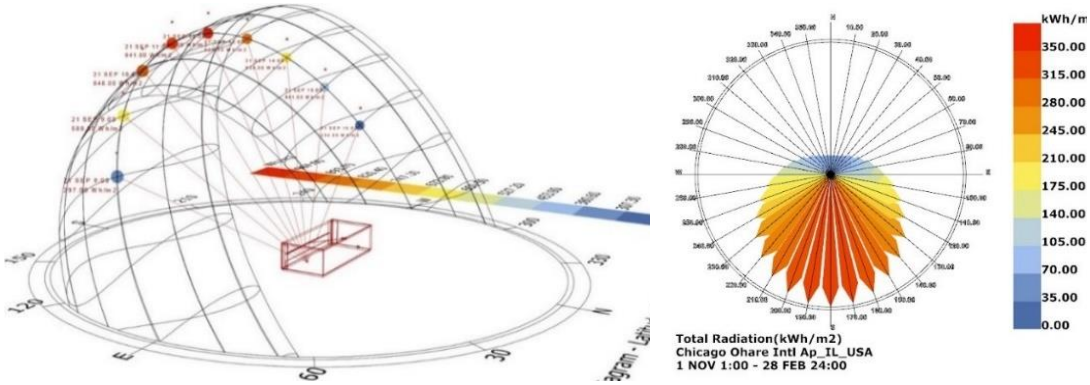


Figure 2-42: sun path and daylight analysis, Grasshopper.

2.7 Daylighting systems control via parametric design

Advanced daylighting systems can be exploited to engage with architecture to improve building environment and enhance buildings' energy performance [129]. Architecture has become more vivid as it has been redefined with different descriptive features such as smart [128], green, sustainable [112], passive [204, 205], active [136], dynamic [206] and adaptive buildings [21], while all these characters are directed to the same target; comfortable, healthy and economically-viable environment. In order to achieve an energy-efficient adaptive building, innovative daylighting systems along with parametric design based on Building Information Modelling (BIM) should be essential tools to control indoor performance with responding to outdoor conditions. The context of architectural practice, parametric design and innovative daylighting system can help to improve building performance for higher energy efficiency.

2.7.1 Louvres design

Louvres design were investigated in previous researches [195] using the parametric approach by exploring all possible screen configurations in daylighting [207]. The method was done by using a parallel computing algorithm that allows a better understanding of the effect of the louvres parameter and their interaction on daylighting performance. These parameters consist of louvres count, louvres depth ratio, tilt angel, window to wall ratio and reflectively, which were connected parametrically to give 1600 items, and they are divided to 200 groups as shown in Figure 2-43. The process was working in a parallel simulation by linking Grasshopper with Radiance through "Diva" plugin, which used to generate Radiance and EnergyPlus interface engines [208].

The study summarised that increasing the louvres count from 3 to 10 leads to a decrease of sDA (spatial Daylight Autonomy) from 40% to 30% respectively, at 30% Window Wall Ratio (WWR) with 1.5 depth ratio. However, the sDA decreased from 76-61% at 50% WWR with the same depth ratio. However, when increasing the depth ratio from 0.75 to 1.5 with 20% WWR, the sDA decreased by 40%, but this decline diminished as WWR increased till it disappeared at 60% WWR where sDA reached the highest value of 100%. In general, louvres count was found that they have no remarkable influence on the sDA with relevant to the louvre depth ratio, which relatively has more impact on the sDA. The utility of this study is that all parameters were explored in all screens; thus, the evaluation of the experiment was practical, and the classification for the parameters was accurate via identifying the optimum solution. However, the disadvantage of studying many parameters together did not achieve accurate results for the overall performance, so it would be better to study each parameter individually while fixing the others.

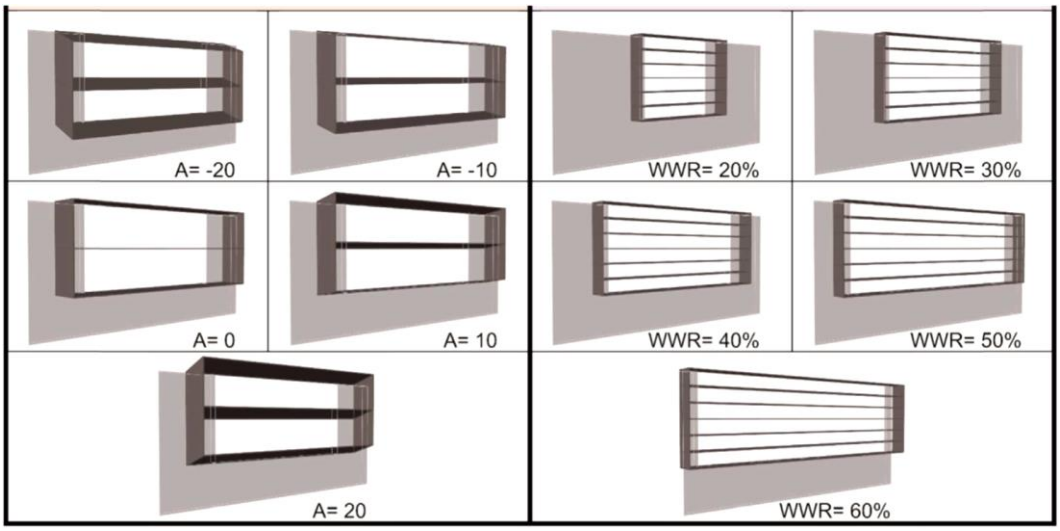


Figure 2-43: the louvre parameters. A= screen tilt angle, WWR= window to wall ratio [195]

El-Sheikh and Gerber [209] also instigated louvres through studying the design of intelligent building skin and its impact on daylighting

performance, using the parametric approach. The method of this study is done by using Grasshopper, Rhino, Diva and Galapagos as parametric tools to control and design exploration of semi-autonomous and fully autonomous configurations of an exterior building envelop louvre system. The system was created to respond to the daylighting conditions and occupants' performance. The study summarised that daylighting performance was improved in the interior spaces putting in consideration the occupants' preferences and building's requirements, and using the automation of independent tilt angles can improve the Building Intelligent Skin system to two times better than a conventional system, concerning daylight harvesting.

Sjarifudin and Justina [210] as well investigated automated louvres by using a new kind of design method called parametric camshaft. The method of this study is done by simulating a workspace in Jakarta with a variation of shading angles aiming to provide sufficient daylight inside the workspace. The study summarised that the occupants' visual comfort could be achieved by varying the shading opening angles between 15° and 75°. However, Jaepil, Taekyoung, Euisoon and Gensong [207] using parametric louvres in their study to optimise the thermal performance in the building, by analysing the best adjustment for the louvres. The study investigated the louvres' performance from three aspects; the distance from the glazing, the louvre's depth and the louvre's tilt angle. The simulation of this study was conducted using Rhinoceros, Grasshopper, Ecotect and Galapagos. A recent literature by Maria and Aris [12] investigated dynamic and automated shading systems, using sensor points and controlled algorithms which responding to the sun moment and weather conditions.

The review concluded that the most popular automated system and motorised Venetian blinds could achieve 20% and 50% in energy saving for cooling and lighting respectively, comparing to conventional louvres.

2.7.2 Skylight design

A study by Goncalo, Jose and Vitor [21] investigated responsive skylight system aims to create a skylight system that responds to environmental conditions and internal functional demands. The system uses three aspects; location, time and sky conditions. This paper studied the process to control daylight dynamically, using a Tetra-Script pavilion prototype, which targets to provide adequate illumination and low visual contrast. The experiment was conducted parametrically using an environmental software analysis to generate criteria to evaluate the results. The model was responding to the sun in a Heliotropic response, which is a natural phenomenon of some species of plants that follows the sun movement in order to receive more sunlight, such as the snow buttercup. The automation of this experiment was done parametrically using Grasshopper, and the configuration of the pavilion is determined by a small set of variables including basic room, tessellation and texture were the static adaptions, and the aperture degrees of the skylight panels adapted automatically [211], see Figure 2-44 and Figure 2-45.

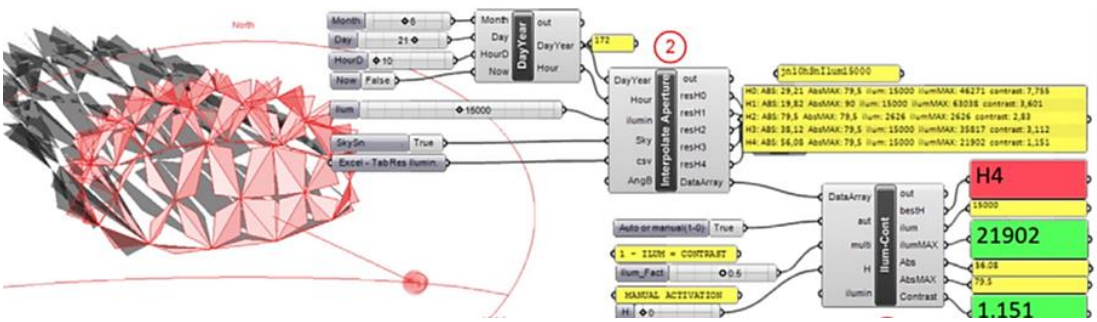


Figure 2-44: the controlling process using Grasshopper [21].

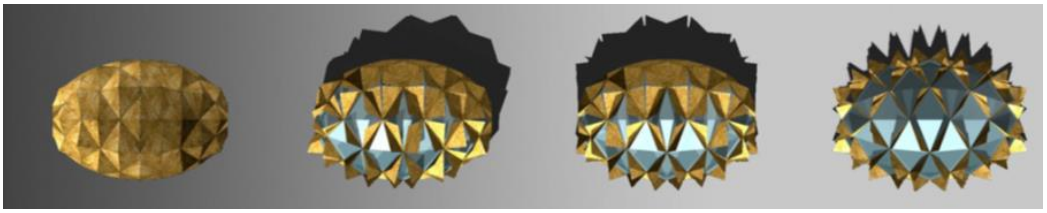


Figure 2-45: The Tetra-Script pavilion concept, controlled parametrically [21].

The calculated results by using the interpolation method revealed an approximate illuminance error between 4.3% and 7.3%, which considered low as an accuracy aspect. The parametric design system used for the generation of skylight configuration can be applied to any pavilion shapes, with other geometries, at any location. Configurations of daylight performance in real-time consider as an advantage of the responsive system [212]. The full results of the study were stored in a database, which contained daylight simulation, heuristics, apertures values, and the best-case worst-case situations. This database can be used to determine the aperture of the skylights that provide the required illuminance and resulting visual contrast value.

Further research made by Michela, Peter, Axel and Rudi [205] who also investigated the performance-oriented of a large roof structure for semi-outdoor space. The study aimed to enhance the environmental performance of the space in the early stages of the design process, in addition to studying passive solar strategies that reduce the need of imported energy via analysing the daylight and thermal comfort. The study used parametric geometry to generate design alternatives, and the exploration performance was studied using a parametric tool called "ParaGen" which is a plugin in Grasshopper capable of studying structural system and their form performance criteria using genetic algorithms [213], see Figure 2-46. The research summarised that in order to achieve passive

strategies for thermal comfort; the temperature should be decided by the physics of the form instead of building engineer, besides the location of its mass, size, the orientation of the openings, and shading in order to achieve zero-energy space [214].

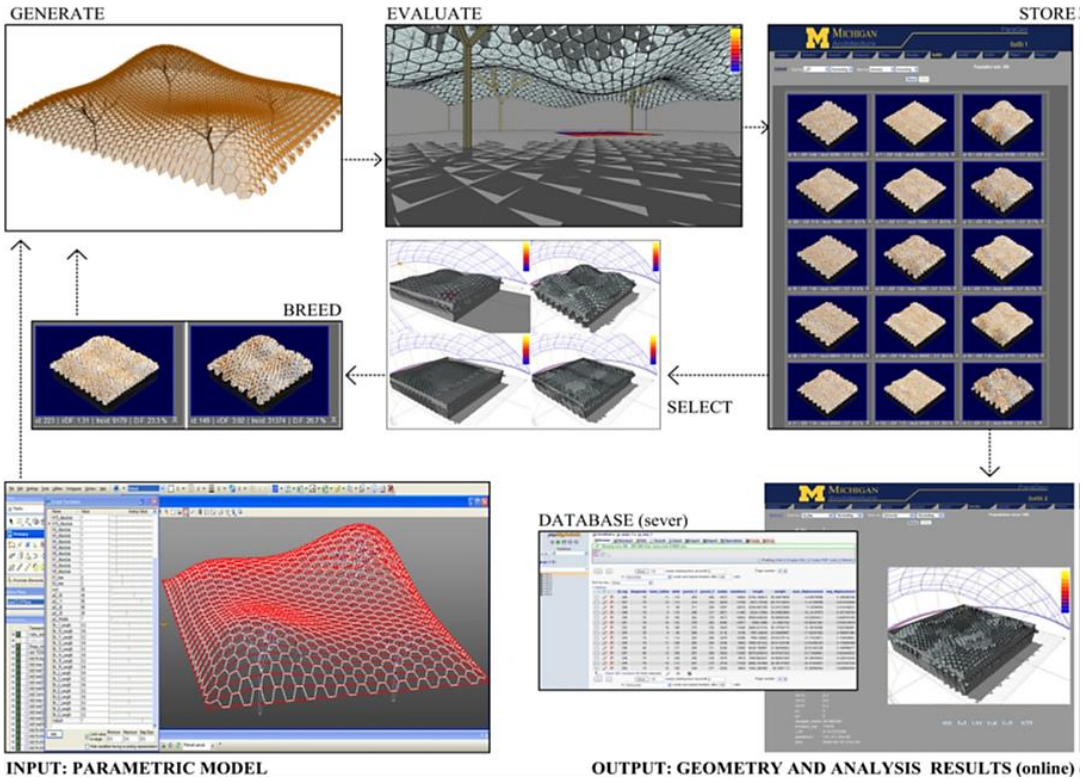


Figure 2-46: The ParaGen plugin cycle [205].

The study found that the lowest ratio between the yearly incident solar radiation and daylight factor was around 3.5 times smaller than the highest ratio. Accordingly, this parametric software was utilised to search for the optimum opening settings, and better energy-related aspect, which resulted in a successful potential based on the case study. The study summarised that parametric design approach could provide full control to deal with complex geometries, which offers clear visual interface as well as a wide variety of different scripts. Furthermore, increase the versatility of the design process, which gives further variations of the geometric models.

In the same issue, M. Turrin, E.Van, A.Kilian and S.Sariyildiz [215] investigated using parametric design to improve the performance of a large span roof in Bologna. The study aims to exploit the use of renewable resources in the site by reducing the summer overheating, enhance the daylight and provide proper ventilation to the project. The parametric design here was employed to manipulating with the structural morphology of the building by controlling the apertures based on a variety of size and distribution, in order to meet the requirements of passive building. The 3D geometry of the structural roof consists of ETFE pneumatic modules, which is controlled by a movable layer adjusted to three positions, where the closed position provides an opaque state, and open position can allow the light to penetrate between patterns [216, 217]. The study found that to achieve the best balance between a low solar factor and a high daylight transmission; the apertures opening angles should be between 60 and 70 degrees, which conducts approximately 30% of solar energy transmission (G-value) which was the best-measured value to improve thermal comfort in summer.

Patric, Paul, and Kera [218] suggested multiple designs of an atrium at the University of Massachusetts in Lowell in order to lit the building floors and bring daylight deep into buildings' spaces. They used the parametric approach in design processes such as Diva for Rhino and Grasshopper. The methodology of the study depends on using reflective systems to exploit the daylight and bring the light into the building's interior surfaces, by analysing many systems techniques used in different buildings as shown in Figure 2-47.

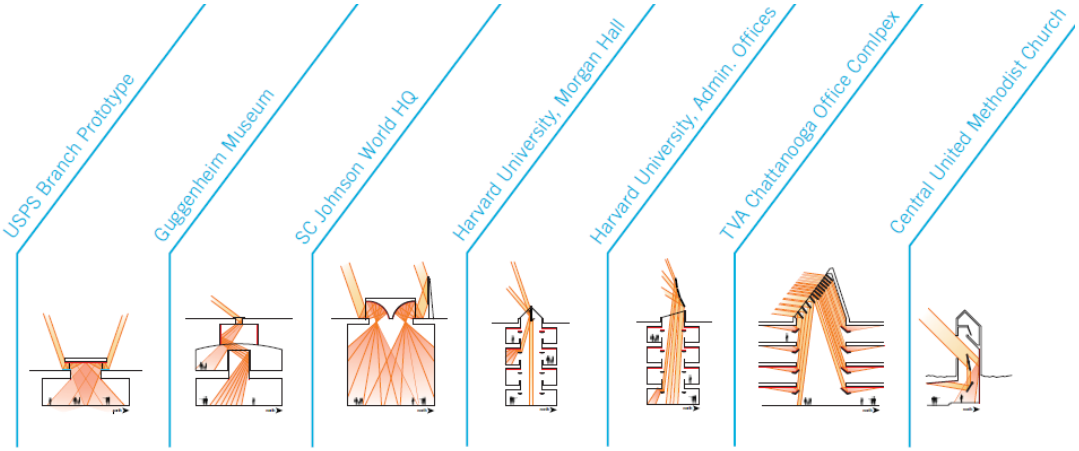


Figure 2-47: Different types of reflective system design [218].

The reflective systems used in this study is a paring of two main daylighting techniques; the first is a large north-facing window as a source of diffuse light, and the second is a south-facing mirrored reflector hung within inside the atrium skylight as shown in Figure 2-48.

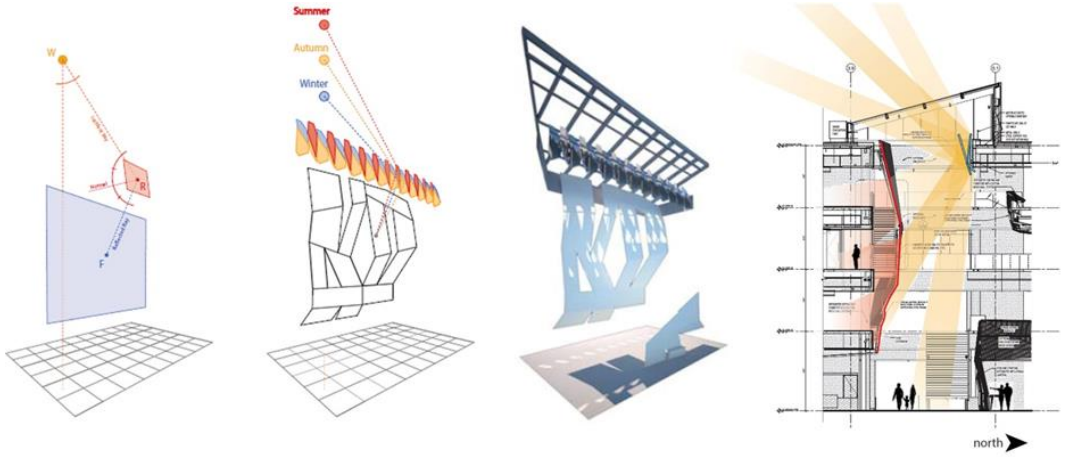


Figure 2-48: daylighting redirecting strategies at University Crossing [218].

Jong and Bharat [219] proposed an innovative technique to lit a gymnasium hall in Korea, which is parametrically bio-inspired by superposition compounds eyes of animals [220, 221] which can absorb a wide range of light better than human eyes. The system consists of reflecting superposition optics which can capture and distribute daylight inside the building dome structure, furthermore, it can respond to the sun movement. The proposed biomimetic model was designed parametrically via using Rhinoceros 3D and Grasshopper. The roof surface of the

gymnasium was subdivided to cuboid structure that was formed as a tapered rectangular prism. Each façade component inside the cube can adjust itself to respond to the sun movement, by shifting the bottom of the components to meet the functional requirements based on climatic state, see Figure 2-49.

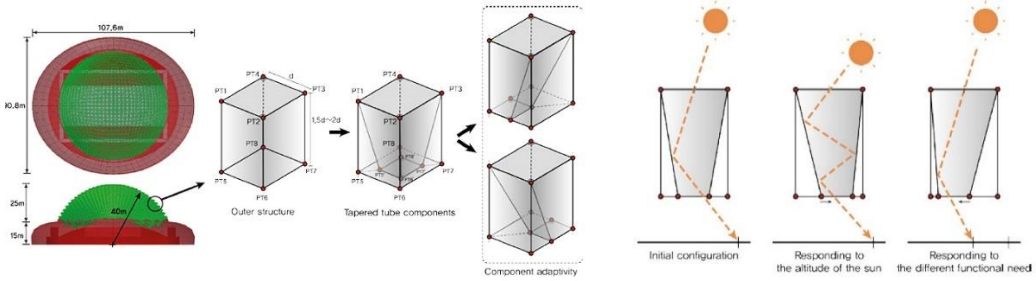


Figure 2-49: Configuration of adaptive façade components.

The Kinetic mechanism of such system can adapt itself corresponding to two different objectives; firstly, keeping the playing area illuminated responding to different sun positions, and secondly, changing illuminance conditions for the needed fictional purposes. The study summarised that parametric design tools provide broad design explorations, and opens more opportunities for innovative building systems to adapt on their own to environmental changes and to become more passively energy-efficient via exploiting natural resources. However, in order to perform correctly, the system still needs a high number of sensors to respond to the environmental changes, besides, the complexity of electromechanical and maintenance cost.

2.7.3 Mass and shadows study

William, Aswin and Heru [171] used a parametric approach in their study as a tool to solve problems during the design process regarding site planning and massing. The study was conducted on an office tower in Jakarta. The study aimed to evaluate the feasibility of using parametric

design method. Therefore, the method being employed in this study to solve each problem individually by creating a formula in Grasshopper containing all data with a specific parameter. The shadows were investigated in this study by analysing the neighbouring buildings that overshadow the site, which was utilised by the sun-path diagram to create a trace of building's shadow at specific hours, see Figure 2-50.

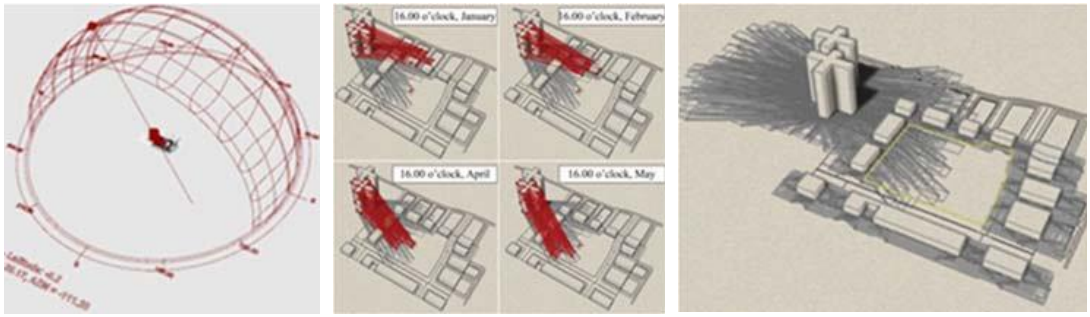


Figure 2-50: Overshadow of neighbouring buildings [171].

The overshadow study concluded that the western part of the site would be more comfortable in the afternoon as it is overshadowed by surrounding buildings after 3 pm, from February to October. Likewise, in Figure 2-51 searching for the most comfortable area along the year, while this overshadowed area will be allocated as public spaces for human activities. The utility of parametric design in this condition is the ease of controlling sun location, which can be iterated during daytime based on specific location imported from the weather file.

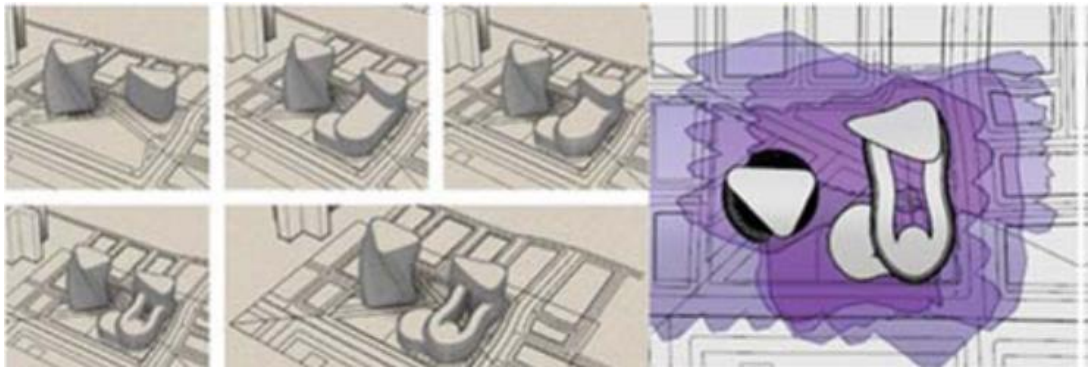


Figure 2-51: Analysis of overshadowing area [171].

The mass is another aspect, was investigated in this study to obtain the optimum solution by reducing the heat gain, where, the mass is considered as the landmark for this site. The parametric approach was utilised in this building to decrease the solar heat gain by determining the rotation degree of the building, which influences on the aesthetic, structural forms, and the tilted wall which can influence on the interior spaces, see Figure 2-52. The simulation concluded that; the influence of rotation the building 90° would decrease the heat gain to 1.32126 Wh/m^2 which was the lowest value of heat gain. The study summarised that parametric design is more practical than traditional methods in terms of real-time coordination and accuracy.

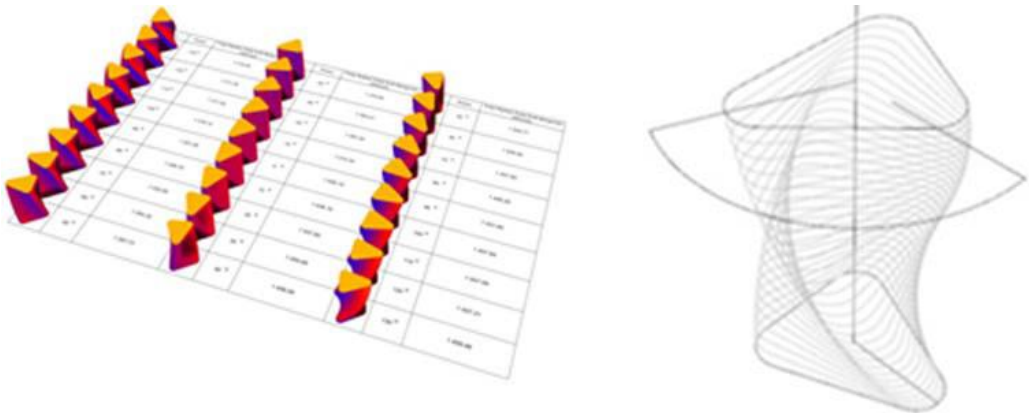


Figure 2-52: Building a mass study with solar radiation [171].

According to the morphological concept, Vasiliki and Odysseas [222] proposed a parametric residential building in Cyprus that designed based on the climatic and functional issue. The design method of the building depends on solar radiation and daylight in this location, and how parametric design could help to perform this design and provide many design alternatives as a bioclimatic system [223]. The study aims to provide sufficient daylight in all the building's spaces and exploiting the solar energy for the heating aspect. These climatic parameters will be connected parametrically, in order to manipulate with the orientation of

the unit to meet the environmental requirements. The model was conducted using Grasshopper as a parametric software, and the daylight analysis was done using Geco as an engine to Ecotect software which is used as an environmental software. The study proposed four solutions for the residential building, which can cover all possible bioclimatic requirements, considering the structure system, orientation and atheistic aspect, see Figure 2-53.

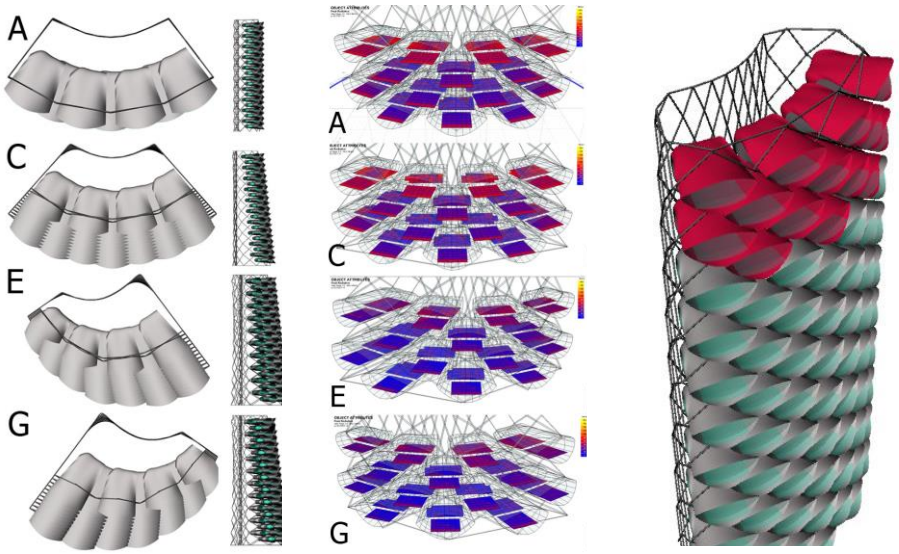


Figure 2-53: The four solutions for the system's geometry and the environmental analysis for each solution [222].

The study found that lighting and solar energy can be reduced to desirable results by adding extra canopy started with 3 m and ended with 1.5 m from east to west respectively. Moreover, the study recommended adding some bioclimatic elements, including passive heating and cooling systems. The study concluded that the performance of daylight and ventilation levels could be improved by using parametric design approach, via changing the morphology parameters through bioclimatic analysis. Comparing to other buildings in the same area, the use of bioclimatic principals can enhance the quality of people's lives, regarding morphological and functional aspects.

2.7.4 Fenestration design

El Daly [112] investigated fenestration allocation design to optimise daylight inside a multipurpose building in Cairo. He claims that conventional windows are now debatable issue concerning environmental rating system (LEED) [224]. He integrated parametric design as a heuristic algorithm with the LEED rating system to achieve the required daylight amounts with a minimum amount of solar radiation inside the building. The design aimed to find suitable allocations for windows to comply with LEED requirements. The reason for using the heuristic algorithm in this study is to solve the problems in limited steps, and find the optimum solution among all possible parameters.

The model was built in Grasshopper with the aid of Geco plugin, in order to generate Ecotect to calculate the daylight analysis. Then the optimisation of the data done with a genetic algorithm tool called "Galapagos", which considered the as an optimisation tool used in such parametric design, see Figure 2-54.

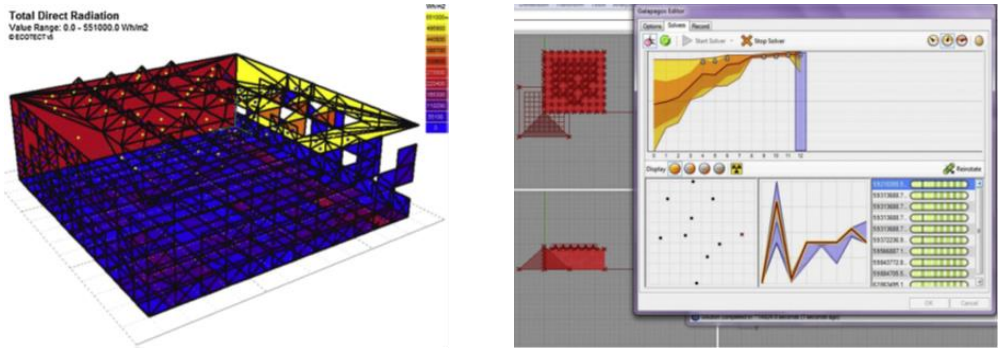


Figure 2-54: Grid analysis by Ecotect (left), Galapagos interface (right) [112]

The optimisation method in this study contributed to decreasing total solar radiation loads to 26%, which was lower than the total loads calculated in the initial parameters. Accordingly, the study summarised that optimisation by using a parametric design based on LEED

requirements could be achieved by using three main steps. Firstly, design the LEED requirements parametrically. Secondly, the automatic selection of solutions through the integration between the simulation program and the heuristic algorithm, and the last one is choosing the optimum solution for the façade design. Burak and Sofia [225] investigated using generative algorithms as well to explore design alternative for the fenestration system of a building in a hot climate territory in Cyprus. The study aimed to customise shading devices for the building, which can optimise daylight, and reduce solar heat gain. The method of this study was conducted by using Diva, Grasshopper and Galapagos. The ambient bounces settings in the study were kept at 2 in Radiance parameters to speed up the simulation process; however, this influence on the accuracy level of the values of the Daylight Factor (DF). The study concluded that average DF was increased by 25% - 67% in all alternatives. Accordingly, integrated parametric design software can improve the performance of the buildings, moreover, provide several alternatives for the design in the early stages.

Pil and Steffen [226] investigated the parametric method in Grasshopper to generate different fenestration systems for a room that fulfils performance criteria regarding indoor climate, daylight and energy saving, see Figure 2-55. The method includes a new plugin in Grasshopper called ICE bear which can simulate annual indoor climate, daylight and energy performance of complex geometries based on hourly weather data. This tool is used simultaneously with Galapagos optimisation algorithm in order to generate design solutions based on the designer conceptual idea. This method aims to reach maximum energy used for the building operation (25 kWh/m^2/year) while fulfilling thermal class II without having

more than 100 h above 26 C°, and minimum Daylight Autonomy (DA) of 60% in a point in the middle of the room. The study concluded that the method could generate an almost optimum solution based on designer concepts, which can achieve indoor environmental requirements.

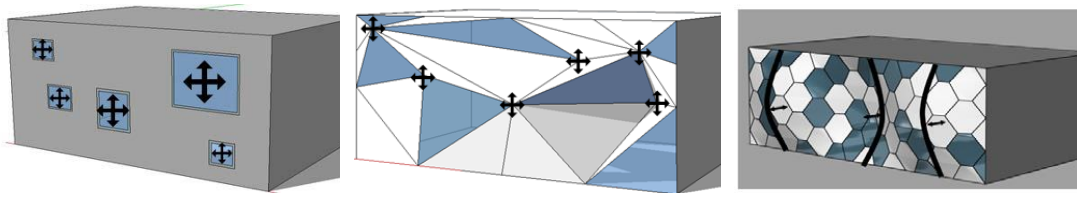


Figure 2-55: Examples of parametric models concepts and variables [226].

2.7.5 Windows design

Ma and Hiroatsu [227] used parametric design in their study to optimise daylight and heat gain inside an office building in Beijing. The study method depends on finding the best size window area on each wall to minimise energy consumption and maximise the useful daylight illuminance. The experiment was done by creating the model in Grasshopper based on Rhinoceros, and the climatic simulation was done using Ladybug and Honeybee as engines to EnergyPlus, Radiance and DAYSIM, in order to study the environmental state parametrically. Additionally, the study used Galapagos plugin to achieve the role of optimisation, which provides a generic platform for the application of evolutionary algorithms to be used in a wide variety of problems by non-programmers. Moreover, Galapagos, as mentioned previously, can provide simple operation, fast speed of calculation results and produces a range of optimised solutions.

The study found that the south-oriented window is the best orientation, followed by north according to this selected territory, which aims to minimise the annual total thermal energy. Whereas, heating energy in this location is needed more than cooling energy. Furthermore, the study concluded that vertical window with height 3.063 m and width 1.959 m is

the optimum solution in 63% of the time for daylight illuminance level greeter than 300 lx, comparing to square and horizontal window with the same area. Generally, the study summarised that parametric design could optimise the selection of window design strategy concerning illuminance level and energy analysis, to minimise the annual total thermal energy and obtain the best orientation. Also, it can improve the design quality in an early stage and provide solution strategy for building design.

2.7.6 Façade design

In Abu Dhabi, Aedas [228] developed "Al-Bahr Tawers" the tow 25 story office towers which were parametrically designed and inspired from an Islamic architectural element called "Mashrabiya", via using the tessellation of the hexagonal shape to create a mosaic scene in the façade, see Figure 2-56. The façade consists of 1000 panels of connected triangular screens arranged in a series of scalable hexagonal shape, which is folding up to protect the façade from direct solar radiation.

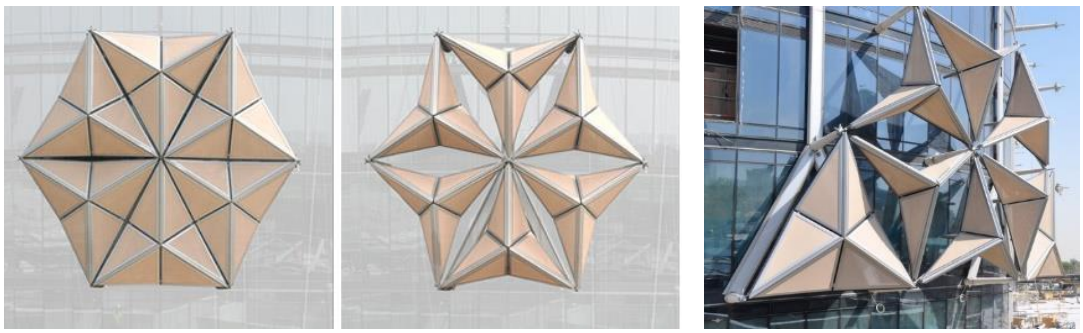


Figure 2-56: Transformation of the hexagonal shape in the façade [228].

The hexagonal shape is responding automatically to the sun movement in an adaptive fitting system [229], to achieve better daylight performance and energy saving. The design succeeded to reduce heat gain and glare by 50%, meanwhile, giving the Islamic atheistic shape. Moreover, parametric façade together with solar thermal panels for hot-water heating and

photovoltaic panels on the roof, minimise the need of electrical lighting and cooling energy and reduce the total CO_2 emissions by over 1750 t per year.

Narangerel and Lee [230] investigated in the same area using south-oriented 3D façade patterns to enhance daylight performance and reduce electricity consumption in Korea without any urban context. The design process was done by using Ladybug and Honeybee, see Figure 2-57.

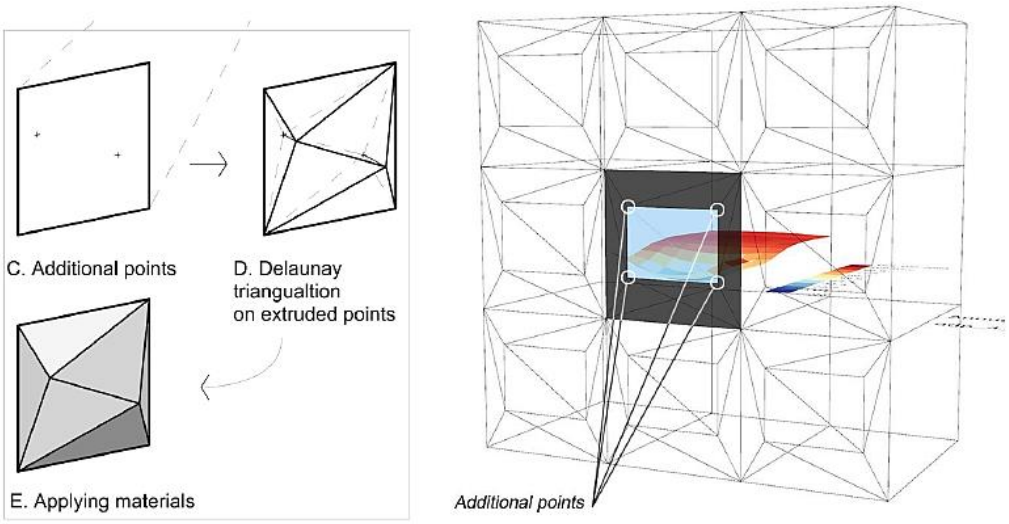


Figure 2-57: Façade geometry generation [230].

The model was created by increasing the points on the rectangular building façade units and connect them with the vertices' corner of the façade apertures. The method of this study suggested the optimal extrusion lengths at the given points and the combination of materials of the surfaces which were generated from the Delaunay triangulation through multi-objective optimisation [213]. The suggested method in this research showed high flexibility and compatibility of generating any façade design using the proposed technique. The authors claimed that the method could be used effectively to create several design alternatives of an office building and to assess the daylighting performance according to a given location. The study summarised that façade model could save energy and enhance daylighting performances.

In similar research, Elliot and Christoph [231] used parametric design and energy simulation tools to determine the influence of daylight on façade's shading designs and the expected energy used in the building, cost optimisation for the building and the amount of carbon emitted from the building. The study conducted by using Grasshopper for simulation modelling, EnergyPlus Based on Diva for the environmental studies, and Galapagos for design optimisation. The study summarised that the designer should put into consideration the climatic changes and how to deal with the physical parameters of a static building to match the environmental changes over time. Accordingly, parametric design can anticipate varieties of scenarios for the building to get the optimised performance.

Mohmoud and Elghazi [232] investigated in kinetic facades [206, 233] using parametric design to optimise the daylight in a south-oriented façade in Cairo. The façade consists of a movable hexagonal pattern which is controlled using Grasshopper in order to study the daylight distribution inside the building, aiming to achieve the requirements of LEED v4. The study showed an improvement in daylight between 20-50% through the four seasons, comparing to traditional facades. The method of this study was based on the kinetic system, via controlling the rotation of hexagonal components in the façade, as shown in Figure 2-58.

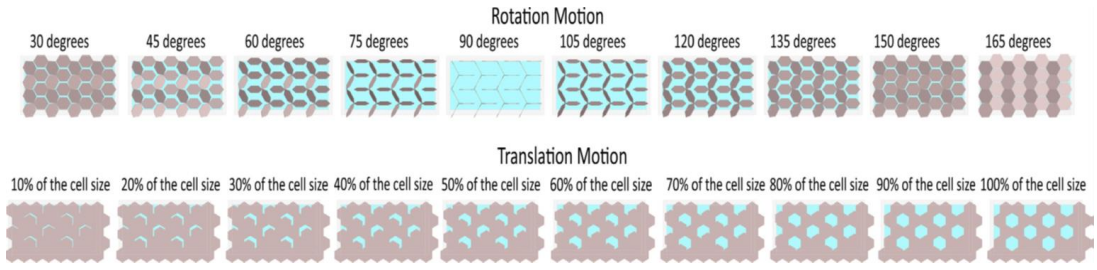


Figure 2-58: Patterns of the rotation motion for the kinetic façade [232].

2.7.7 Prototypes design

Elghazi, Wagdy, Mohmed and Hassan investigated daylight optimisation by [234] using Kaleidocycle design technique in a residential façade in Cairo based on Origami, in order to enhance the daylighting in a living room and achieving the requirements of LEED V4 [235]. The methodology of this research was focusing on using the parametric of Kaleidocycle logic, which was conducted by applying parametric design based on Rhinoceros, Grasshopper and Diva as an engine to Radiance and DAYSIM [236].



Figure 2-59: Origami forms based on geometrical rules [234].

It can be observed in Figure 2-59 that the origami is a folding paper techniques, which offers a finite set of paper shapes based on sequence and relationships between surface and points, which can be defined by rules, moreover, it is a type of manual algorithm that can be translated into parametric shapes [237].

The study investigated the concept of Kaleidocycle skin by using the Origami technique. Kaleidocycle is defined as rotating rings of tetrahedrons which usually used with the mathematical exercises. Each tetrahedron in the cycle is linked to its predecessor and successor at opposite edges, where the movement technique treats each tetrahedron as an independent element [238]. The process of this research was done using a genetic algorithm, by using "Galapagos" component in order to optimise the results. The results showed that Kaleidocycle rings with 30 cm size and 64°

rotation angle achieved 100% of daylight distribution which exceeded LEED V4 requirements (75%) and accepted Daylight Availability standard. The research summarised that LEED V4 requirements could be achieved via using parametric techniques; besides, the integration of daylight simulation tools and genetic algorithm contributes to achieving better daylight performance.

Another research in the same area investigated in using origami concept with parametric design, done by Avergauw, Lalegria, Kroovers and Niels [239]. The study concentrated on using an adaptive shading system which can respond to the environmental circumstances. This system is based on a curved-line folding technique which depends on kinematic behaviour. This technique provides vast opportunity to generate flexible shapes, which can be conducted by pushing specific endpoints in the geometrical shape using the small curved lines which can be easily squeezed, see Figure 2-60.

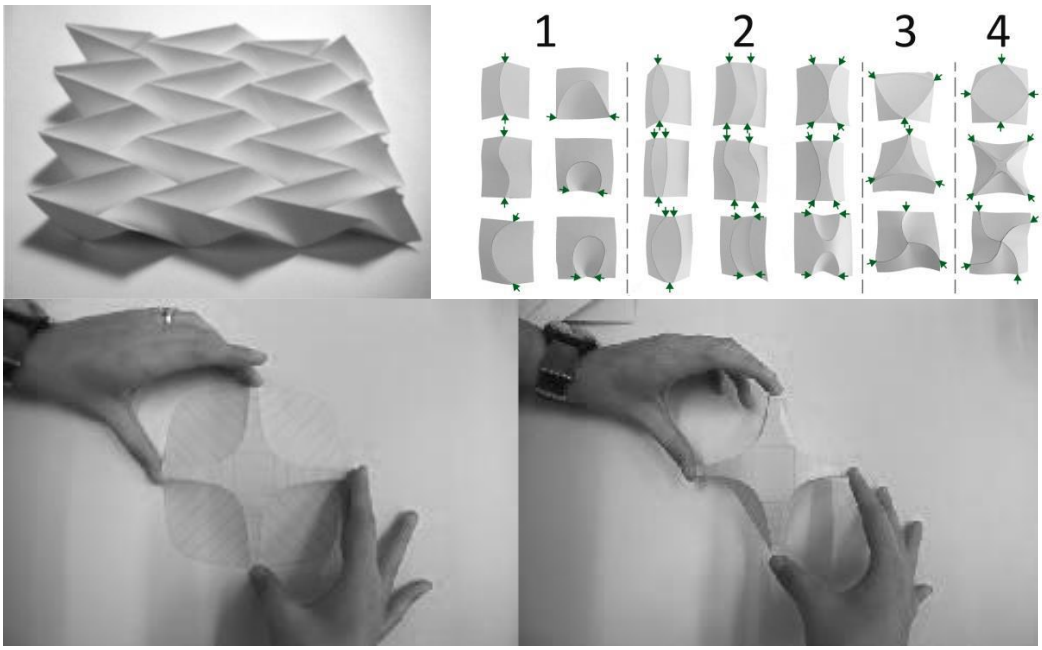


Figure 2-60: The kinematic behaviour using the curved line adaptive [239].

The significant character of this system that it can give higher displacement in its formation with low forces added to its vertices [240].

The model morphology was created and controlled parametrically using Grasshopper. The study aims to save energy consumption and enhance indoor comfort by using the concept of kinematic behaviour based on parametric design. The study resulted that using adaptive shading parametrically can improve daylight exploitation and energy saving.

Gomaa and Jabi [241] investigated in intricate facades using parametric tools (Autodesk Revit and 3D Max) in order to evaluate and compare the performance of daylighting analysis by using these two software. The experiment was done by making three types of the model; using Revit, 3D Max and a physical scaled model. The physical scaled model was conducted by 3D printing and laser cutting processes, which was used as a reference case for comparison purposes. The initial test performed in a simple unglazed opening room. The next set of tests used three types of parametric pattern to form the façade geometries, as shown in Figure 2-61, which approximate some of the commonly used shapes in new building envelopes.

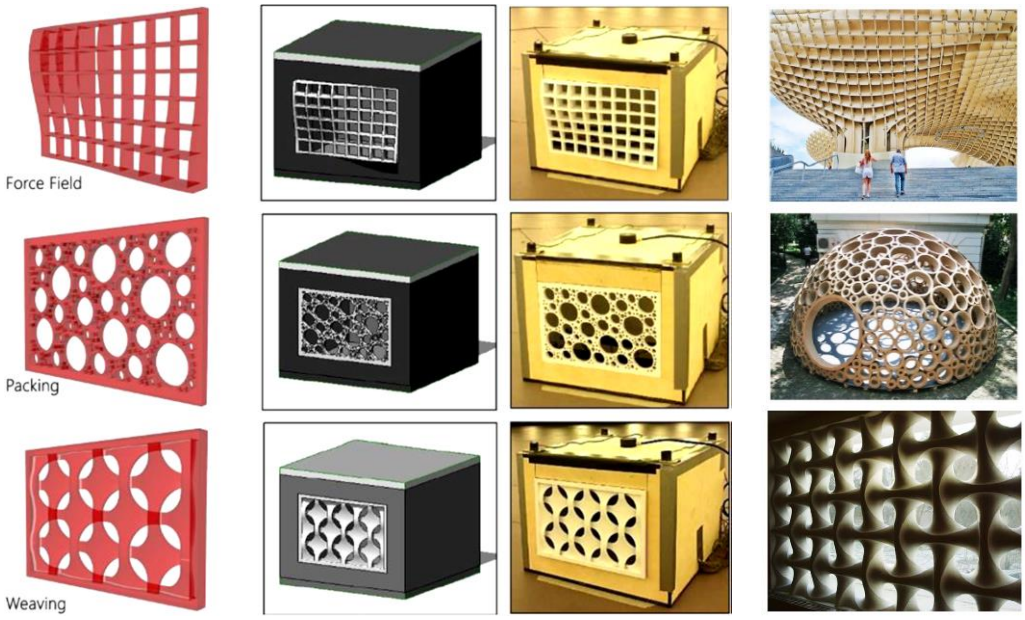


Figure 2-61: The three chosen patterns in three modelling types [241].

The daylighting analysis was performed using the available tools in each software. The assessment of results depends mainly on evaluating the differences in illuminance values which reported from each software and then comparing them to the values of the physical model. The study summarised that Rivet is better in using fast and straightforward geometries with daylight analysis when high levels of accuracy are not needed, however, in contrast with 3D Max, which considered to perform better with sophisticated geometries. Additionally, the rapid progress of parametric modelling which integrated with fabrication technologies has made the daylighting analysis of complex geometries less reasonable, comparing to the real model. Therefore, the existing daylight simulation tools need validations and crucial upgrades in order to control the gap between predictions and physical reality.

2.7.8 Photovoltaics design

Hend, Ayman, Paolo, Robert and John [242] investigated in the integration between photovoltaics technology and buildings' structure, while they are recommended renewable energy source. The main aim of this study was using parametric design with photovoltaics membrane structure, in order to solve complex relations within the membrane formation. For instance, the membrane's geometry, layout orientation, shadowing, analyse the daylight pattern on the membrane surface, calculate the stress distribution in different weather conditions and the maximum deflection allowed for the membrane surface under different loading conditions. The study argued that these former aspects could be integrated parametrically, via using Grasshopper, while this parametric approach could provide multiple facilities in a real-time process for these

complex aspects. The study summarised that parametric method could optimise many environmental aspects such as maximum daylighting absorption and energy saving. However, the study required more research to analyse more geometrical solutions with different structural parameters.

2.8 Summary

This literature review reveals the influence of parametric design on daylighting performance and energy saving, especially for complex projects and innovative concepts, while it can provide quick iteration, real-time results, data analysis, time-saving, integrated relations and the optimisation characteristic. Table 2-1 summarises daylighting performance and energy saving in some previous studies via using parametric design.

Table 2-1: Daylight performance and energy saved within parametric design

Reference	Type of Daylighting Design	DF Improvement	sDA Improvement	Reduce Solar Heat Gain	Energy Saving
[195]	Louvres design		100%		
[12]	Automated shading system				50%
[205]	Skylight design				35%
[215]	Skylight design			30%	
[112]	Fenestration design				26%
[225]	Fenestration system	67%			
[226]	Fenestration system		60%		
[234]	Façade design	100%			
[228]	Façade design			50%	

Chapter 2 has presented a literature review about light, daylighting and their metrics. Then the literature went through parametric design from its origin, principle, implementation and applications, and precisely the relation between parametric design and daylighting research. The parametric design has been getting popular in recent years to address the design complexity of modern buildings, by applying advanced modelling

tool to refine the design parameters simultaneously. The parametric design has been used widely in the areas of architecture, structural design, urban planning, fashion design, etcetera, while its applications for daylighting research are still growing.

The most common software used for this aspect is Grasshopper based on Rhinoceros 3D as a parametric modelling approach. Grasshopper is developed to connect multiple plugins in one canvas in order to facilitate the relationship between different disciplines in the same simulation approach. For daylighting simulation; Diva, Ladybug and Honeybee are used as plugins to generate comprehensive simulation daylight analysis. These plugins are connected to Grasshopper and used as an engine to Ecotect, EnergyPlus, OpenStudio, Radiance and DAYSIM, in addition to defining a specific territory by using EPW weather file. The genetic algorithmic plugin "Galapagos" is used as an optimisation tool to find the best solution. The advantage character of this parametric software revealed in the capability to control and amend all the design elements individually or integrated, and any modification or alteration in the ambient will influence on the whole model simultaneously. Therefore, the parametric approach as a design tool can improve the performance of daylighting and energy saving in the early stage of design.

Chapter 3 Parametric Control of a Rotating Louvre Consisting of Parametrically-angled Mirrored Slats, Methodological study

3.1 Introduction

Daylighting plays an essential role in designing energy-efficient buildings in terms of saving energy and visual comfort for the occupants [243] and increasing their productivity [244]. Additionally, the more uniform daylight and good distribution could save much more energy than the sharply changed daylight distribution [245]. Nevertheless, heat gain from the windows contributes significantly to increase cooling loads, and large windows could produce glare problems, especially in south-facing facades [246, 247].

Buildings' design may face several illumination issues such as orientation, size, room depth, surrounding obstacles, and many other factors which limit to receive sufficient daylight. To overcome those issues, some daylighting systems have been practiced to improve daylighting performance inside buildings; such as light shelves [248], Venetian blinds [12], louvres [12, 137, 249], optical louvre system (OLS) [137], roller shutters [250], electrochromic glazing [3, 251, 252], thermotropic windows [253], translucent insulating panels [251], laser-cut panels [254] prismatic glazing [255], photo-bioreactors, , light pipes [144], fibre optics [148], CPCs [256], light wells, and other fenestration systems [3, 112, 257]. According to statistical studies [42, 57, 249, 258, 259], such daylighting systems can save electric lighting by 20-40% from total energy.

Many researchers investigated the utilisation of Venetian blinds and optical louvre system (OLS) to reflect incident sunlight into buildings [50], which produced significant results. However, these results were limited at specific times due to their static state in relation with sun movement, which influences on the uniformity and steadiness of the reflected light, and therefore, reduces the occupants' visual comfort [137]. They may also have some drawbacks such as limited times of the provided daylight, risk of glare or excessive light, which probably lead to visual discomfort for occupants and use of artificial light instead.

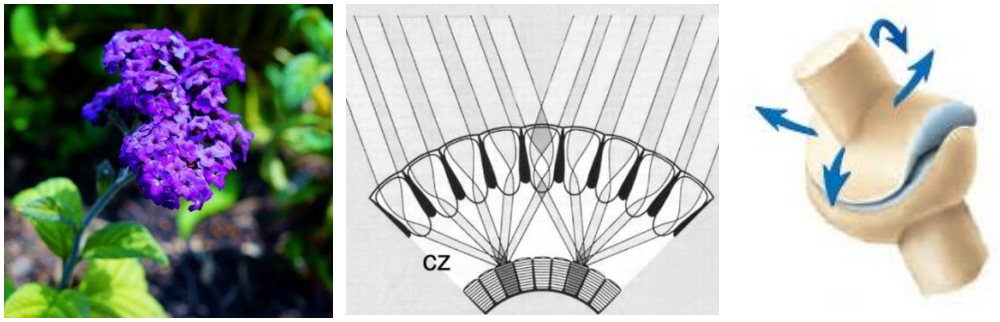
However, when using responsive tools such as automated louvre, daylight harvesting can be dramatically improved, due to its real-time response to the sun movement [129], which can keep the reflected light not just uniform but also relatively steady during the daytime, which accordingly can improve visual comfort and increase the energy saving [212]. This characteristic will be discussed in details in this chapter.

A case study of the proposed method will be conducted for an office building model in New Cairo in Egypt. According to previous researches [12, 71], highly glazed facades and open floor offices spaces required the use of dynamic solar shading controlled with a cut-off strategy to minimise the risk of overheating and optimise the use of daylight. Consequently, this chapter will investigate controlling the slats' rotation automatically using parametric design [205].

3.2 Methodology description of the parametric daylighting louvre

The parametric daylighting louvre system is inspired by three different organisms. The "Heliotrope plant" which can ultimately respond to the sun

movement [211], and is used in our study as a response method. The "Superposition compounds eyes" is a visual behaviour in the bees which can redirect the collected light to a specific point in their retina [260], which used in our study as a reflection method. The "Saddle joint" is a type of connection in the human bones [261], which used in our study as a movement mechanism, see *Figure 3-1*. Practically, the study uses an integrated daylighting louvre system which can respond automatically to the sun movement. The integrated system consists of four main parts; *rotating louvre, electrochromic window, thermochromic window and chamfered ceiling*. The whole system is connected and controlled parametrically using Grasshopper.



(a) (b) (c)

Figure 3-1: Heliotrope plant (a), Superposition compounds eye (b) and Saddle joint (c)

3.2.1 Parametric daylighting louvre software control

The daylighting louvre system is controlled using Grasshopper software. Grasshopper is a plugin for Rhinoceros 3D software, used to generate 3D parametric models [186, 262]. Grasshopper is a flexible algorithmic software used as a scripting language to deal with different parameters via specific formulas in order to define the model. These formulae appear as canvas connections which can be amended and controlled parametrically in a separate graphical interface [263]. Grasshopper software can help designers to quickly generate complex parametric forms with no formal

scripting background [98]. It can provide full control and accurate manipulation of the model's elements by defining form-generation components, which can be optimised through the use of sliders and mathematical expressions, or even with simple scripting. Grasshopper and Rhinoceros 3D have separate interfaces, where the formula is created in Grasshopper screen, and the model is revealed in Rhinoceros viewport screen as shown in *Figure 3-2*.

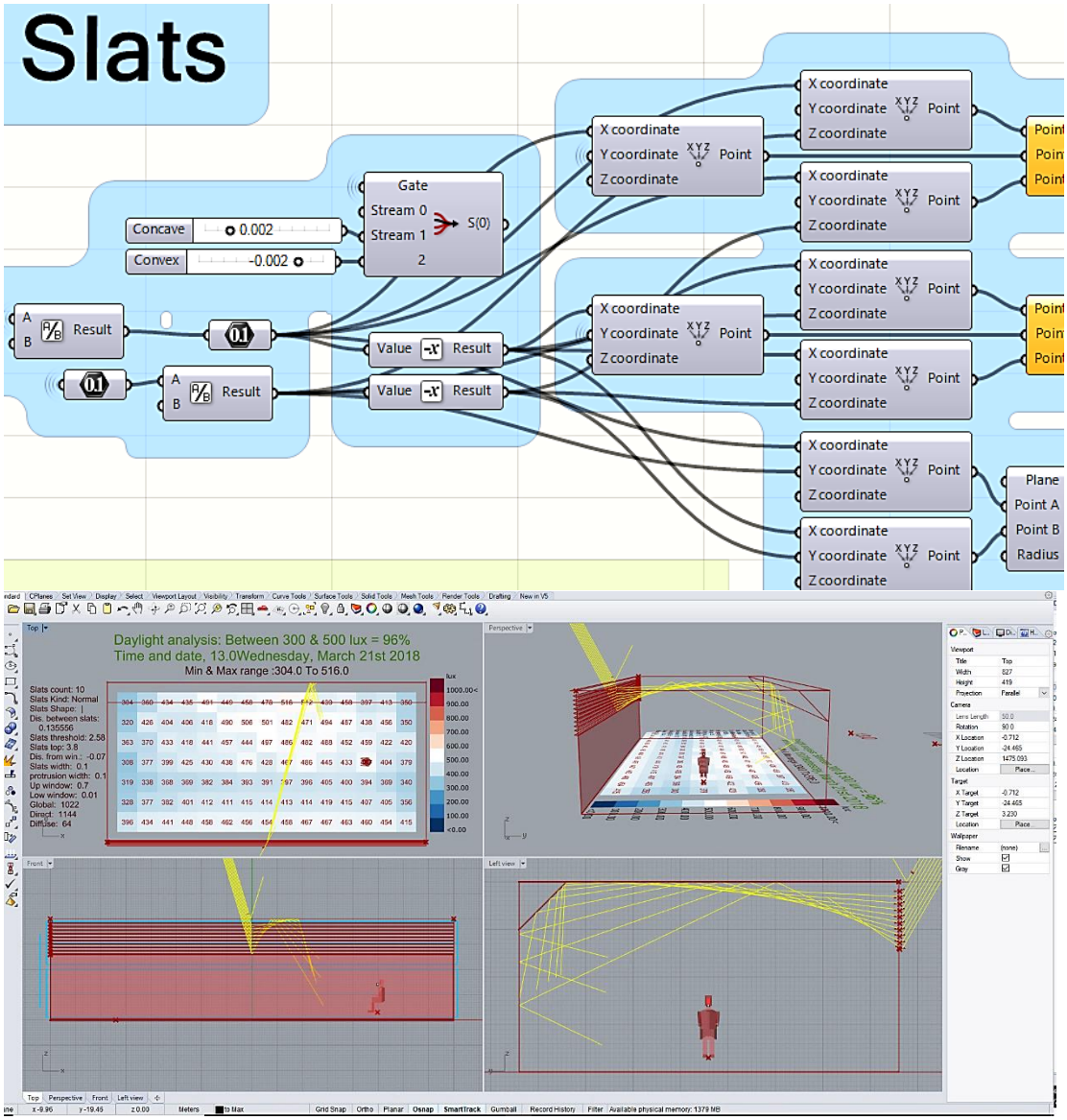


Figure 3-2: Grasshopper interface showing the canvas of sliders and connections (Top). Rhinoceros 3D interface showing the model viewport (Bottom).

Grasshopper has the flexibility to connect multiple plugins in one canvas based on the project needs. In our study "Honeybee" and "Ladybug" are

used as an environmental software plugins [264]. Honeybee plugin is used to generate "Radiance" software as a lighting simulation analysis tool which developed by Ward [265], it is based on backward ray-tracing algorithm used for daylighting calculations [208] see Figure 3-3. Meanwhile, Ladybug plugin is used as an engine to generate DAYSIM to get the weather data, sun-path, time and date related to a specific location, via using EPW weather file which can be downloaded online for any specific location around the world (https://energyplus.net/weather).

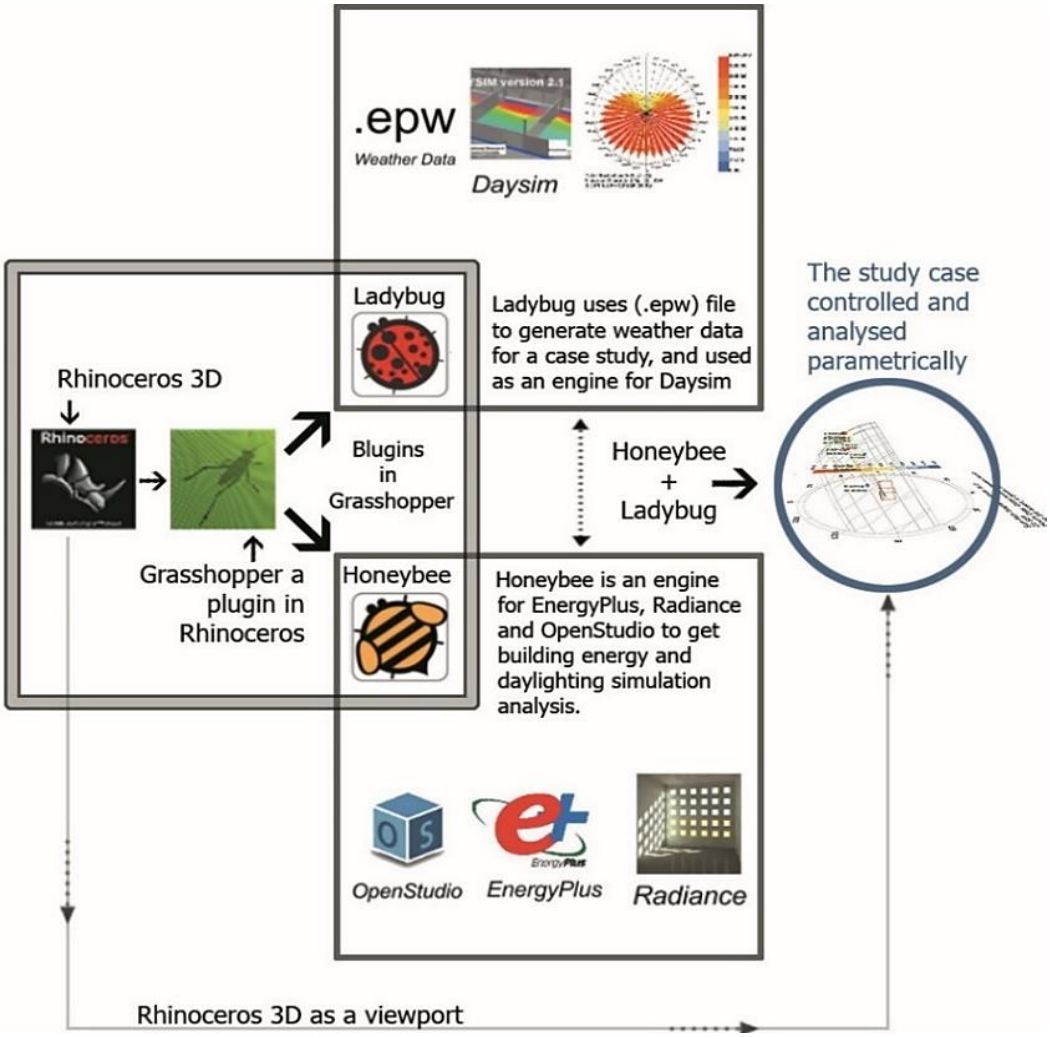


Figure 3-3: links between Rhinoceros, Grasshopper, Honeybee and Ladybug to generate an environmentally conscious model [262-264].

This thesis proposes a formula created in Grasshopper software to control the slats' rotation, where these slats act like a snow buttercup

flower following the sun direction to receive more light, a process known as *Heliotropic* response [21]. The Grasshopper formula for the proposed parametric louver is attached in the Appendix C.

For a daylight simulation and analysis calculation, test points are used inside the examined area at the desk level 0.75 m to calculate the illuminance level, see Figure 3-4. The results of the test points represent the illuminance value of each single point, where, the sum of all points are calculated to determine the percentage average for the whole area for the daylight illuminance within the range 300~500 lx. The illuminance range 300~500 lx in our study is used as a standard threshold level for visual comfort, based on the information in section 2.3.4. Figure 3-4 is a sample image for a daylight simulation analysis for an example office room, where the blue area represents a low illuminance level and the red area is a high illuminance level, while the light blue area represents the recommended illuminance level range which should be between 300 and 500 lx.

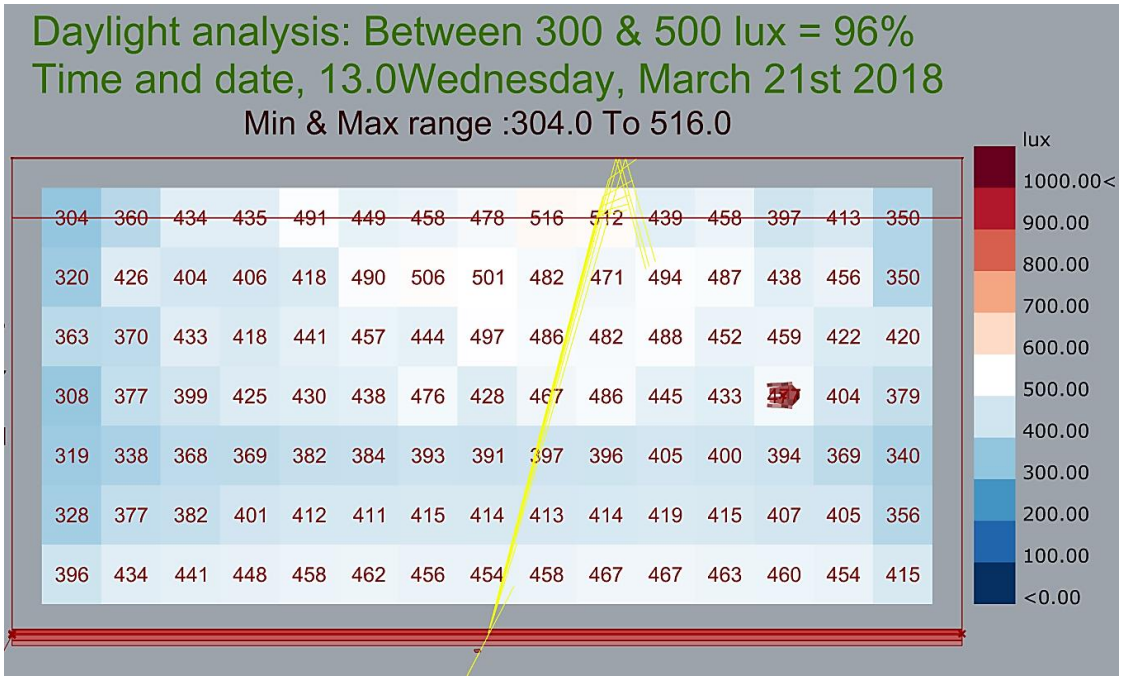


Figure 3-4: Sample daylight simulation analysis for an example office room

3.2.2 Parametric daylighting louvre main components:

1. Rotating louvre with parametrically-angled mirrored slats

The louvre system consists of aluminium slats with 90% reflectivity, the slats are parametrically-angled with individual rotation angle for each slat but can be rotated with the same angle, and their rotation pivots aligned with their sides. The slats' rotation reacts to the sun movements, where each slat has its unique angle in order to reflect the incident light to the specific target patches on the ceiling, and then the ceiling works as a source of light to illuminate the room as shown in Figure 3-5. These slats are controlled parametrically and modified accurately using Grasshopper. The louvre should be installed in a south-oriented façade at the upper part of the window and preferred to be used in the sunny territories.

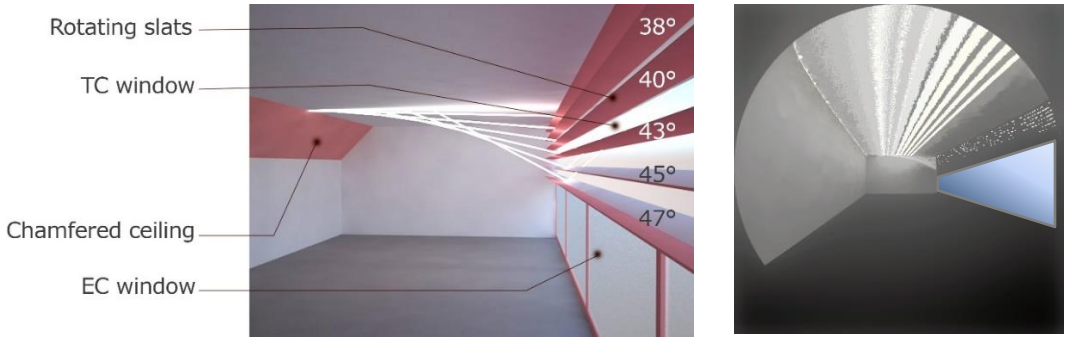


Figure 3-5: Real map perspective view from 3D Max showing the elements of the proposed daylighting louvre system (left), Fisheye map from Radiance showing the reflected light on the ceiling (right).

2. Electrochromic glazing

Electrochromic (EC) glazing is an advanced kind of glass capable of transferring from transparent to translucent phase [266] under the action of a voltage or current. This advanced material can disperse the incident sunlight to diffuse light. This kind of glazing used in our study as a source of diffuse light to the area near to the window, while, it is installed at the lower part of the window and can be controlled parametrically using Grasshopper based on solar intensity, see Figure 3-5. EC materials were

suggested for glazing applications in 1983 by Lampert [267], Svensson and Granqvist [268]. The technology of EC materials has been recently applied in extensive window glazing for visual comfort, pleasant indoor environment and energy saving. This type of glazing can save up to 45% of total energy when compared to single static glazing [33, 160].

3. Thermochromic glazing

Thermochromic (TC) materials originally based on colour-changed composites that sensitive to temperature. Thermochromism refers to dramatic phase change, which occurs when a material is melted [269]. Therefore, thermochromic glazing can change its colour, responding to solar intensity [270]. In our study, thermochromic glazing used to control the intensity level of the daylight coming from solar radiation and sky dome, while, it is installed at the upper part of the window, see Figure 3-5. TC materials have been suggested for glazing applications in 1986/1987 by Jorgenson and Lee [271], and Babulanam et al. [272].

4. Chamfered ceiling

Adding a simple modification to the ceiling at the deep-plan room can make a remarkable improvement to the illuminance level at this area. A study by A. Freewan [140] indicated that adding curvature to the ceiling at the end of a room can enhance the illuminance performance at this area. The current study claims that adding a chamfered ceiling in 45° at the end of the room can significantly improve the uniformity of the light and increase the illuminance level up to 10% [273], see Figure 3-5.

3.2.3 Parametric daylighting louvre control mechanism

The main method of the parametric louvre based on reflective slats which can automatically rotate with responding to the sun movement at daytime in order to collect and redirect the incident sunlight to the ceiling, then the reflected lights on the ceiling act as a diffuse light to the room, see *Figure 3-6*. The system is so-called "Parametric Louvre" or "Parametrically-angled Mirrored Slats" because the slats are parametrically rotated, where every single slat has a specific rotation angle, aiming to redirect sunlight to specific chosen targets points on the ceiling, and these targets are fixed. These targets can be changed parametrically based on the depth of the room to provide more coverage and distribution. During the sun movement; the slats rotate accordingly with responding to the sun direction in order to keep the reflected light constant at these targets. This process is controlled parametrically using an algorithmic formula in Grasshopper, and this formula is changeable and editable. The formula concept is depending on keeping the opposing two angles (δ) shown in *Figure 3-7* above the slat equal - wherever the sun direction - where the first angle is the intersection between incident sunlight and slat, while the other angle is the intersection between reflected light and the slat. The tilt angle of the slat (β) calculated as next:

$$\beta = \Omega - \delta \text{ or } \delta - \theta$$

$$\theta = \tan^{-1} u/v$$

Where; (δ) is the opposing two angles over the slat. (Ω) is the solar profile angle, (θ) is the angle between reflected light and ceiling. (u) is the distance from the centre of the slat to the point (a), (v) is the distance

from the point (a) to the target point (b), and (β) is the slat tilt angle, see *Figure 3-6* and *Figure 3-7*.

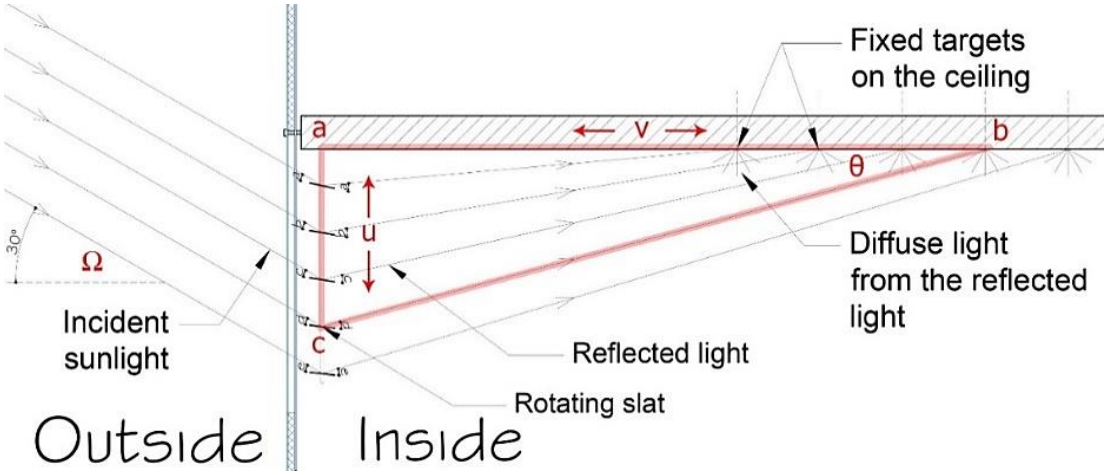


Figure 3-6: Cross-sectional view of the room showing the incident sunlight reflected by the rotating mirrored slats to a fixed target, resulting in diffuse light to the occupants. Every single slat has a specific rotation angle according to the target position, which is related to the slat.

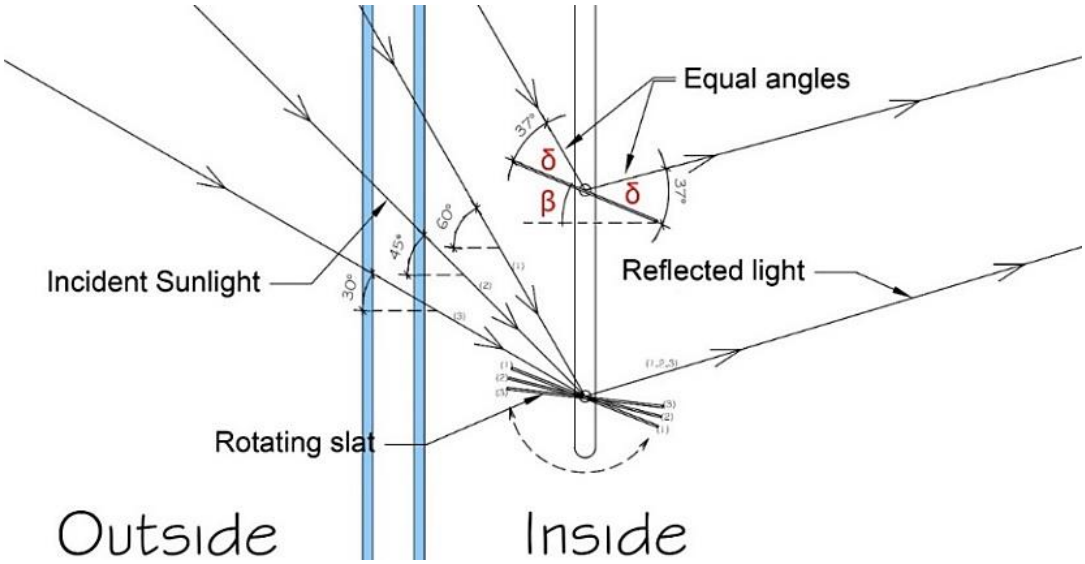


Figure 3-7: Cross-sectional view of the slats showing sun altitude outside is changing during daytime, and the slats are rotating responding to sun movement in order to keep the reflected light towards the fixed target points on the ceiling, and this process conducted via keeping the opposing angles (Ω) equal wherever the sun position.

The required tilt angle (β) in our study, should reach to the cut-off angle (β*) which is defined as the slat tilt angle beyond where no direct radiation is being transmitted through the slats. It is the most typical automatic blind control used in several previous studies [274], see *Figure 3-8*(c), where: β*= β required.

Distance between slats in this study is critical aspect because; if it is tiny as shown in *Figure 3-8*(b), it will utterly prevent the penetration of

sunlight, but may have the risk of blocking the reflected light to the ceiling. In contrast, if the distance between the slats is larger than a specific limit as shown in *Figure 3-8*(a), it will reflect the whole coming light from direct sunlight, however, still, have the risk of incident sunlight penetration. Therefore, the critical distance (y) shown in *Figure 3-8*(c) should be tuned to achieve the balance between the two main functions to obtain the optimum performance.

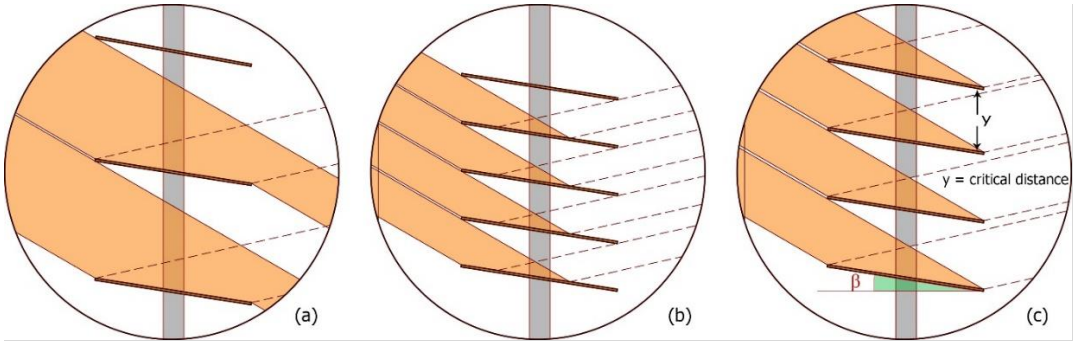


Figure 3-8: a comparison showing the influence of the distance between slats on the light reflected; (a) big distance, (b) small distance, and (c) is the critical distance which is acceptable according to the balance achieved with the cut-off angle β (required β).*

It should bear in mind that for individual control, every single slat has its unique rotation angle because each slat has its specified target over the ceiling. However, for comprehensive control, the whole slats have the same rotation angle during each movement, see Figure 3-9. Comparing to regular Venetian blinds, the reflected beams with the conventional blinds are parallel; however, the reflected beams with the parametrically-angled mirrored slats are spread out and separated. It is difficult to make a complex process to control several functions and find a compromise at the same time, whereas, this should be conducted by computerising. Therefore, utilising parametric design in this kind of complicated process is highly recommended, and it can be conducted via a formula created in Grasshopper. In this case, the cut-off angle (β*) is a unique angle for every single slat, as shown in Figure 3-7. The reason of using fixed targets on

the ceiling is to keep the reflected beams horizontally constant, parallel to the window, and moving in a straight line in one path according to sun azimuth as shown in Figure 3-10. Accordingly, this method can keep the daylight uniform and distributed inside the room.

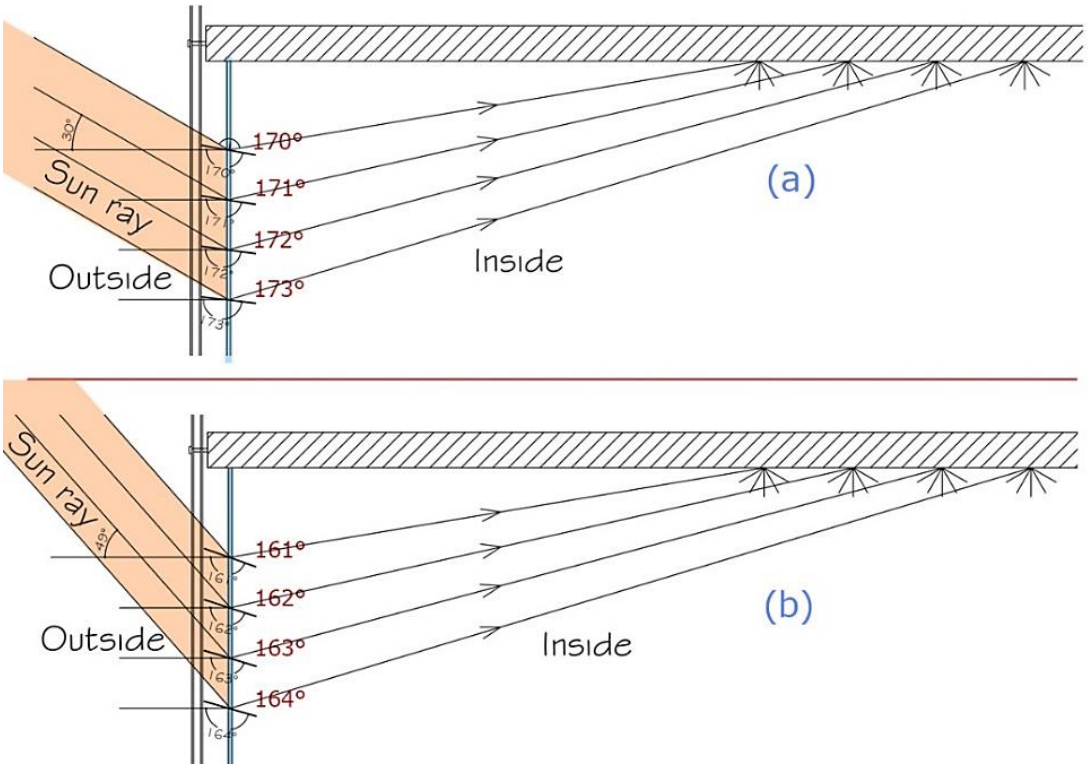


Figure 3-9: it can be noticed the 1° rotation difference between case (a) and case (b); meanwhile, each salt has its unique rotation angle.

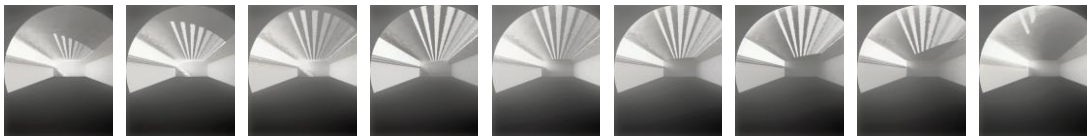


Figure 3-10: Radiance maps inside the room showing the parallel reflection on the ceiling during the daytime from 9 a.m.: 5 p.m.

The advantage of using parametric design in this process is to facilitate achieving maximum coverage of daylighting inside the room, via adapting the slats to accurately collect sunlight and reflect it to the ceiling as shown in Figure 3-8(c). At the same time, the slats acting as a shading device to protect the occupants from direct sunlight and heat gain, which leads to reducing cooling demands up to 30% based on previous studies [249, 275]. It should bear in mind that Energy coming from the sun is short-

wave and carries little heat. The heat has only occurred when a surface absorbs the solar energy and then radiated as long-wave infrared energy. In our case, the reflected solar energy is not an issue, because it remains short-wave and does not cause any heat gain [276]. Additionally, the parametric slats can keep the reflected light more steady and distributed on the ceiling during the working hours; which can provide visual comfort for the occupants. Consequently, electric light can be saved during the daytime as long as the reflected lights are constant and available [259].

3.3 Case Study description of the Parametric Louvre

A case study of the proposed method has been conducted for a deep-plan office room located in New Cairo in Egypt. The office room model was built in Grasshopper based on Rhinoceros 3D with dimensions 4m height, 7m depth and 18m length. The model has two main parameters; the slats control and timing. The Parametric Louvre System consists of aluminium slats with 90% reflectivity, which located at the upper part of the window as shown in Figure 3-11. The slats parameters control are listed below.

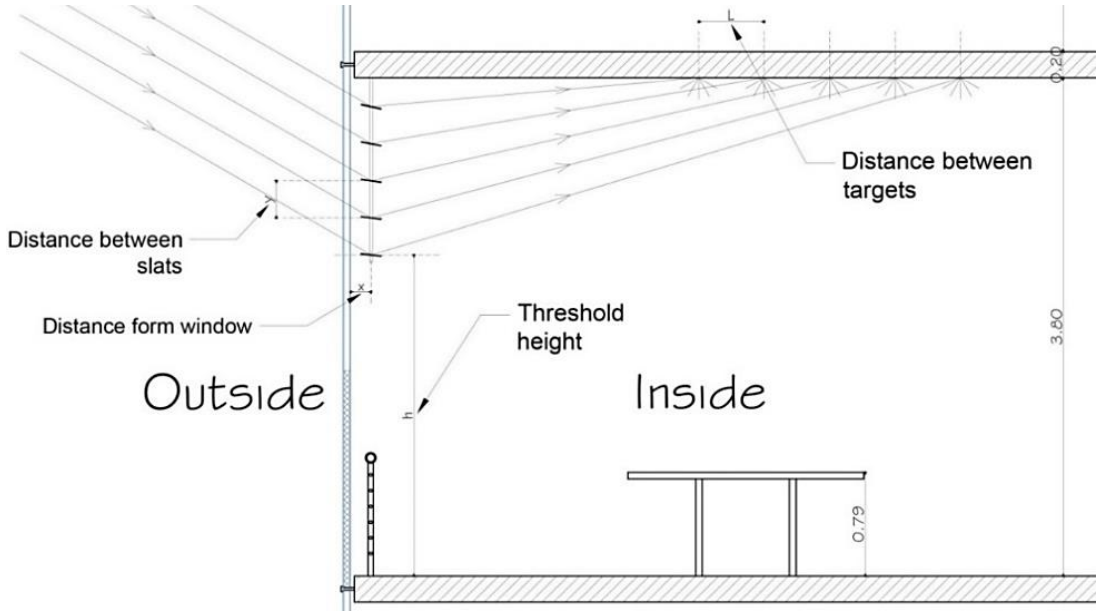


Figure 3-11: Cross-sectional for the office showing the controlled parameters; x: slats distance from the window, y: the distance between slats, L: the distance between targets, h: slats' threshold from the finish floor.

1. *The slat dimensions (length, width, and thickness).*
2. *The slat shape (flat – concave – convex).*
3. *The count of slats based on solar altitudes.*
4. *The distance between the slats (y) based on the slats' count.*
5. *The threshold of the slats (h).*
6. *The distance between the targets (L) based on room depth.*
7. *The slats location (inside or outside the window).*
8. *Tuning the tilt angle of the whole system, based on season change.*

The slats should perform two functions simultaneously; firstly, redirect incident sunlight to the ceiling, and secondly, prevent direct sunlight from penetrating inside the workstation, through using specific cut-off angles [274] with a specific critical distance between the slats. In order to achieve optimum performance, these two functions should be controlled in balance; via keeping the critical distance between the slats homogeneous with sun altitude. The formula in Grasshopper is tuned to react to sun movement when changing time or date automatically, using clear sky with direct sunlight. Ladybug plugin provides full sun path parameters via EPW weather file. In order to understand the hypothesis of this study, we will study three different cases from summer to winter (21st of June, 21st of September and 21st of December), see *Figure 3-12*.

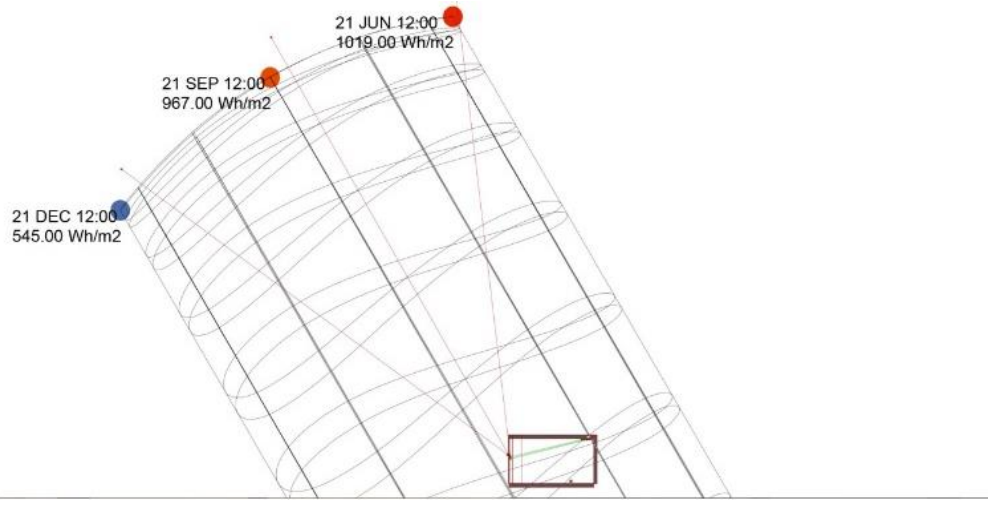


Figure 3-12: Sun path exported form Rhinoceros 3D, on June 21st, September 21st, and December 21st and sun altitudes 83.3°, 60.2°, and 36.4° respectively at zenith time.

3.4 Examining the Parametric Louvre in an example office room in New Cairo in three different seasons, to evaluate the daylight performance

The modelling experiment was conducted for three seasons; on the 21st of June, 21st of September and 21st of December, which are representing maximum, equinox, and minimum of sunlight availability throughout the year respectively. The model is a south-oriented office room in New Cairo and exposed to direct sunlight with a clear sky. The room is 18m length, 7m depth, and 4m clear height, and the slat unit in our case will be set to 10cm width and 1mm thickness. Firstly, we will study the sun-path and its coverage percentage area inside the room before adding the slats. Then adding the slats based on the attitude of sun coverage, in order to adapt the slats to react adequately with the variation of the altitude of the incident sunlight. The reflected lights in our cases are concentrated in 5 meter depth starting from the end of the room, while, the area near to the window is already illuminated with sufficient natural light, see *Figure 3-13*.

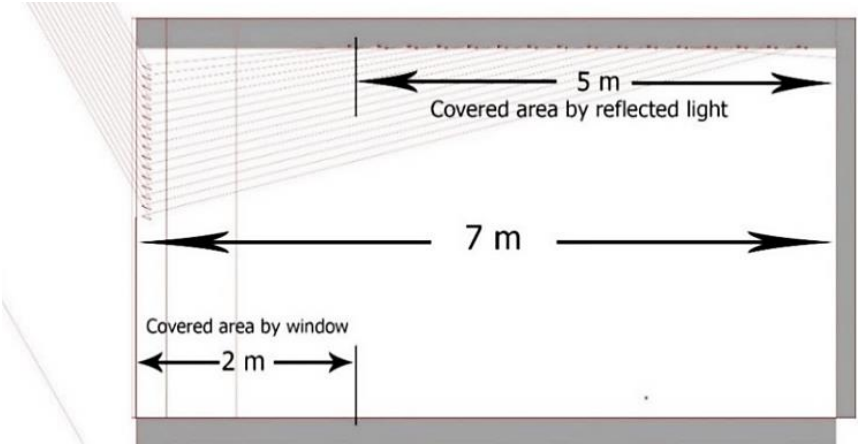


Figure 3-13: cross-section in the workstation showing the covered area by reflected light

3.4.1 Case 1: clear sky with the sun on the 21st of December

In this case, winter season in Cairo, 21st of December sun altitude is 36.4° at zenith time, see *Figure 3-12*. Meanwhile, it can be noticed in Figure 3-14 that direct sun light is low at this time and covering more than

80% of the room from 8 a.m. to 5 p.m. Therefore; the slats count should be increased to prevent the penetration of direct sunlight inside the room.

This process was done in Grasshopper by changing the distance between the slats, in order to create a balance between the cut-off angle (β*), the reflected light and the critical distance between the slats (y), see *Figure 3-15* (detailed section).

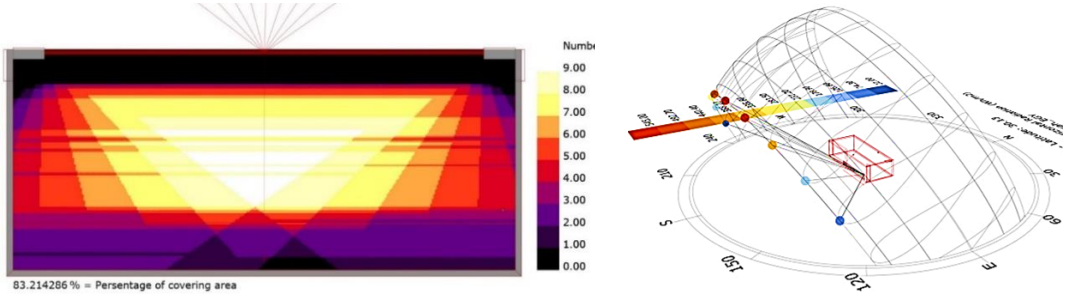


Figure 3-14: Top view of the office room showing hourly illuminated coverage area (83.2% coverage) from 8 a.m. to 5 p.m. on the 21st of December (left), Sun path (right)

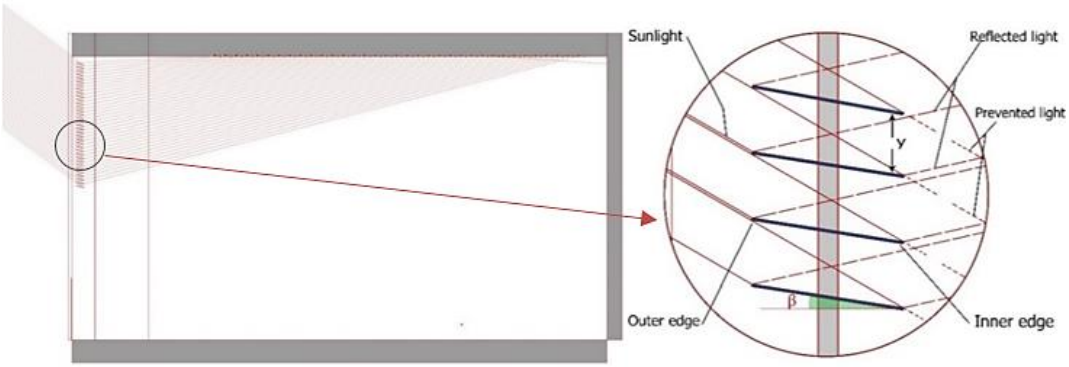


Figure 3-15: (left); cross-sectional view on the workstation showing sun rays at zenith time with 36.4° altitude on December 21st, using a high number of slats [35 slats], (right); detailed section for the slats

The ray passed through the top outer edge of the slat is prevented by the inner edge of the bottom slat. Consequently, the amount of light passes between the two slats is prevented from passing to the room, while, redirected to the ceiling, and so on for the other rays. Meanwhile, the insolation intensity of sunlight is low according to Lambert's Law, because in winter season; a unit beam of the sunray is steep which resulting coverage of a larger area, accordingly, receiving less energy per unit of an area [22]. Therefore, high number of slats will compensate the weakness

of sun radiation (545 W/m^2) at this time, see Figure 3-16, by reflecting maximum sunlight into the ceiling as shown in *Figure 3-15* (left). The slats settings are shown in *Table 3-1*.

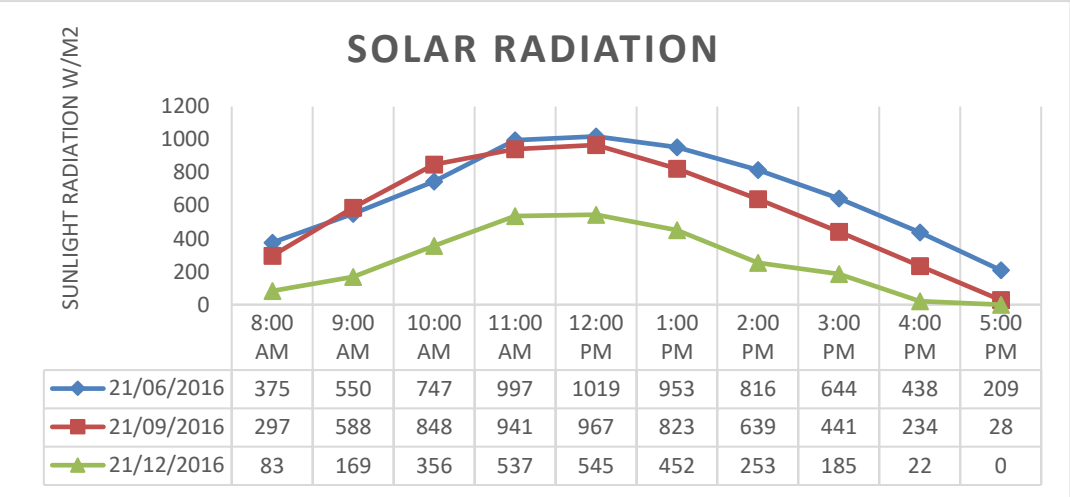


Figure 3-16: Solar radiation in Cairo on the 21st of June, 21st of September and 21st of December from 8 a.m. to 5 p.m.

Table 3-1: Slats settings

Slats parameters in meter	*21st Dec.*	*21st Sep.*	*21st Jun.*
Distance between targets (L)	0.14	0.3	0.3
Distance form window (x)	0.1	0.1	-1
Horizontal shift between slats	0	0	0.06
Threshold height (h)	2	2	2
Distance between slats (y)"critical distance"	0.047	0.1	0.1
Number of slats	35	16	16
Target form wall	0.3	0.3	0.3

The first and last three hours of the working hours from 8 a.m. to 11 a.m., and 2 p.m. to 5 p.m. respectively, sun altitudes are low. It can be noticed in Figure 3-14 (purple colour) that sunlight is penetrating deep into the end of the room, and the influence of solar radiation at these 6 hours is relatively low, while maximum solar radiation at this period is 356 W/m^2 at 10 a.m., see Figure 3-16. Therefore, we can utilise the solar intensity by providing diffuse light at this period via using translucent glass with 30% translucency [252, 277] within the automated slats (will be investigated in details in *Chapter 4*). The middle three hours from 11 a.m.

to 2 p.m.; sun altitudes are relatively high (comparing to the first three hours) and the intensity increases gradually, which should be sufficient to be reflected using the parametric louvre.

3.4.2 Case 2: clear sky with the sun on the 21st of September

In this case, autumn equinox on 21st of September, where daytime and night are equal (12 hours each) and sun altitude is 60.2° at zenith time. At this time, it can be noticed in *Figure 3-17* that sunlight is covering just 22% of the room; meanwhile, daytime is more extended than the winter season. According to the increase in sun altitudes, the number of slats was decreased (moved away from each other) in order to match the higher angles of sunray at this time, see Figure 3-17. In such a case, daylight is needed to cover deep inside the room, while approximately 80% of the room is dim and not exposed to direct sunlight.

Indeed, a higher altitude of the sun means more insolation intensity according to Lambert's Law [22], consequently, based on Figure 3-16 the increase in solar radiation at this time will compensate the lack of slats via reflecting larger intensity of the sunlight. Although, count of slats, in this case, is lower than in winter season, however, we can receive approximately the same intensity from reflected light as in winter season.

In Figure 3-16 it can be noticed that solar radiation on the 21st of September at noontime is 967 W/m²; however, it is 545 W/m² at the same time on 21st of December, which is approximately equal to the morning of September 21st 588 W/m². Which means that the minimum of solar radiation in September is approximately equal to the maximum of solar radiation in December. Therefore, this difference can be compensated by controlling the number of reflected lights (slats count). Moreover, solar

intensity on this date is sufficient to provide daylight during the daytime, except the first and last hours from the working hours. Therefore, automated slats can work effectively during six hours of the day, while, diffuse light can be implemented in the remaining two hours via using translucent glass [252] as mentioned in "Case 1".

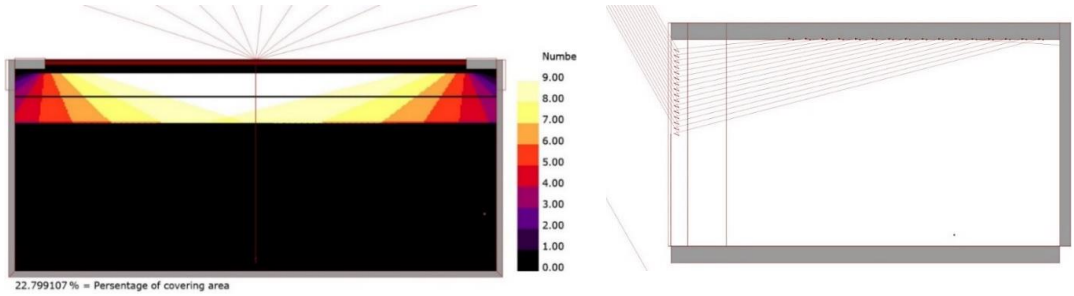


Figure 3-17: Top view of the office room showing hourly illuminated coverage area (22.7% coverage) from 8 a.m. to 5 p.m. on the 21st of September (left), Cross-sectional view for the workstation showing sun rays at zenith time 60.2° altitude, using low number of slats [16 slats]. (Right)

3.4.3 Case 3: clear sky with the sun on the 21st of June

At this time of the year summer season, 21st of June is the longest day over the year and sun is approximately vertical at zenith time, see *Figure 3-12*, accordingly, the office room is almost dark during daytime as shown in Figure 3-18. Hence, sun rays cannot strike the slats as long as they are vertically deployed; accordingly, reflected light is hardly obtained because of the vertical path of the sun rays as shown in Figure 3-18. Therefore, the slats should be tilted in an inclined sequence order to receive maximum sunlight. Moreover, this action will work as a shade to protect the window from incident sunlight during the day. The slats settings listed in *Table 3-1*.

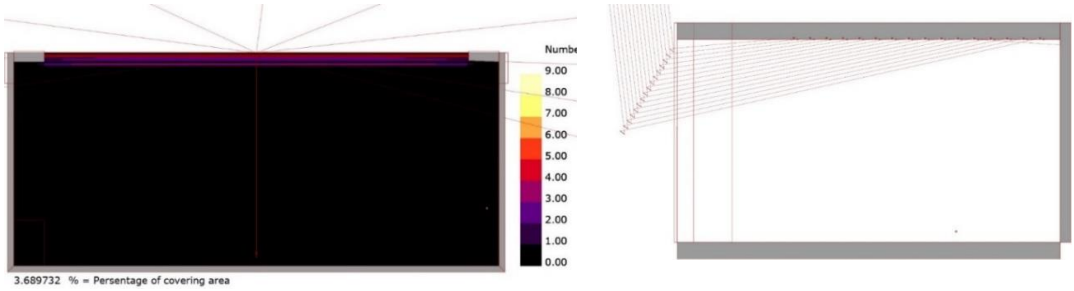


Figure 3-18: Top view of the office room showing hourly illuminated coverage area (3.7% coverage) from 8 a.m. to 5 p.m. on the 21st of December (left), Cross-sectional view for the workstation showing sun rays at zenith time with 83.3° altitude, using tilted blinds [16 slats]. (Right)

3.5 Cases study comparison and analysis

A comparison analysis is conducted between the three previous cases at 8 a.m., 10 a.m. and 12 p.m., using a plain window, conventional slats and the Parametric Louvre in the office room. All parameters of the conventional slats were set similar to the automated slats, except the rotation parameter, where the conventional slats were set in a horizontal state with no rotation angle. As mentioned before, each slat in the automated slats has an individual rotation angle which response parametrically to the sun movement.

Figure 3-19 is showing a comparison maps of daylight distribution in the office room using a plain window, conventional slats and the Parametric Louvre System on 21st of December, 21st of September and 21st of June respectively at 8 a.m. In September and June in the automated case, sunlight is blocked and successfully reflected, however, in December the incident light is penetrating between the slats according to the low inclination of the sun; however, this issue will be addressed in *Chapter 4* by using translucent glass. In the typical case, the slats were set to be in a horizontal state, which is considered the best static way to utilise daylight [278]. The conventional slats at this time are showing lower efficiency in reflecting light comparing to the parametric ones. Although, some reflected light is revealed in December, however, still insufficiently distributed.

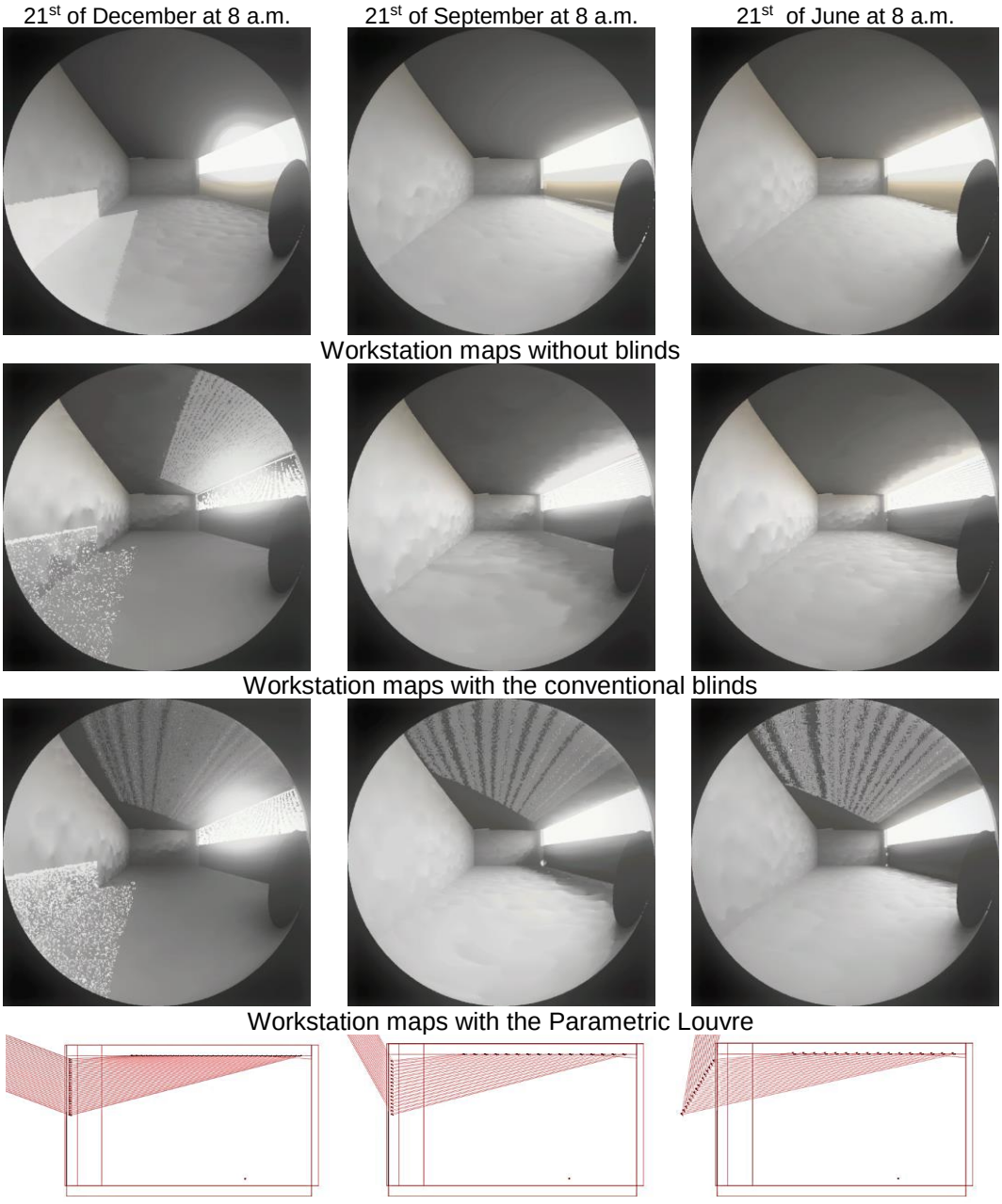


Figure 3-19: Radiance maps for the office room at 8 a.m. on 21st of December, 21st of September and 21st of June, from left to right (top), raytracing and solar altitudes (bottom)

In *Figure 3-20*, same conditions at 10 a.m.; the reflected light with the Parametric Louvre looks steady and uniform on the three mentioned dates. Moreover, it can be noticed that reflected light in December at this time is approximately blocked and reflected comparing to 8 a.m. The conventional slats at this time still unsuccessful to reflect sunlight efficiently. Nevertheless, they are slightly showing better performance in December but still not distributed.

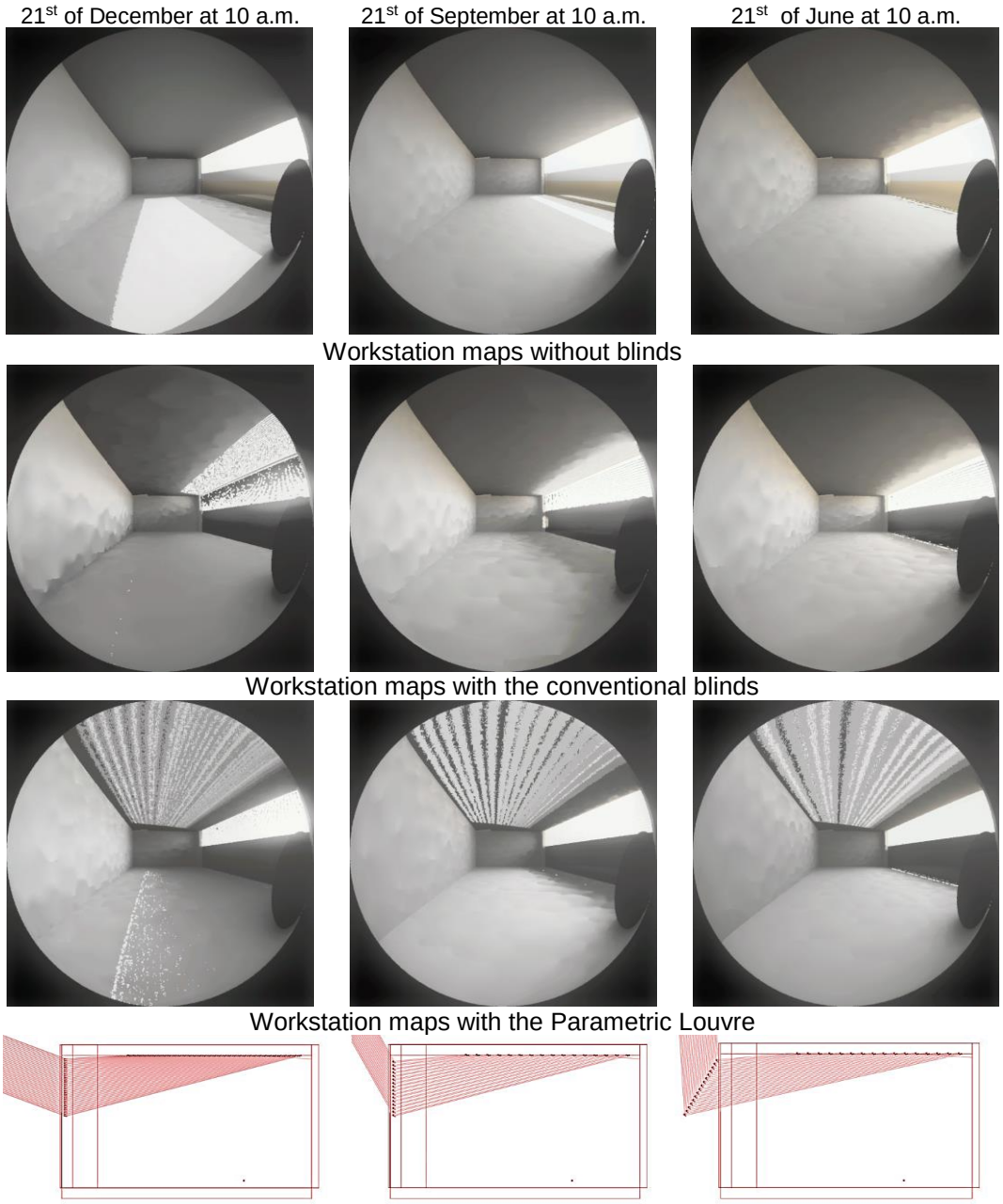


Figure 3-20: Radiance maps for the office room at 10 a.m. on 21st of December, 21st of September and 21st of June, from left to right (top), raytracing and solar altitudes (bottom)

In *Figure 3-21*, same conditions at 12 p.m., the Parametric Louvre reveals the best performance on all dates, while they succeeded to reflect and block sunlight efficiently; moreover, the reflected daylight is distributed well on the whole ceiling. On the other hand, the conventional slats blocked the light successfully, but still insufficient to illuminate the office room.

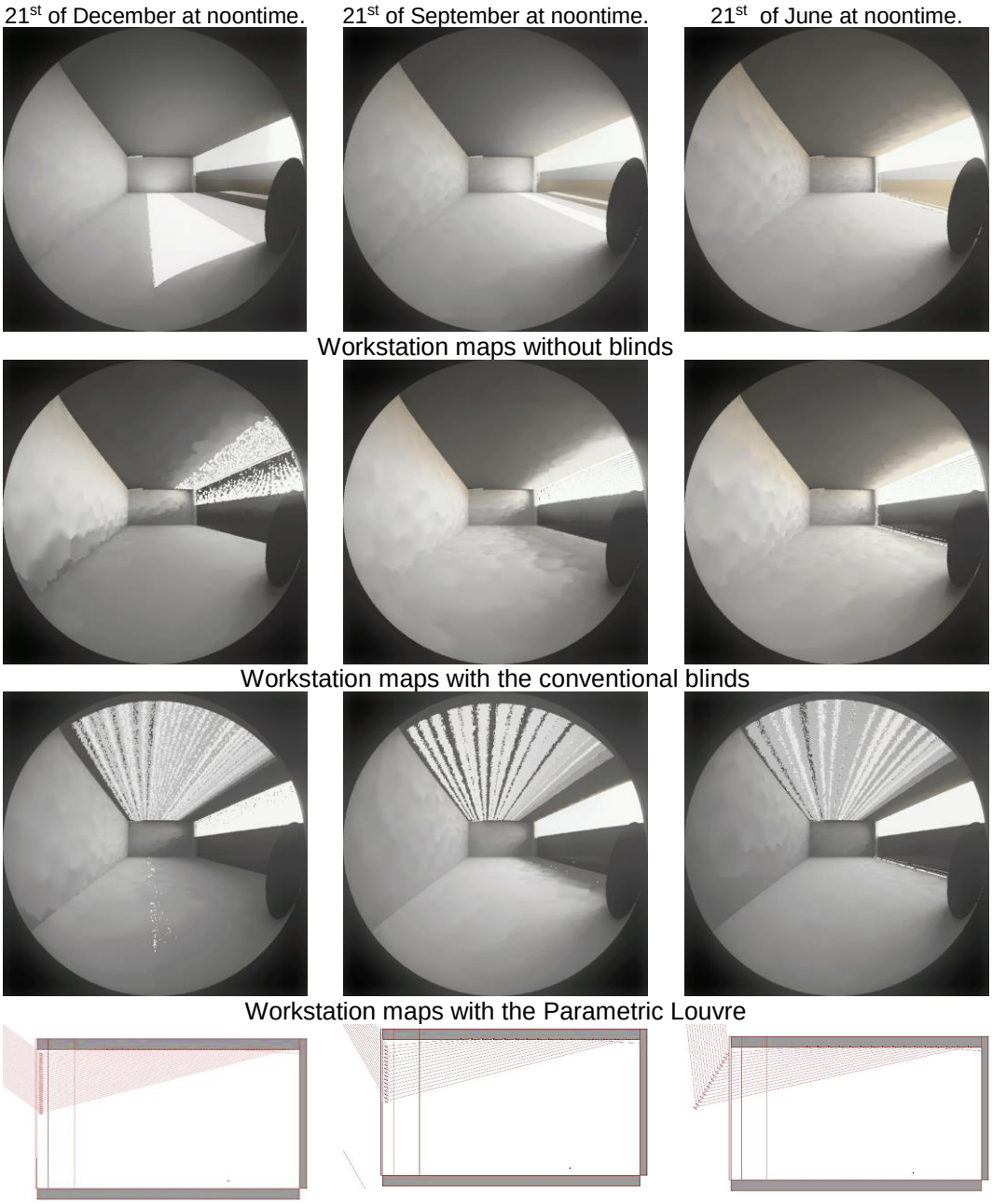


Figure 3-21: Radiance maps for the office room at 12 p.m. on 21st of December, 21st of September and 21st of June, from left to right (top), raytracing and solar altitudes (bottom)

3.6 Summary

Parametric Louvre was used to illuminate a south-oriented office room in Cairo using direct sunlight with a clear sky. The slats were controlled parametrically and respond automatically to the sun movement in a heliotropic response. The experiment performed at three different times of the year; 21st of December, 21st of September and 21st of June, and these specific dates were chosen to cover all possible circumstances of daylight exposure. While, these dates represent the maximum, equinox and minimum of sunlight exposure throughout the year.

The slats were set vertically at the upper part of the window on December and September, where the sun inclinations are sufficient to be reflected into the ceiling and provide natural light. However, sun altitude in June is very high to be caught by such vertical slats. Therefore, the slats were tilted in an inclined sequence, in order to receive maximum sunlight. The Parametric Louvre System, among all cases, was showing the best performance of providing natural daylight, blocking direct sunlight and distributing light. Although, conventional slats succeeded to prevent incident sunlight and to provide natural light, however, the provided daylight still insufficient and not well distributed.

To summarise, Parametric Louvre System succeeded to provide distributed daylight in a south-oriented room and protect from direct sunlight, simultaneously. Therefore, this system can be used instead of artificial light to save electrical energy. *Chapter 4* will discuss the validity of such a system via using 1:20 physical prototype.

Chapter 4 Prototyping and Validation of the Parametric Louvre

4.1 Introduction

Automated daylighting systems can achieve up to 50% of energy-saving comparing to 20% of the stationary systems at their best performance [279]. However, the performance of these automated systems is still limited due to their inadequate performance, control difficulties and users' preferences [12]. Recently, the parametric design has been implemented in these automated systems to improve their performance and solve potential lack of daylight coverage, while, it can combine different parameters and complex relations, simultaneously [123]. *Chapter 4* will investigate the Parametric Louvre System (PLS) with individually-angled mirrored slats (based on *Chapter 3*) [247] by implementing automation control in a physical prototype. The PLS was used as a daylighting system which can provide evenly distributed daylight inside the room [273]. The study aims to demonstrate the validity and performance of the proposed PLS in a mock-up study and also the application of microcontrollers in the prototype as a controlling method [280]. Microcontrollers have been utilised previously in several types of research to improve energy efficiency and comfort conditions [129, 281, 282]. The validation process starts with specifying the prototype location by inserting the EPW file in the "Ladybug" component, likewise, time and date inserted as an input data in Grasshopper. Then, the input data should be calculated via Grasshopper's formula to obtain the slats' rotation angels. After that, the values of the angle are sent immediately to Arduino board

as a microcontroller via a specific plugin known as "Firefly". Finally, Arduino board gave signals to the servo-motors with the specified angles, which should accordingly rotate the slats, see Figure 4-1.

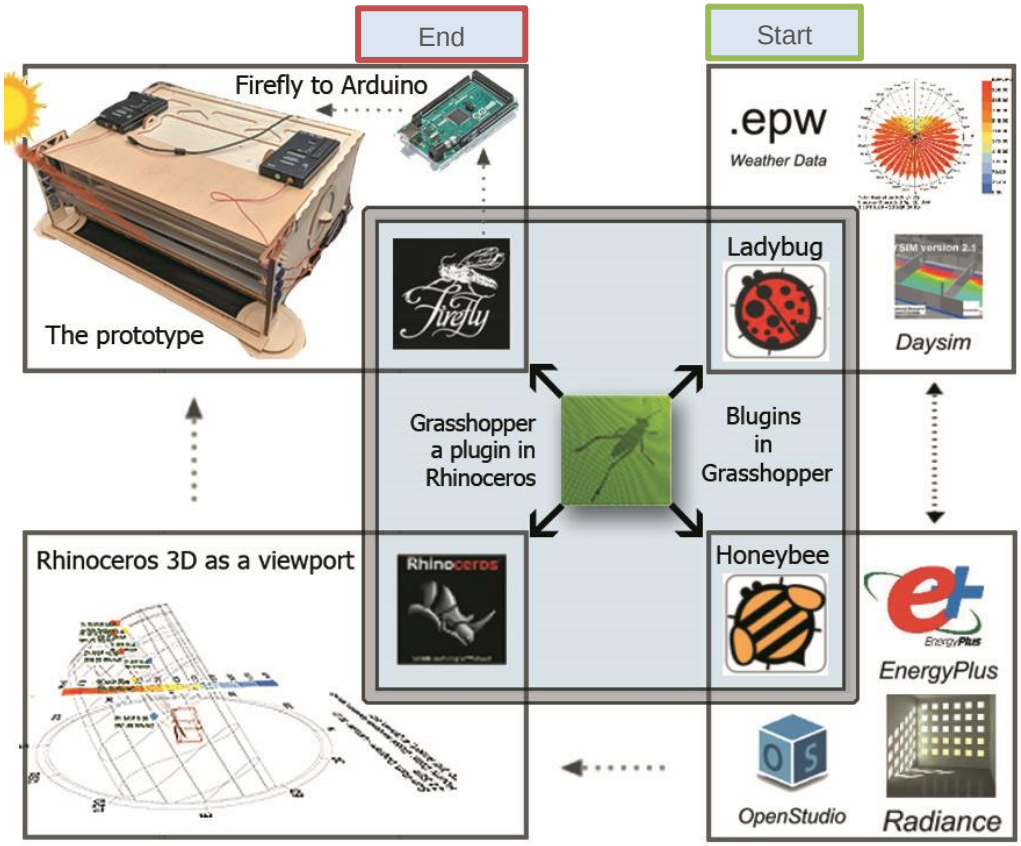


Figure 4-1: Conceptual diagram showing the relation between Software, Hardware, Sensors and Actuators

4.2 Prototyping the Parametric Louvre

A scaled prototype was created to validate the results obtained from the computer simulation of the parametric louvre in an example office room [273, 279]. The prototype was built with a scale of 1:20 for the office room of 8m depth, 4m height and 12m width. The prototype was made of an assembled laser-cut 3mm plywood and with a movable ceiling. The full south side was fitted with the louvred window. The walls and ceiling were matt white painted to give a typical 80% reflectivity, while the floor was covered with standard grey carpet. A side circular access opening was created to take a snapshot of the interior with a wireless controlled camera,

see Figure 4-2. The test was carried out at the University of Nottingham in May, July and August where the sky conditions are relatively stable. Time was selected in the middle of the day between 10 a.m. and 3 p.m. The validation method of this study is based on the interconnection of three main parts; the physical part which contains the hardware and all physical controllers, the digital part which contains the software and all digital controllers, and the measurement part which contains the sensors and the measurement devices.

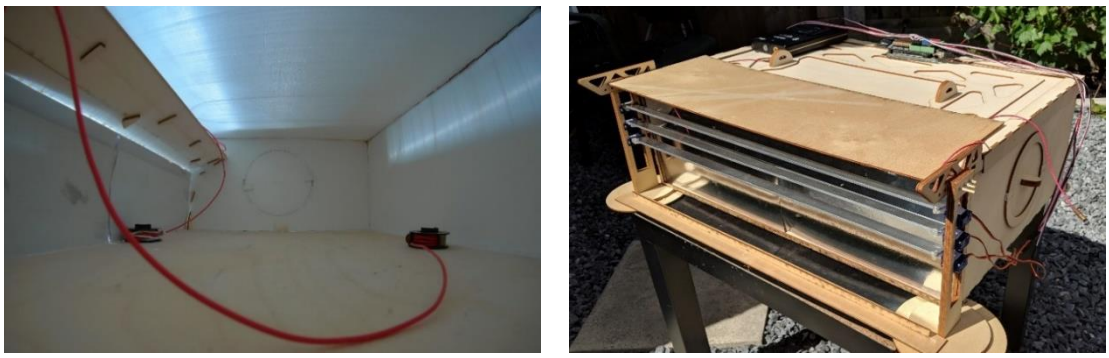


Figure 4-2: 1:20 scaled prototype for daylighting system validation

4.2.1 The physical part of the prototype

1. The Parametric Louver

The parametric louvre consists of aluminium slats covered with mirrored film with 75% reflectivity. The louvre was installed at the upper part of the window as seen in Figure 4-2. Rotation of the slats were actuated by a micro-servo motor.

2. Micro servo motor

As an actuator in the control of motion, the micro servo motor used with the prototype is brand "9g Micro Servo Motor (4.8V)". Its accuracy is 1 degree, and it can rotate up to 180° in one direction. As mentioned previously, a set of slats can be actuated with a single micro-servo motor theoretically, however, for better balance, two micro-servo motors were

fixed at the two ends of each slat to control its rotation. The signal for a required rotation degree is delivered from an electronic board known as Arduino board.

3. Arduino board description

Arduino is an open-source electronics platform based on easy-to-use hardware and software, and it has been utilised in many fields due to its distinctive capabilities and low cost. It is a microcontroller based on Integrated Circuits and has been mainly exploited to control micro servo motors and robotic kits. Arduino can be therefore used as a mediator between the digital simulation and the real model. 'Arduino MEGA 2560' was chosen in our study due to its capability to control several parameters [283]. It has 54 digital binary codes (1/0) pins and 16 analogous inputs/outputs [284]. In our experiment, Arduino MEGA 2560 is attached to an expansion shield known as "DFRobot Mega" as shown in Figure 4-3, which facilitates a connection to the Micro Servo Motor. It is utilised to take all the information and data from the computer and deliver them to the actuators via an algorithmic software called Firefly.

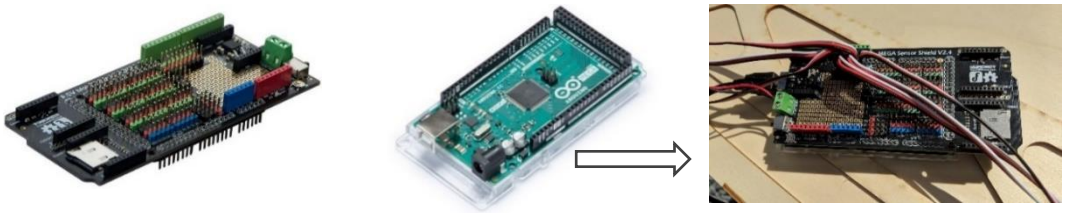


Figure 4-3: The expansion shield on the left side is attached to the Arduino MEGA 2560 board in the middle to form the final shape of the board on the right side

4.2.2 The digital part of the prototype

The connection between the computer and the Arduino board is a physical connection using the USB connection. Behind the computer screen, this connection translated to Grasshopper and Firefly as shown in Figure 4-4. Firefly is an open-source software plugin and can be

downloaded as a plugin in Grasshopper (refer to section *3.2.1*) to serve as a bridge between Grasshopper and the Arduino microcontroller [285]. The interface components of Firefly is a translation of the Arduino board's input/output pins [129]. It allows the components of Grasshopper to open a connection to the serial port, read the rotation angles in Grasshopper, and deliver it out into Arduino. In general, Arduino must be defined to the computer in order to send and receive data from Firefly via a novel communication protocol called "Firefly Firmata" [286], see Figure 4-4

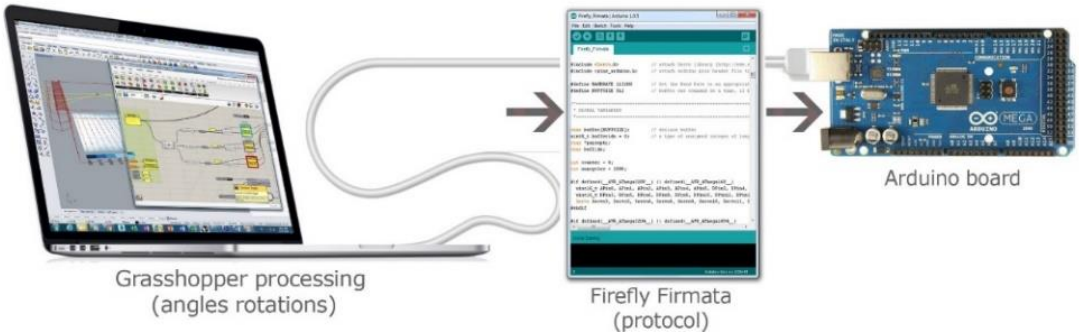


Figure 4-4: Connection process from the computer to Arduino via Firefly Firmata protocol

4.2.3 The measurement part

Two photosensors were used inside the prototype to detect the illuminance level over the floor; the sensor height is 3 cm from the floor; the first one was set 5 cm away from the window, and the other sensor set 5 cm away from the back wall, as shown in Figure 4-5. Both sensors were connected to two lux meters to display the illuminance level individually. It should be considered that test points in the Grasshopper represent the photosensors in the prototype. Two lux meters (HAGNER LUXMETER, MODEL E2-X) were connected directly to the photosensors to read the illuminance level inside the room, see Figure 4-5.

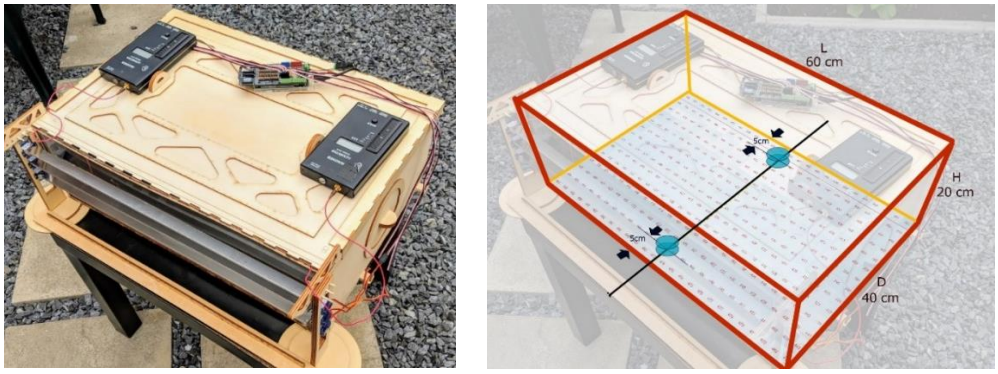
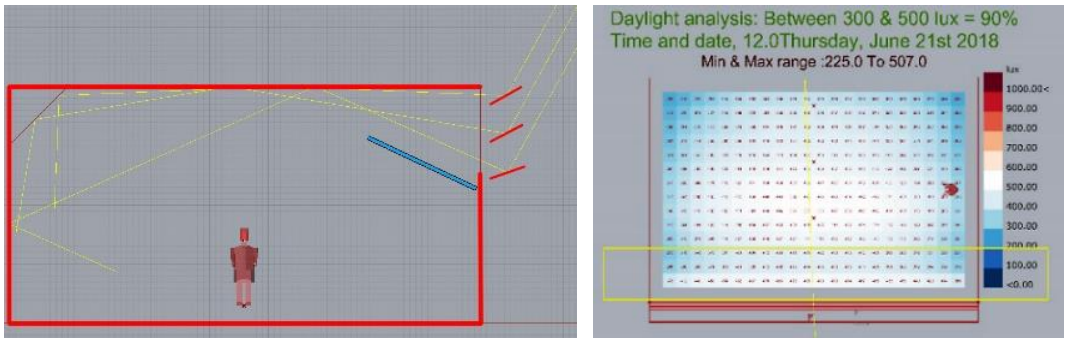


Figure 4-5: The sensors positions inside the prototype

4.2.4 Limitations of the experimental design

1. Addition of fixed shade

A single shading plate was fixed directly under the lowest mirrored slat [279] to absorb any downward or leaked light to avoid potential glare near the window [274], as shown in Figure 4-6.



Daylight coverage 90% with a shading plate

Figure 4-6: A single shading plate adjacent to the Parametric Louvre System

2. Number and size of the slats

For the full-scale model, the number of slats in the *simulation* was set to 10; the dimensions were supposed to be 12m length, 15cm width and 3mm thickness. However, when rescaling these parameters to match the prototype size 1:20, the results were inaccurate due to its small size. Rescaling and cutting a mirrored stainless steel to 7mm width and 60cm length influenced badly on its shape properties, which became like a spiral shape, in addition to its surface which became concave. Moreover, it was difficult to fix and rotate a fragile slat along the 60cm length, which resulted

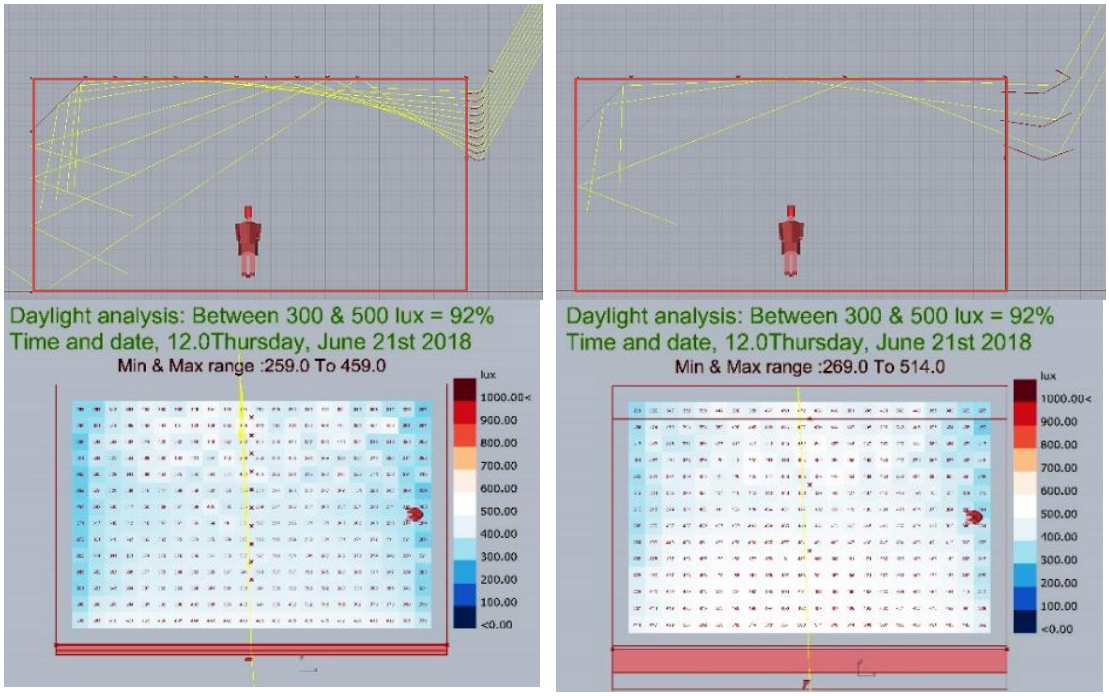
in a zigzag reflection over the ceiling, see Figure 4-7. To improve the accuracy control; number of slats was changed from 10 to 3 and the dimension of each slat was changed to be 3 cm wide (equivalent to 60cm in the full scale) and 2 mm thick with the same length 60 cm. Polished aluminium slats (with 75% specularity) were replaced with the stainless steel slats due to their strength and lightweight, see Figure 4-2.



Figure 4-7: The initial setting of the prototype with ten mirrored slats

It should be considered that the number and size modifications of the slats would not influence the function of daylighting performance and its validation as long as the settings in the simulation are adjusted accordingly. Both parameters were examined in the simulation in order to produce the same result and performance as shown in Figure 4-8.

By examination, the simulation with ten slats and 0.7cm width was giving daylight coverage average 92% on the 21st of June at noontime. Meanwhile, changing the number of slats to 3 with a specific equivalent distance (2.7 cm) [247] between them and 3 cm width was giving almost the same daylight coverage average 92%, see Figure 4-8. The percentage value here represents the percentage coverage area with the daylight illuminance between 300-500 lx, which was chosen according to the European and CIE standards [16].



Daylight coverage 92% with 10 slats Daylight coverage 92% with 3 slats

Figure 4-8: Daylight coverage for 10 and 3 mirrored slats, respectively

It should bear in mind that this chapter focuses only on validating the performance of the PLS regardless of the intensity level of the daylight. The bottom window accordingly was also ignored in this test and replaced with an opaque surface, while it will be discussed in Chapter 5.

4.2.5 Sky conditions

Three main sky conditions were studied for the simulation, clear sky with sun, intermediate sky and overcast sky [287]. The analysis of Daylight hours for the location of Nottingham reveals that the sky is clear, intermediate and overcast during 17%, 47% and 34% of the year respectively, based on the criteria in Table 4-1 [33]. The study uses Radiance for daylight analysis via Ladybug components in Grasshopper.

Table 4-1: Sky types

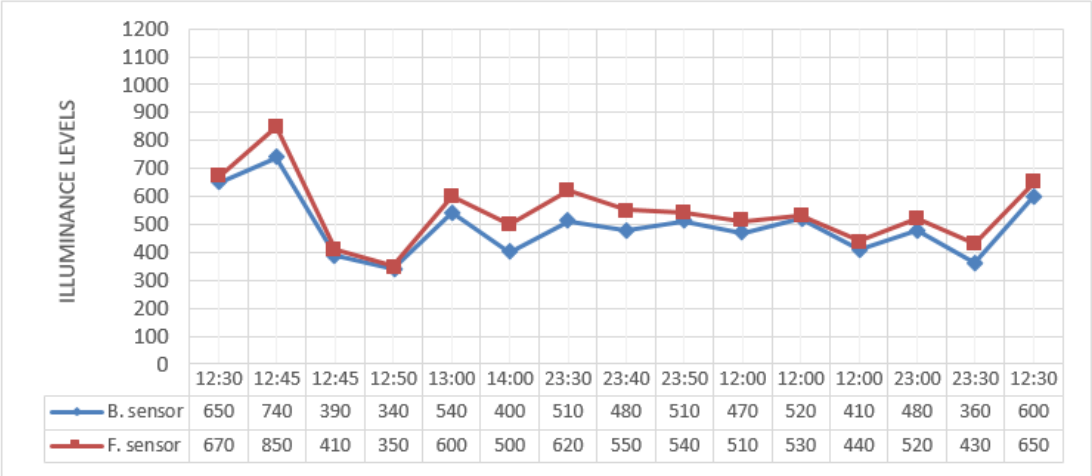
CIE sky type	*Condition*
Clear	Direct normal irradiance is more than 200% of diffuse horizontal
Intermediate	Direct normal is between 5% and 200% of diffuse horizontal
Overcast	Direct normal is less than 5% of diffuse horizontal

4.3 Monitoring results of the Parametric Louvre at different times and dates

Firstly, the results have been monitored in random days in May, July and August to evaluate the system's performance in the long term. Then the simulation results have been validated with the prototype results by choosing specific days with different sky conditions. Daylight hourly monitoring has been made inside the prototype in May, July and August in different chosen days when the sky condition is steady, between 10 a.m. and 3 p.m., see

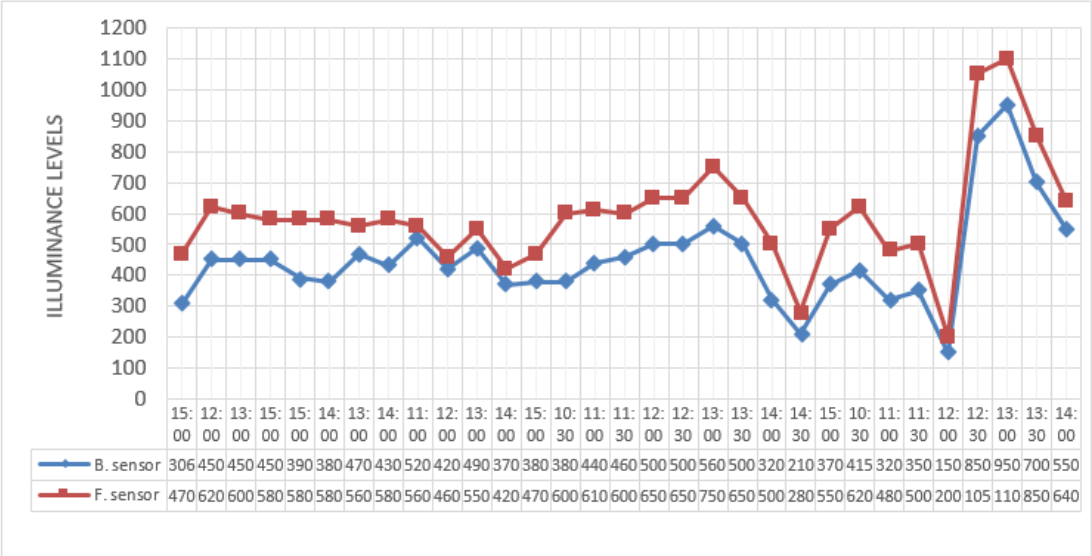
Figure 4-9*, Figure 4-10* and *Figure 4-11*. A predominant illuminance level is seen between 300~600 lx. Sky conditions at this green illuminance range were varying between intermediate and overcast. While the illuminance levels ranging between 600 – 1500 lx are relatively higher due to the influence of direct solar radiation in the bright sky condition.

In terms of the uniformity of daylight distribution, the automated louvre system provided a satisfactory performance and partly met our design expectation. Although, the recommended illuminance level for visual comfort in office buildings supposed to be between 300~500 lx according to CIE standards [16, 34, 288], howerver, a previous study [45] claimed that lighting level between 100~2000 lx could meet human visual comfort based on occupants' survey. Therefore, if the illuminance range 100~2000 lx considered as an acceptable range for occupants, the proposed Parametric Louvre system can be considered as a promising application in office buildings to save electrical energy. As mentioned previously, this study is focused only on validating the distribution performance of the Parametric Louvre regardless of the intensity level of the daylight.



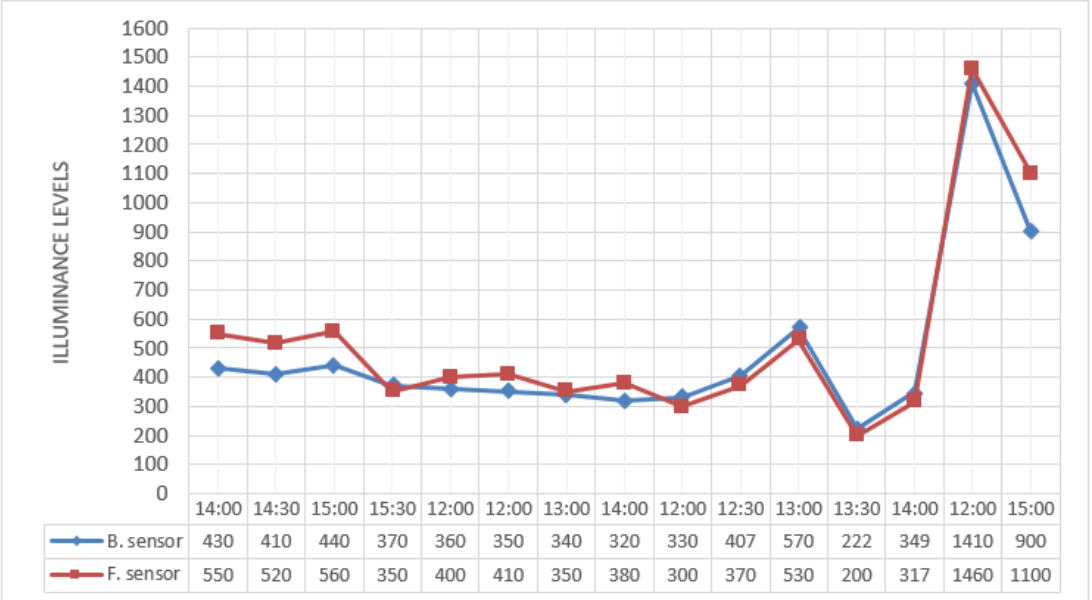
	12:30	12:45	12:45	12:50	13:00	14:00	23:30	23:40	23:50	12:00	12:00	12:00	23:00	23:30	12:30
B. sensor	650	740	390	340	540	400	510	480	510	470	520	410	480	360	600
F. sensor	670	850	410	350	600	500	620	550	540	510	530	440	520	430	650

Figure 4-9: Daylight hourly monitoring in May on random days between 11 a.m. and 3 p.m.



	15:00	12:00	13:00	15:00	15:00	14:00	13:00	14:00	11:00	12:00	13:00	14:00	15:00	10:30	11:00	11:30	12:00	12:30	13:00	13:30	14:00	14:30	15:00	10:30	11:00	11:30	12:00	12:30	13:00	13:30	14:00
B. sensor	306	450	450	450	390	380	470	430	520	420	490	370	380	380	440	460	500	500	560	500	320	210	370	415	320	350	150	850	950	700	550
F. sensor	470	620	600	580	580	580	560	580	560	460	550	420	470	600	610	600	650	650	750	650	500	280	550	620	480	500	200	105	110	850	640

Figure 4-10: Daylight hourly monitoring in July on random days between 10 a.m. and 3 p.m.



	14:00	14:30	15:00	15:30	12:00	12:00	13:00	14:00	12:00	12:30	13:00	13:30	14:00	12:00	15:00
B. sensor	430	410	440	370	360	350	340	320	330	407	570	222	349	1410	900
F. sensor	550	520	560	350	400	410	350	380	300	370	530	200	317	1460	1100

Figure 4-11: Daylight hourly monitoring in August on random days between 1 p.m. and 3 p.m.

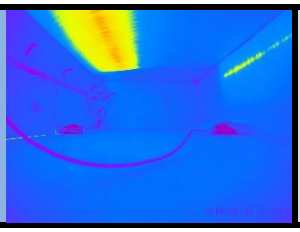
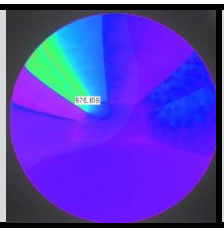
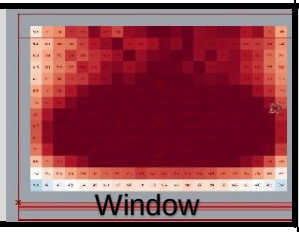
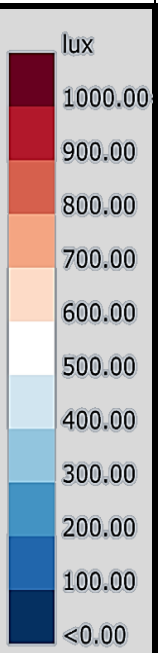
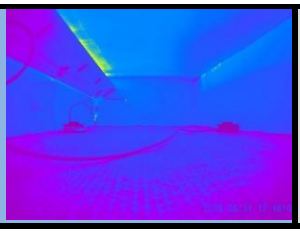
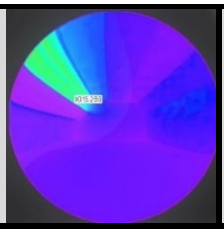
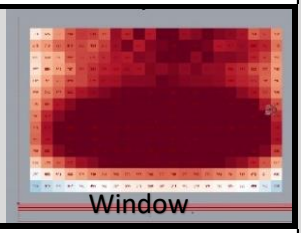
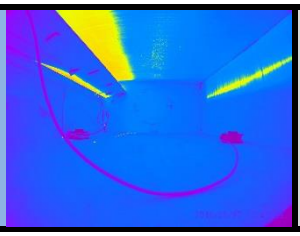
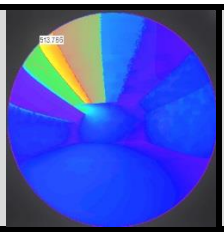
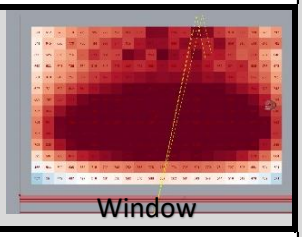
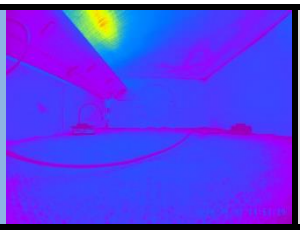
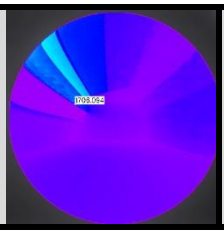
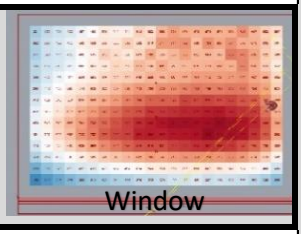
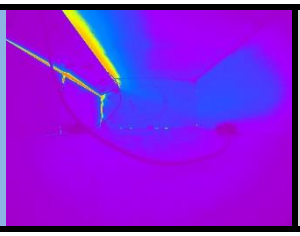
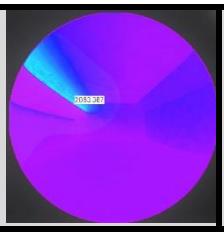
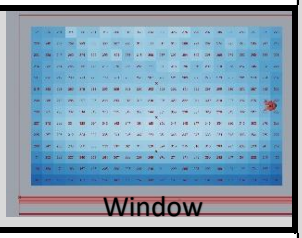
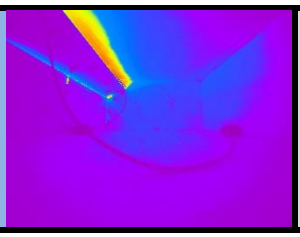
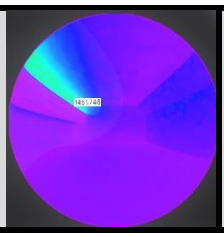
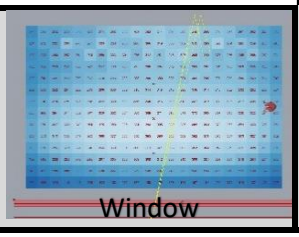
4.4 Validation of the Parametric Louvre

The examination has been performed to validate the results of the prototype with the simulation results in Grasshopper by comparing the real illuminance maps with the rendered maps in the simulation. The real illuminance maps of the test were captured by using an action camera inside the prototype, then, an effect of "light-scale gradient" was applied on the maps to produce the HDRI illuminance maps as shown in Table 4-2. This effect can change a real map with normal colours to false colour map.

HDRI maps in were generated in Grasshopper by using "Honeybee False Color" component, valued in luminance cd/m^2. The luminance performance of the daylight can be seen in the bluish colours in the maps, where, the blue colour means more intensity and the purple colour means lower luminance levels. Luminance levels in the prototype were ranging between 50~2200 cd/m^2. However, for light intensity measurements, illuminance (Lux) values are preferable for such study [53, 258, 289].

In Table 4-2, under the sunny conditions, the recorded values at the back and front sensors in the prototype were 1385 lx as a minimum value and 1460 lx as a maximum value respectively, which considered relatively high. Under the overcast sky condition, the illuminance values were ranging between 300 – 570 lx, which is considered satisfactory. The reason behind this balance reveals beyond the type of illuminance coming from the skydome as a contribution of diffuse radiation based on Table 4-1.

Table 4-2: A comparison between the HDRI maps in the prototype and the simulation as a validation study, in addition to the daylight analysis map to indicate the illuminance values.

Date & time	Sky condition	Measurements: B/F Sensors values	Measurements: HDRI real map from the prototype	Simulation: HDRI fish eye false colour from Grasshopper (cd/m2: 11000, 9900, 8800, 7700, 6600, 5500, 4400, 3300, 2200, 1100, 0)	Simulation: B/F points equivalent to the sensors	Simulation: Daylight illuminance analysis maps from Grasshopper (top view)	Illuminance scale. Accepted range: 300~500 lx
Case 1							
31-7-2018 13 :00	Sunny	1385 / 1430			1140 / 1450		
Case 2							
31-8-2018 13 :00	Sunny	1410 / 1460			1393 / 1426		
Case 3							
7-8-2018 13 :00	Intermediate with sun	850 / 1150			974 /1211		
Case 4							
31-8-2018 15 :00	Intermediate with sun	900 / 1100			785 / 938		
Case 5							
9-8-2018 12 :00	Overcast	330 / 300			382 / 292		
Case 6							
9-8-2018 13 :00	Overcast	570 / 530			325 / 411		

In Case "1" the effect of direct solar radiation revealed on the ceiling near to the window which accordingly increases the illumination of the room, due to the influence of direct sunlight. In this case, the simulation recorded; 1140 lx at the back and 1450 lx at the front, which are equivalent to the sensors' records; 1385 lx at the back room and 1430 at the front, respectively. In Case "3", the simulation recorded; 974 lx back and 1211 lx front, which are equivalent to the sensors' records; 850 lx and 1150 lx back and front, respectively.

An illuminance difference can be noticed between two sky conditions Case "4" and Case "1" due to the contribution of diffuse light from the skydome according to *Table 4-1*. In Cases "5 & 6" due to the overcast sky condition, the mirror slats reflect only the diffused light caused by the skydome, which accordingly conducted a moderate illuminance distribution inside the room. Cases "2 & 4" are relatively similar to Cases "1 & 3", respectively, due to their similar conditions.

Overall, the values resulted from the sensors were relatively close to the values in the simulation, which considered a promising outcome for such a validation study. The white matt surfaces of the walls and ceiling were playing an essential role in the daylight illuminance distribution inside the room due to their diffuse reflection, particularly when daylight is reflected onto the ceiling, which acts as a source of light to the room. For instance, the first quarter of the ceiling is responsible to lit the first 2/3 part of the room as seen in Table 4-2. While, the end corner of the ceiling within the wall at the back is responsible to lit approximately the last 1/3 part of deep inside the room [140]. Whereas, the wall acts as a second reflection to the room, see Table 4-2 (top view maps). This analysis aims

to find a compromise between these two illuminated areas to keep within an accepted range [273]. Direct solar radiation and diffuse horizontal radiation are changing and varies based on the location type and climate classification [22, 290], which influence as well on the illuminance level inside the room.

4.5 Summary

Parametric Louvre has been introduced in this chapter as a prototyping model for validation purpose. The study has followed a typical procedure, starting with Grasshopper as a parametric control tool and ending with the final physical prototype and its validation.

Validation is a crucial step to assess the performance of the proposed system. The test results indicated that the proposed system succeeded to provide a relatively uniform distribution of daylight. This validation study was performed for two main aims, to validate the system's performance and demonstrate its practicality as a control method. The first aim focuses on the capability to distribute the daylight inside the room with respond to the sun movement. Compared to static systems which cannot provide uniform daylight inside the room and even the automated shading systems which only used for protection from direct sunlight, the parametric louver system can successfully achieve both functions by providing steady uniform daylight and simultaneously protect from direct sunlight. The second aim focuses on the ability to execute and control such a system by using small actuators and simple electronic board.

This validation was performed by using a mediator known as "Arduino board" between the prototype and the parametric control of Grasshopper (digital to the physical world). Different kinds of tools can be connected to

the Arduino such as sensors, monitors, micro-servo motors and actuators based on the needed role. Overall, the simulation outcomes were promisingly close to the sensors values in the prototype within a reasonable difference. This validation study will be used as a steady base to use 'Arduino board within the actuators' as a controlling mechanism method, in addition to a step forward to improve the performance of such system via applying integrated parametric control which will be discussed in the next chapter.

Chapter 5 Combining the Parametric Louvre with Advanced Glazing and Chamfered Ceiling for Better Daylighting Uniformity

5.1 Introduction

Advanced louvres and other types of shading devices [12] are used to maximise the benefits of daylight [68], reduce solar heat gain in the summer, [291] save energy[71, 292], provide visual comfort and improve the occupants' efficiency [4, 258]. However, a previous study revealed that 80 – 90% of respondents believed that conventional window blinds are used only as a shading device to protect from excessive light more than thermal comfort and energy saving [293]. It has been found that using automated blinds can reduce the users' behaviour of turning on the electric light, which can save electrical energy up to 30% due to the utilisation of daylight [258]. In order to improve daylight penetration; reflective shelves [56, 248] and optical louvre systems (OLS) [137] have been used as Light Guiding System (LGS) to redirect sunlight into the deep interior of a building. Likewise; advanced type of smart-glass [294] such as Electrochromic (EC) and Thermochromic (TC) glazing, which also known as switchable glasses, are used as a Fenestration System (FS) to protect from glare and heat gain inside a room [295]. It is essential to keep the daylight within an accepted range for visual comfort [296] to control the occupants' interaction with the window shadings [293]; therefore, switchable windows can be used to adjust the interior daylight illumination level according to solar radiation intensity.

Although daylight penetration has been improved to various extents with those reported daylighting designs [297], the desired uniform distribution of daylight inside a room remains a challenge. EC and TC glazing in the current study will be utilised within the Parametric system to control and enhance the penetration of solar radiation inside the building [266] near to the window. Moreover, a simple shift will be added to the ceiling shape to improve the illuminance distribution at the deep-end of the room. Therefore, this chapter endeavours to integrate between; the Parametric Louvre, the advanced windows and the ceiling shape, aiming to maximise the use of daylight inside the building and to achieve daylight uniformity distribution within illuminance range of 300~500 lx [16, 17]. The proposed system will be introduced in Section *5.2*, while the combinations of these elements will be studied in five phases. Each phase will be investigated individually to identify the most suitable combination aiming to reach the desired daylight distribution. The performance of each element will be clarified in comparison in Section *5.3* at specified dates and then throughout some selected months [273].

5.2 Modelling method of the proposed system in an example office room by using Grasshopper

A south-oriented example office room is modelled with 4 m height, 7 m depth and 18 m length. The slats were set at the upper portion of the window between 2.2 m and 4 m height from the floor. A mirrored surface was added to the slats at the upper side with 70% reflectivity, while the bottom side of the slats is black matt painted with 0% reflectivity to absorb any specular light coming from the mirrored side of the following slat, and decrease any potential scattered light [248, 274]. Walls were set to white

matt with 80% reflectivity, while, the floor was set to dark matt with 0% reflectivity to absorb any potential reflections. Daylight illuminance will be measured using test points created in Honeybee, refer to section 3.2.1. The test points were set at desk level 70 cm high from the floor to measure the illuminance values at this level [16]. The grid size of the test points was set to 0.5 m, i.e. four points each square meter, as shown in Figure 5-1. EPW weather file was used for the location of Cairo in Egypt.

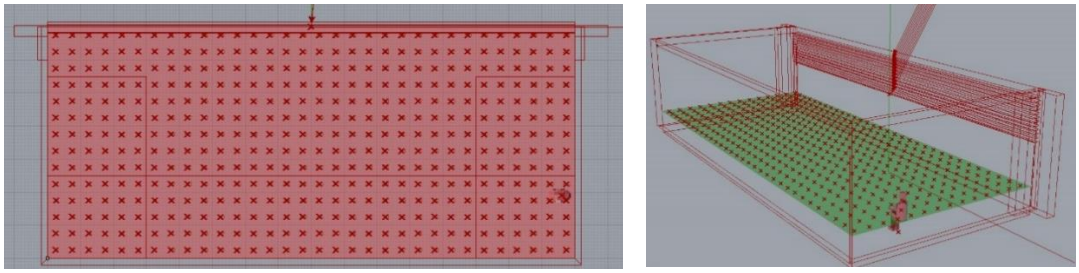
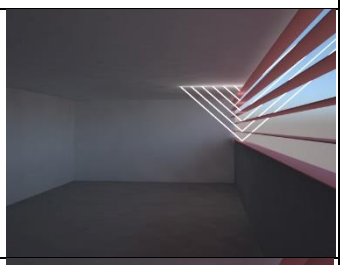
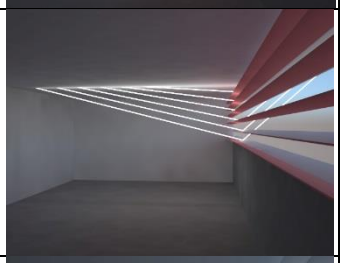
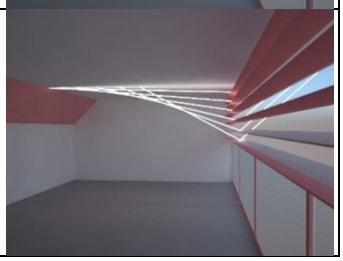


Figure 5-1: The test points distribution, top view exported from Rhinoceros 3D (Left), perspective view (Right)

5.3 Evolution phases of the integration between the Parametric Louvre with the advanced glazing and the chamfered ceiling by using parametric design

Daylight performance inside the room will evolve through five phases via changing parameters and adding elements, aiming to achieve better daylight distribution, see *Table 5-1*. Firstly, the comparison will use a fixed time and date at 12:00 p.m. on the 21st of September, in order to demonstrate the modelling method and to understand the phases from a precise ray-tracing study [247]. The chosen time and date represent equinox time, where, sun rays can give moderate tendency, meanwhile, count of slats were set to 12 based on sun altitude. Later on, time and date will be changed, in order to reveal the suitability and efficiency of the system at different times and dates throughout the year. It would also be seen that the number of slats will be adjusted for different months.

Table 5-1. List of modelling phases (changes between the phases appear in red italic).

Phase number	louvre type	Fixed slats addition	Glazing addition	Chamfered ceiling addition	Rendered image, exported from V-ray (3D Max)
Phase 1	*Conventional* louvre	No	No	No	
Phase 2	*Parametric* normal louvre	*Yes*	No	No	
Phase 3	Parametric *reversed* louvre	Yes	No	No	
Phase 4	Parametric reversed louvre	Yes	*Electrochro mic* glazing	No	
Phase 5	Parametric reversed louvre	Yes	Electrochro mic glazing	*Yes*	

5.3.1 Phase 1; using conventional louvre

In Phase 1, the slats' width of the louvre was set to 10 cm and 0° tilt angle at their conventional shape, which is considered the best state of utilising daylight [278], putting in consideration the influence of specular and diffuse light coming from the louvre and the skydome [274]. The louvre is not controlled parametrically, so the reflected light would not go to any specified points as expected in the other modelling phases. In other

words, the louvre in this phase is static and not responding to the sun movement similar to the Optical Louvre System (OLS) [137], therefore, as long as the sun moves; the light will be reflected to different points on the ceiling, unlike the fixed target points for the parametrically controlled louvre in the other modelling phases. The lower portion of the window under the louvre was opaque in Phase 1, 2 & 3 to demonstrate particularly the effect of the reflected light produced by the louvre.

5.3.2 Phase 2; applying parametric control to the rotating louvre with the addition of fixed slats shade

The louvre in Phase 2 was set parametrically to respond to the sun movement, where, reflected light is redirected to some specific targets on the ceiling wherever the sun moves (this method was demonstrated in section *3.2.2*) [247]. In this phase, fixed slats were added to the rotating mirrored louvre (as a protrusion) in a parallel direction with the reflected beams and connected through the rotation axis, as shown in Figure 5-2. These fixed slats are black matt painted with 0% reflectivity with 25 cm length, to absorb any potential scattered light. Because, the study focused on the influence of the redirected light only.

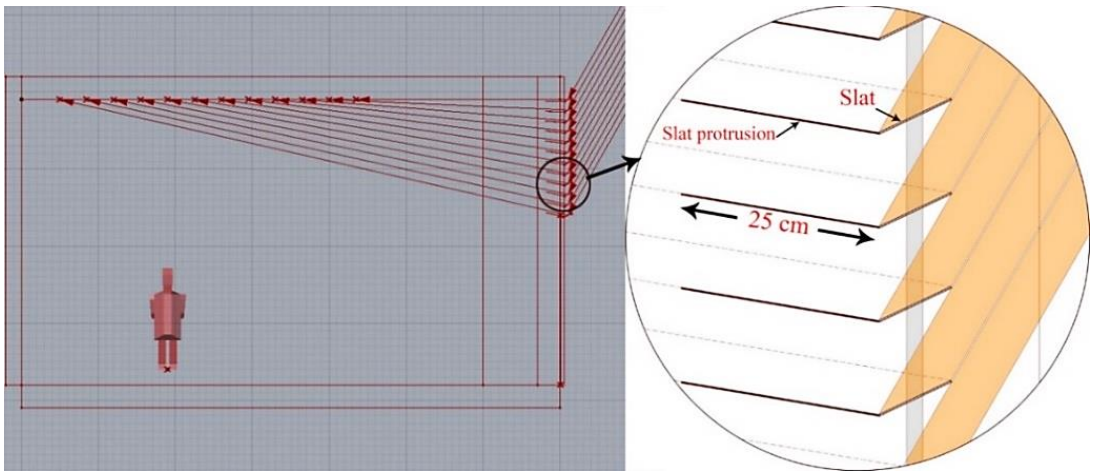


Figure 5-2: Detailed cross-section for the fixed slats shade.

In Phase 2, the louvre reflected the sunlight to the ceiling in a typical sequence, that is, the uppermost slat reflects light to the closest point from the window, and the second slat reflects light to the next target further from window, et cetera, as shown in Figure 5-2. The targets were specified parametrically in Grasshopper at some fixed points on the ceiling. That means as long as the sun moves, the louvre will respond to its movement in a Heliotropic response [21], to reflect sunlight to the fixed targets. Distance between the targets are equidistant, the first target is 240 cm away from the window, and the last target is 50 cm away from the wall.

5.3.3 Phase 3; reversing the slats' targeting of the rotating louvre, parametrically

The settings in this phase are similar to Phase 2, except for the slats' targeting sequence, which was reversed parametrically, that is, the uppermost slat reflects light towards the farthest point from window (the closest point to wall) and the lowermost slat reflects light to the target point closest to the window, etcetera, see *Figure 5-3* and *Table 5-1*.



Figure 5-3: Side view of the reversed targeting sequence.

5.3.4 Phase 4; Adding Electrochromic and Thermochromic windows to the Parametric Louvre

In addition to the previous phase, an Electrochromic (EC) glass [298] was added to the lower portion of the window below the louvre, as shown in *Table 5-1*. EC window is an advanced type of switchable glass. It has

been chosen for this study because of its significant function of light transmission control which can transfer from transparent to translucent state [252, 266, 294] by a small applied voltage between double glazing void [266] or electronic pulses applied to thin film attached to the window via operator controller. EC window will work as a source of diffuse light to lit the area near to the window within 2 m depth [299]. The amount of diffuse light provided by EC window is controlled parametrically in Grasshopper [295] based on the needed amount of illuminance, which was assigned between 300 ~ 500 lx and adapted by using test points at the desk level.

The adaptation process will be specified by using a specific component in the Honeybee plugin called "Honeybee Translucent Material" [300]. This component has several parameters such as 'reflectivity, specularity, diffuse transmission and roughness'. Whereas, "Diffuse transmission" is responsible for the translucency function. Diffuse transmission can be set between 0.01 (almost opaque) and 1 (transparent), while any value in-between specifies the transmittance amount. A formula was created in Grasshopper to control daylight penetration (solar intensity). The formula represents a relation between diffuse transmission and solar radiation intensity. Following many trials, the diffuse transmission of translucent material was determined at 0.01 ~ 0.07 (as a translucency level), in order to control the daylight illuminance within 300 ~ 500 lx at the adjacent area to the window, under the prevailing clear sky condition in New Cairo. For instance, if solar radiation is 790 W/m²; the diffuse transmission will be automatically set to 0.01, so the daylight penetration will be reduced from 20,000 lx to 400 lx.

EC materials can be altered and adjusted automatically via using a dimmer controller in order to control the solar energy transmittance [301], which accordingly is controlled parametrically in our case using Grasshopper within the whole system [273] aiming to stabilise the penetrated illuminance level at the desk level between 300 ~ 500 lx.

Thermochromic window has been added at the upper part of the window to control the intensity penetration of solar radiation. *(TC will be investigated in Chapter 7)*

5.3.5 Phase 5; adding a chamfered ceiling to the Parametric Louvre

In this phase, the integration of all phases is completed after applying a simple modification to the ceiling. This modification revealed in a chamfered section added at the farthest end of the ceiling, as shown in Figure 5-4 (Bottom). A previous study by A. Freewan [140] proved that adding a curved shape to the ceiling at the end of the room can improve light distribution up to 10%. In our study, the results show that chamfered ceiling is giving better distribution by approximately 3% more than the curved ceiling, while it acts as a second diffuser reflector, as shown in *Figure 5-4*. Furthermore, the chamfered ceiling is more practical and more manageable in installation. The chamfered ceiling was installed at the end of the room at a 45° angle with the ceiling.

To summarise, the integration between the previous five phases can be considered as an "Integrated Parametric Louvre" as an upgraded phase of the "Parametric Louvre", which can dramatically maximise the use of daylight inside the building.

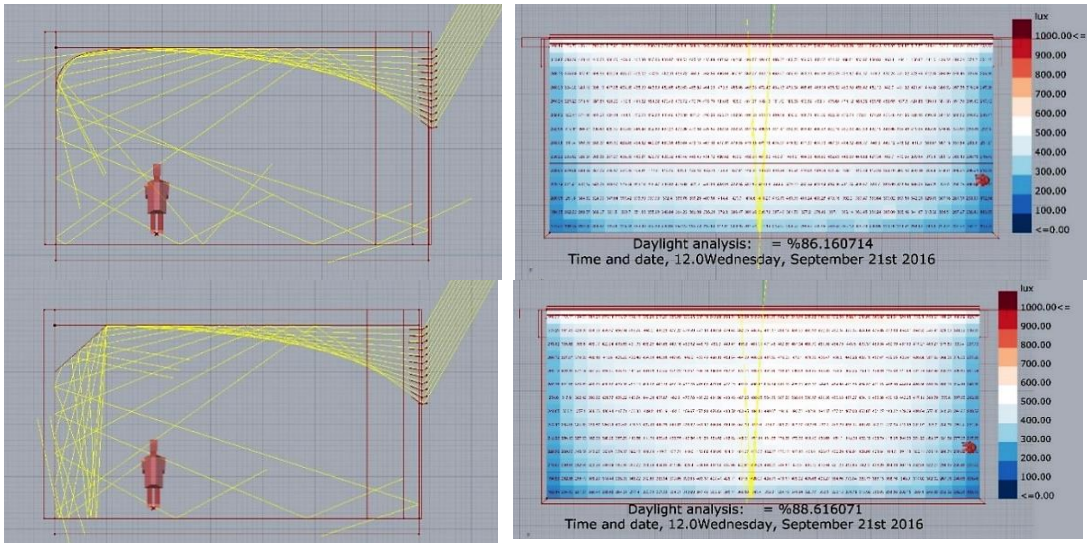


Figure 5-4: Comparison between the curved and chamfered ceiling, using raytracing and test points. The curved ceiling results in 86% area between 300~500 lx (Top), while the chamfered ceiling results in 88.6% between 300~500 lx (Bottom).

5.4 Comparison study between the phases of the Integrated Parametric Louvre on the 21st of September at noontime

A comparison study has been illustrated in Figure 5-5 with two analysis criteria, raytracing analysis and illuminance map at the desktop level, aiming to determine the percentage area coverage for the required daylight illumination between 300 ~ 500 lx. It is worth to mention that the raytracing analysis is for illustration only, and does not mean specular reflective surfaces. It can be observed in Figure 5-5 Phase 1 that almost 100% of the room at the desktop level exceeding 1000 lx at the chosen date and time. The reason for this excessive amount of light is the high intensity of solar radiation which increases the scattered light, and then produces an excessive illumination. Therefore, the slats should be set to 45° tilt angle to block off sunlight completely and allow diffuse light penetration only as shown in Figure 5-6. However, even so, this leads to a noticeable contrast in daylight distribution with a much brighter pattern near the window, as seen in Figure 5-6 (Right). Although all rays were

blocked, daylight analysis revealed irregular distribution, starting from 1000 lx near to the window and ending with 200 lx near to the wall.

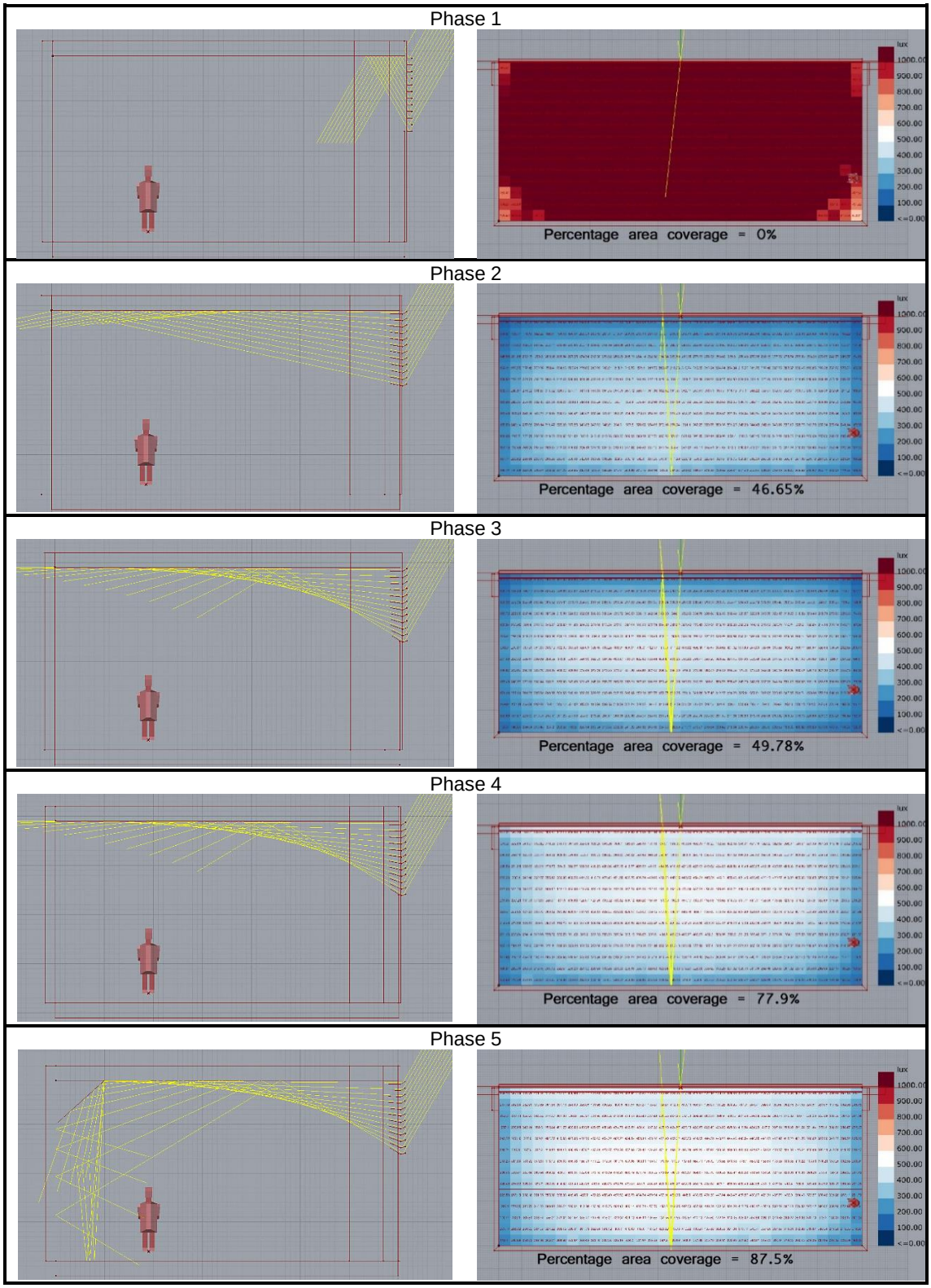


Figure 5-5: side view, illustrating raytracing study; starting from the top with conventional slats, and ending with the Parametric sequence-reversed louvre with EC window and chamfered ceiling, respectively (Left). The percentage coverage area for the daylight illuminance range between 300 - 500 lx (Right).

In Phase 2, daylight illuminance distribution gives acceptable value of 46.6% coverage for the daylight illuminance range of 300~500 lx, due to the parametrically rotated slats, in addition to the added fixed slats which helped to shade any excessive light at the area near the window. The results of daylight distribution were achieved mainly from the reflected light. In Phase 3, a fundamental change can be observed in the raytracing due to the reversed targeting sequence, in addition to the difference in daylighting coverage which increases from 46.6% to 49.7%, resulted an improvement in daylight distribution at the given ranges 300 ~ 500 lx.

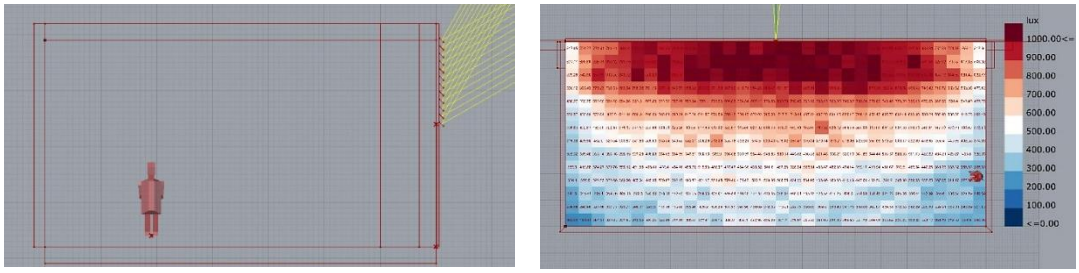
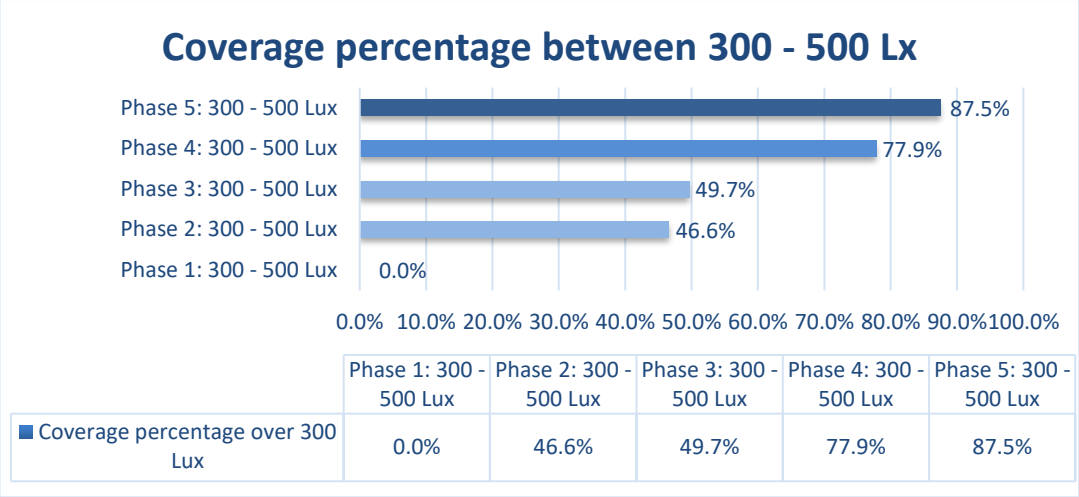


Figure 5-6: Conventional slats with 45° tilt angle (Left) side view, (Right) top view.

In Phase 4, 28% enhancement has been achieved after adding the electrochromic window, which influenced the coverage area near to the window, via providing sufficient amount of daylight at this area. Consequently, daylight coverage area increased in this phase to 77.9%, which considered a significant improvement compared to the previous one, as shown in Figure 5-7.

In Phase 5, a full distribution is covering the whole area after adding the chamfered ceiling, which achieved 87.5% area coverage for the daylight illuminance range of 300~500 lx. The chamfered ceiling in this phase has an obvious impact on the illumination at the deep area of the room by 10% improvement compared to Phase 4, as shown in Figure 5-5.

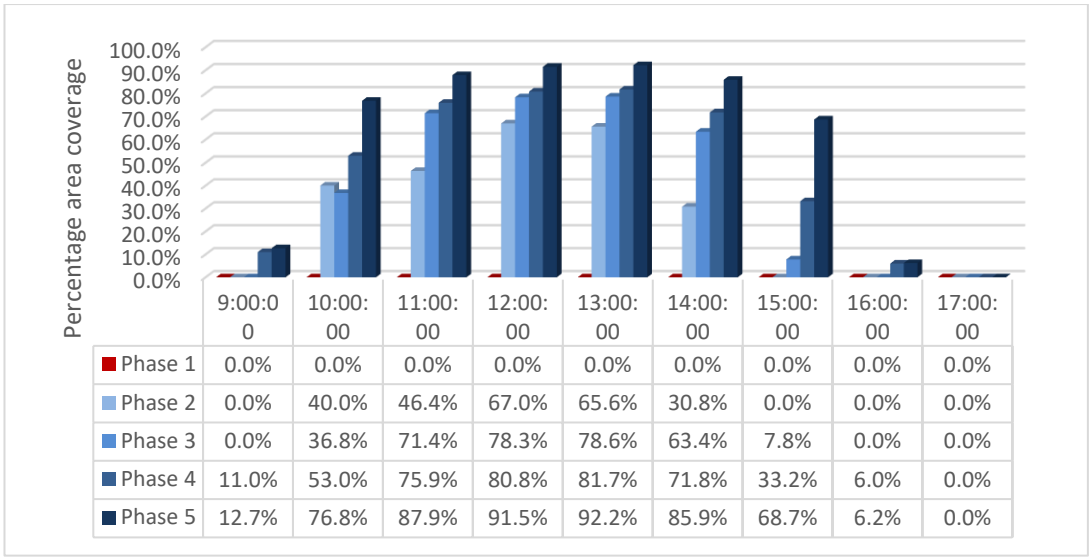


	Phase 1: 300 - 500 Lux	Phase 2: 300 - 500 Lux	Phase 3: 300 - 500 Lux	Phase 4: 300 - 500 Lux	Phase 5: 300 - 500 Lux
Coverage percentage over 300 Lux	0.0%	46.6%	49.7%	77.9%	87.5%

Figure 5-7: Bar graph showing the coverage percentage between 300 ~ 500 Lx for the five phases on September 21st at noontime.

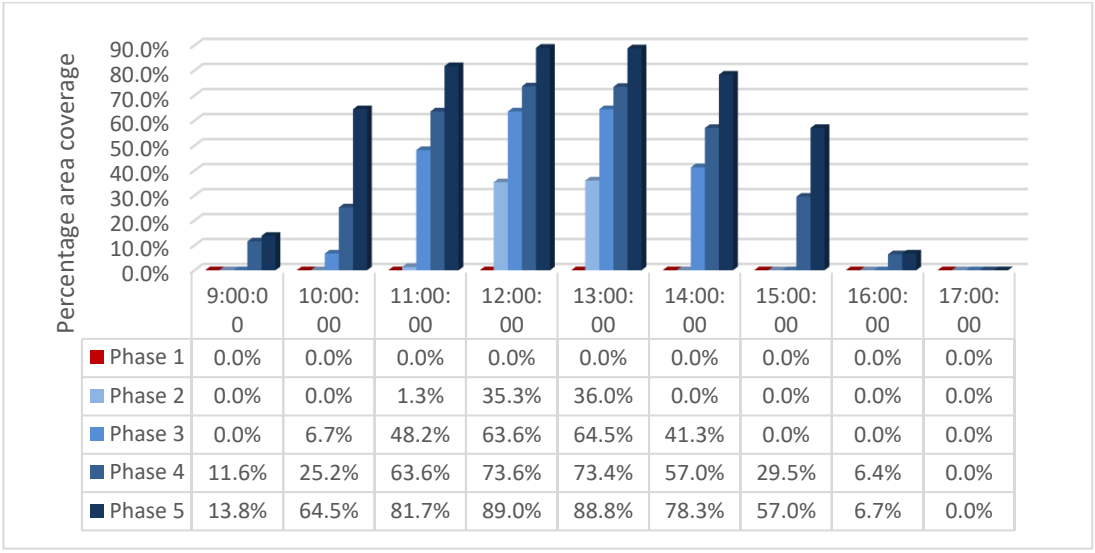
5.5 Comparison study for the Integrated Parametric Louvre during the working hours on the 21st of each month from June to December

Further comparisons were made for these five phases on the 21st of the months from June to December, respectively, during the regular working hours. In these comparisons; the number of slats and their tilt angle were changed parametrically, according to the changes of solar trajectories in different seasons. In winter, sun altitude is lower than in other seasons, and solar radiation is relatively weak. Therefore, the number of slats should be increased in order to prevent the penetration of sunlight due to its low inclination at this time, and simultaneously reflect larger amount of daylight to compensate the weakness of solar radiation [22]. For the latitude of new Cairo, the sun altitude reaches 83° at the zenith in the summertime in June [290]. As well, the first target point on the ceiling needs to be changed parametrically to 40 cm away from the window in November and December in order to compensate solar radiation weakness at the deep room area, while the EC window transmittance was increased to allow more daylight.



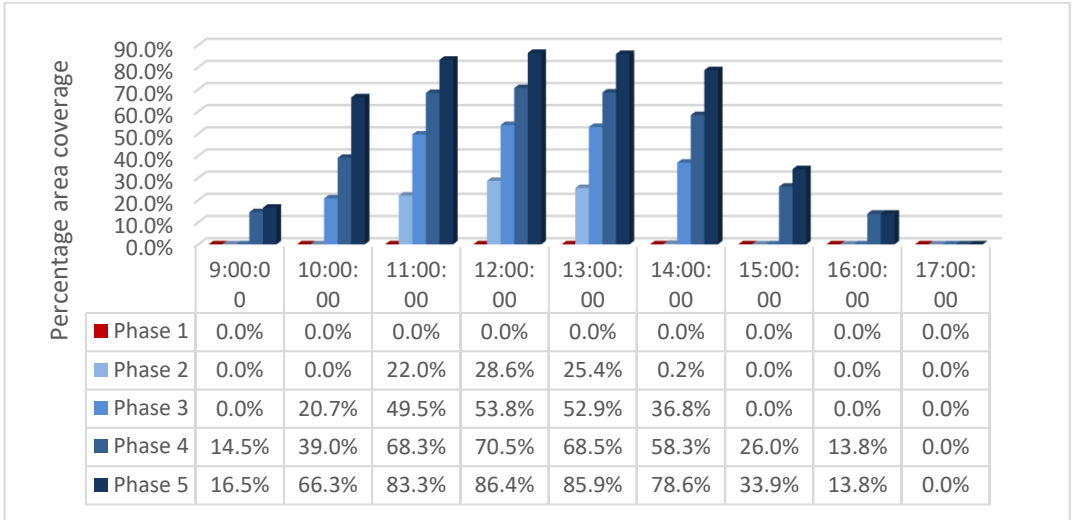
	9:00:00	10:00:00	11:00:00	12:00:00	13:00:00	14:00:00	15:00:00	16:00:00	17:00:00
Phase 1	0.0%	0.0%	0.0%	0.0%	0.0%	0.0%	0.0%	0.0%	0.0%
Phase 2	0.0%	40.0%	46.4%	67.0%	65.6%	30.8%	0.0%	0.0%	0.0%
Phase 3	0.0%	36.8%	71.4%	78.3%	78.6%	63.4%	7.8%	0.0%	0.0%
Phase 4	11.0%	53.0%	75.9%	80.8%	81.7%	71.8%	33.2%	6.0%	0.0%
Phase 5	12.7%	76.8%	87.9%	91.5%	92.2%	85.9%	68.7%	6.2%	0.0%

Figure 5-8: Coverage percentage for the daylight illuminance range of 300 - 500 lx during working hours on 21st of June



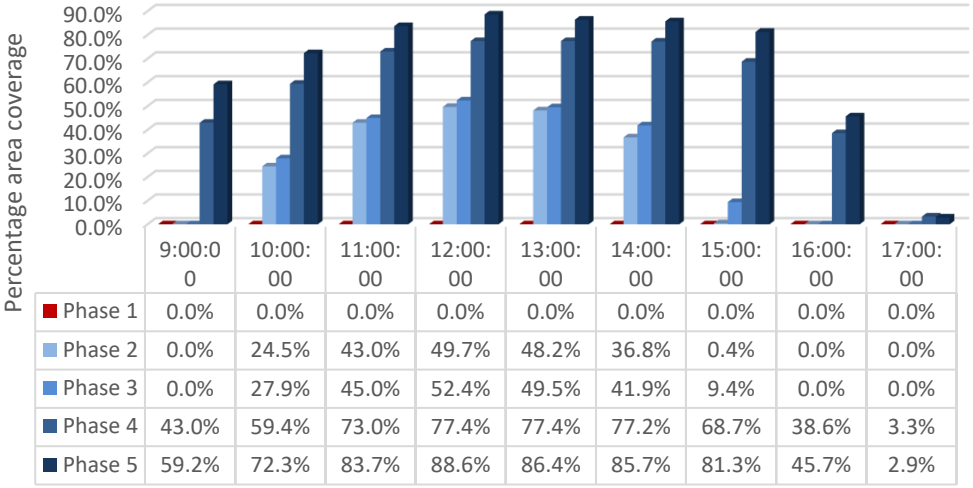
	9:00:00	10:00:00	11:00:00	12:00:00	13:00:00	14:00:00	15:00:00	16:00:00	17:00:00
Phase 1	0.0%	0.0%	0.0%	0.0%	0.0%	0.0%	0.0%	0.0%	0.0%
Phase 2	0.0%	0.0%	1.3%	35.3%	36.0%	0.0%	0.0%	0.0%	0.0%
Phase 3	0.0%	6.7%	48.2%	63.6%	64.5%	41.3%	0.0%	0.0%	0.0%
Phase 4	11.6%	25.2%	63.6%	73.6%	73.4%	57.0%	29.5%	6.4%	0.0%
Phase 5	13.8%	64.5%	81.7%	89.0%	88.8%	78.3%	57.0%	6.7%	0.0%

Figure 5-9: Coverage percentage for the daylight illuminance range of 300 - 500 lx during working hours on 21st of July



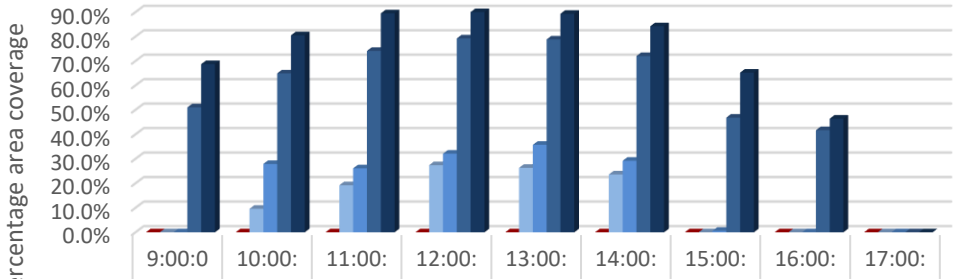
	9:00:00	10:00:00	11:00:00	12:00:00	13:00:00	14:00:00	15:00:00	16:00:00	17:00:00
Phase 1	0.0%	0.0%	0.0%	0.0%	0.0%	0.0%	0.0%	0.0%	0.0%
Phase 2	0.0%	0.0%	22.0%	28.6%	25.4%	0.2%	0.0%	0.0%	0.0%
Phase 3	0.0%	20.7%	49.5%	53.8%	52.9%	36.8%	0.0%	0.0%	0.0%
Phase 4	14.5%	39.0%	68.3%	70.5%	68.5%	58.3%	26.0%	13.8%	0.0%
Phase 5	16.5%	66.3%	83.3%	86.4%	85.9%	78.6%	33.9%	13.8%	0.0%

Figure 5-10: Coverage percentage for the daylight illuminance range of 300 - 500 lx during working hours on 21st of August



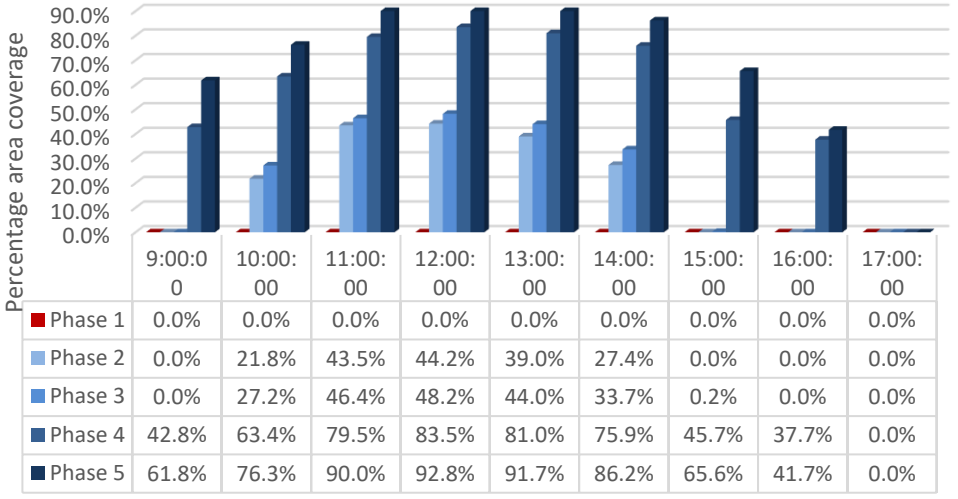
	9:00:00	10:00:00	11:00:00	12:00:00	13:00:00	14:00:00	15:00:00	16:00:00	17:00:00
Phase 1	0.0%	0.0%	0.0%	0.0%	0.0%	0.0%	0.0%	0.0%	0.0%
Phase 2	0.0%	24.5%	43.0%	49.7%	48.2%	36.8%	0.4%	0.0%	0.0%
Phase 3	0.0%	27.9%	45.0%	52.4%	49.5%	41.9%	9.4%	0.0%	0.0%
Phase 4	43.0%	59.4%	73.0%	77.4%	77.4%	77.2%	68.7%	38.6%	3.3%
Phase 5	59.2%	72.3%	83.7%	88.6%	86.4%	85.7%	81.3%	45.7%	2.9%

Figure 5-11: Coverage percentage for the daylight illuminance range of 300 - 500 lx during working hours on 21st of September



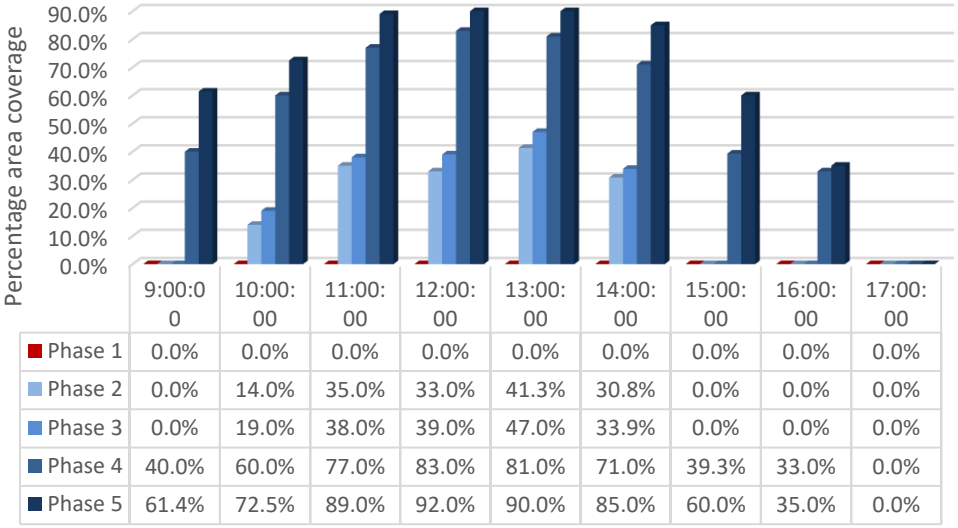
	9:00:00	10:00:00	11:00:00	12:00:00	13:00:00	14:00:00	15:00:00	16:00:00	17:00:00
Phase 1	0.0%	0.0%	0.0%	0.0%	0.0%	0.0%	0.0%	0.0%	0.0%
Phase 2	0.0%	9.6%	19.2%	27.4%	26.3%	23.6%	0.0%	0.0%	0.0%
Phase 3	0.0%	27.9%	26.1%	32.1%	35.7%	29.2%	0.6%	0.0%	0.0%
Phase 4	51.0%	64.9%	74.1%	79.2%	78.8%	72.0%	46.8%	41.7%	0.0%
Phase 5	68.7%	80.5%	89.5%	91.7%	89.3%	84.2%	65.2%	46.4%	0.0%

Figure 5-12: Coverage percentage for the daylight illuminance range of 300 - 500 lx during working hours on 21st of October



	9:00:00	10:00:00	11:00:00	12:00:00	13:00:00	14:00:00	15:00:00	16:00:00	17:00:00
Phase 1	0.0%	0.0%	0.0%	0.0%	0.0%	0.0%	0.0%	0.0%	0.0%
Phase 2	0.0%	21.8%	43.5%	44.2%	39.0%	27.4%	0.0%	0.0%	0.0%
Phase 3	0.0%	27.2%	46.4%	48.2%	44.0%	33.7%	0.2%	0.0%	0.0%
Phase 4	42.8%	63.4%	79.5%	83.5%	81.0%	75.9%	45.7%	37.7%	0.0%
Phase 5	61.8%	76.3%	90.0%	92.8%	91.7%	86.2%	65.6%	41.7%	0.0%

Figure 5-13: Coverage percentage for the daylight illuminance range of 300 - 500 lx during working hours on 21st of November



	9:00:00	10:00:00	11:00:00	12:00:00	13:00:00	14:00:00	15:00:00	16:00:00	17:00:00
Phase 1	0.0%	0.0%	0.0%	0.0%	0.0%	0.0%	0.0%	0.0%	0.0%
Phase 2	0.0%	14.0%	35.0%	33.0%	41.3%	30.8%	0.0%	0.0%	0.0%
Phase 3	0.0%	19.0%	38.0%	39.0%	47.0%	33.9%	0.0%	0.0%	0.0%
Phase 4	40.0%	60.0%	77.0%	83.0%	81.0%	71.0%	39.3%	33.0%	0.0%
Phase 5	61.4%	72.5%	89.0%	92.0%	90.0%	85.0%	60.0%	35.0%	0.0%

Figure 5-14: Coverage percentage for the daylight illuminance range of 300 - 500 lx during working hours on 21st of December

Generally, it can be seen that the electrochromic window and chamfered ceiling playing a crucial role in improving daylight distribution during the working hours, especially at the first and last hours. For instance, at 9 a.m. and 3 p.m. on the 21st of September, there is almost no direct sunlight shining on the south-facing window, and the Integrated Louvre delivers limited daylight at the time, so this lack of direct sunlight can be compensated by the diffuse light from the EC window.

During the working hours, the design of Phase (5) is providing relatively constant distribution from 10 a.m. to 3 p.m. with a percentage area coverage of 70 ~ 80%. Then this coverage is strongly stooped till reaching 0% at 5 p.m. At 9 a.m. around 40% of illumination covering the desktop area, accordingly, electrical light can be used to compensate the lack of natural daylight, and the electric light should be then gradually swished off till approaching 10 a.m. On the contrast, at 4 p.m., 50% of electrical light can be used to compensate the diminishing of daylight, then this backup should gradually increase to 100% at 5 p.m. Therefore, we can deduce that electrical light should be used partially only in the first and last two

hours of the day for the location of Cairo. Accordingly, using the proposed integrated design can save the lighting electricity consumption up to 80% during the working hours.

It can be seen in Figure 5-8 that the influence of the reflective slats is relatively evident in June, when the sun altitude is almost at zenith, therefore, the slats are playing a significant role in collecting more sunlight, as revealed in Phase 3 in Figure 5-8, which is giving higher values compared to the following months. On the other hand, in October, November and December, the design of Phase (5) is more relied on the use of the EC window and chamfered ceiling as shown in Figure 5-12**,** Figure 5-13 and Figure 5-14, where, solar altitudes are dramatically low, especially at 9 a.m. and 4 p.m. and accordingly produces lower Intensity.

5.6 Analysis discussion for the Integrated Parametric Louvre

When analysing the "False colour fisheye maps" in Figure 5-15, we can observe that light distribution in Phase 2 is more uniform than Phase 3 at the first impression, however, light distribution on the ceiling is not our purpose. The reflected light striking the ceiling surface shows a somewhat strong effect in Phase 3 comparing to Phase 2, which contributes better distribution of daylight at the desk level. Additionally, it can be observed in Phase 2 in Figure 5-15 a blue area on the wall, which means that the wall absorbed the reflected light on the ceiling as a second bounce rather than to the working area. While, the blue area on the wall in Phase 3 is relatively weak and faded, which means that the reflected light is more concentrated onto the horizontal area.

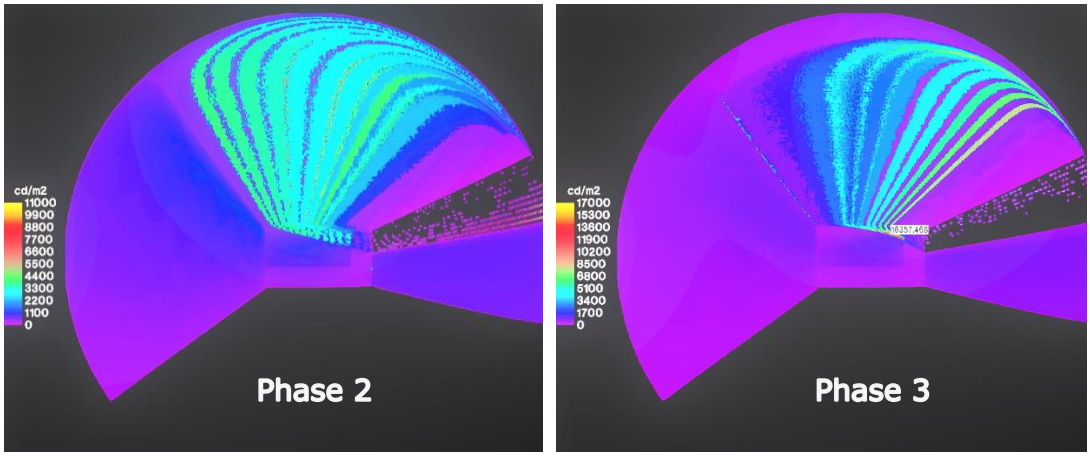


Figure 5-15: False-colour fisheye maps exported from Honeybee plugin; showing the reflected light distribution on the ceiling. Phase 2 (Left), Phase 3 (Right).

Regarding the sequence of the louvre; the reflection from the lowermost slat in Phase 2 may have a risk of being blocked by any obstacles in the room, while it is the closest slat to the occupants. However, in Phase 3 this issue was relatively solved by reversing the targeting sequence parametrically, which means that the uppermost slat will reflect light to the farthest target point on the ceiling with little risk of blocking, and likewise for the next slats respectively.

Excluding Phase 1 from the design, we can observe that the edges and corners in the room are relatively dim, due to the interception of light by the walls and the so-called penumbra effect [156] which may somewhat also influence on this illuminance reduction. These small areas near to the edges can be ignored because the occupants rarely use them in general workstations [302], which is usually half of a meter away from the walls. Accordingly, if the edges and corners which is around 12% of the total floor area were ignored in daylighting evaluation, the percentage area coverage for the daylight illuminance range of 300 ~ 500 lx would reach 100% for even more number of working hours. Therefore, it is reasonable to neglect

those edge areas in daylighting evaluation in order to give a more reasonable result for the office room.

Overall, each element in this integrated daylighting system has a significant utility for a specific time and function. Each element can perform higher in sometimes, to compensate for the weakness of the other elements at other times, and vice versa. Therefore, the combination of different utilities contributes to achieving a better distribution of daylight.

5.7 Summary

Chapter 5 investigated a combination between different architectural elements parametrically, in order to achieve more uniform daylight distribution inside an example office room, with New Cairo chosen as a location for the case study. The proposed design has been identified through a multi-step comparison study employing parametric design approach, aiming to improve the daylight distribution within the usable range of 300 ~ 500 lx. The first phase starts with fixed shade slats, and the daylighting system was then upgraded to the automated slats in Phase 2. Then the slats targeting sequence was reversed in Phase 3, which has slightly improved daylight distribution. In Phase 4, an EC and TC glasses have been added to the lower part and upper part of the window to control the penetration of daylight parametrically, resulting in a noticeable improvement in this phase. Finally, a chamfered ceiling was added in the interior design to complete the integrated system in Phase (5). The whole system was integrally connected and controlled parametrically using Grasshopper as a parametric software based on Rhinoceros 3D.

The first part of this chapter covers the detailed designs for the five phases at a specific time and date, in order to clarify the raytracing

distribution from the results and daylighting analysis. Then the following part reveals daylight performance for seven months from June to December on the 21st of each month during the working hours, to give a more comprehensive comparison.

The integrated designs in Phases (4) and (5) succeeded to improve daylight distribution inside the room by achieving an average 80% of the area coverage for the daylight illuminance range of 300 ~ 500 lx for most of the working hours. By neglecting the edges and corners of the room while they are not usually used; the percentage area coverage for the required daylight range can be even higher by an additional 10%. Accordingly, this integrated system based on parametric control is expected to save up to 80% of electrical lighting energy consumption.

This chapter focused on improving daylight distribution in a south-oriented deep-plan room in New Cairo by using Integrated Parametric Louvre. The following chapter will investigate the Integrated Parametric Louvre performance throughout the year in different orientations.

Chapter 6 Evaluating the Integrated Parametric Louvre in different orientations and throughout the year

6.1 Introduction

In buildings, daylighting is a primary source of lighting and a special element in enhancing architecture [36], which is improved recently by using advanced tools, software, and innovative daylighting systems [75]. Such new systems are using several methods [12, 123] based on different criteria such as type of building, location, orientation, and climate changes [22].

This Chapter will investigate the capability of providing daylight in an example office room in different circumstances, by using the preceding Integrated Parametric Louvre based on parametric control. Such a system was investigated previously in *Chapter 4* in a South oriented room in Egypt [273] and succeeded to achieve more than 80% of daylight availability during the working hours. The current Chapter will examine the performance of the system in different orientations, and then investigate the efficiency of this system throughout the year during the working hours in a different location such as the UK territory.

The method of this study, as usual, is based on parametric control using Grasshopper [263] for Rhinoceros 3D [262]. As mentioned formerly, Grasshopper is a flexible algorithmic software that can deal accurately with complex relations. The study will focus on the efficiency of provided daylighting by using this Integrated Parametric Louvre via analysing multiple comparisons, which can reveal the amount of energy saved [279].

6.2 Model description of the Integrated Parametric Louvre and Conventional Static Louvre for a comparison study

The proposed system has been applied in an example office room in Birmingham location in the UK, by using the EPW weather file and comparing it with a conventional louvre system in the same conditions.

1. *The room design*

The room dimensions are 18 m length, 8 m depth and 4 m clear height. Global horizontal radiation was used for the examination as a source of solar radiation measurement, and Climate Based Sky was used for the sky type to create the real condition of the ambient, where, the sky is not expected to be clear during the year in such type of territory. The experiment depends on two primary sources of light; firstly, the direct light, which is coming from sunlight with a clear sky that should be exploited by the reflective slats, and secondly, the diffused light coming from the skydome and clouds that should be exploited by the window. The slats are located at the upper part of the window from the outside, with 2.2 m height from the floor.

2. *The Conventional Static Louvre (CSL) design*

The Conventional Static Louvre (CSL) is a static system that consists of external aluminium slats, which arrayed vertically in a fixed sequence with zero tilt angle, the distance between each slat is 15 cm with 1 cm thickness and 15 cm depth, and assembled outside of the window.

3. *The Integrated Parametric Louvre (IPL) design*

The proposed Integrated Parametric Louvre (IPL) uses three main tools based on *Chapter 4* [273]. The first tool is the "mirrored slats" with 75%

reflectivity, the switchable windows and the chamfered ceiling with 45° tilt angle, see Figure 6-1. The number of slats was set to 10, with a fixed distance between each base on the threshold height of 2.2 m. Each slat is 15 cm depth, 1 cm thickness, and 18 m width to cover the room façade. The reflected light over the ceiling was set to fixed targets where the closest target is 3 m away from the window, and the farthest target is 7.4 m from the window.

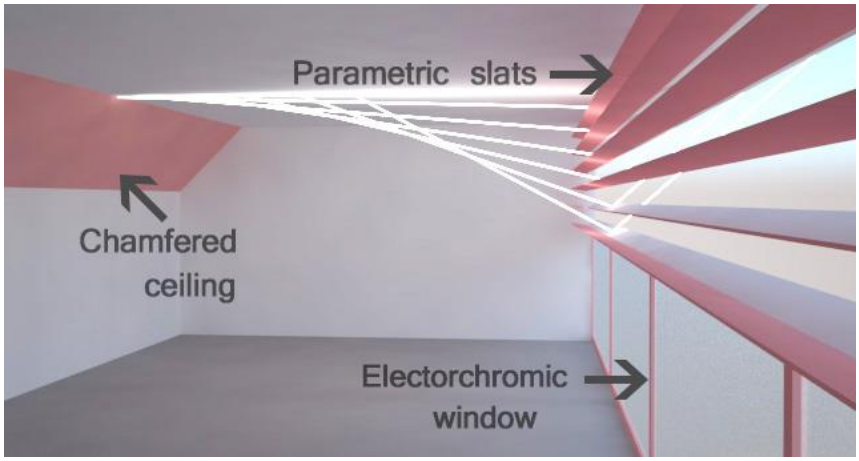


Figure 6-1: The proposed integrated parametric louvre, showing the three main tools (Rendered in V-Ray for 3D MAX).

6.3 Comparison criteria between the Integrated Parametric Louvre and the Conventional Static Louvre in different orientations

A comparison study has performed between two different systems; the IPL and the CSL. The office room will be examined in five different orientations; West, Southwest, South, Southeast, and East by using unified criteria, as shown in Figure 6-2. The daylight performance test will be performed on each orientation during the working hours from 9 a.m. to 5 p.m., on the 21st of June, 21st of September and 21st of December. The test will measure hourly coverage percentage of daylight over the whole room area, by using a one-meter square grid of test points at the desk level 0.75 m height. The experiment was tuned to achieve the illuminance

range 300 ~ 500 lx based on the guidance of the Chartered Institution of Building Services Engineers (CIBSE), a professional institution for lighting guide in the UK, which recommends the range of 300 ~ 500 lx as a standard daylighting level for offices spaces [303] and human visual comfort [16]. On the other hand, previous research claims that lighting level between 100~2000 lx can meet human visual comfort based on occupants' survey [45]. However, our study will focus on using the lighting level standard of 300~500 lx, putting into consideration the potential of scattered light and glare effect. Meanwhile, if we consider 100–2000 lx as a useful range for occupants, our study should be on the safe side.

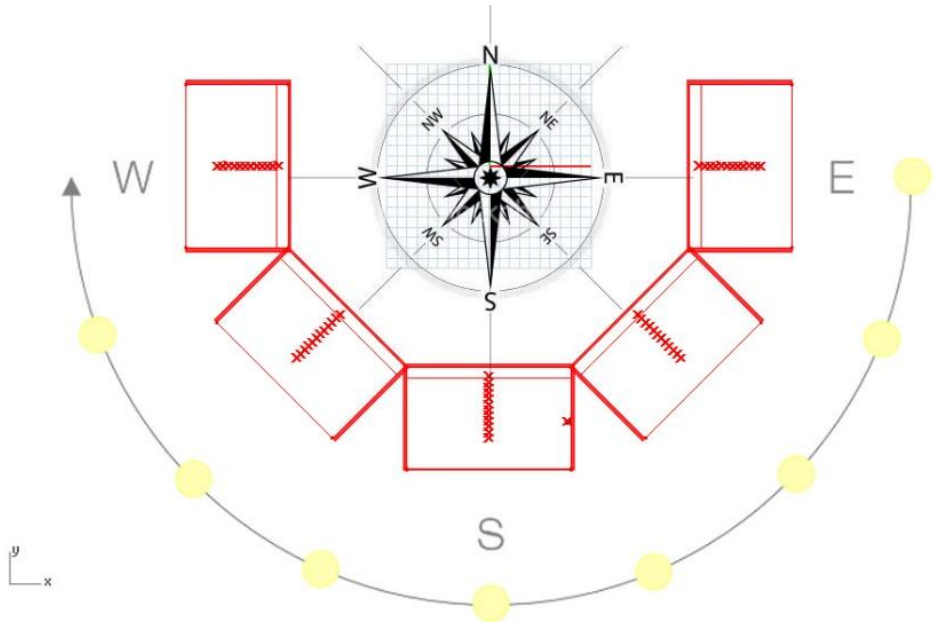


Figure 6-2: The five different orientations of the office room.

In Section *6.4*, the test will be performed during the working hours from 9 a.m. to 5 p.m. throughout the year on the South orientation, by using the integrated system. The test will clarify the illumination average per unit area by using radiation metrics Wh/m². Then, the results will be compared to the standard radiation needed for the office room by using EnergyPlus, which calculates 4.8 Wh/m² as a recommended luminous for the selected office room within the applied conditions.

6.3.1 Daylight coverage percentage analysis for the IPL and CSL on the 21st of June, 21st of September and 21st of December

The daylight analysis has been performed from 9 a.m. to 5 p.m., via using CSL and IPL at the south orientation only to clarify the simulation process and to understand the difference in coverage range between the two systems. The accepted range should be between 300~500 lx for human visual comfort.

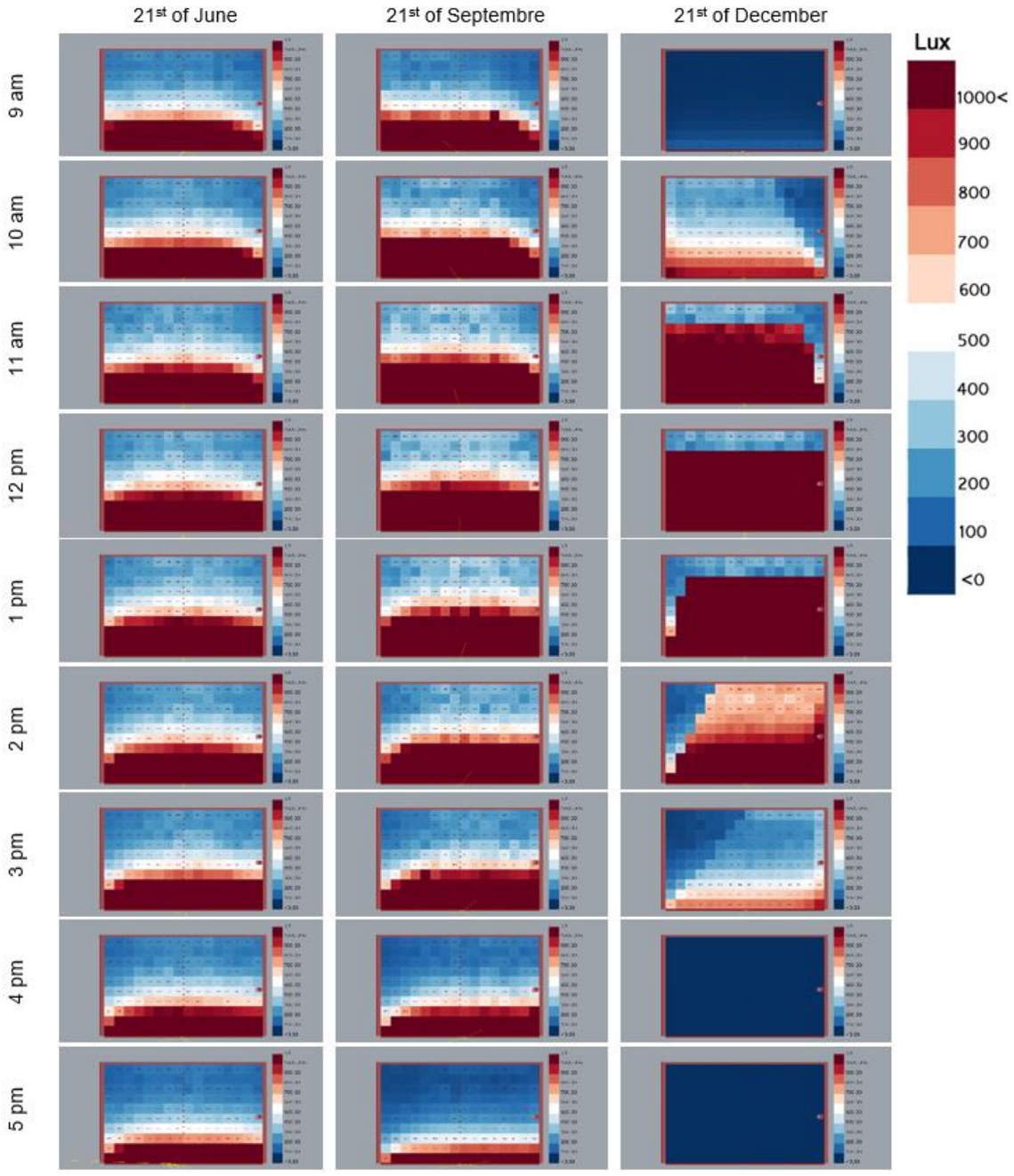


Figure 6-3: Daylight coverage percentage analysis during the working hours using the CSL for a south-oriented office room on 21st of June (a), 21st of September (b), and 21st of December (c).

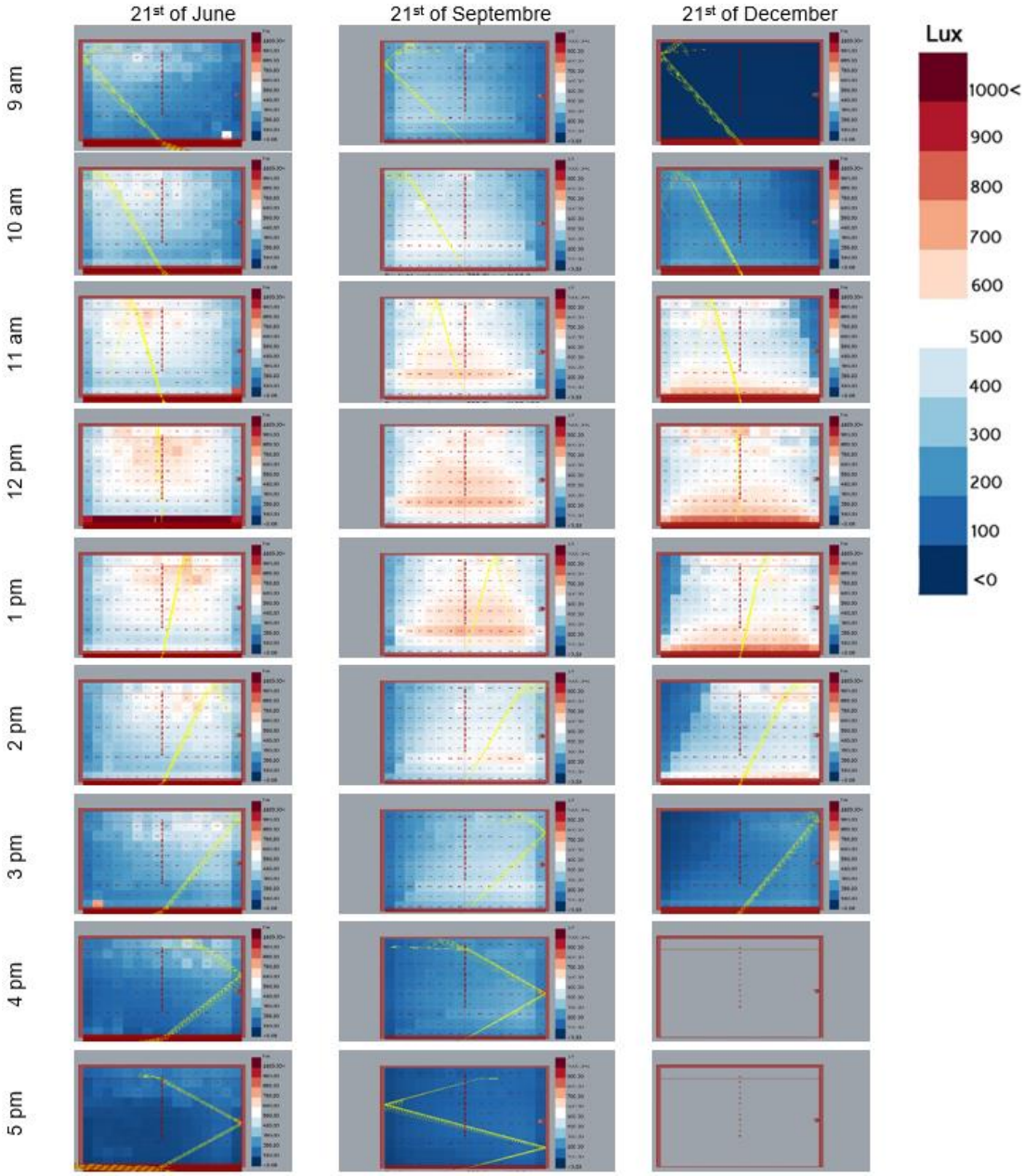
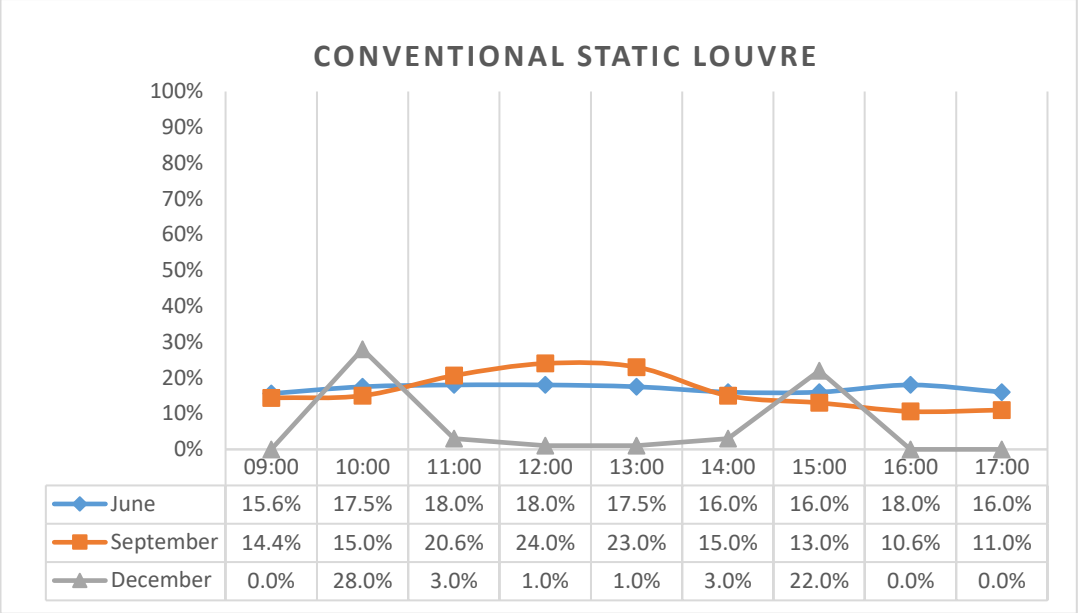


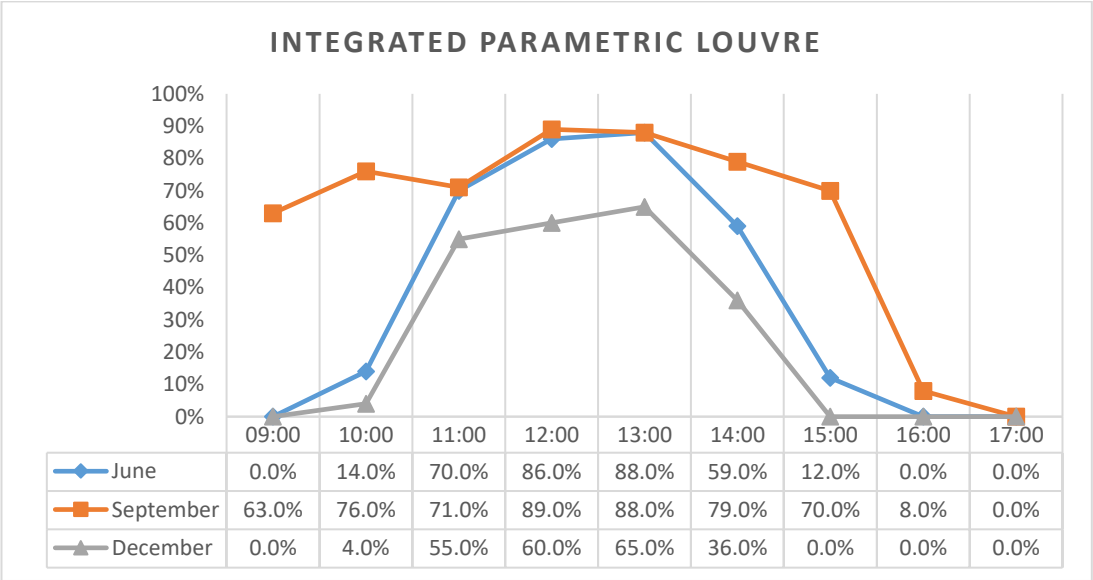
Figure 6-4: Daylight coverage percentage analysis during the working hours using the IPL for a south-oriented office room on 21st of June (a), 21st of September (b), and 21st of December (c).

The daylight coverage percentage by using both systems in Figure 6-3 and Figure 6-4 are summarised in the following diagrams. It can be seen in Figure 6-5 that daylight coverage percentage within the CSL did not exceed 28% of the recommended range 300~500 lx during the daytime in all months. However, in Figure 6-6, daylight coverage percentage reached 90% by using the IPL system.



	09:00	10:00	11:00	12:00	13:00	14:00	15:00	16:00	17:00
June	15.6%	17.5%	18.0%	18.0%	17.5%	16.0%	16.0%	18.0%	16.0%
September	14.4%	15.0%	20.6%	24.0%	23.0%	15.0%	13.0%	10.6%	11.0%
December	0.0%	28.0%	3.0%	1.0%	1.0%	3.0%	22.0%	0.0%	0.0%

Figure 6-5: Coverage percentage between 300~500 Lx during the working hours in 21st of June, 21st of September, and 21st of December by using the CSLS for the South oriented room.



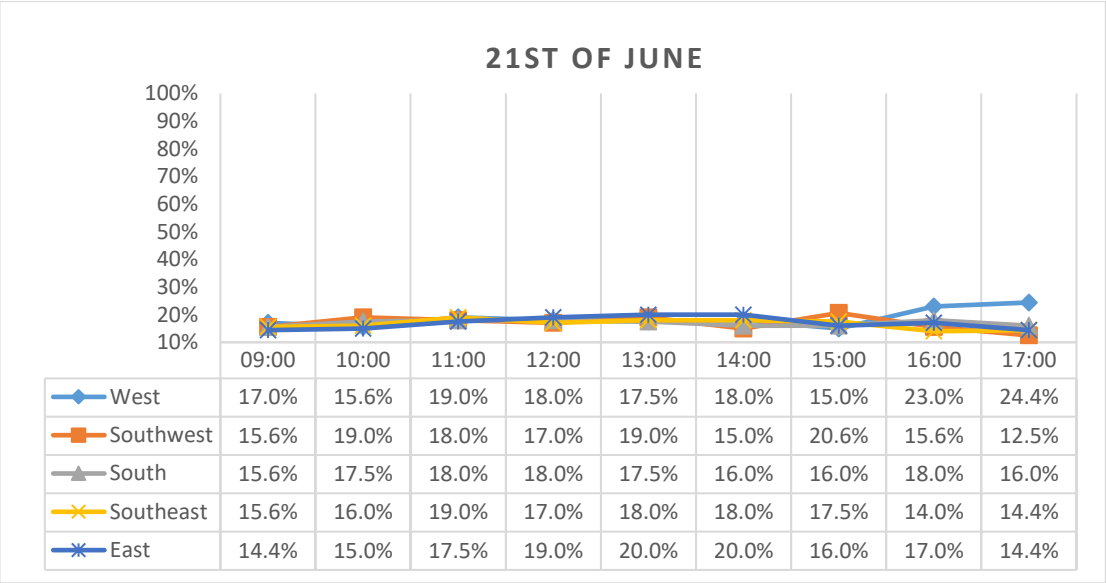
	09:00	10:00	11:00	12:00	13:00	14:00	15:00	16:00	17:00
June	0.0%	14.0%	70.0%	86.0%	88.0%	59.0%	12.0%	0.0%	0.0%
September	63.0%	76.0%	71.0%	89.0%	88.0%	79.0%	70.0%	8.0%	0.0%
December	0.0%	4.0%	55.0%	60.0%	65.0%	36.0%	0.0%	0.0%	0.0%

Figure 6-6: Coverage percentage between 300~500 Lx during the working hours in the 21st of June, 21st of September, and 21st of December by using the integrated parametric louvre for the South oriented room.

6.3.2 Daylight coverage percentage analysis on the 21st of June, 21st of September, and 21st of December for the CSL in different orientations during the working hours

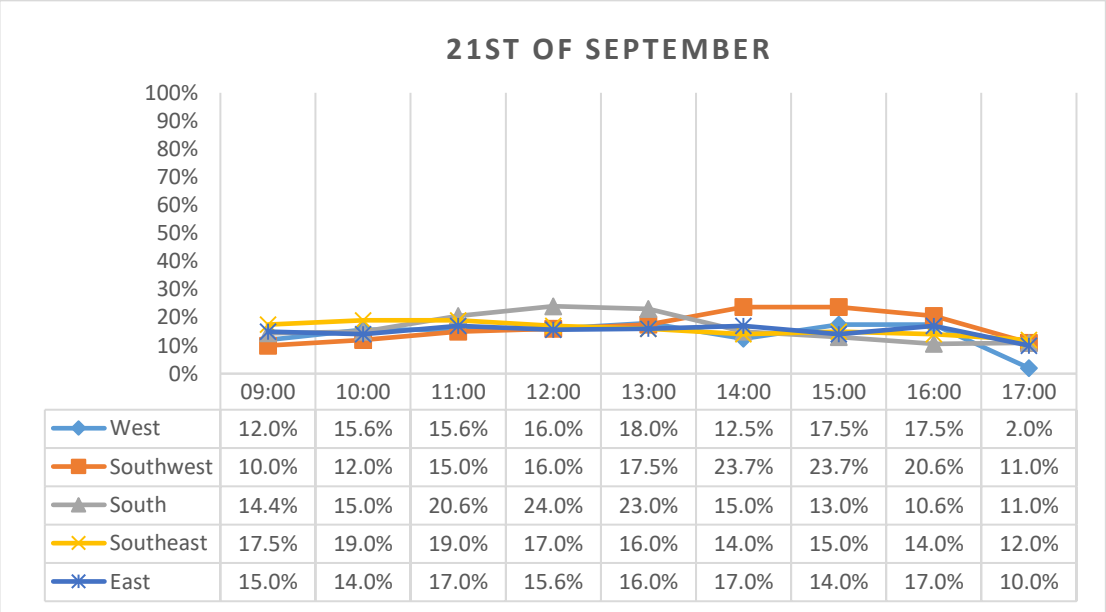
It can be observed in Figure 6-7 and Figure 6-8 that the conventional system does not exceed 25% coverage in June and September, however, it reaches 38% coverage on December at its peak due to the low inclination of the sun altitude, as shown in Figure 6-9, where it can reach more in-

depth coverage inside the room. Additionally, the illumination coverage is relatively constant during the daytime in June and September, while there is a notable variation during the daytime in December. Furthermore, it can be observed in Figure 6-10 that the coverage percentage in all different orientations are almost equal, which means that the conventional system has no tangible effect when changing orientation.



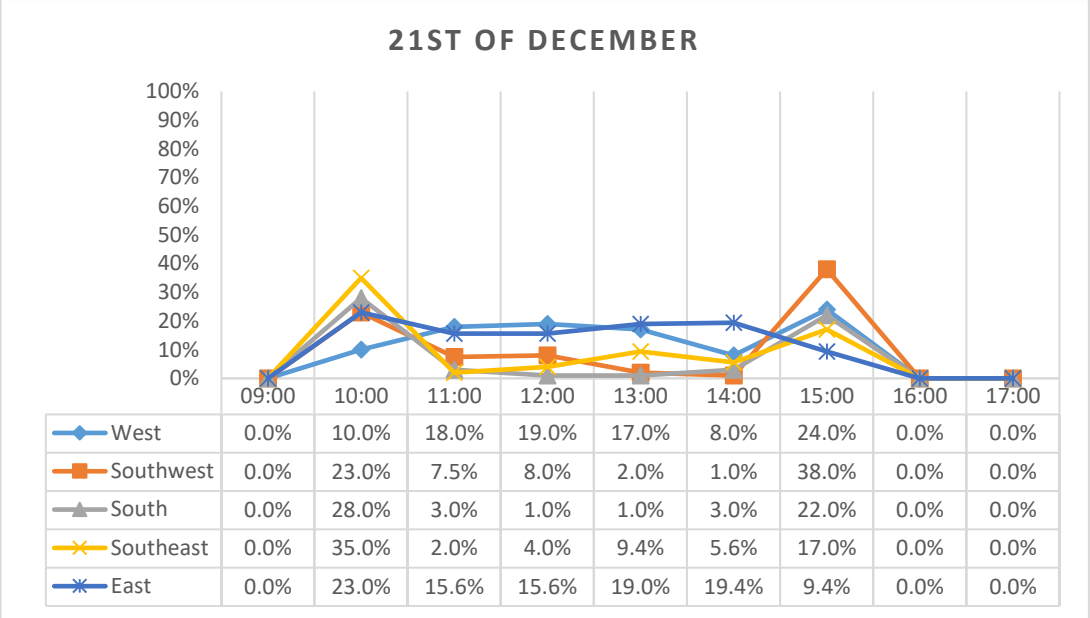
	09:00	10:00	11:00	12:00	13:00	14:00	15:00	16:00	17:00
West	17.0%	15.6%	19.0%	18.0%	17.5%	18.0%	15.0%	23.0%	24.4%
Southwest	15.6%	19.0%	18.0%	17.0%	19.0%	15.0%	20.6%	15.6%	12.5%
South	15.6%	17.5%	18.0%	18.0%	17.5%	16.0%	16.0%	18.0%	16.0%
Southeast	15.6%	16.0%	19.0%	17.0%	18.0%	18.0%	17.5%	14.0%	14.4%
East	14.4%	15.0%	17.5%	19.0%	20.0%	20.0%	16.0%	17.0%	14.4%

Figure 6-7: Coverage percentage between 300~500 Lx during the working hours for the office room through five orientations on the 21st of June, using the CSL.



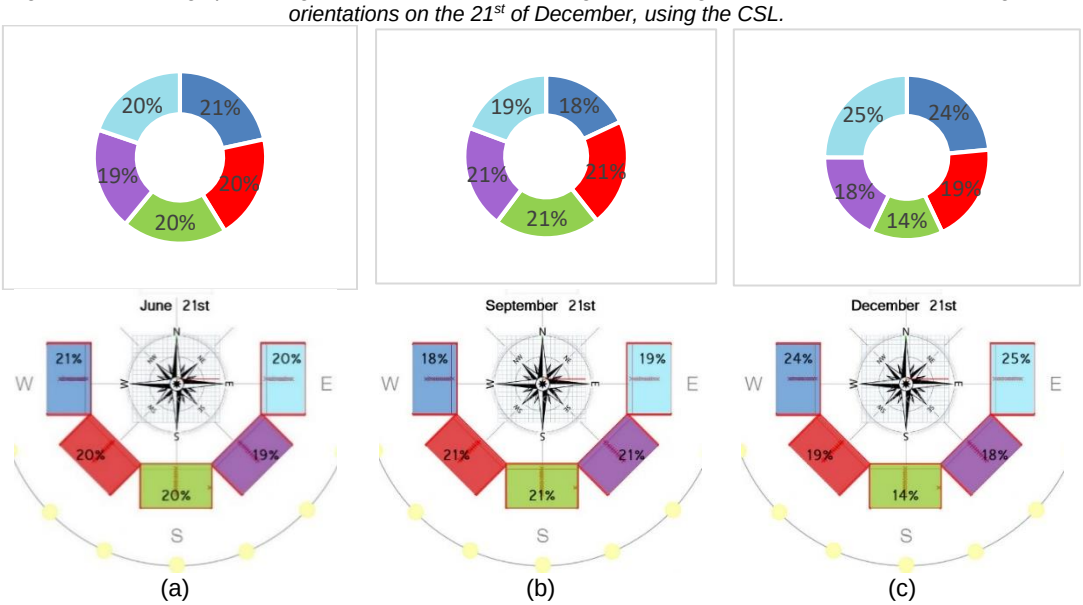
	09:00	10:00	11:00	12:00	13:00	14:00	15:00	16:00	17:00
West	12.0%	15.6%	15.6%	16.0%	18.0%	12.5%	17.5%	17.5%	2.0%
Southwest	10.0%	12.0%	15.0%	16.0%	17.5%	23.7%	23.7%	20.6%	11.0%
South	14.4%	15.0%	20.6%	24.0%	23.0%	15.0%	13.0%	10.6%	11.0%
Southeast	17.5%	19.0%	19.0%	17.0%	16.0%	14.0%	15.0%	14.0%	12.0%
East	15.0%	14.0%	17.0%	15.6%	16.0%	17.0%	14.0%	17.0%	10.0%

Figure 6-8: Coverage percentage between 300~500 Lx during the working hours for the office room through five orientations on the 21st of September, using the CSL.



	09:00	10:00	11:00	12:00	13:00	14:00	15:00	16:00	17:00
West	0.0%	10.0%	18.0%	19.0%	17.0%	8.0%	24.0%	0.0%	0.0%
Southwest	0.0%	23.0%	7.5%	8.0%	2.0%	1.0%	38.0%	0.0%	0.0%
South	0.0%	28.0%	3.0%	1.0%	1.0%	3.0%	22.0%	0.0%	0.0%
Southeast	0.0%	35.0%	2.0%	4.0%	9.4%	5.6%	17.0%	0.0%	0.0%
East	0.0%	23.0%	15.6%	15.6%	19.0%	19.4%	9.4%	0.0%	0.0%

Figure 6-9: Coverage percentage between 300~500 Lx during the working hours for the office room through five orientations on the 21st of December, using the CSL.



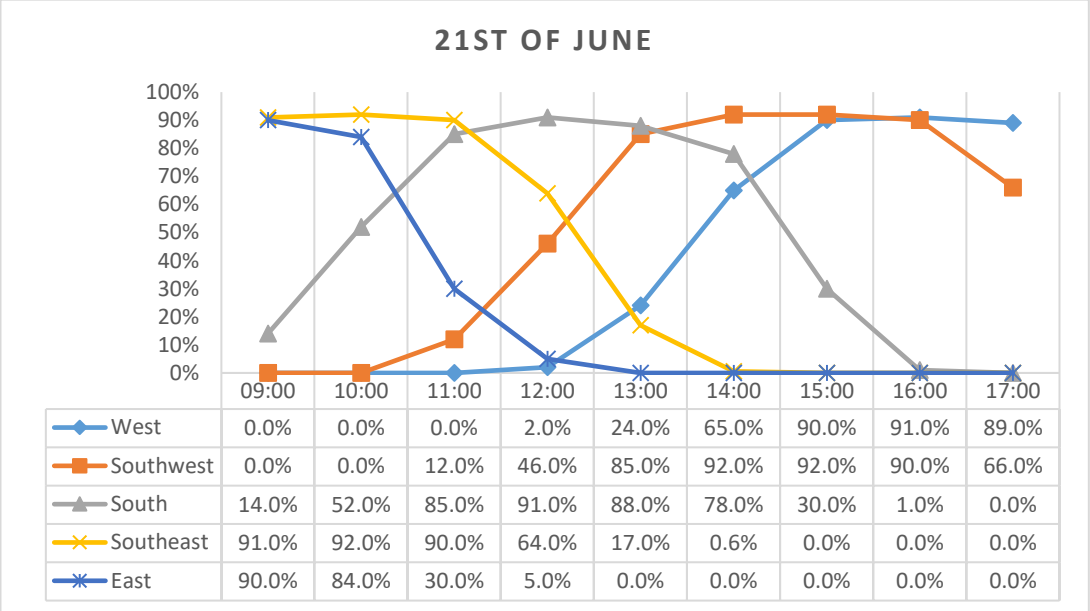
(a) (b) (c)

Figure 6-10: Daylight average coverage percentage in the 21st of June (a), 21st of September (b), and 21st of December (c) by using the CSL on the five orientations.

6.3.3 Daylight coverage percentage on the 21st of June, 21st of September and 21st of December for the IPL in different orientations

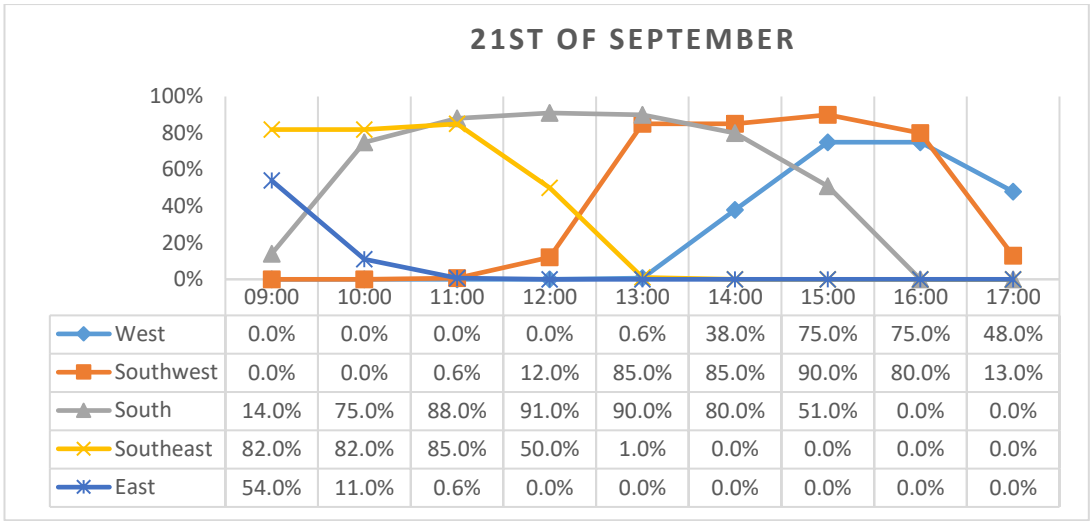
It can be observed that daylighting coverage percentage achieves more than 90% in all of the orientations with some fluctuations due to the difference in directions, see Figure 6-11, Figure 6-12 and Figure 6-13. It is worth mentioning that South and Southwest orientations are giving the best daylight coverage when comparing to other orientations in all of the

seasons. It can be seen in Figure 6-13 that the South orientation is giving the best performance from 11 a.m. to 2 p.m. only. The reason that the daytime is relatively short in December at this specific territory, where the sun altitudes in the morning and the evening are low and probably have potential blocking by trees and surrounding obstacles. In Figure 6-14 it can be seen noticeable variations between the five orientations when using the IPL, especially with the South and the Southwest orientations, while they are giving the highest daylight coverage when comparing to the other orientations. That means that these two orientations should be considered in the early stages of design for better energy saving when using the proposed integrated system.



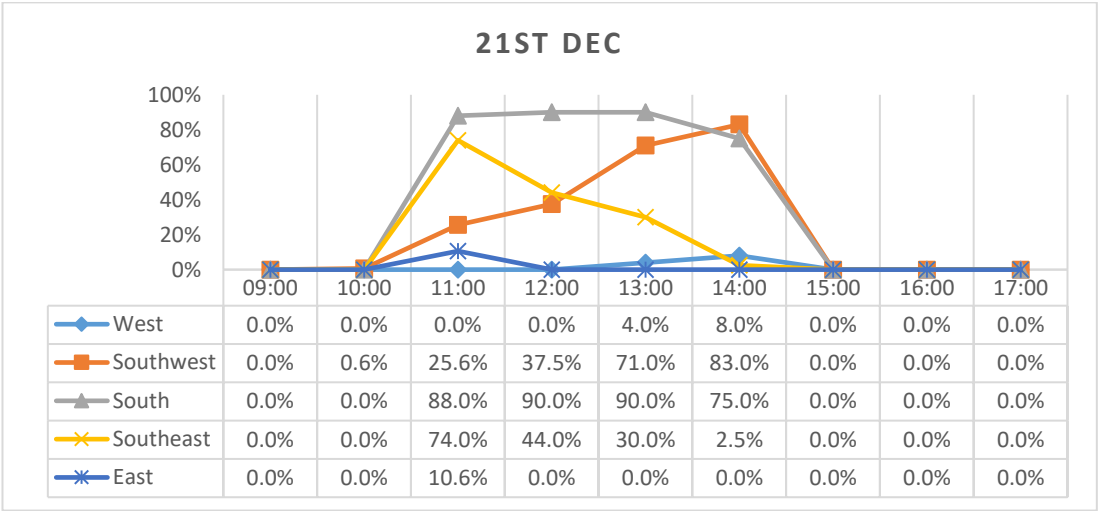
	09:00	10:00	11:00	12:00	13:00	14:00	15:00	16:00	17:00
West	0.0%	0.0%	0.0%	2.0%	24.0%	65.0%	90.0%	91.0%	89.0%
Southwest	0.0%	0.0%	12.0%	46.0%	85.0%	92.0%	92.0%	90.0%	66.0%
South	14.0%	52.0%	85.0%	91.0%	88.0%	78.0%	30.0%	1.0%	0.0%
Southeast	91.0%	92.0%	90.0%	64.0%	17.0%	0.6%	0.0%	0.0%	0.0%
East	90.0%	84.0%	30.0%	5.0%	0.0%	0.0%	0.0%	0.0%	0.0%

Figure 6-11: Coverage percentage during the working hours for the office room through the five orientations on the 21st of June, using the IPL.



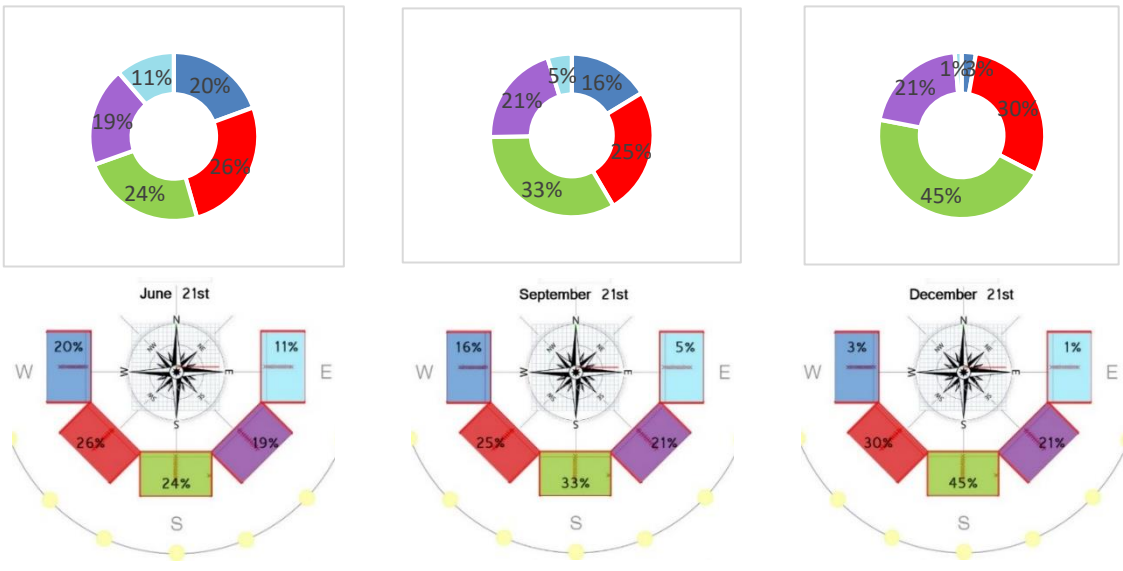
	09:00	10:00	11:00	12:00	13:00	14:00	15:00	16:00	17:00
West	0.0%	0.0%	0.0%	0.0%	0.6%	38.0%	75.0%	75.0%	48.0%
Southwest	0.0%	0.0%	0.6%	12.0%	85.0%	85.0%	90.0%	80.0%	13.0%
South	14.0%	75.0%	88.0%	91.0%	90.0%	80.0%	51.0%	0.0%	0.0%
Southeast	82.0%	82.0%	85.0%	50.0%	1.0%	0.0%	0.0%	0.0%	0.0%
East	54.0%	11.0%	0.6%	0.0%	0.0%	0.0%	0.0%	0.0%	0.0%

Figure 6-12: Coverage percentage during the working hours for the office room through the five orientations on the 21st of September, using the IPL.



	09:00	10:00	11:00	12:00	13:00	14:00	15:00	16:00	17:00
West	0.0%	0.0%	0.0%	0.0%	4.0%	8.0%	0.0%	0.0%	0.0%
Southwest	0.0%	0.6%	25.6%	37.5%	71.0%	83.0%	0.0%	0.0%	0.0%
South	0.0%	0.0%	88.0%	90.0%	90.0%	75.0%	0.0%	0.0%	0.0%
Southeast	0.0%	0.0%	74.0%	44.0%	30.0%	2.5%	0.0%	0.0%	0.0%
East	0.0%	0.0%	10.6%	0.0%	0.0%	0.0%	0.0%	0.0%	0.0%

Figure 6-13: Coverage percentage during the working hours for the office room through the five orientations on the 21st of December, using the IPL.



(a) (b) (c)

Figure 6-14: Daylight average coverage percentage in the 21st of June (a), 21st of September (b), and 21st of December (c) by using the IPL on the five orientations.

6.4 Potential energy saving throughout the year for the IPL

Two main criteria should be considered in our study; firstly, the accepted illuminance range 300 ~ 500 lx, which considered as a visual comfort criterion. Secondly, the electrical energy saved when the provided daylight is above 300 lx regardless of the maximum level 500 lx, which considered as an energy-saving criterion. That means, whenever the available daylight is over 300 lux at any part of the room, the electrical light at this part will automatically turn off, and vice versa, whenever the available light is less than 300 lux the electrical light will automatically turn on. The succeeded system should achieve the two criteria simultaneously of providing visual comfort and saving energy.

For instance, on the 21st of June at 11 a.m., by using the proposed system; 70% of the room was provided with daylight. Furthermore, the available daylight ranged between 300 ~ 500 lx, which means that the system achieved both criteria of saving 70 % of electrical lighting energy in the room and reaching the visual comfort, as shown in Figure 6-4. Accordingly, the electrical light will turn on automatically at the dimming parts of the room and the electrical energy consumption at this time should be 1.35 Wh/m². On the other hand, by using the CLS system at the same time and date, the accepted coverage average for visual comfort is only 18%. Although, 70% of the room is provided with daylight and only 30% of the electrical light should be turned on; however, this system did not succeed to achieve the two criteria due to failure of achieving visual comfort. Furthermore, at this time, the occupants will probably use the blinds or roller shades to protect from excessive sunlight.

Table 6-1: Daily average of electrical lighting energy consumption Wh/m² at the desk level in Birmingham, UK by using the IPL.

Days/months	Jan	Feb	Mar	Apr	May	Jun	Jul	Aug	Sep	Oct	Nov	Dec
1		2.7	2.5		2.3	2.3		2.3	1.8		2.7	3.3
2		4.5	4.2		2.4	2.7		2.3		2.5	3.2	
3	3.1	4.5	4.1	1.8	2.2		2.7	2.3		2.5	2.4	
4	4.4	3.5		2.9	1.9		2.7	2.0	2.1	3.7		4.1
5	4.5			2.1	1.9	2.6	2.8		1.9	2.7		3.0
6	3.0		3.1	2.3		2.7	2.6		1.4	2.6	2.7	2.7
7	3.3	3.5	3.8	2.0		2.8	2.6	2.1	1.8		2.7	3.2
8		2.7	3.1		2.0	2.5		2.4	1.7		3.5	3.1
9		4.5	1.9		2.0	2.7		2.1		3.0	4.3	
10	4.0	1.0	2.5	2.5	2.1		2.7	1.9		2.4	3.7	
11	3.0	4.5		2.1	2.0		2.6	2.2	1.9	2.5		3.0
12	3.2			2.3	2.1	2.5	2.5		1.5	2.2		4.5
13	3.6		1.8	2.3		2.7	2.7		2.1	2.4	2.8	4.5
14	3.7	2.7	2.3	2.1		2.4	2.6	2.2	2.1		2.7	3.5
15		2.1	1.9		2.5	2.6		2.1	2.6		2.7	3.5
16		2.8	3.2		2.2	2.2		2.1		3.3	3.0	
17	4.5	2.5	2.3	2.0	2.3		2.5	2.3		4.4	3.0	
18	2.7	2.4		2.4	2.3		2.5	2.1	2.3	4.3		3.2
19	4.5			2.2	2.3	2.5	2.5		2.3	2.3		3.0
20	2.9		2.2	2.3		2.8	2.5		1.7	2.2	2.6	3.6
21		2.6	3.2	2.7		2.8	2.3	1.8	1.8		3.1	3.1
22		2.3	2.1		2.6	2.9		2.1	2.0		3.4	4.5
23	4.2	2.8	2.0		2.4	2.7		2.2		4.4	4.1	
24	3.1	2.3	1.8	2.7	2.6		2.3	2.1		2.3	4.1	
25	4.5	2.7		2.6	2.3		2.3	1.9	2.3	3.0		3.6
26	4.2			2.5	2.0	3.0	2.4		3.1	2.6		3.0
27	4.5		2.1	2.3		2.3	2.1		2.3	2.6	3.2	3.1
28		2.7	2.2	2.3		2.7	2.3	2.2	2.6		3.2	3.5
29		2.6	2.2		2.5	2.7		1.9	2.6		3.3	4.1
30	2.6		2.7		2.6	2.7		2.2		2.5	3.4	
31	3.6		2.6		2.5		2.3	2.1		2.2		
IPL system Wh/m²	3.67	2.96	2.59	2.32	2.26	2.62	2.50	2.13	2.09	2.84	3.17	3.48
CSL system Wh/m²												
Average over 300 lx	1.58	2.18	1.86	0.95	0.11	0.07	0.28	0.56	1.93	2.60	1.86	0.81
Average 300~500 lx	3.30	3.45	3.59	4.04	4.39	4.43	4.22	3.94	3.13	3.34	3.41	4.22
Nominal energy consumption												
Wh/m²	4.50											

In our case, potential electrical lighting consumption can be achieved by applying the proposed IPL system in the selected office room, as shown in Table 6-1. The test points inside the office room recorded the daily average of electrical lighting consumption during the working hours throughout the year, putting into consideration the two days off during the week, which were not accounted. The monthly averaged from daily electric lighting energy consumption are also included at the bottom of the table and shown in Figure 6-15 for both integrated and conventional systems, via considering the two criteria above. The results in Table 6-1 from the integrated system were using the two criteria simultaneously; however, the results in the CLS system were using each criterion separately. The nominal energy consumption of electric lighting corresponds to the electric lighting level at 500 lx. For the selected office room, DAYSIM gave a value of 4.5 Wh/m² as the nominal electric lighting energy consumption.

Figure 6-15 reveals the monthly electrical lighting consumption by using both IPL and CSL systems, according to the standard electrical consumption. It can be observed that the CSL system (in yellow) gives the best electrical energy saving during the year comparing to the IPL. However, the CSL did not achieve the other criteria of visual comfort. Therefore, this system (in yellow) cannot be considered as an advantageous system. On the other hand, when comparing the performance of both systems within the same criteria, we can observe that the IPL can save more energy, in addition to the well-distributed daylight as shown in Figure 6-4 comparing to Figure 6-3.

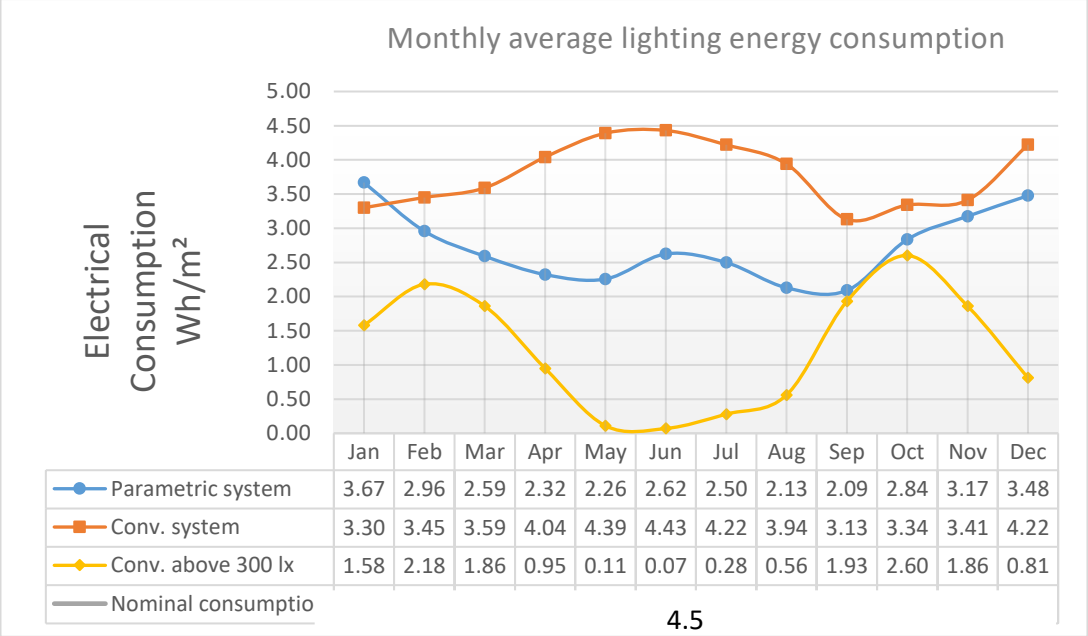


Figure 6-15: Monthly consumed electrical lighting in the office room by using the IPL system.

Table 6-2 shows the potential daylight coverage achieved by using the IPL system during the working hours in the selected office room. The test points inside the office room recorded the daily average daylighting coverage percentage during the working hours throughout the year, putting into consideration that the weekend days were not accounted for in the results. The monthly averaged from daily daylighting coverage percentages is shown at the bottom of the table.

For monthly average daylight coverage percentage of the IPL, we can observe in Figure 6-15 relatively lower daylight coverage in November, December and January compared to the other months, due to the decrease in solar altitude which causes weak solar radiation in addition to the shortage of the daytime hours especially in such territory like the UK.

Table 6-2: Daily daylight coverage percentage for the daylight illuminance range of 300~500 lx at the desk level in Birmingham, UK by using the integrated parametric louvre.

	Jan	Feb	Mar	Apr	May	Jun	Jul	Aug	Sep	Oct	Nov	Dec
1		40%	44%		49%	48%		50%	61%		41%	26%
2		0%	7%		46%	41%		48%		45%	29%	
3	36%	0%	10%	60%	52%		41%	48%		45%	46%	
4	3%	22%		36%	58%		40%	56%	54%	17%		10%
5	0%			54%	58%	42%	38%		57%	39%		34%
6	34%		31%	49%		40%	42%		68%	43%	39%	41%
7	27%	23%	15%	55%		38%	42%	53%	59%		40%	28%
8		39%	32%		55%	44%		47%	63%		22%	32%
9		0%	57%		55%	39%		53%		33%	4%	
10	12%	78%	44%	45%	54%		40%	57%		46%	17%	
11	34%	0%		53%	55%		43%	51%	57%	45%		34%
12	29%			48%	54%	44%	45%		66%	52%		0%
13	21%		60%	48%		41%	39%		54%	47%	37%	0%
14	18%	39%	48%	53%		46%	42%	51%	54%		40%	22%
15		53%	58%		45%	43%		53%	42%		39%	22%
16		37%	29%		51%	52%		53%		27%	33%	
17	0%	45%	49%	55%	49%		44%	49%		3%	34%	
18	39%	46%		46%	48%		45%	54%	50%	5%		30%
19	0%			52%	50%	44%	44%		50%	48%		34%
20	35%		52%	50%		38%	44%		63%	51%	43%	19%
21		42%	30%	39%		37%	49%	59%	60%		31%	31%
22		49%	53%		43%	36%		53%	55%		25%	0%
23	7%	37%	56%		47%	41%		51%		3%	9%	
24	31%	48%	61%	39%	43%		48%	54%		49%	10%	
25	0%	40%		42%	48%		49%	57%	48%	34%		19%
26	6%			44%	55%	33%	47%		31%	43%		33%
27	0%		54%	50%		50%	54%		48%	43%	29%	32%
28		40%	52%	50%		39%	48%	51%	43%		29%	23%
29		42%	52%		44%	40%		58%	42%		26%	8%
30	42%		39%		43%	41%		52%		45%	25%	
31	19%		43%		45%		50%	54%		51%		
Parametric system	**19%**	**34%**	**42%**	**48%**	**50%**	**42%**	**44%**	**53%**	**54%**	**37%**	**29%**	**23%**

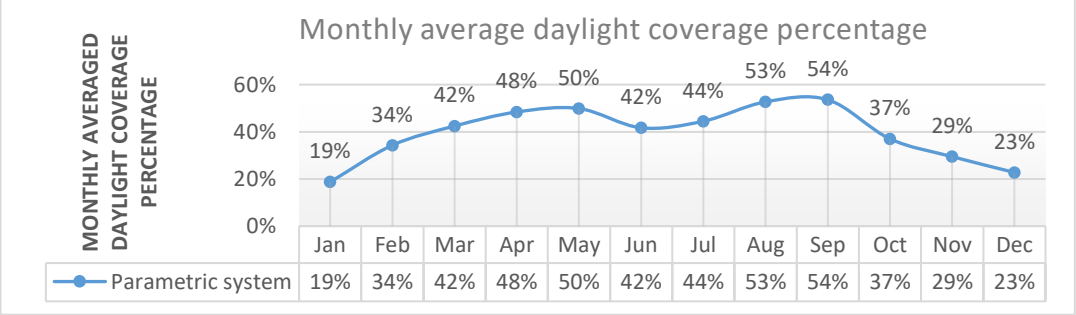


Figure 6-16: Monthly averaged daylight coverage percentage in the office room for the daylight illuminance range of 300 ~ 500 lx by using the integrated system.

It is remarkable to bear in mind that the measured daylight coverage was considered only at the daylight illuminance range of 300~500 lx, however, in some cases the daylight illuminance may exceed or even fall behind this range within a small value, which consequently not accounted in the calculations, therefore resulting in lower coverage values [304]. The simulation results from Radiance / DAYSIM may be primarily affected by the chosen number of bounces and test points to control the radiation quality, which can be adjusted from the "rad Parameters component" in the simulation settings. Putting into consideration that this may take much longer time in rendering, in addition to the computer performance factor. Accordingly, this may influence the analysis quality and the accuracy of the results [305]. While this study was investigating annual daylight performance based on hourly analysis, therefore, the simulation settings were set to the medium level in order to save time. Figure 6-17 reveals the difference between the analysis accuracy levels in the office room on the 1st of February at noontime, whereas, the render time consumed with the high resolution map took ~3 minutes, while the medium resolution map took ~1 minutes and the low resolution map took ~50 seconds. For a reasonable results, our study was using the medium resolution level.

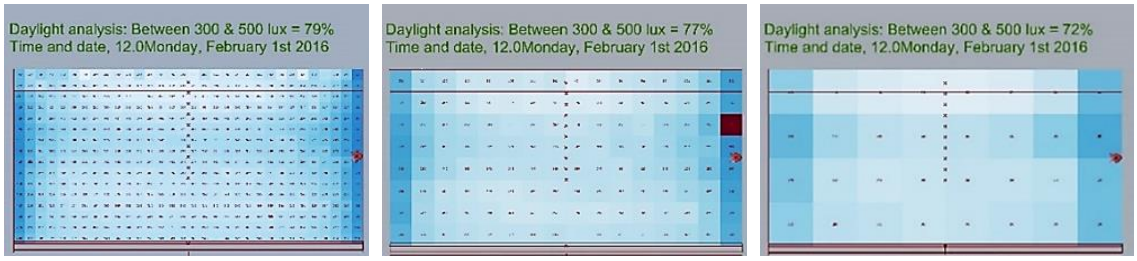


Figure 6-17: Daylight analysis by using different accuracy settings for the same time and date, showing 79%, 77% and 72% of daylight coverage for high, medium and low settings, respectively.

It is worth to mention that the IPL system can save up to 40% as an average of potential electrical energy. However, in consideration to the

points mentioned above, regardless the small limitations within (300~500 lx) due to rendering time and computer performance, the IPL system can probably reach up to 50% of potential savings, based on the required illuminance level.

6.5 Summary

Daylighting can be utilised in different ways to achieve better performance and enhance occupants' visual comfort. The Integrated Parametric Louvre system was examined previously in *Chapter 4* in a South oriented office room for a specific date that achieved 80% of energy saving. The current Chapter examined the suitability of such a system for installation in five orientations. The IPL system achieved the highest results at two orientations (South, Southwest) which records better coverage of daylight during the day in June, September and December compared to other orientations.

The IPL system has also been evaluated throughout the year in the territory of the UK, which reveals promising results comparing a conventional static louvre system. Regarding the fluctuation nature of the selected territory, the study found that the using the Integrated Parametric Louvre can achieve an average of 50% saving of electric lighting energy consumption when it is applied throughout the year. The following chapter will focus on improving the coverage and performance of the Integrated Parametric Louvre.

Chapter 7 Proposing an Innovative Control Method to Increase the Daylighting Stability, via using Dual-axis and Double-layer Parametric Louvre

7.1 Introduction

Architecture as an inanimate; is strongly influenced by the surroundings from different aspects such as design, shape, function, orientation, mass, etcetera, and in some cases, architecture itself can respond to climate changes and sun movement. Some species can adapt to the surroundings by changing their phases in order to survive; likewise, architects inspired by these species to create more sustainable architecture. One of the inspiring plants known as heliotrope, which can react and respond to the sun movement whenever the sun moves, in order to receive as much as possible of solar energy. Modern architecture can inspire this utter response to increase the use of daylight and save more energy. This chapter proposes an innovative control method which can respond to both solar altitude and azimuth simultaneously, to maximise the utilisation of the sun for more uniform and steady daylight distribution inside the deep-plan room, by using specific algorithm in Grasshopper. While azimuth orientation was rarely considered as a parameter [306] or even exploited by daylighting devices [307].

7.2 Hypothesis control development mechanism of the Integrated Parametric louvre (IPL)

An innovative type of IPL is introduced in this chapter, which can utterly respond to the sun movement. Typically, the IPL was used to reflect direct sunlight towards a fixed path over the ceiling inside the deep-plan room, and then the illuminated ceiling acts as a source of light to the occupants. However, the newly proposed method is to keep this reflected light constant towards fixed target points on the ceiling during the daytime, consequently, keep the light distribution more uniform inside the room.

Parametric design as a tool is used to find a compromise between changeable parameters such as altitude, azimuth, intensity and the physical parameters of the louvre system and tuning windows to maintain the provided light within the range 300~500 lx to meet the occupants' visual comfort according to CIE standard [308]. The study analyses the percentage of daylighting coverage for the range 300~500 lx at the desktop level across the office room. General daylighting systems can achieve 30~50% of daylight coverage in their best cases [123] within the accepted range of illumination. However, the current proposed system can achieve up to 75~95% in various climate conditions throughout the year.

Computer software is developed orderly to create intricate graphical drawings; accordingly, parametric software is produced to deal with complex geometries with different parameters [123]. New Cairo in Egypt was selected as a region for the office room while this location represents a hot arid territory with dominant clear sky condition. Annual hourly data analysis for this location revealed that the sky is clear, intermediate and overcast during 53%, 37% and 10% of the year, respectively, based on

the criteria in Table 7-1 [33], which means that the availability of solar radiation can reach up to 90% during the year in this location.

Table 7-1: Definitions of sky types

CIE SKY TYPE	CONDITION
CLEAR	Direct normal irradiance is more than 200% of diffuse horizontal
INTERMEDIATE	Direct normal is between 5% and 200% of diffuse horizontal
OVERCAST	Direct normal is less than 5% of diffuse horizontal

The new proposed system consists of IPL coated with 90% specular reflection, these slats can follow the sun movement in all directions, while, they can rotate around two axes to appropriate with all solar angles, except steep angles less than 10 degrees with the façade, aiming to increase the availability of daylight during the daytime.

7.2.1 Integrated Parametric Louvre based on One-axis rotation control (the original system)

This type of daylighting system has been investigated in previous chapters by using rotating mirrored slats with one-axis rotation for each. Such a system is parametrically controlled using algorithmic formula created in Grasshopper. The system can reach up to 50% of daylight autonomy within 300~500 lx coverage in a typical office room at the desk level throughout the year [279].

The slats in the IPL consists of 10 rows and the distance between each row is 17 cm, giving about 170 cm height of the louvre system. Each row consists of two parts, a rotating mirrored slat and a fixed shade slat, and each slat is 20 cm width, see *Figure 7-1*. The rotating slats assigned as a mirrored coated surface with 90% reflectivity and they are controlled independently based on solar altitudes. Although every single slat in each row has a specific inclination angle due to its target's direction on the ceiling, however, they all rotate at the same magnitude. On the other hand,

the fixed shade slats are assigned as dark matt material and work as shading part to prevent glare or any excessive light passing between the rotating slats. The rotation process is performed from a hinged axis (X-axis) around a tangent line between both slats, as shown in *Figure 7-1*.

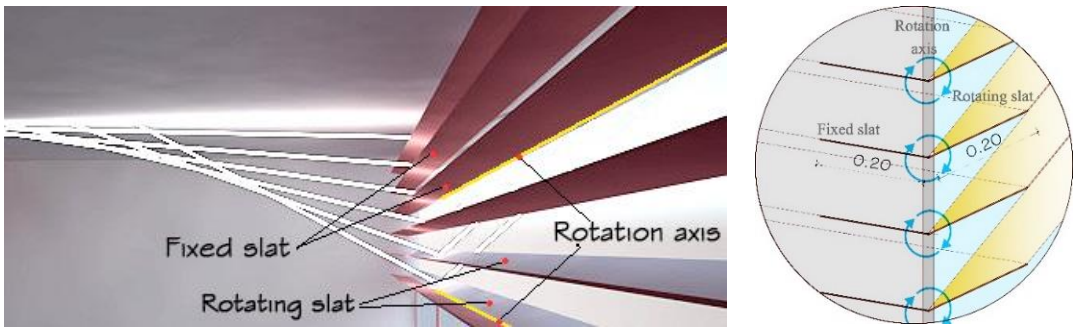


Figure 7-1: One-axis rotation control system

The process of this system is based on responding to the sun movement to collect as much as possible of daylight and reflect it onto fixed paths over the ceiling inside a deep-plan room; then the ceiling works as a source of light inside the room [247]. However, it is worth to bear in mind that these slats can respond only to solar altitudes, not solar azimuths, which means that the illuminated patch of the reflected light on the ceiling will move by time in a longitudinal path as shown in *Figure 7-2*.

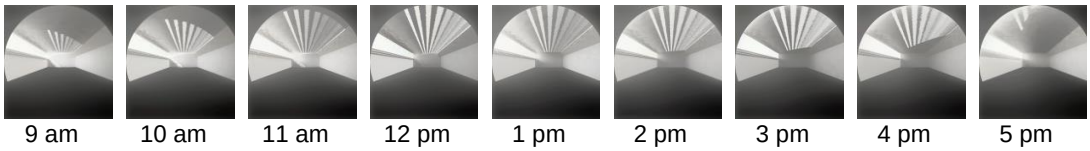


Figure 7-2. Radiance illuminance maps showing the illuminated path is moving over the ceiling from 9 a.m. to 5 p.m. on the 21st of September.

Concerning the sun movement, the illuminated area inside the room should be at its maximum performance when the incidence plane of sunlight is perpendicular to the south-facing façade. However, the illuminated area decreases gradually when the sun moves to the west or comes from the east, as indicated in *Figure 7-3*. Consequently, these

rotating slats can provide uniform daylight inside the room but still not constant enough, especially, at the late and early time of a day.

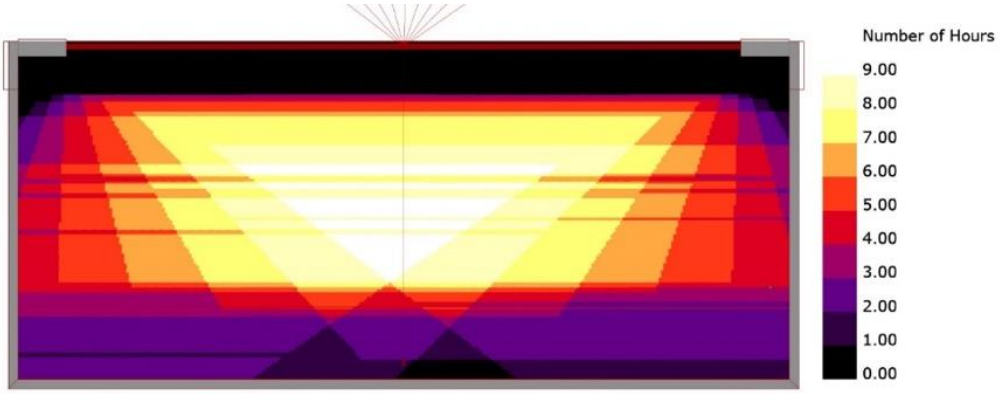


Figure 7-3. Hours of daylight autonomy for the range of 300-500 lx at the desktop level on the 21st of September.

7.2.2 Integrated Parametric Louvre based on Dual-axis rotation control (the new proposed system – 1st alternative)

Dual-axis or biaxial rotation control inspired by "saddle joint" which forms a flexible biaxial connection between two bones that can move in all directions except for axial rotation [261]. The slats in this system can rotate in two directions simultaneously in order to follow the sun movement in all directions. This response aims to track sunlight wherever it moves and redirects it to specific fixed targets on the ceiling, see *Figure 7-4*.

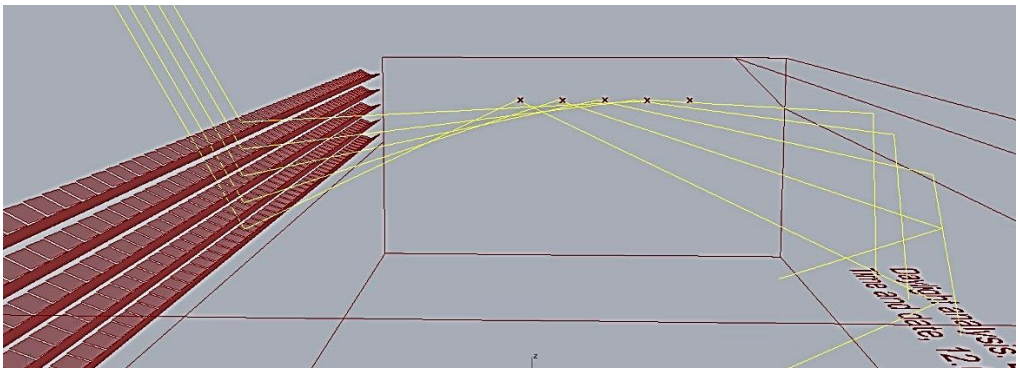


Figure 7-4: Dual-axis parametric louvre – raytracing study

This method is almost likewise the original method, which consists of the same two parts (the rotating part and fixed part); however, the rotating part consists of deployed slats divided into consecutive segments as shown in *Figure 7-5*. Every single slat is hinged from its corner where

it can rotate in a biaxial rotation from this corner around X and Y pivots. While the opposite corner is fixed in a moveable bar which can control the movement of the slats. The movable bar can move horizontally and vertically to tune the reflection surface with the sun movement and keep the reflected ray in a fixed target, see Figure 7-6.

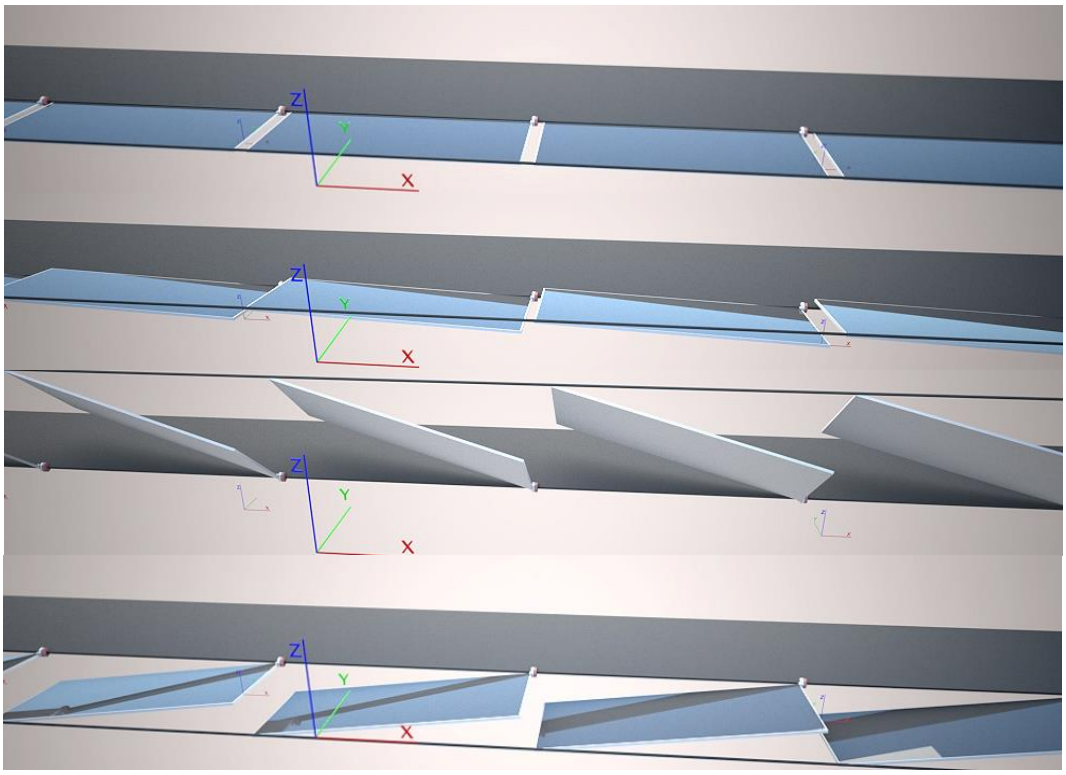


Figure 7-5: Dual-axis rotation movements.

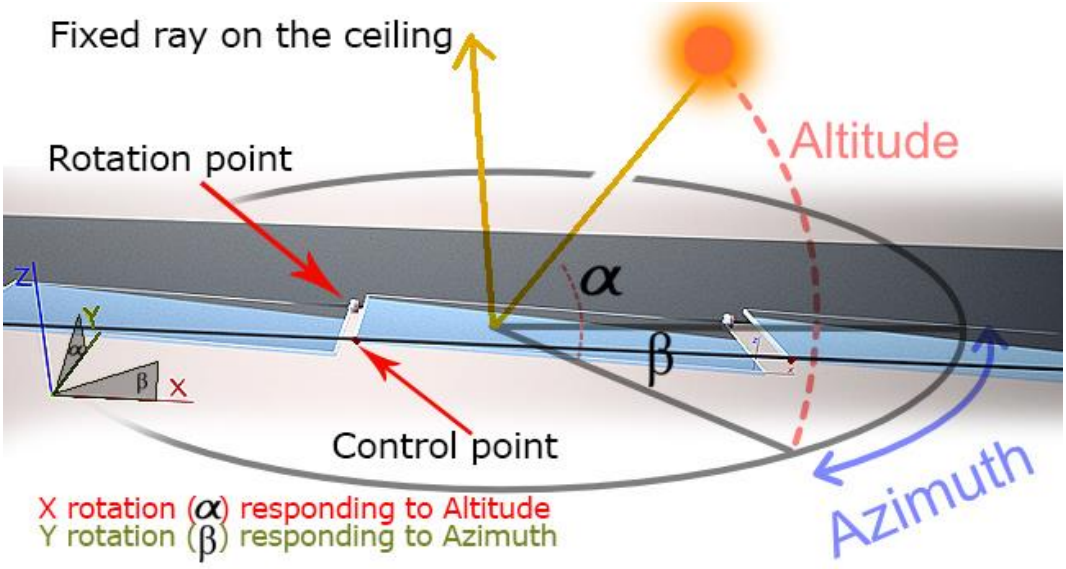


Figure 7-6: Dual-axis rotation control

Every single slat has two-rotation angles Beta (β), and Alpha (α), which varies parametrically in a biaxial rotation around its pivot in the (X-Y) coordinates using specific algorithmic formula created in Grasshopper, see *Figure 7-7*. The formula is solving the relation between the vector of the reflected ray to the ceiling and the vector of the incident ray from the sun by using the "Orient" component which works as a 'heliotropic' [21] mirror surface between the two rays. Thus, the slat's angles β and α should alter simultaneously with the solar altitude and azimuth. Therefore, the reflected light to the ceiling should be steadier during the daytime, see *Figure 7-8*.

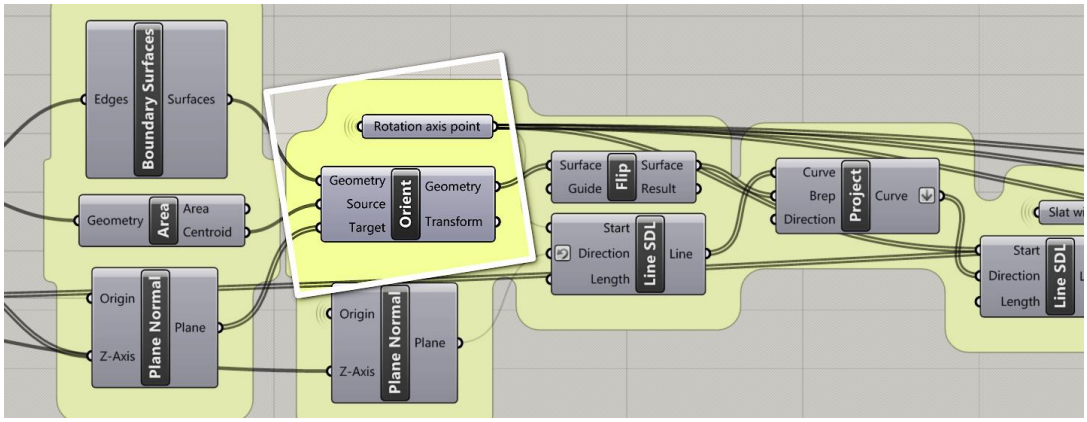


Figure 7-7: Grasshopper formula to control the rotation angles

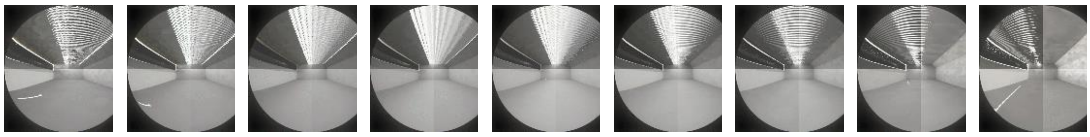


Figure 7-8: Radiance illuminance maps for the Dual-axis rotation control from 9 a.m. to 5 p.m. on the 21st of September.

7.2.3 Integrated Parametric Louvre based on Double-layer rotation control with a combination of horizontal and vertical louvre (the new proposed system – 2nd alternative)

This system consists of two bundles of rotating louvre, one of them is deployed horizontally along the façade and can rotate responding to the sun altitude [247], and the other bundle is deployed vertically in front of the horizontal bundle and can rotate responding to the sun azimuth. The two bundles work parametrically together to keep the reflected light onto

a specific target on the ceiling. This system has two-axis rotations, "Z" axis which define the vertical slats and "X" axis which define the horizontal slats. Sunlight strikes the vertical slats first which can rotate automatically around their "Z" axis by responding to the sun azimuth, in order to redirect the light into a projected surface aligned perpendicularly with the façade. Then the horizontal slats rotate automatically around their "X" axis to reflect the redirected light towards a specific target on the ceiling, see Figure 7-9. Both bundles are connected parametrically and work simultaneously by using a predefined formula created in Grasshopper, with the consideration that each bundle has its unique rotation angle.

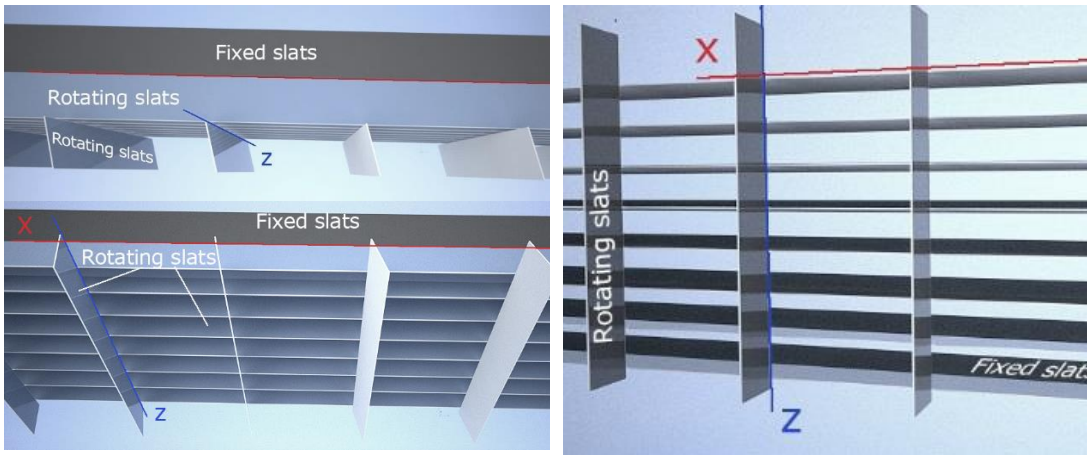


Figure 7-9: Double-layer rotation control

The vertical slats arrayed along the façade with a distance 60 cm between their pivots and the width of each slat is 20 cm. The width of the horizontal slats was determined to 20 cm, while their length is related to the room length and the number of slats was set to 10. Fixed shade slats were attached to the horizontal louvre – likewise the one-axis rotation control system – to prevent potential glare or any excessive light passing between the slats.

7.2.4 Addition of a Thermochromic (TC) glass

Thermochromic material is an advanced type of glass can adapt its transmission level based on solar intensity [12, 309], accordingly, the higher solar heat it absorbs, the less light level is passing through it [158]. TC glass in our study has been installed at the upper part of the window next to the slats, in which it can keep the reflected light from the slats at a constant intensity. For more efficient daylighting system, this window can help to keep the number of slats fixed and no need to increase or decrease their number to compensate, while, such window will do the function of keeping the solar intensity in balance. In Grasshopper, test points were used over the window using "TestPoints component" in Honeybee to measure the intensity of solar radiation, which then can tune the window transparency to control the amount of the penetrated light.

7.3 A comparison study between the one-axis, dual-axis and double-layer Integrated Parametric Louvre

A comparison is given here between the two proposed systems and the original one [279]. The analysis was conducted for a deep-plan example office room in New Cairo with 18 m length and 8 m depth, aiming to cover the whole office with permanent steady and uniform daylight within 300~500 lx. The percentage daylight coverage is defined as the ratio of the area with the daylight illuminance of 300~500 lx relative to the total floor area, and it was measured using test points at the desk level at 75 cm above the floor [16] and 50 cm between each point. The study ignored the edge area within 50 cm from the walls around the room, while the illuminance level at this area is usually between 100~300 lx and even not exploited by the occupants. Generally, illumination in the overall area

should not decrease below 100 lx at any time during the day [34]. By ignoring the 50 cm area around the inner walls, the opportunity of achieving 300-500 lx should be higher. The illuminance values at those test points were used to calculate the percentage daylight coverage for the acceptable range 300~500 lx. Usually, 70% coverage for the daylight range of 300-500 lx is acceptable for typical daylighting systems [12, 123, 248]. Primarily, this study aims to achieve over 90% of daylight coverage. The rest 10% can be considered as uncertainty and sensitivity factors [304], which most likely close to the required range, that does usually have slightly more than 500 lx or less than 300 lx within the range 50 lx, which can be accepted or even ignored and do not need to be compensated with electrical lighting. The location, New Cairo, represents a hot arid territory, where the sunny weather is dominant throughout the whole year, and the sun altitude reaches 83° at zenith time in summer. The ray-tracing study can be seen in Figure 7-10 at 9 a.m., 12 p.m. and 3 p.m. on the 21st of September as a standard case.

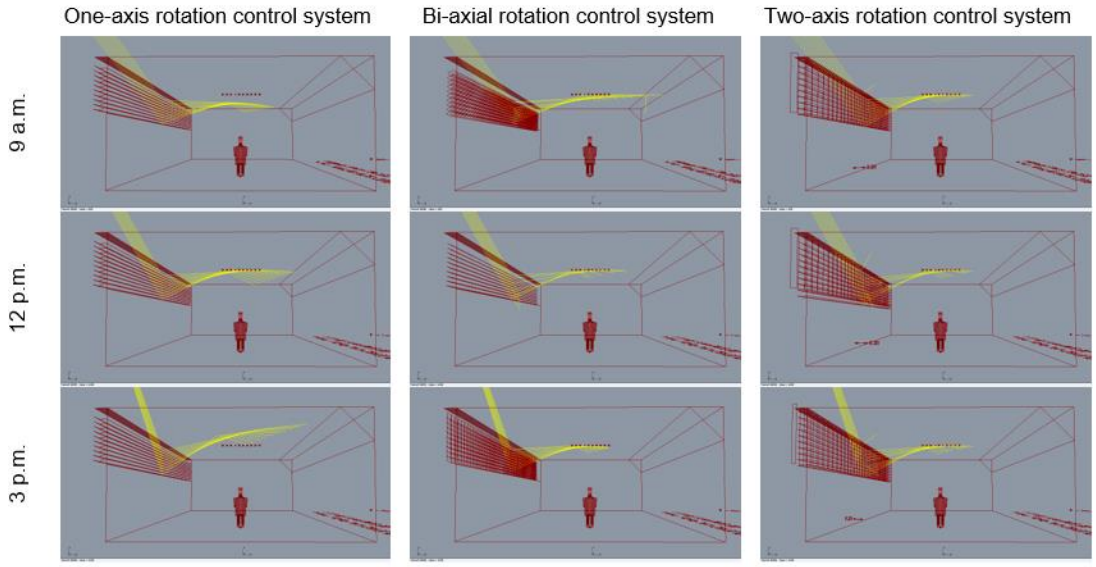


Figure 7-10: Perspective view showing the ray-tracing directions for the One-axis, dual-axis and double-layer rotation control systems respectively, at 9 a.m., 12 p.m. and 3 p.m. on the 21st of September.

In Figure 7-11, the points in the middle of the room are representing the targets. It can be seen that the raytraced light at the 'One-axis' case is moving along the room in different directions, while, the dual-axis and double-layer louvre systems are respecting the targets during the daytime. Accordingly, the daylight coverage should be more constant during the working hours comparing to the One-axis rotation control system.

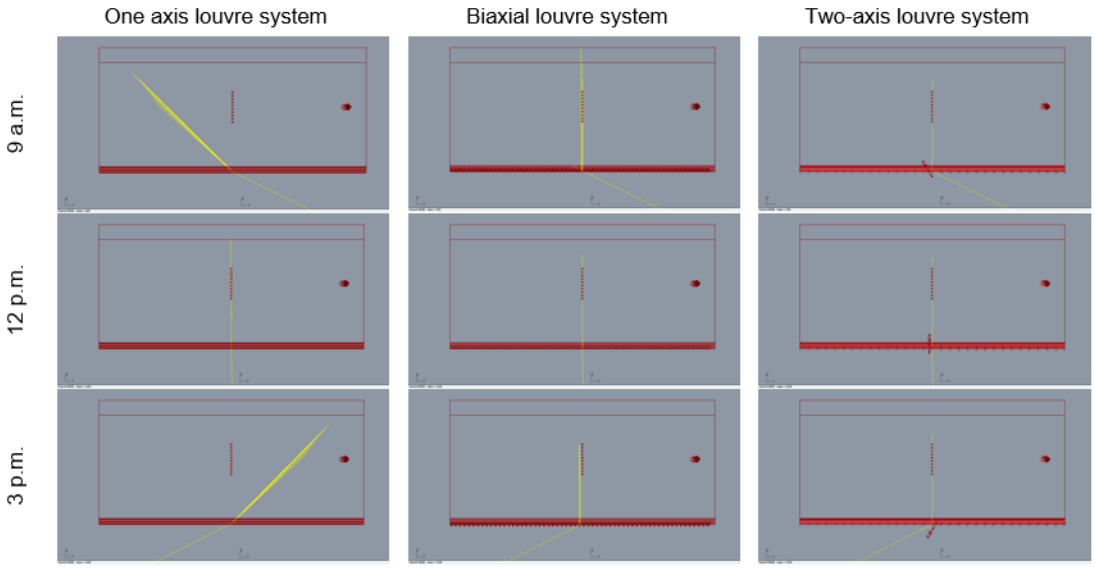


Figure 7-11: Top view for the office room showing the ray-tracing directions for the One-axis, dual-axis and double-layer systems respectively, at 9 a.m., 12 p.m. and 3 p.m. on the 21st of September.

A comparison study has been made in four different dates throughout the year in order to cover all the possibilities of sun positions. The selected dates are 21st of March, 21st of June, 21st of September and 21st of December while, they are representing different seasons and different altitudes, see Figure 7-12, Figure 7-13, Figure 7-14 and Figure 7-15.

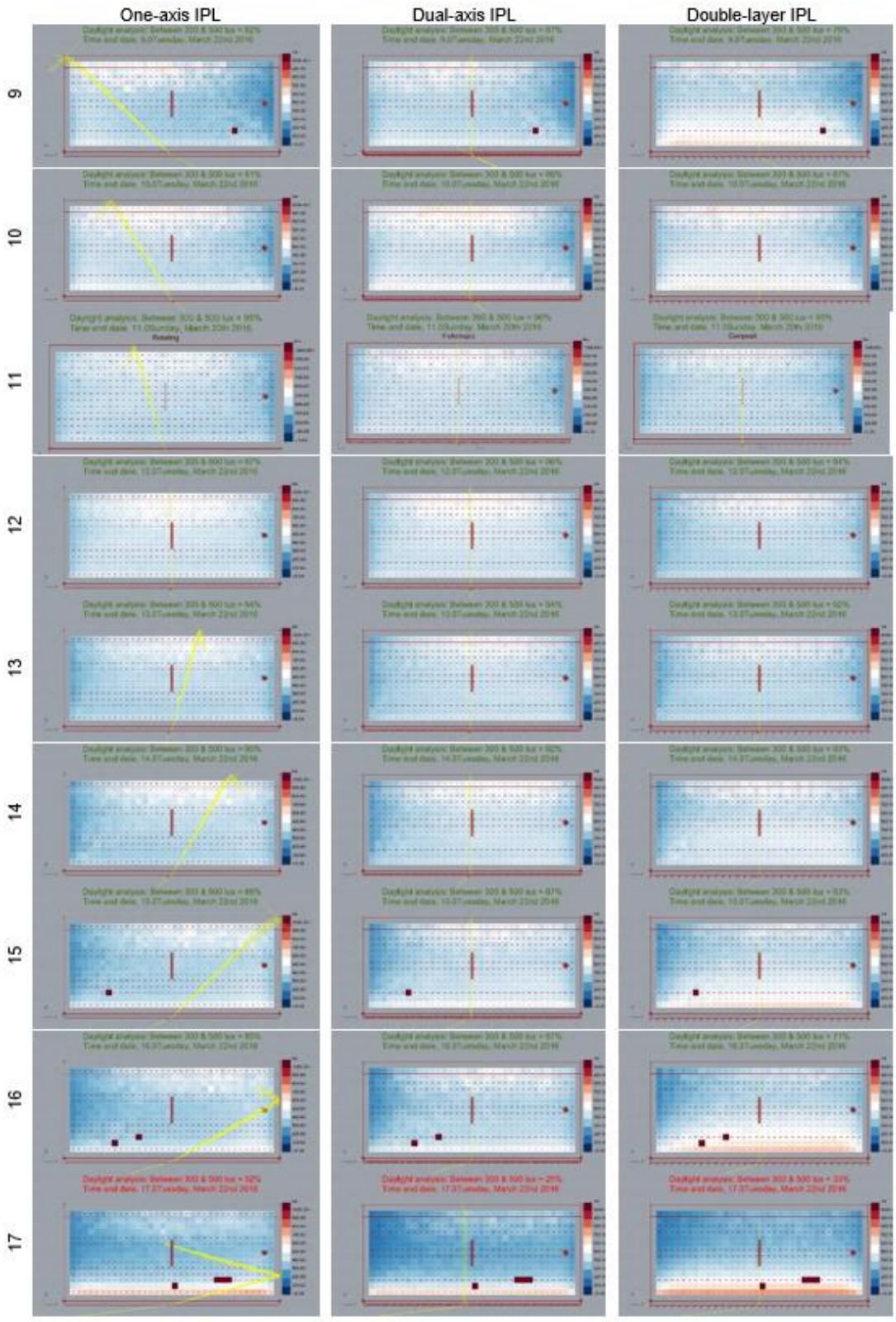


Figure 7-12: Daylight coverage for the One-axis, dual-axis and double-layer IPL systems, respectively on the 22nd of March

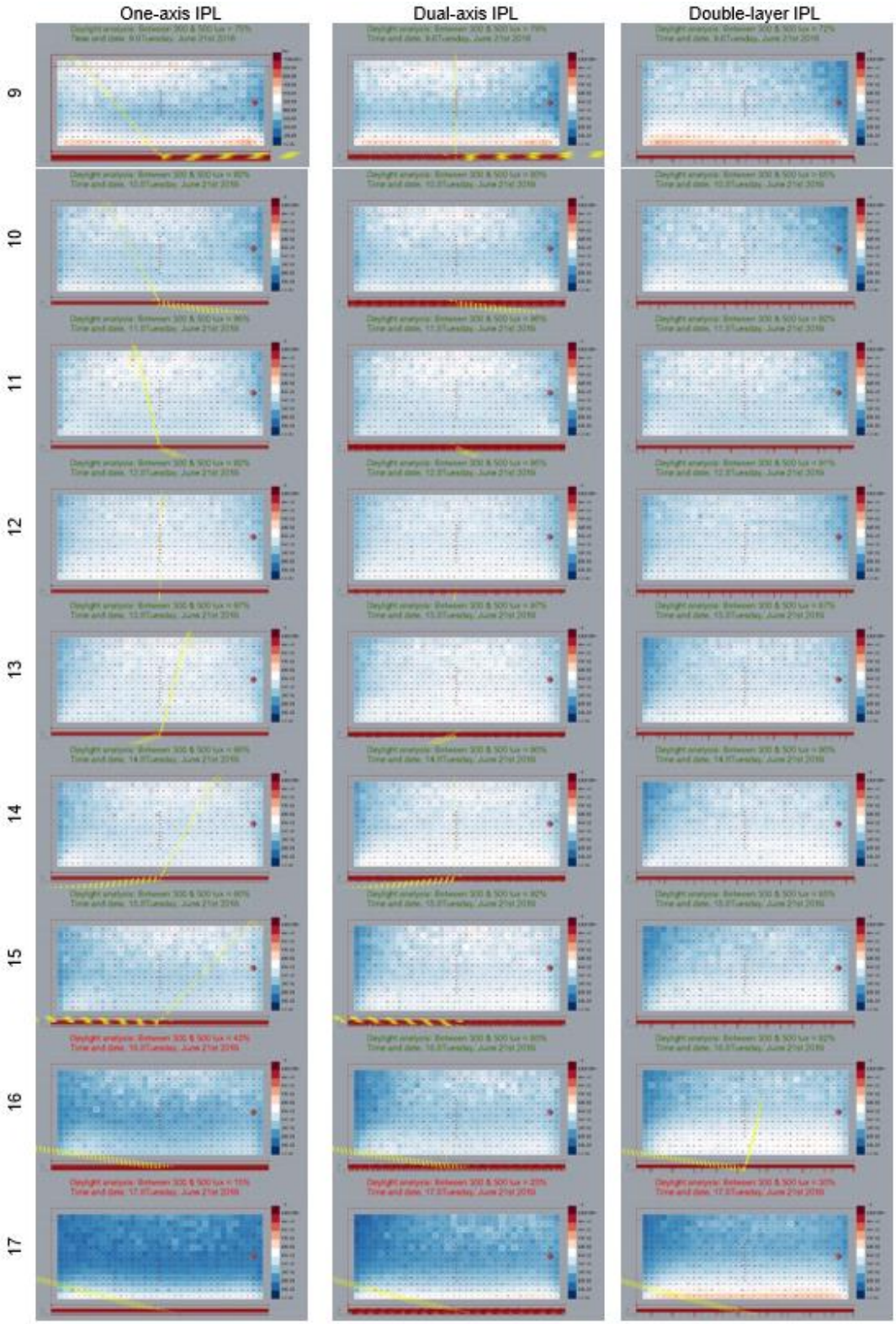


Figure 7-13: Daylight coverage for the One-axis, dual-axis and double-layer rotation control systems, respectively on the 21st of June

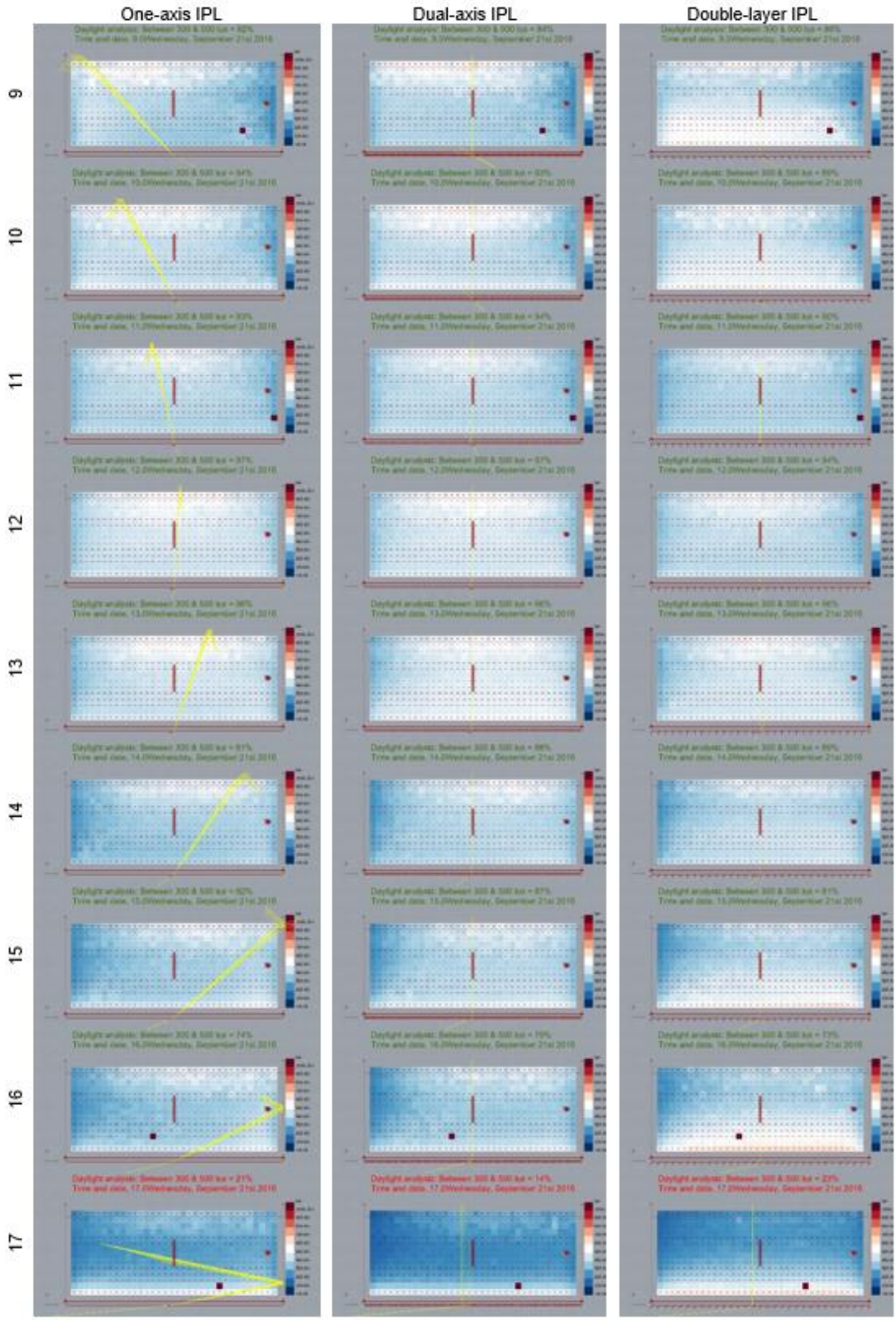


Figure 7-14: Daylight coverage for the One-axis, dual-axis and double-layer IPL systems, respectively on the 21st of September

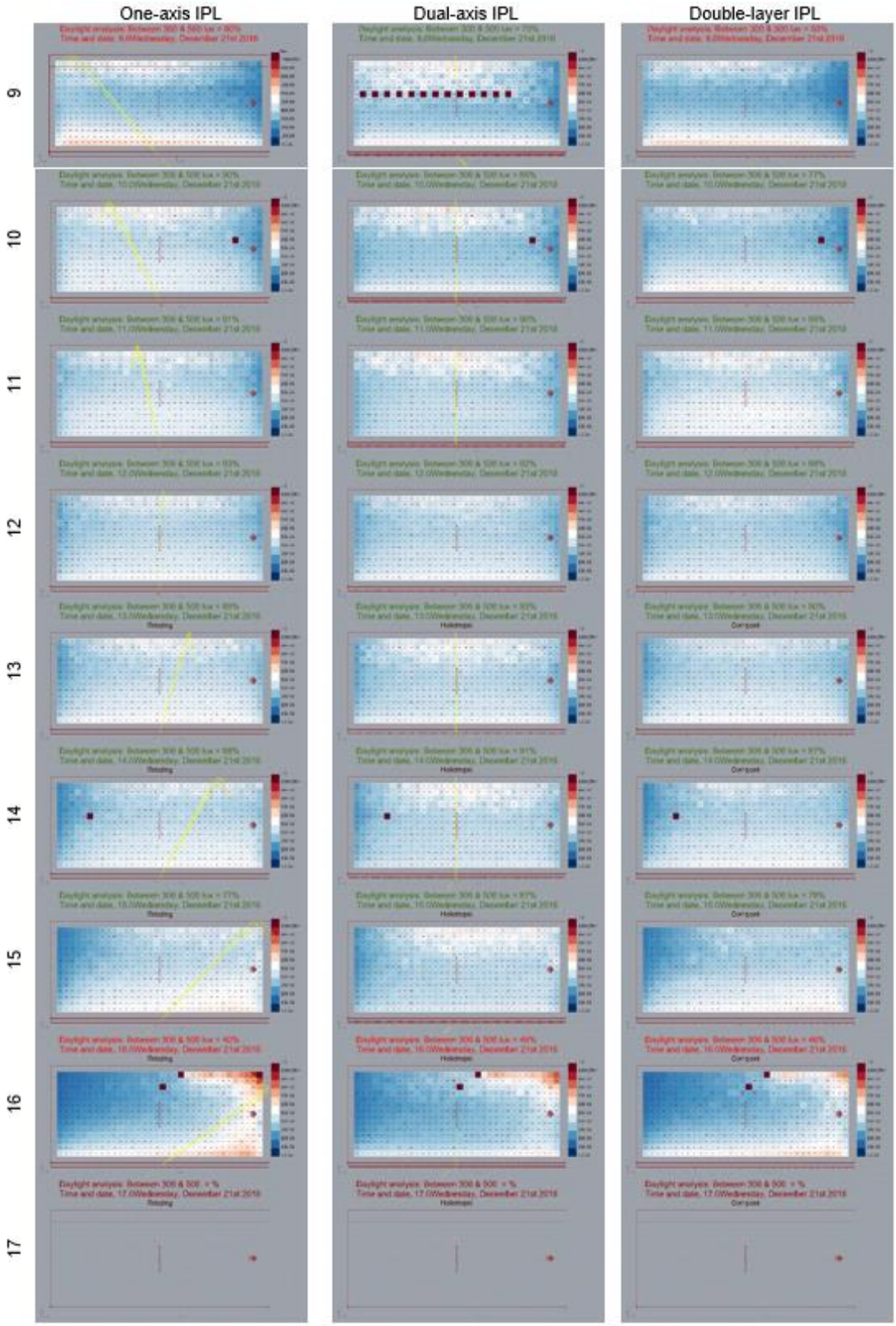


Figure 7-15: Daylight coverage for the One-axis, dual-axis and double-layer IPL systems, respectively on the 21st of December

7.4 Results and discussion between the one-axis, dual-axis and double layer Parametric Louvre

In Figure 7-17, Figure 7-18, Figure 7-19 and Figure 7-20 it can be observed that the coverage is almost same between the three systems, however, slightly better performance revealed in the dual-axis system especially at 4 pm in March, June and September due to the contribution of the fixed targets. Meanwhile, in Figure 7-12 to Figure 7-15 it can be seen a dark blue area in all systems at the left side near to the wall at the late hours and even on the right area in the morning hours. Although, the new proposed systems; systems supposed to provide constant light while they use fixed targets method, however, some areas still could not receive enough light. See Figure 7-8 comparing to Figure 7-2 for more clarification.

From a different point of view, we can find that sun position in the skydome has a substantial contribution on the daylight coverage inside the room [288], in addition to the influence of redirected rays on the ceiling. It can be observed in Table 7-1 that the contribution of the diffuse light from the skydome has the majority effect, which dramatically influences on the daylight transmittance through the upper part of the window (TC window).

Although, the upper part of the window is covered by a bundle of slats which should protect from direct sunlight, however, the contribution of the bright diffuse area around the sun – besides the skydome – dramatically influences on the direction of the illuminated area inside the room, as seen in Table 7-2. Meanwhile, the lower part of the EC window is directly influenced by the sunrays.

Data in Table 7-2 demonstrates the window tuning values which calculated by Grasshopper to optimise the penetration of the daylight at the desk level within illuminance range 300~500 lx. The results in Table 7-2 shows that the DHI has a significant influence on the upper TC window, in addition to GHI, respectively. However, the EC window is primarily influenced by GHI in addition to DNI, respectively. It can be seen in Figure 7-16 that values of solar radiation over the EC window is primarily following the attitude of GHI.

Table 7-2: Solar radiations on September 21st from 9 a.m. to 5 p.m. in New Cairo by using One-axis rotation control in New Cairo location

Day time	(GHI) Global horizontal irradiance	(DNI) Direct normal irradiance	(DHI) Diffuse horizontal irradiance	Solar radiation over the EC win.	TC tuning	EC tuning	Coverage %
9	297	128	214	207	0.80	0.04	84%
10	588	497	200	407	0.65	0.02	92%
11	848	883	94	582	0.90	0.01	93%
12	941	969	96	644	0.90	0.01	97%
13	967	1051	94	659	0.90	0.01	96%
14	823	915	152	567	0.75	0.01	88%
15	639	788	177	434	0.7	0.02	84%
16	441	691	164	292	0.9	0.03	82%
17	234	568	127	144	0.95	0.05	21%

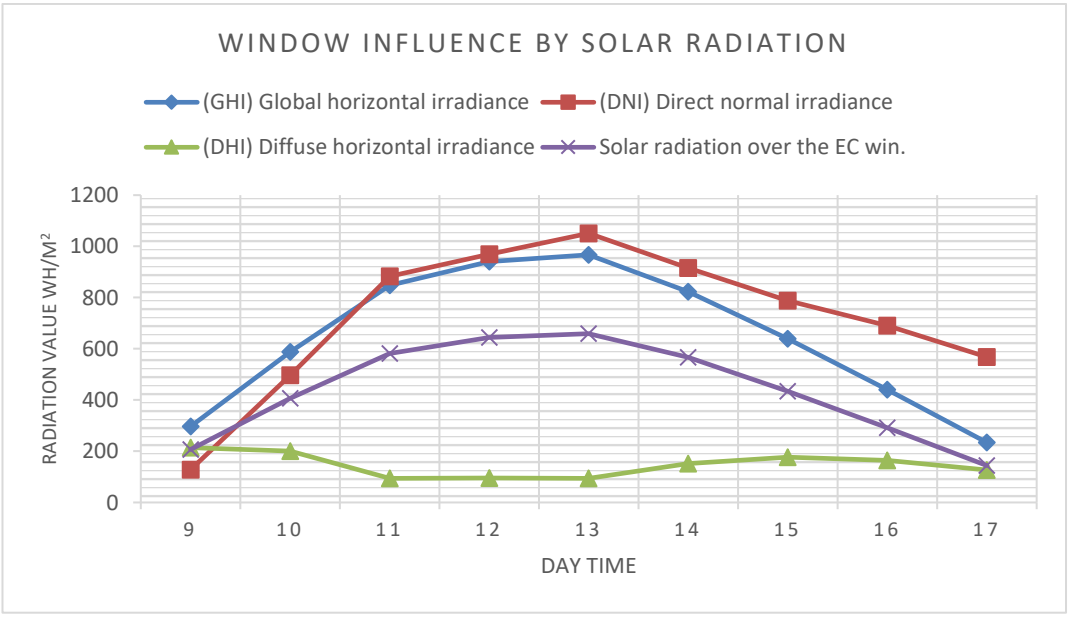
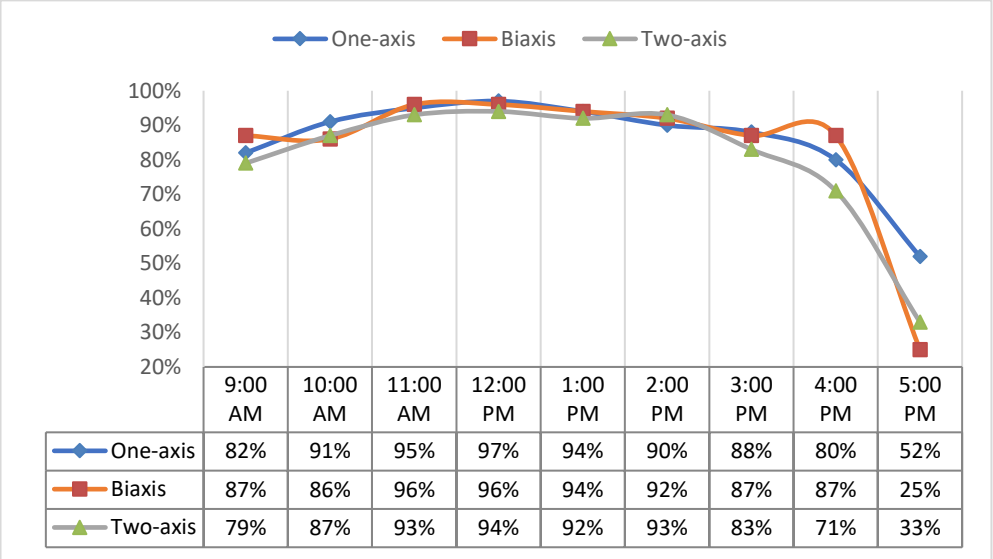


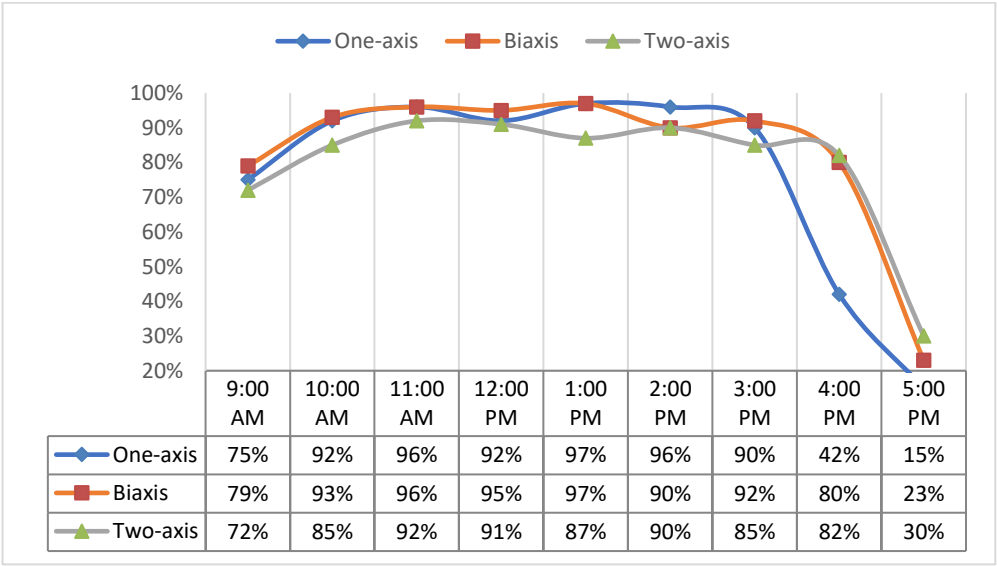
Figure 7-16: The influence of solar radiation on the window surface.

The upper window transmittance assigned between 0.35 (nearly opaque) – 0.95 (almost transparent). Therefore, the window transmittance will automatically decrease when, GHI and DHI increase, and vice-versa. Likewise, the lower EC window is influenced by the amount of solar radiation strikethrough based on GHI and DNI values. Both windows controlled parametrically using algorithmic formula created in Grasshopper, summarised in a simple diagram in Figure 7-21.



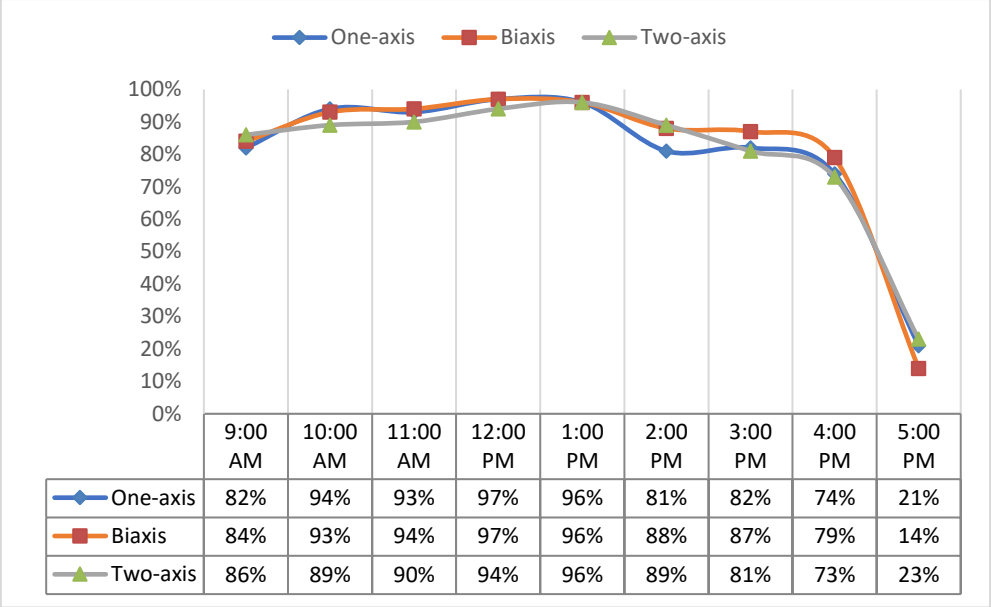
	9:00 AM	10:00 AM	11:00 AM	12:00 PM	1:00 PM	2:00 PM	3:00 PM	4:00 PM	5:00 PM
One-axis	82%	91%	95%	97%	94%	90%	88%	80%	52%
Biaxis	87%	86%	96%	96%	94%	92%	87%	87%	25%
Two-axis	79%	87%	93%	94%	92%	93%	83%	71%	33%

Figure 7-17: Percentage daylight coverage during working hours on the 21st of March of the One-axis, dual-axis and double-layer systems



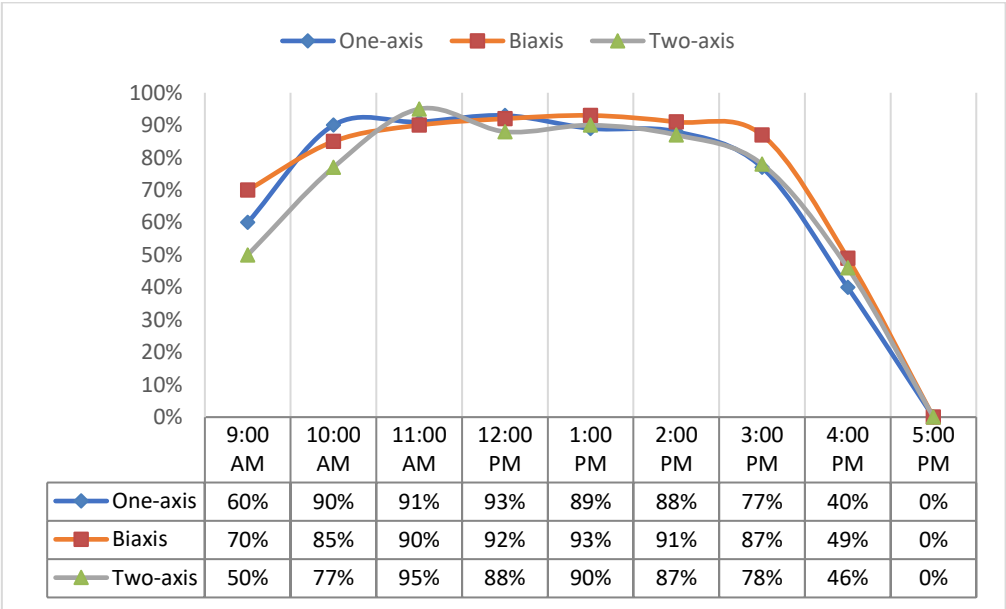
	9:00 AM	10:00 AM	11:00 AM	12:00 PM	1:00 PM	2:00 PM	3:00 PM	4:00 PM	5:00 PM
One-axis	75%	92%	96%	92%	97%	96%	90%	42%	15%
Biaxis	79%	93%	96%	95%	97%	90%	92%	80%	23%
Two-axis	72%	85%	92%	91%	87%	90%	85%	82%	30%

Figure 7-18: Percentage daylight coverage during working hours on the 21st of June of the One-axis, dual-axis and double-layer systems



	9:00 AM	10:00 AM	11:00 AM	12:00 PM	1:00 PM	2:00 PM	3:00 PM	4:00 PM	5:00 PM
One-axis	82%	94%	93%	97%	96%	81%	82%	74%	21%
Biaxis	84%	93%	94%	97%	96%	88%	87%	79%	14%
Two-axis	86%	89%	90%	94%	96%	89%	81%	73%	23%

Figure 7-19: Percentage daylight coverage during working hours on the 21st of September of the One-axis, dual-axis and double-layer systems



	9:00 AM	10:00 AM	11:00 AM	12:00 PM	1:00 PM	2:00 PM	3:00 PM	4:00 PM	5:00 PM
One-axis	60%	90%	91%	93%	89%	88%	77%	40%	0%
Biaxis	70%	85%	90%	92%	93%	91%	87%	49%	0%
Two-axis	50%	77%	95%	88%	90%	87%	78%	46%	0%

Figure 7-20: Percentage daylight coverage during working hours on the 21st of December of the One-axis, dual-axis and double-layer systems.

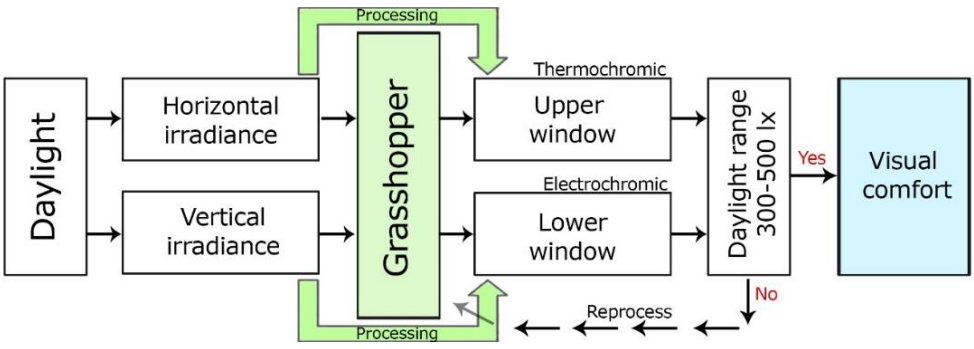
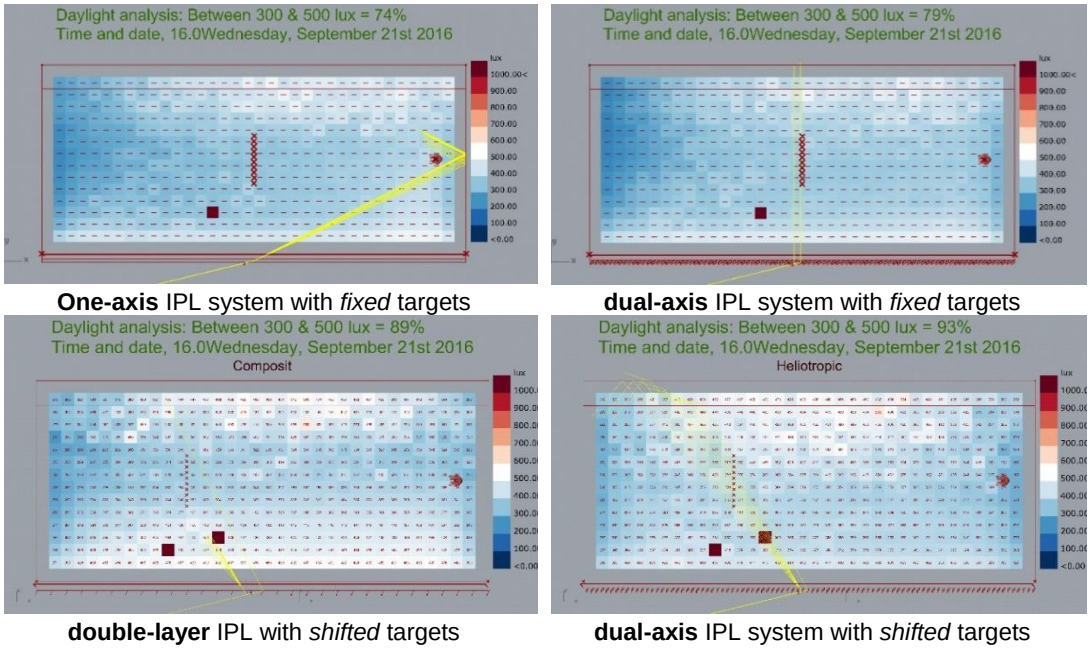


Figure 7-21: A diagram showing the process in Grasshopper to control the window transmission.

Although, the proposed two systems should be able to compensate the lack of daylight at all times while they can reflect the sunlight to a fixed targets, however, the results in Figure 7-19 and Figure 7-20 shows lack of daylight availability starting at 4 p.m. due to a sharp steep in the solar azimuth in addition to its weak intensity. Promisingly, this issue can be solved via changing the positions of those target points on the ceiling to the less illuminated area, thanks to parametric control that allows changing different parameters simultaneously. For instance, at 4 p.m. if we move the target points 3 meters to the left on the ceiling, the reflected light will be directed onto the dark blue area and compensate the weakness of daylight at this time, see *Figure 7-22*.



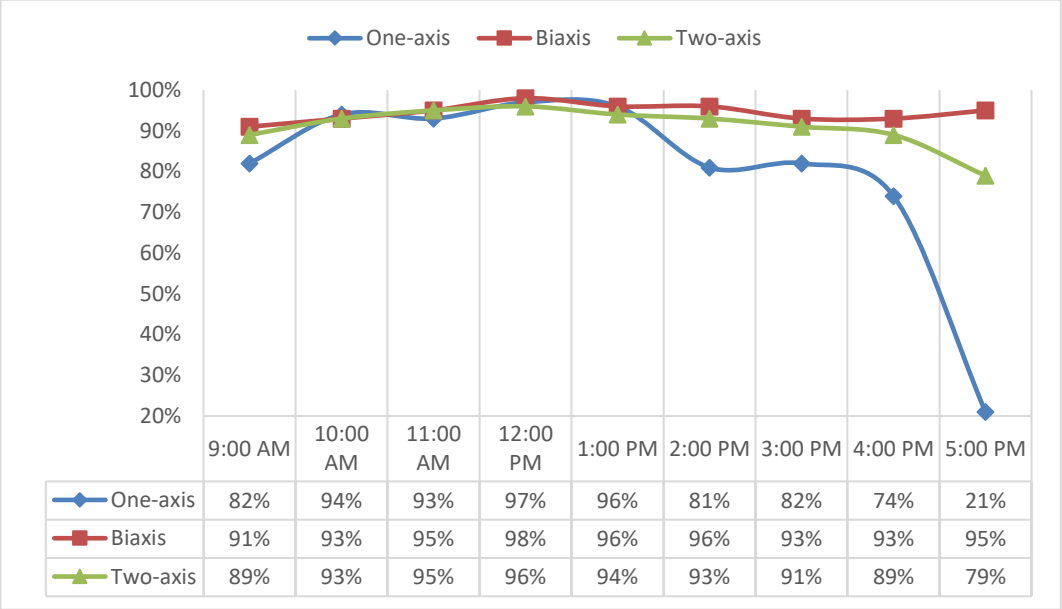
One-axis IPL system with *fixed* targets | **dual-axis** IPL system with *fixed* targets

double-layer IPL with *shifted* targets | **dual-axis** IPL system with *shifted* targets

Figure 7-22: Daylight coverage before and after moving the targets at 4 p.m. on the 21st of September.

Significantly, we can observe that the blue area near to the wall is almost disappeared after moving the targets to the left side, which improved the daylight at this area. More than 10% increment has been obtained (from 79% to 93%) comparing to the original target positions, and this shift of targets position could be considered as a promising method

for energy saving at this late time of the day. After applying this shift during the day, we can observe substantial improving at the early and late hours, as shown in *Figure 7-23*. It can be seen that the double-layer IPL is giving illuminance performance ranging between 79–96%, which is above the accepted range 70%. Meanwhile, the dual-axis IPL is ranging between 91–98%, which is above the targeted amount 90%; accordingly, daylight availability is almost constant during the daytime and no need for electrical lighting.



	9:00 AM	10:00 AM	11:00 AM	12:00 PM	1:00 PM	2:00 PM	3:00 PM	4:00 PM	5:00 PM
One-axis	82%	94%	93%	97%	96%	81%	82%	74%	21%
Biaxis	91%	93%	95%	98%	96%	96%	93%	93%	95%
Two-axis	89%	93%	95%	96%	94%	93%	91%	89%	79%

Figure 7-23: Percentage daylight coverage of the three systems after applying the shifted targets, on the 21st of September

7.5 Summary

A comparison analysis was conducted for the south-oriented office room in New Cairo location to evaluate the daylight availability during the daytime by using three daylighting systems with different methods. The whole daylighting systems were controlled parametrically using predefined algorithmic formula created in Grasshopper within its environmental plugins. *Chapter 7* aimed to evaluate the performance of each system by using the improved redirecting method.

It has been mentioned previously in *Chapter 6* that using "One-axis method" in the Integrated Parametric Louvre can save around 50% of electrical light throughout the year. However, by using the fixed targets method based on dual-axis and double-layer Parametric Louvre, more uniform and constant daylight can be achieved, which can save more than 70% of electrical light. At the first instance, daylight analysis results revealed that the three systems were dramatically converged, although the new proposed two systems (dual-axis and double-layer IPL) should provide constant reflected light on the ceiling. The data analysis revealed that the skydome has a significant influence on the provided daylight in addition to the reflected sunlight. Consequently, the study found that when shifting the targets on the ceiling to the low light area, it will significantly compensate for the lack of daylight at this area.

Therefore, dual-axis and double-layer IPL can be considered as promising methods for such daylighting systems while they can provide up to 90% and 80% respectively of daylight coverage during the daytime inside the room. Accordingly, electrical light can be saved during working hours. On the other hand, the addition of the Thermochromic window increased the daylight stability, while, it can control the penetration of daylight based on solar intensity. Besides, more practical Integrated Parametric Louvre has been achieved, while, no need to increase or decrease the number of slats to compensate for the intensity level.

Chapter 8 Adaption of the Parametric Louvre to slim and curved slats to increase its feasibility

8.1 Introduction

As mentioned in the previous chapters, the Integrated Parametric Louvre can be used to protect buildings' envelope from negative effects of solar radiation, optimise useful daylight, achieve occupants' comfort and save energy. However, cost, quality, efficiency and maintenance are still crucial challenges for such a system. Therefore, practical and feasible aspects should be taken in to account to increase the benefits of the system. Although, some innovative daylighting systems such as light-shelves and Himawari can optimise the use of daylight, however, their big size can be a potential obstacle to be introduced widely to the market. As well as cost and maintenance, which should be considered at the early stage of the system's design [75]. Therefore, manipulating with the parameters of such systems can probably increase their feasibility [310].

A previous study investigated the possibility to reduce the size of daylight redirecting micro-prism system while remaining its optical performance [311], aiming to achieve more practical use. Other study used three-dimensional textile to improve daylight performance via manipulating with the shape and using small size apertures [312]. As a daylight penetration, Penumbra effect plays an important role in such cases, which efficiently occurred when reducing the size of the apertures of any fenestration system [156]. This phenomenon mitigates the intensity of the light, reduces potential glare and provides diffuse light. This chapter focuses on a further practical and feasible system in two ways. Firstly, by

reducing the slats' size without affecting their illuminance performance. Secondly, by changing the slats' shape to originate lighter weight and graceful shape, which accordingly can ease the installation process. The study went through several steps by changing size and shape to achieve the aims, as mentioned earlier.

8.2 Reducing the slat's size of the Parametric Louvre

In the previous chapters, the slat width of the Parametric Louvre was chosen to be 10 or even 15 cm for both rotating mirrored slats and fixed shade slats, which accordingly should be used outdoor as a louvre shading device next to the window due to its big size [8]. This chapter investigates reducing the slat width in order to be installed indoor or even within double glazing for more handy control. The following figures reveal the performance of daylight distribution and Daylight Glare Probability (DGP) inside an example office room when the slat width is gradually reduced from 25 cm to 2.5 cm at seven intervals.

8.2.1 Simulation of reducing the slat's width of the Parametric Louvre in seven intervals

DGP is an abbreviation of Daylight Glare Probability, which influences on the occupants' visual comfort inside the office room. Glare, is defined as the contrast lowering effect within a visual field due to the presence of bright light sources, or a difference between a dark and bright area, or even light occurred from a shiny surface. DGP is considered the most recent index to evaluate glare from daylight. Usually, the fisheye lens is used to measure its level. In our case, DGP was measured using a virtual person sitting at the desk level facing a side wall, see Figure 8-1.

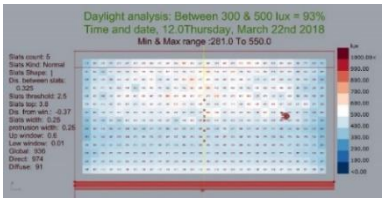
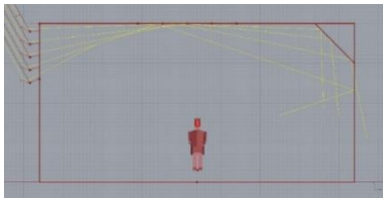
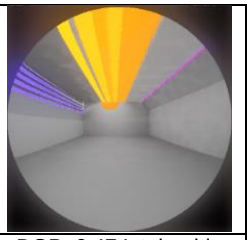
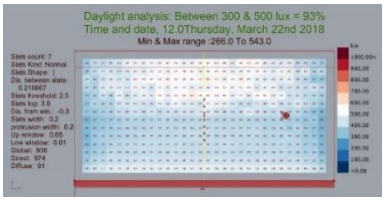
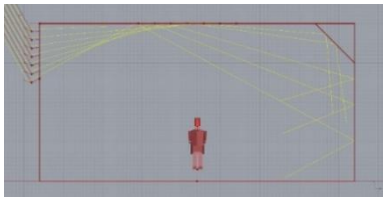
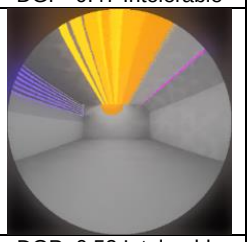
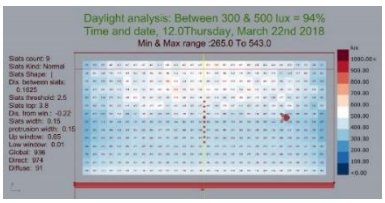
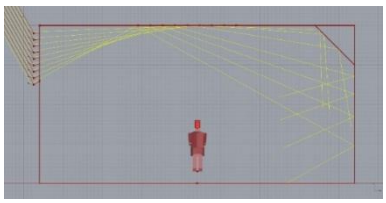
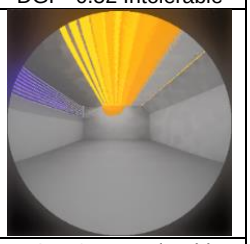
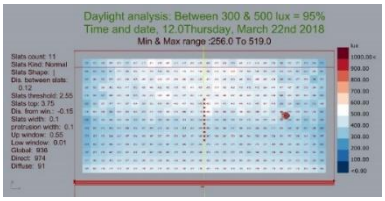
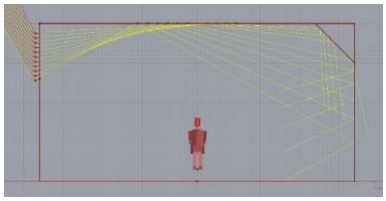
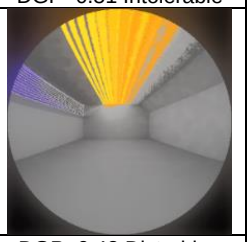
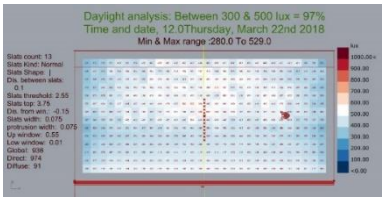
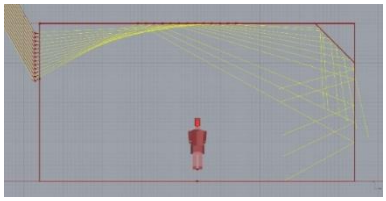
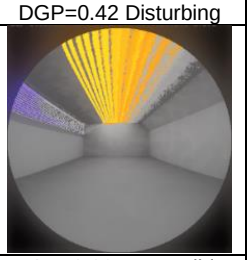
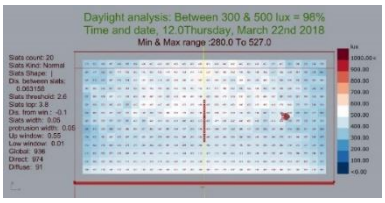
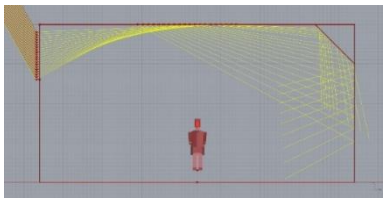
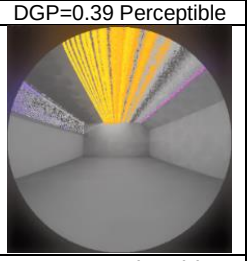
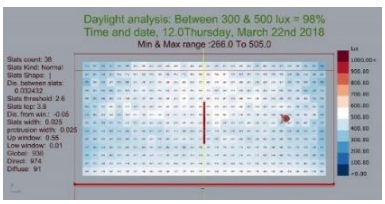
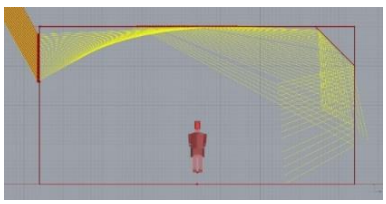
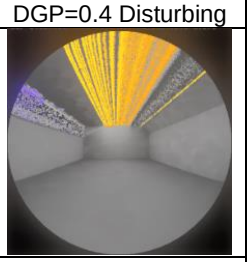
Case (1)			
	Daylight coverage analysis 93%	25 cm – 5 slats	DGP=0.47 Intolerable
Case (2)			
	Daylight coverage analysis 93%	20 cm – 7 slats	DGP=0.52 Intolerable
Case (3)			
	Daylight coverage analysis 94%	15 cm – 9 slats	DGP=0.51 Intolerable
Case (4)			
	Daylight coverage analysis 95%	10 cm – 11 slats	DGP=0.42 Disturbing
Case (5)			
	Daylight coverage analysis 97%	7.5 cm – 13 slats	DGP=0.39 Perceptible
Case (6)			
	Daylight coverage analysis 98%	5 cm – 20 slats	DGP=0.4 Disturbing
Case (7)			
	Daylight coverage analysis 98%	2.5 cm – 38 slats	DGP=0.38 Perceptible

Figure 8-1: Flat Parametric Louvre shape – applied in an example office room in New Cairo on the 22nd of March at noontime, showing; top view – daylight analysis percentage, side view – raytracing study and DGP map, respectively.

8.2.2 Prototyping the reduced size of the Parametric Louvre via using 1:1 mock-up (2.5 cm slat width)

A prototype scale 1:1 has been created for the Parametric Louvre as an experimental study to validate the reduced size of the louvre. The mock-up frame was made of acrylic by using laser cut. The mock-up was assembled in a square shape 80 * 80 cm height and width as a window frame. Two sides of the frame have been perforated at 29 vertical apertures with 22 cm equidistant between each aperture and Ø 0.5 cm for each. These 29 apertures were used as guide for Ø 0.5 cm aluminium rods, which used as a single rotation guide axis for the slats. One side of these rods were attached with 29 gears controlled by "rack and pinion" system, whereas, all the slats have the same rotation magnitude, but with an individual angle for each, see Figure 8-2. Therefore, "rack and pinion" as an accurate controller system can rotate all the slats simultaneously with a prior specified rotational angle for each slat. Rack and pinion movements are controlled by one stepper motor mounted at the top of the acrylic frame. The stepper motor is controlled by Arduino Uno based on Firefly as a plugin in Grasshopper (similar steps as in *Chapter 4*).



Figure 8-2: 1:1 mock-up for the Parametric Louvre made of laser cut acrylic and aluminium slats

8.2.3 Validating the reduced slats' size of the Parametric Louvre via using 1:1 mock-up (2.5 cm slat width)

A validation study has been made for the Parametric Louvre using scale 1:1 mock-up, in a meeting room at the University of Nottingham. The mock-up was mounted in the upper part of a south-oriented window. The lower part was covered with black fabric, while, the area near to the window has been ignored in this study. The room is 10 m length and ~8 m depth, and 3.8 m height. Before this validation study, the mock-up has been tested in a lecture room oriented to the southwest, in order to calibrate the measurements tools and verify the mock-up control. This test room was 8 m length and 6 m depth and 2.7 m height. In this case, the mock-up was mounted at a lower level at 1 m height, while, the lower part was just a simple wall. The test has been performed at 2 p.m. in a clear sky condition with direct sunlight, on the 21st of May, see Figure 8-3.



Figure 8-3: the two images showing the difference between opened and closed state (off/on) of the Parametric Louvre mock-up

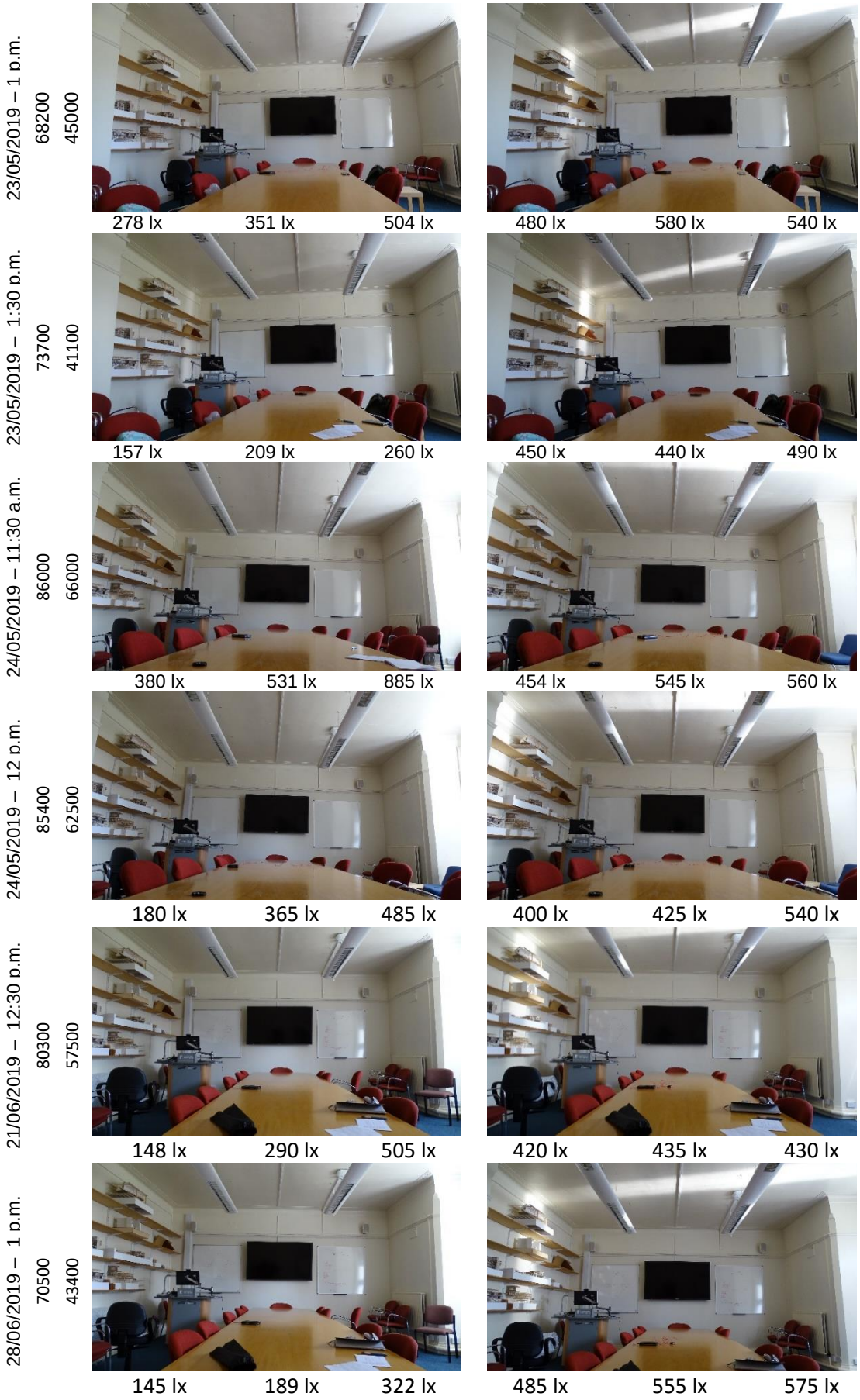
The illuminance has been tested in the off/on states of the Parametric Louvre mock-up using two sensors and lux meters (similar as in *Chapter 4*). The sensors have been located in 1.5 and 3 m away from the wall, at the front desk along under the illuminated patch, where, the desk is 0.75 height from the floor.

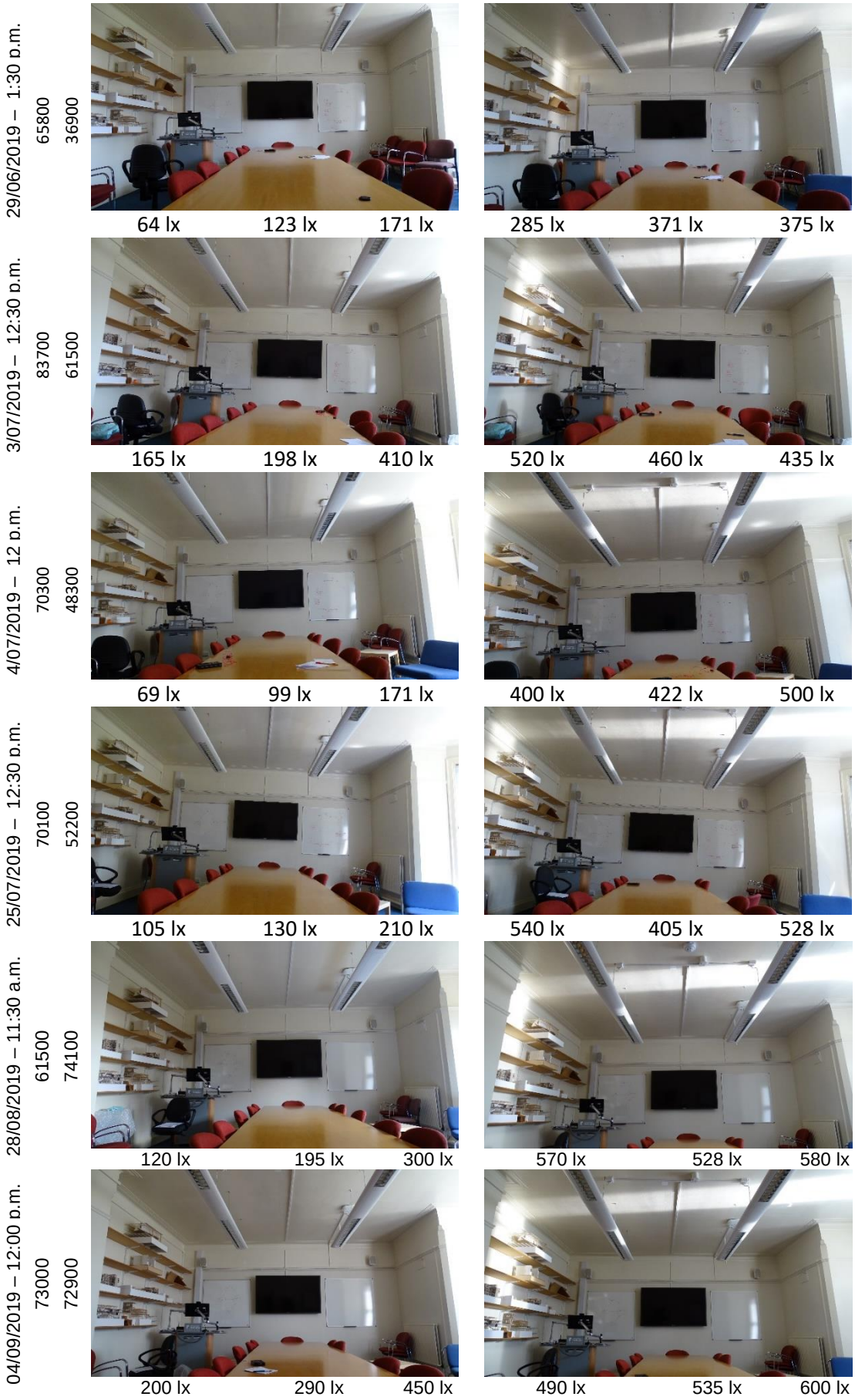
In the standard window (Off state) the sensors recorded 87 lx and 109 lx respectively, however, in the (On state) the sensors recorded 313 lx and 308 lx respectively, which meets the recommended illuminance threshold 300~500 lx. We have to put in consideration that the illuminated patch width is relatively small, which potentially produces lower intensity than expected. However, if it is applied on a broader scale, the contribution of the reflected light can probably increase.

For the validation study, as mentioned previously, the test has been made in the meeting room between 11 a.m. and 1 p.m. on selected sunny days in May, June, July, August and September. The test time was limited between 11 a.m. and 1 p.m. due to the small size of the mock-up, because, the illuminated patch decreases before and after these times and the contribution of the reflected light become lower. Meanwhile, the test was performed to validate the efficiency of the Parametric Louvre in its optimum performance. The sensors have been located in three positions under the illuminated patch at 1.2, 2.2, and 3.4 m away from the wall facing the window. The test has been performed using off/on states; therefore, six figures have been recorded for each time, in addition to the horizontal and vertical illuminance for the solar radiation at this time, see Table 8-1.

Table 8-1: comparison between off/on states using three different sensors in a meeting room at the University of Nottingham, from May to August in selected sunny days with clear sky condition

Date – Time Horizontal illuminance Vertical illuminance	Off state			On state		
Illum.	at 1.2 m	at 2.2 m	at 3.4 m	at 1.2 m	at 2.2 m	at 3.4 m


23/05/2019 – 1 p.m.
68200
45000
278 lx
351 lx
504 lx
480 lx
580 lx
540 lx
23/05/2019 – 1:30 p.m.
73700
41100
157 lx
209 lx
260 lx
450 lx
440 lx
490 lx
24/05/2019 – 11:30 a.m.
86000
66000
380 lx
531 lx
885 lx
454 lx
545 lx
560 lx
24/05/2019 – 12 p.m.
85400
62500
180 lx
365 lx
485 lx
400 lx
425 lx
540 lx
21/06/2019 – 12:30 p.m.
80300
57500
148 lx
290 lx
505 lx
420 lx
435 lx
430 lx
28/06/2019 – 1 p.m.
70500
43400
145 lx
189 lx
322 lx
485 lx
555 lx
575 lx


29/06/2019 – 1:30 p.m.
65800
36900
64 lx
123 lx
171 lx
285 lx
371 lx
375 lx
3/07/2019 – 12:30 p.m.
83700
61500
165 lx
198 lx
410 lx
520 lx
460 lx
435 lx
4/07/2019 – 12 p.m.
70300
48300
69 lx
99 lx
171 lx
400 lx
422 lx
500 lx
25/07/2019 – 12:30 p.m.
70100
52200
105 lx
130 lx
210 lx
540 lx
405 lx
528 lx
28/08/2019 – 11:30 a.m.
61500
74100
120 lx
195 lx
300 lx
570 lx
528 lx
580 lx
04/09/2019 – 12:00 p.m.
73000
72900
200 lx
290 lx
450 lx
490 lx
535 lx
600 lx

The results in the "off" state reveal a noticeable variation among the illuminance values which gradually increases towards the window; meanwhile, the illuminance levels were still lower than the required threshold level in most cases, which probably considered inappropriate for human visual comfort. Promisingly, in the "on" state, variation between the sensors is relatively reasonable within the range 300~600 lx, which is above the required threshold level. Moreover, the difference between the illuminance values ranges within 100 lx, which is relatively steady compared to the "off" state. It should bear in mind that the chamfered ceiling and the advanced glazing were not considered in the test room, which may significantly influence the steadiness and the distribution of the daylight in the room. For instance, the vertical patch light at the left wall can be exploited by using the chamfered ceiling to give better performance. Additionally, for such an experiment, the limited size of the mock-up reduces the opportunity of maximum daylight harvesting, which can probably yield better performance with a full-scale system. Generally, the results show that the Parametric Louvre can significantly provide 8-meter dim room with constant and steady daylight within an acceptable range, which can achieve visual comfort and save electrical energy.

8.3 Modifying the slat's shape of the Parametric Louvre

In previous chapters, the slats were assumed to be in a flat shape. For a smaller slat width, the study in this section will examine two different slat shapes; the concave shape and the convex shape, see *Figure 8-4*. It should bear in mind that modifying the slat's shape can generate more strength and thinner slat in addition to achieving more limber characteristic and feasible material.

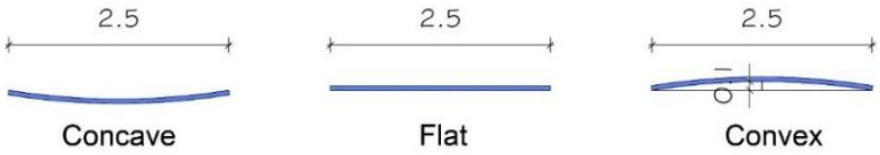


Figure 8-4: Various slat shapes (width in centimetre), height is 0.1 cm

8.3.1 Simulation of reducing the concave slats' width of the Parametric Louvre at seven intervals

Similar to the study on the flat slats, the width of the concave slats was also changed at seven intervals; 2.5cm, 5cm, 7.5cm, 10cm, 15cm, 20cm and 25cm. The simulation consists of; daylight coverage percentage analysis at the desk level, left view of the room revealing light raytracing and Daylight Glare Probability radiance map, as shown in *Figure 8-5*.

8.3.2 Simulation of reducing the convex slats' width on the Parametric Louvre at seven intervals

Likewise, to the previous section, a convex slat has been applied to the Parametric Louvre. The convex slat width was also changed and examined at seven intervals; 2.5cm, 5cm, 7.5cm, 10cm, 15cm, 20cm and 25cm. The simulation consists of; daylight coverage percentage analysis at the desk level, left view of the room revealing light raytracing and Daylight Glare Probability radiance map, see *Figure 8-6*.

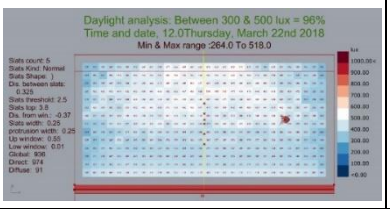
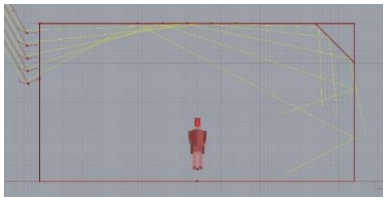
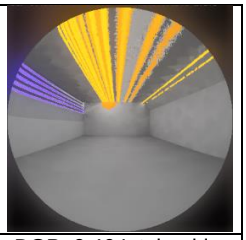
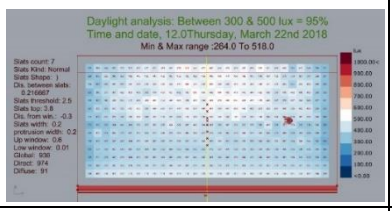
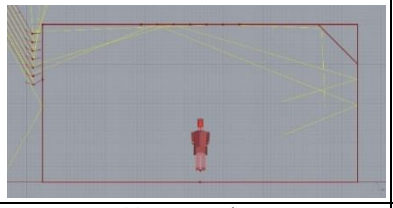
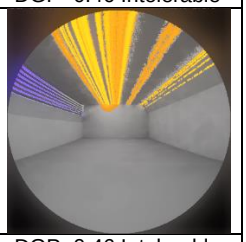
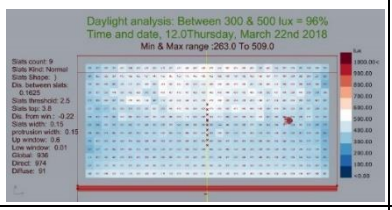
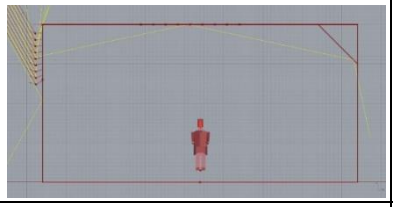
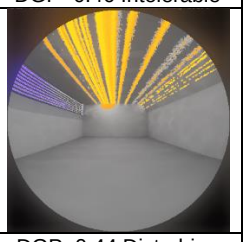
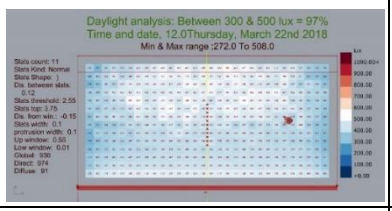
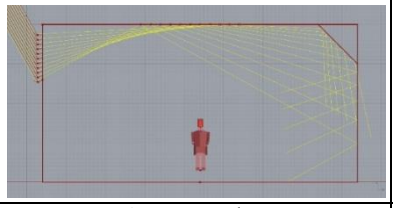
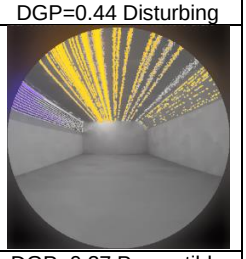
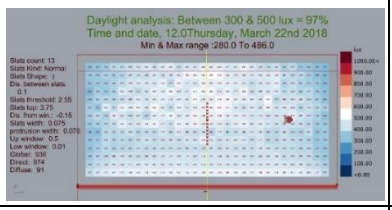
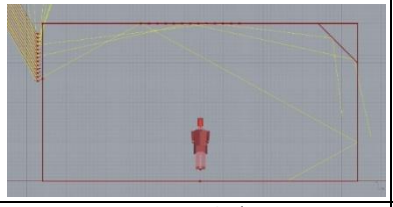
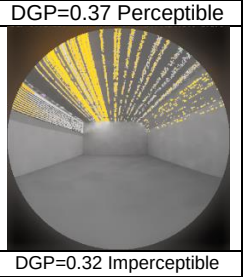
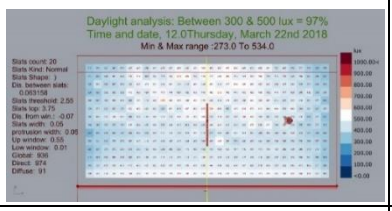
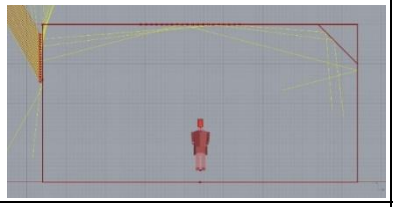
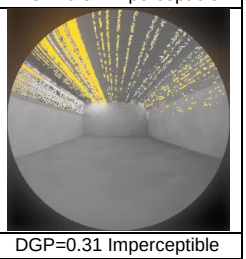
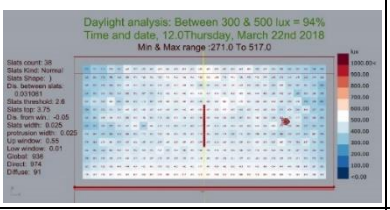
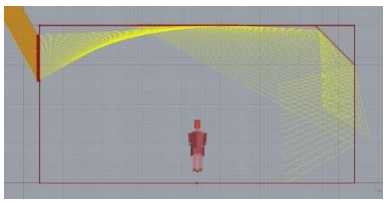
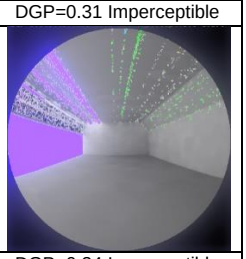
Case (1)			
	Daylight coverage analysis 96%	25 cm – 5 slats	DGP=0.46 Intolerable
Case (2)			
	Daylight coverage analysis 95%	20 cm – 7 slats	DGP=0.46 Intolerable
Case (3)			
	Daylight coverage analysis 96%	15 cm – 9 slats	DGP=0.44 Disturbing
Case (4)			
	Daylight coverage analysis 97%	10 cm – 11 slats	DGP=0.37 Perceptible
Case (5)			
	Daylight coverage analysis 97%	7.5 cm – 13 slats	DGP=0.32 Imperceptible
Case (6)			
	Daylight coverage analysis 97%	5 cm – 20 slats	DGP=0.31 Imperceptible
Case (7)			
	Daylight coverage analysis 94%	2.5 cm – 38 slats	DGP=0.34 Imperceptible

Figure 8-5: Concave Parametric Louvre shape – applied in an example office room in New Cairo on 22nd of March at noontime, showing; top view – daylight analysis percentage(left), side view – raytracing study (middle) and DGP map (right), respectively.

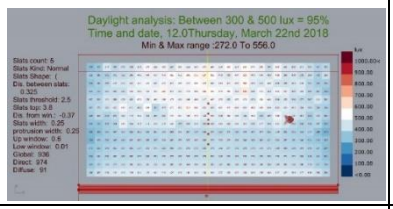
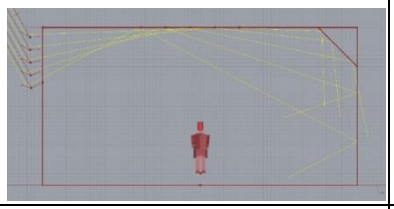
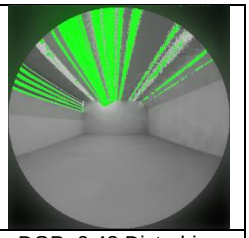
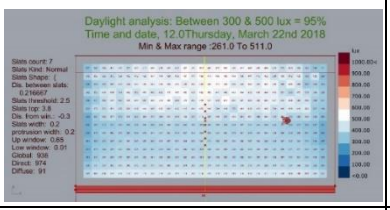
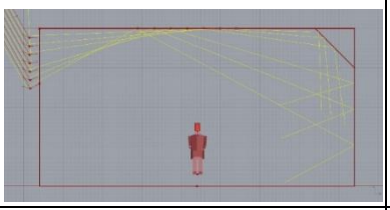
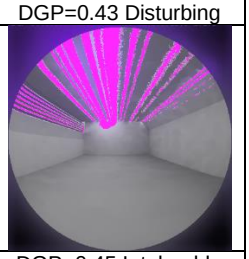
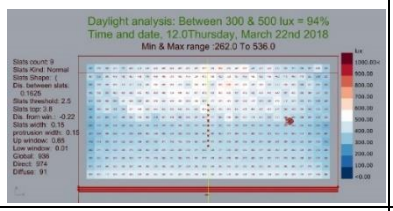
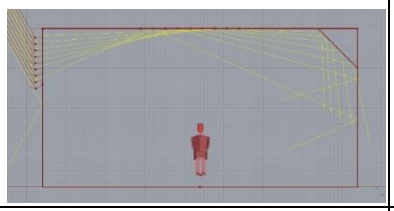
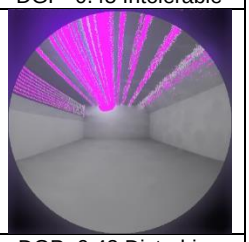
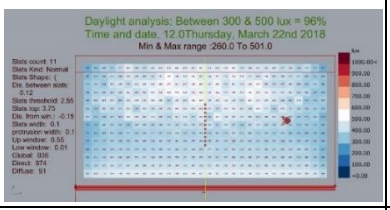
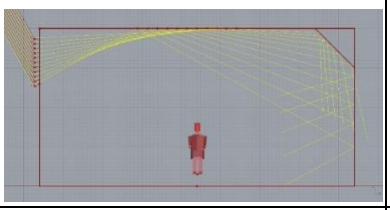
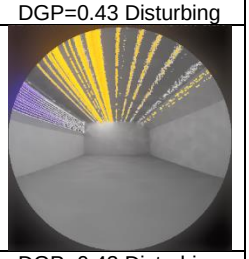
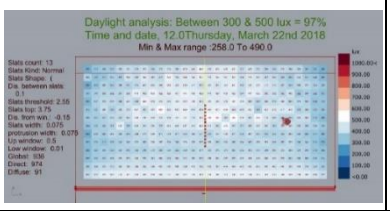
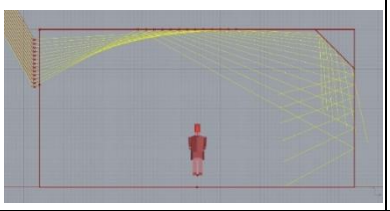
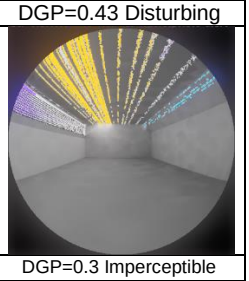
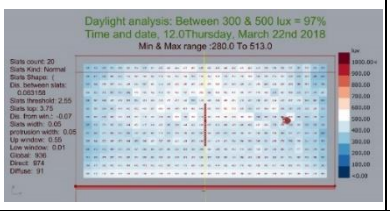
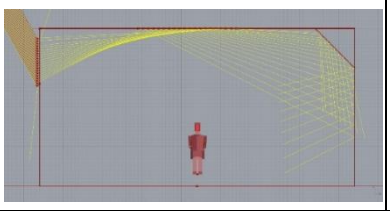
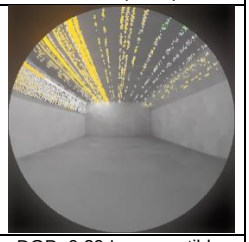
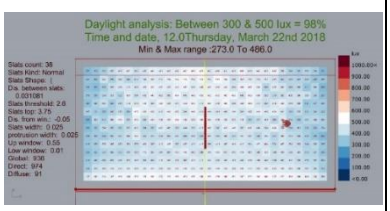
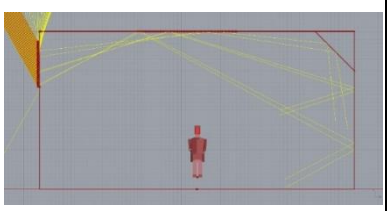
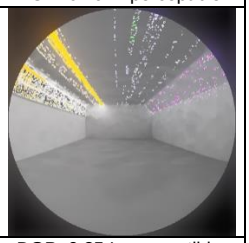
Case (1)			
	Daylight coverage analysis 95%	25 cm – 5 slats	DGP=0.43 Disturbing
Case (2)			
	Daylight coverage analysis 95%	20 cm – 7 slats	DGP=0.45 Intolerable
Case (3)			
	Daylight coverage analysis 94%	15 cm – 9 slats	DGP=0.43 Disturbing
Case (4)			
	Daylight coverage analysis 96%	10 cm – 11 slats	DGP=0.43 Disturbing
Case (5)			
	Daylight coverage analysis 97%	7.5 cm – 13 slats	DGP=0.3 Imperceptible
Case (6)			
	Daylight coverage analysis 97%	5 cm – 20 slats	DGP=0.29 Imperceptible
Case (7)			
	Daylight coverage analysis 98%	2.5 cm – 38 slats	DGP=0.25 Imperceptible

Figure 8-6: Convex Parametric Louvre shape – applied in an example office room in New Cairo on 22nd of March at noontime, showing; top view – daylight analysis percentage (left), side view – raytracing study (middle) and DGP map (right), respectively.

8.4 Examining the Parametric Louvre performance with the reduced slat width and the modified slat's shape on the 21st of June, 23rd of September and 21st of December during the working hours at the New Cairo location

It is apparent from the previous results that modifying the slat size and shape succeeded to achieve promising performance compared to its initial size and its flat shape. Accordingly, these new applied modifications will be examined in different seasons at different times for more validated results and doubtless performance. For convenience in descriptions, the Parametric Louvre with a slat width 2.5 cm will be denoted as (Slim Flat-Parametric Louvre or SF-PL), (Slim Concave-Parametric Louvre or SCC-PL) and (Slim Convex-Parametric Louvre or SCV-PL), respectively.

A comparison has performed between SF-PL, SCC-PL and SCV–PL during daytime from 9 a.m. to 5 p.m. on the 21st of June, 23rd of September and 21st of December to examine the performance of daylight coverage percentage analysis for each shape individually, via using DAYSIM based on Ladybug as a plugin in Grasshopper, see *Figure 8-7*, Figure 8-8 and Figure 8-9 . The test was performed under a clear sky condition with direct sunlight in an example office room by using the EPW weather file of the New Cairo location. As mentioned previously, the comparison here is only for the slim slat of 2.5 cm wide.

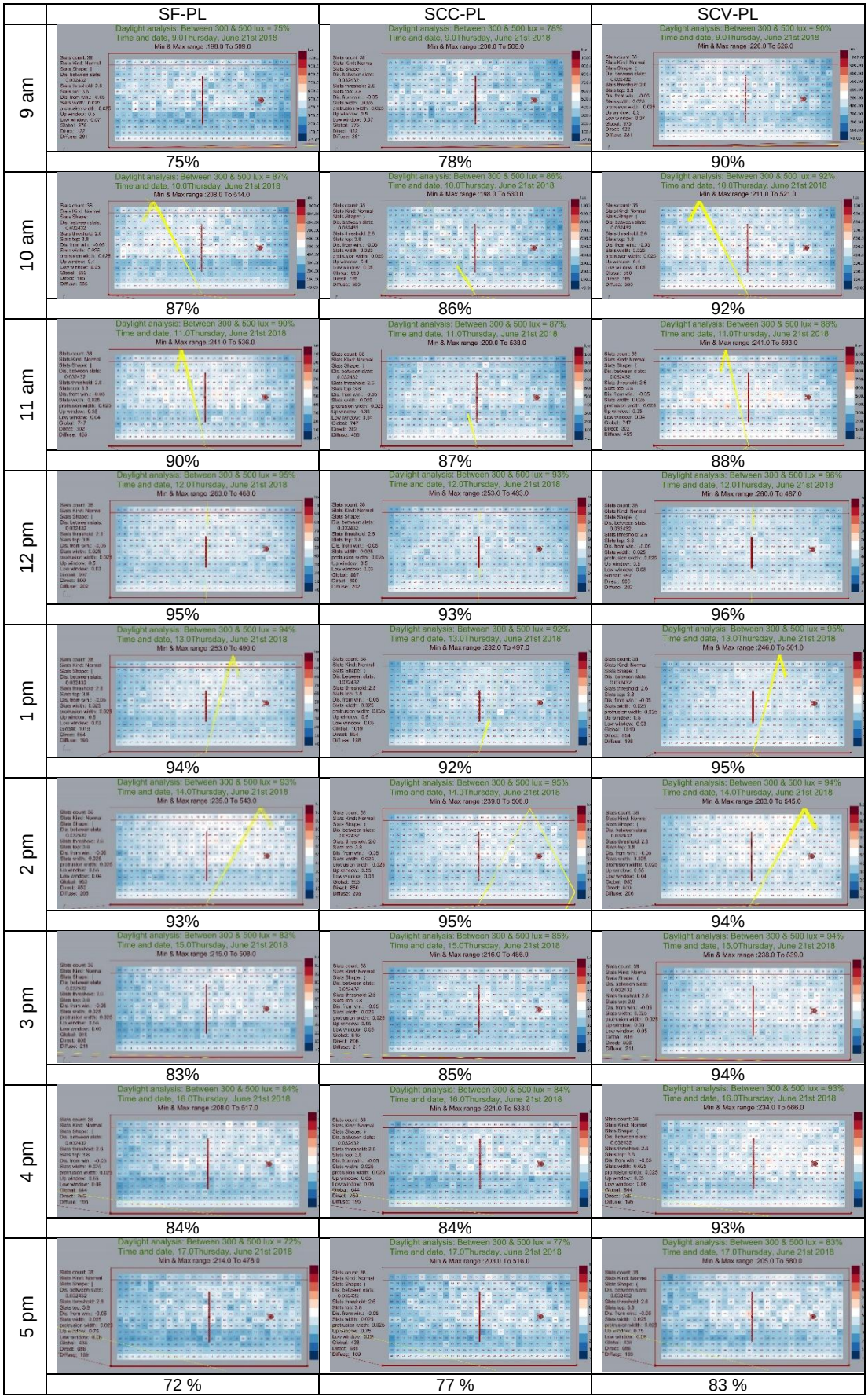


Figure 8-7: Daylight coverage percentage during the daytime on June 21st at New Cairo location for the SF-PL, SCC-PL and SCV-PL

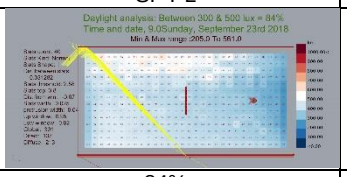
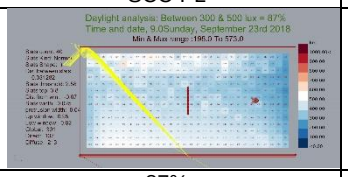
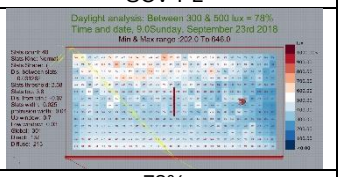
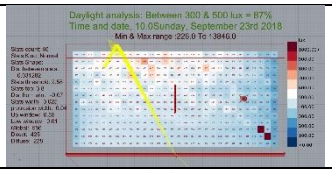
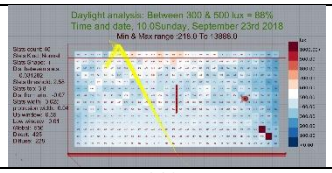
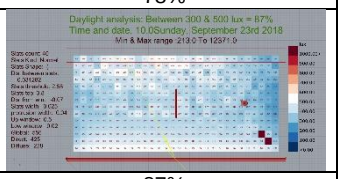
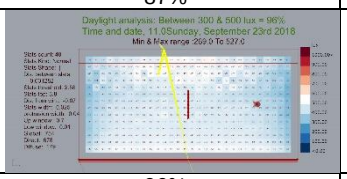
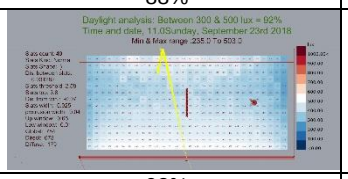
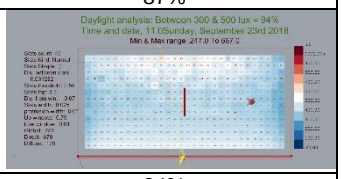
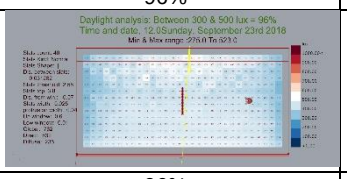
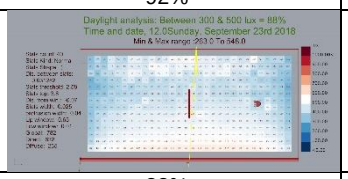
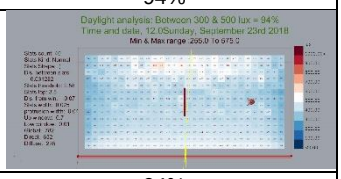
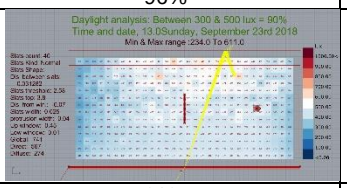
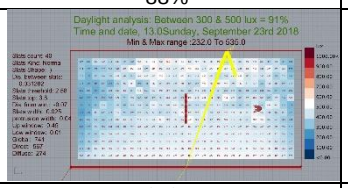
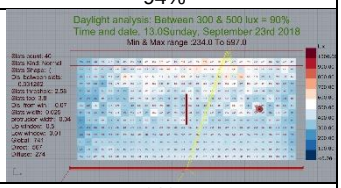
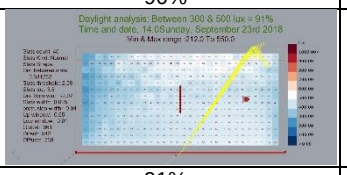
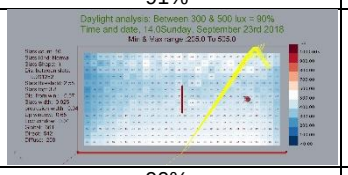
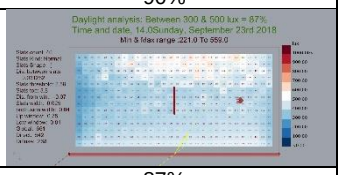
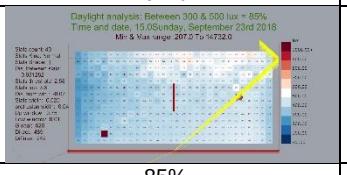
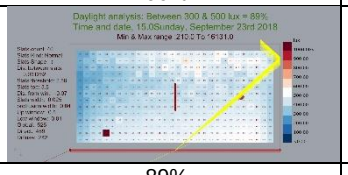
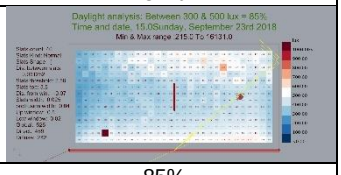
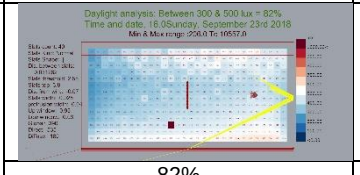
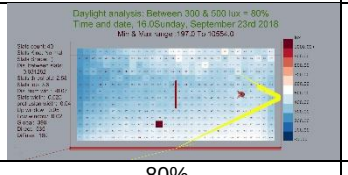
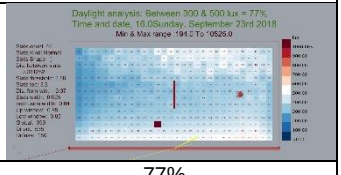
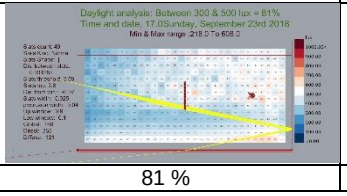
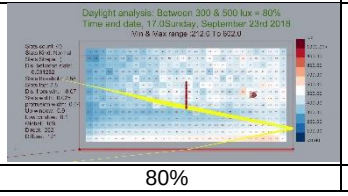
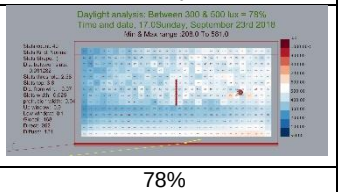
	SF-PL	SCC-PL	SCV-PL
9 am			
	84%	87%	78%
10 am			
	87%	88%	87%
11 am			
	96%	92%	94%
12 pm			
	96%	88%	94%
1 pm			
	90%	91%	90%
2 pm			
	91%	90%	87%
3 pm			
	85%	89%	85%
4 pm			
	82%	80%	77%
5 pm			
	81 %	80%	78%

Figure 8-8: Daylight coverage percentage during the daytime on September 23rd at New Cairo location for the SF-PL, SCC-PL and SCV-PL

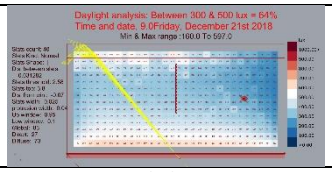
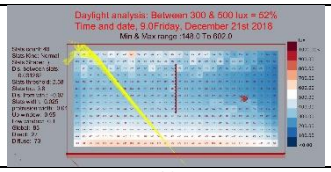
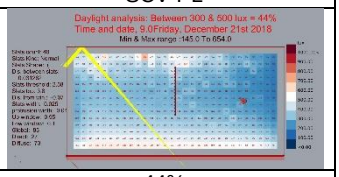
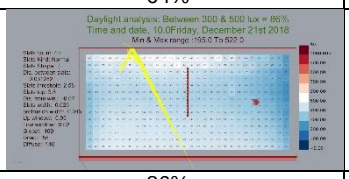
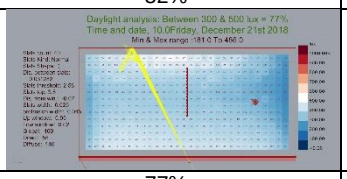
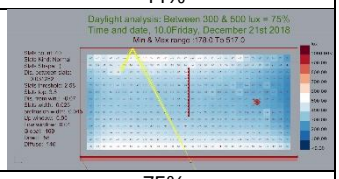
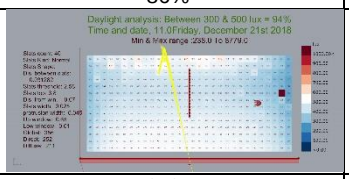
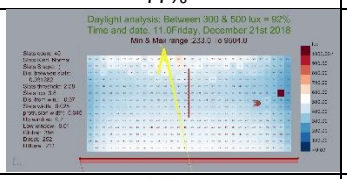
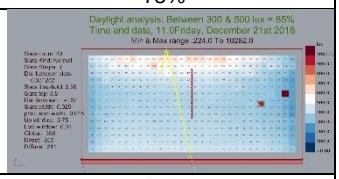
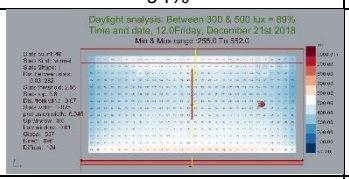
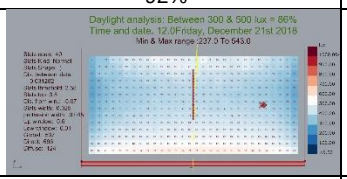
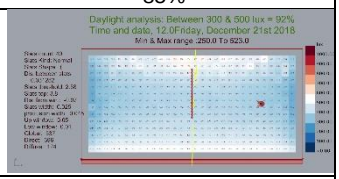
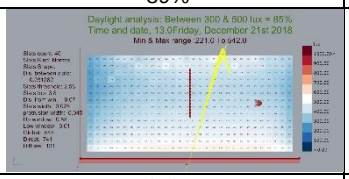
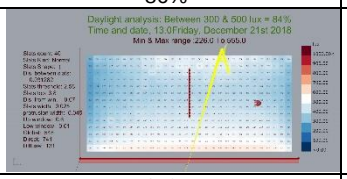
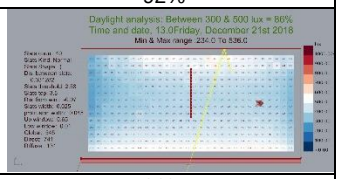
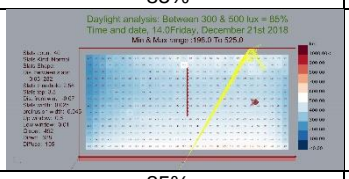
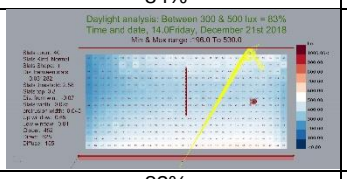
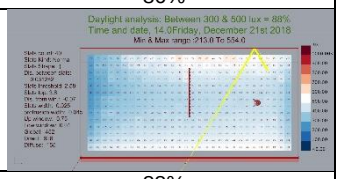
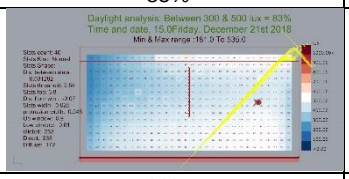
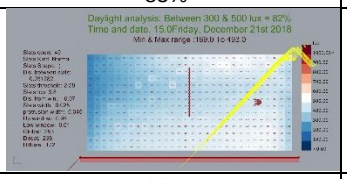
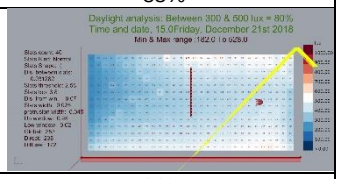
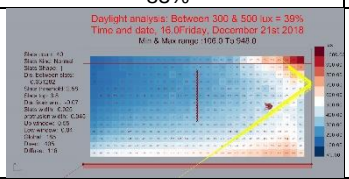
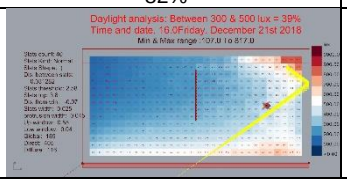
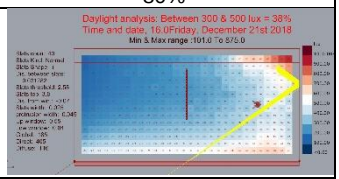
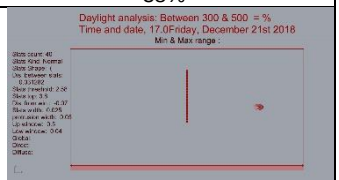
	SF-PL	SCC-PL	SCV-PL
9 am			
	64%	52%	44%
10 am			
	86%	77%	75%
11 am			
	94%	92%	85%
12 pm			
	89%	86%	92%
1 pm			
	85%	84%	86%
2 pm			
	85%	83%	88%
3 pm			
	83%	82%	80%
4 pm			
	39%	39%	38%
5 pm			
	0%	0%	0%

Figure 8-9: Daylight coverage percentage during the daytime on December 21st at New Cairo location for the SF-PL, SCC-PL and SCV-PL

8.5 Results and discussion about the performance of reducing the size and modifying the shape of the Parametric Louver

It can be observed in *Table 8-2,* Table 8-3 and Table 8-4 that daylight coverage percentage has been improved when the slat width is gradually reduced as shown in Figure 8-10. In addition to this aspect, DGP was also decreased gradually to a Perceptible level, which is potentially acceptable for visual comfort [41, 313] as shown in Figure 8-11.

Table 8-2: Comparison results between slats count, daylight coverage percentage, DGP and Glare effect of the Parametric Louvre via using flat slats

Case no.	slats width	slats count	daylight coverage	DGP	Glare effect
(1)	25 cm	5	93%	0.47	Intolerable
(2)	20 cm	7	93%	0.52	Intolerable
(3)	15 cm	9	94%	0.51	Intolerable
(4)	10 cm	11	95%	0.42	Disturbing
(5)	7.5 cm	13	97%	0.39	Perceptible
(6)	5 cm	20	98%	0.4	Disturbing
(7)	2.5 cm	38	98%	0.38	Perceptible

Table 8-3: Comparison results between slats count, daylight coverage percentage, DGP and Glare effect of the Parametric Louvre via using concave slats

Case no.	slats width	slats count	daylight coverage	DGP	Glare effect
(1)	25 cm	5	96%	0.46	Intolerable
(2)	20 cm	7	95%	0.46	Intolerable
(3)	15 cm	9	96%	0.44	Disturbing
(4)	10 cm	11	97%	0.37	Perceptible
(5)	7.5 cm	13	97%	0.32	Imperceptible
(6)	5 cm	20	97%	0.31	Imperceptible
(7)	2.5 cm	38	94%	0.34	Imperceptible

Table 8-4: Comparison results between slats count, daylight coverage percentage, DGP and Glare effect of the Parametric Louvre via using convex slats

Case no.	slats width	slats count	daylight coverage	DGP	Glare effect
(1)	25 cm	5	95%	0.43	Disturbing
(2)	20 cm	7	95%	0.45	Intolerable
(3)	15 cm	9	94%	0.43	Disturbing
(4)	10 cm	11	96%	0.37	Perceptible
(5)	7.5 cm	13	97%	0.3	Imperceptible
(6)	5 cm	20	97%	0.29	Imperceptible
(7)	2.5 cm	38	98%	0.25	Imperceptible

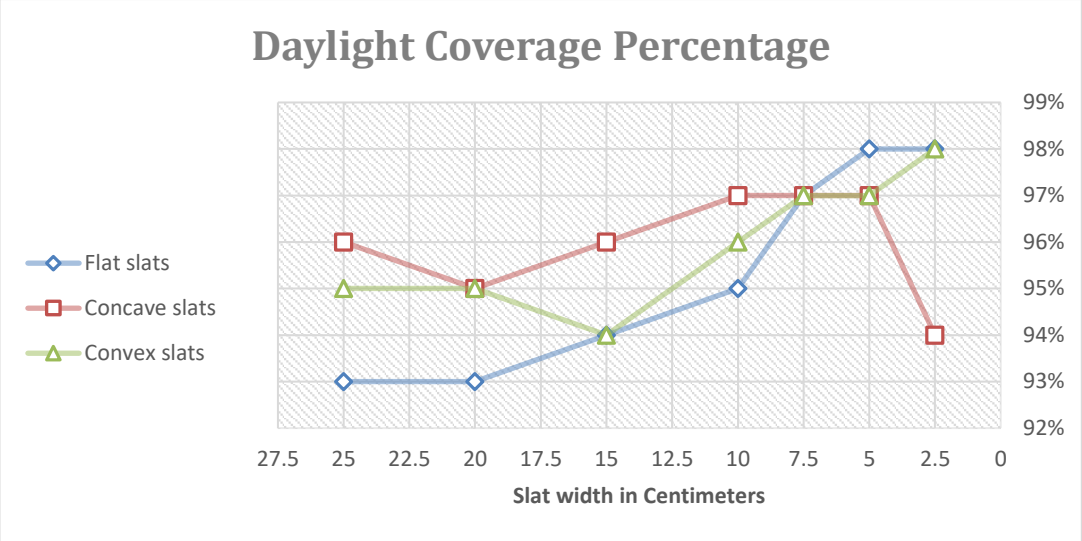


Figure 8-10: Daylight coverage percentage comparison results

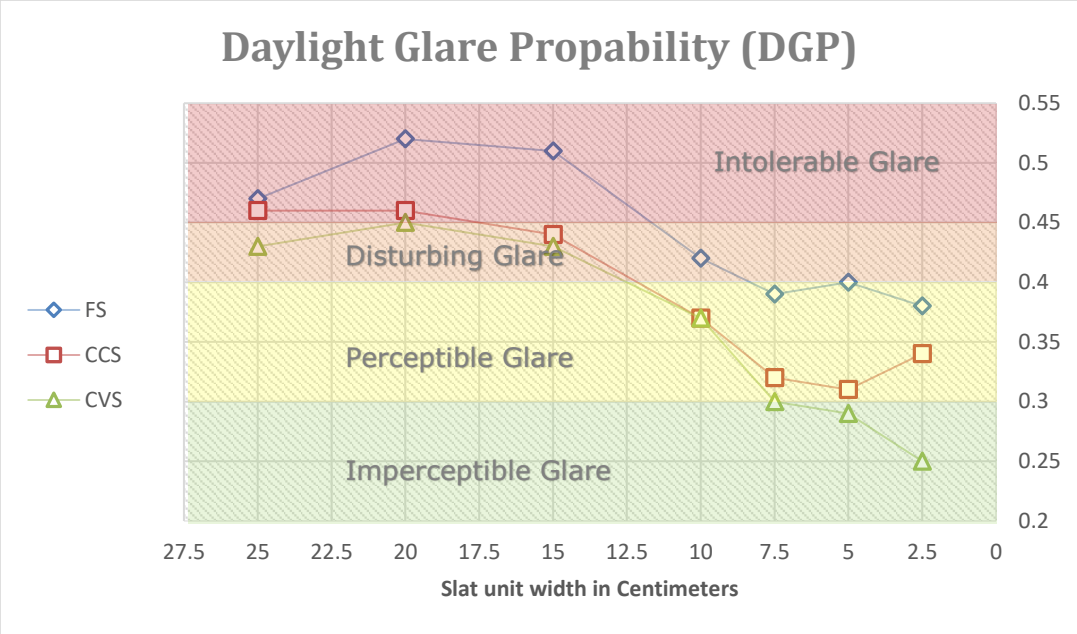


Figure 8-11: Daylight Glare Probability comparison results of the reduced slats' size of the SF-PL, CCS-PL and CVS-PL

8.5.1 The influence of reducing the size and modifying the shape of the Parametric Louver performance

Based on the results in *Table 8-2* and *Table 8-3* it can be observed that daylight coverage by using the concave slats is slightly lower than the flat slats due to the geometrical change of the slat curvature which influences on the reflected light distribution, meanwhile, DGP is slightly decreased in the concave slats compared to the flat one. On the other hand, in Table 8-4, there is a tangible improvement in the performance of the daylight

coverage and glare probability when using the convex shape. It can be seen that daylight coverage percentage reached 98% corresponding to an apparent drop in DGP to 0.25, which considered "Imperceptible" glare at that level in Case (7) compared to other cases. Among all other shapes, the (2.5 cm) convex shape in Case (7) achieved the best performance of daylight coverage and lowest glare, as shown in Figure 8-10 and Figure 8-11, respectively. In addition, the caustics on the ceiling is almost disappeared in such a case, as shown in Figure 8-17.

8.5.2 The outcome of the reduced size and the modified shapes of the Parametric Louver at different times and dates

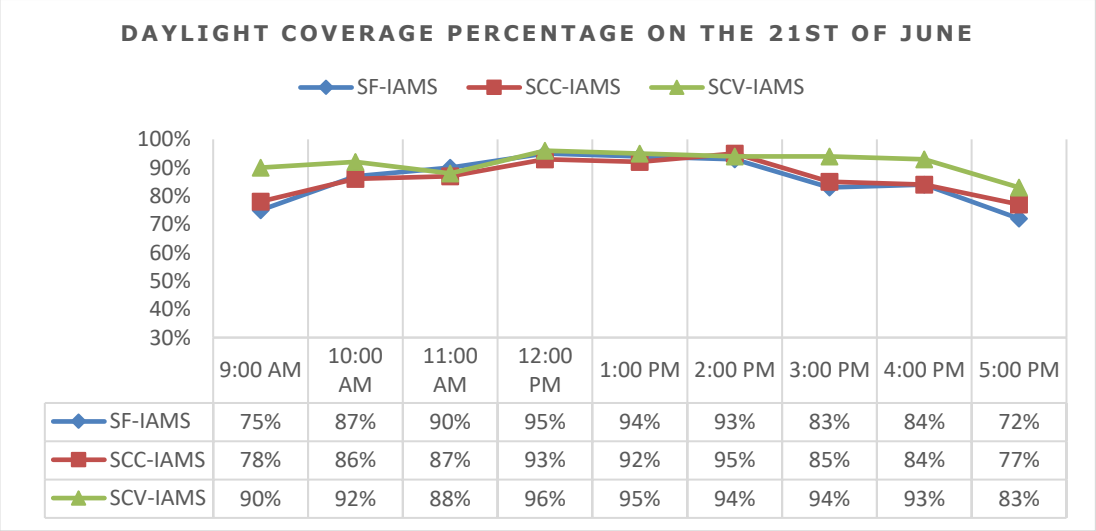
On the 21st of June, among all slats' shapes, the SCV-PL reveals the best performance of daylight during the working hours, especially at early and late hours as shown in *Figure 8-12*. The reason of that is due to the scattering parameter of the convex shape which is more likely to diffuse the received light rather than the flat shape which tends to reflect the same amount of any received light, and even the concave shape which tends to focus the received light as shown in *Figure 8-15*.

Moreover, the SCV-PL plays a vital role with the light received from the skydome, regardless of the direct sunlight. For instance, in Figure 8-7 at 4 p.m. and 5 p.m. on the 21st of June, it can be noticed that the azimuth inclination of the sunbeam is not striking the south window, which means that the received daylight only depends on the light coming from the skydome. Accordingly, this steepness of incident light can be a rational reason for the lack of daylight availability in the SF-PL and SCC-PL cases.

It can be seen in Figure 8-13, on the 23rd of September that the performances of all shapes are almost similar during the daytime, where, the illuminance coverage percentage ranges between 77% - 96%, which

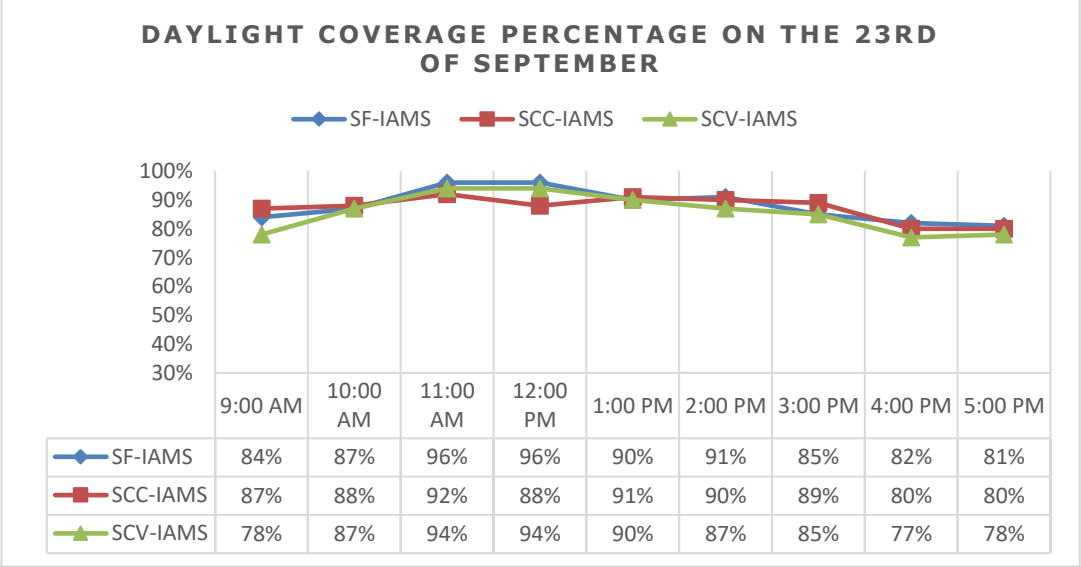
should be sufficient to meet the occupants' visual comfort and save energy. Accordingly, the SCC-PL and SCV-PL can be considered as efficient shapes beside the FS shape.

On the 21st of December, the performance all shapes are almost similar as well, with a slight difference at the morning hours, see *Figure 8-14*. Due to solar weakness and daytime insufficiency, the daylight coverage percentage gradually decreased from 80% at 3 p.m. to 0% at 5 p.m. Meanwhile, daylight coverage performance during the other hours is almost steady of around 85% except at 9 a.m., which is relatively low.



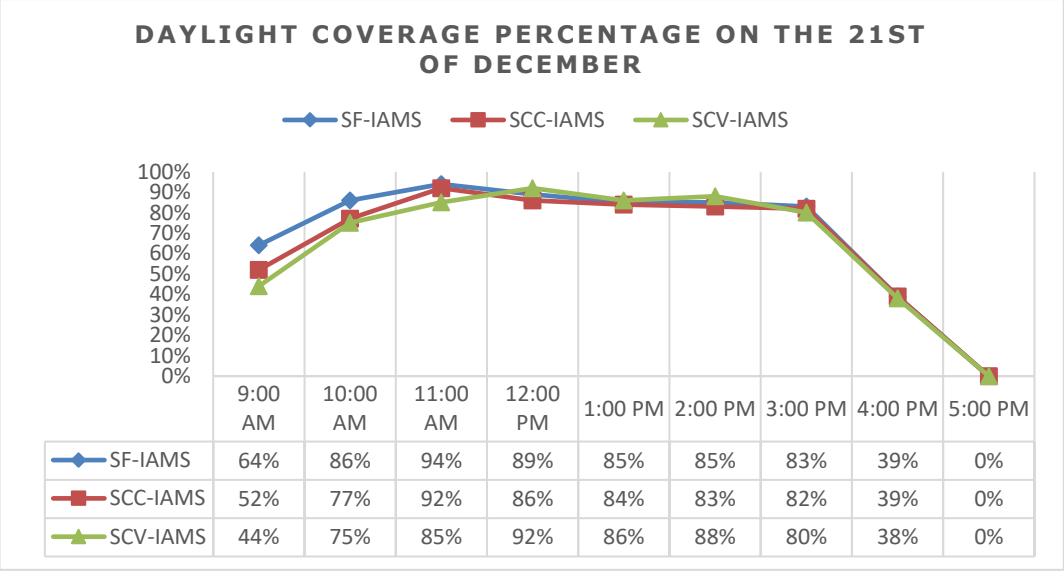
	9:00 AM	10:00 AM	11:00 AM	12:00 PM	1:00 PM	2:00 PM	3:00 PM	4:00 PM	5:00 PM
SF-IAMS	75%	87%	90%	95%	94%	93%	83%	84%	72%
SCC-IAMS	78%	86%	87%	93%	92%	95%	85%	84%	77%
SCV-IAMS	90%	92%	88%	96%	95%	94%	94%	93%	83%

Figure 8-12: 21st of June daylight coverage percentage graph for the SF-PL, SCC-PL and SCV-PL from 9 a.m. to 5 p.m.



	9:00 AM	10:00 AM	11:00 AM	12:00 PM	1:00 PM	2:00 PM	3:00 PM	4:00 PM	5:00 PM
SF-IAMS	84%	87%	96%	96%	90%	91%	85%	82%	81%
SCC-IAMS	87%	88%	92%	88%	91%	90%	89%	80%	80%
SCV-IAMS	78%	87%	94%	94%	90%	87%	85%	77%	78%

Figure 8-13: 23rd of September daylight coverage percentage graph for the SF-PL, SCC-PL and SCV-PL from 9 a.m. to 5 p.m.



	9:00 AM	10:00 AM	11:00 AM	12:00 PM	1:00 PM	2:00 PM	3:00 PM	4:00 PM	5:00 PM
SF-IAMS	64%	86%	94%	89%	85%	85%	83%	39%	0%
SCC-IAMS	52%	77%	92%	86%	84%	83%	82%	39%	0%
SCV-IAMS	44%	75%	85%	92%	86%	88%	80%	38%	0%

Figure 8-14: 21st of December daylight coverage percentage graph for the SF-PL, SCC-PL and SCV-PL from 9 a.m. to 5 p.m.

Although the significant variations in altitudes due to solar solstices [22], thanks to parametric design which capable to control the slats' rotations with respond to these solar fluctuations and accordingly facilitates the manipulation with the targets locations over the ceiling based on solar altitudes [247], which can compensate the weakness spots of daylight inside the room.

8.5.3 Discussion about the reflection behaviour of the Flat, Concave and Convex–Parametric Louver

It can be seen in Figure 8-15 that the concave slat behaviour is similar to the "parabolic trough" where, sunlight is collected and focused to a specific point; however, the concave slats were not tuned to a specific focal point. The light is concentrated at a specific distance then distributed again until reaching the ceiling. The reflected light is slightly concentrated near to the window then distributed in patches, then overlapped at the end of the room. It should be considered that the focal points in the concave case may have a risk of heat concentration on the fabrics material in the interior space, which can be a potential drawback of such a system, as seen in

Figure 8-15. On the other hand, the convex shape tends to disperse the reflected light over the whole ceiling, as shown in Figure 8-16, which considered as an advantage concerning the DGP.

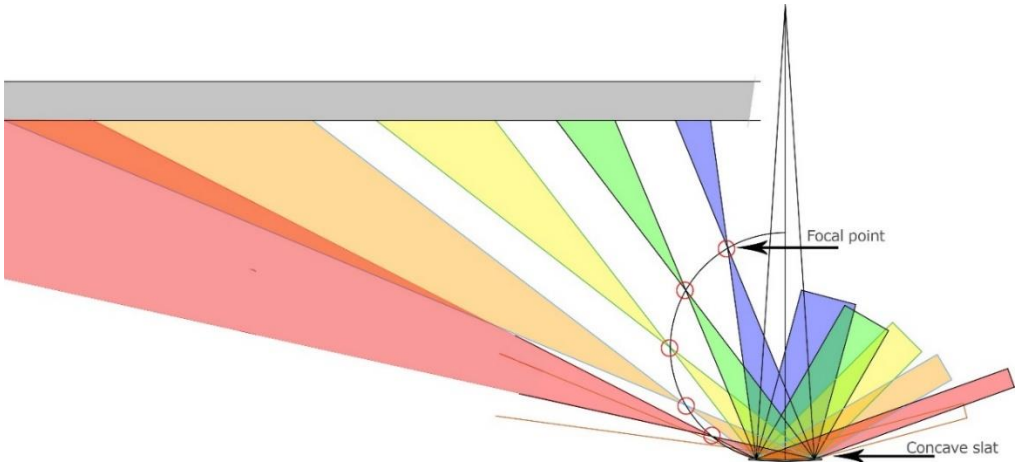


Figure 8-15: Side view showing the shape of the reflected light with a 5 cm concave slat in different inclination angles, the red circles indicate the focal points which may occur a risk for a heat concentration spots

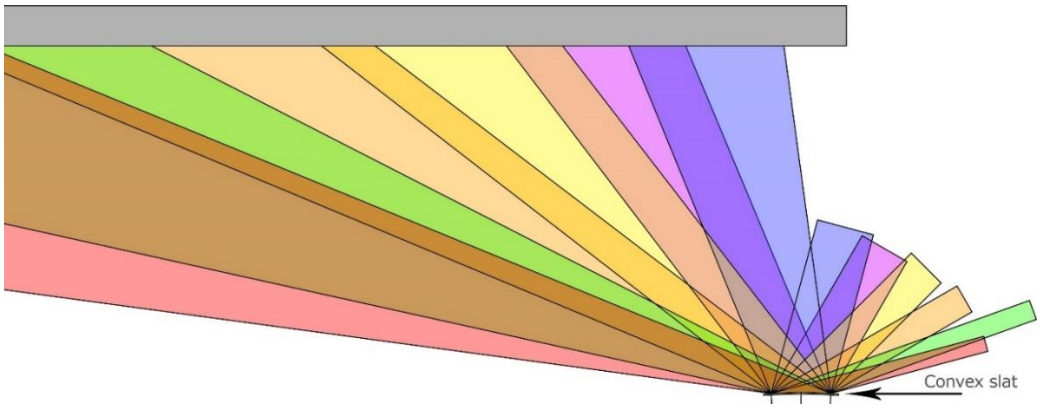


Figure 8-16: Side view showing the shape of the reflected light with a 5 cm convex slat in different inclination angles

In addition to the previous point, it can be seen in the false-colour maps in Figure 8-17 a density difference between the bright stripes on the ceiling, which influences the daylight uniformity in the room. Thanks to the small slats, which dramatically reduced the contrast between the bright stripes and gradually blended, as shown in Cases (7), which can yield better daylight uniformity. Moreover, the false-colour maps in Figure 8-17 reveal caustics patches in cases 01 and 04; however, these caustics were slightly diminished in Case (7), which has no contrast and homogeneously distributed. Besides, we can obviously notice a tangible improvement

among the SF-PL, SCC-PL and SCV-PL in Case (7), respectively, where the SCV-PL is the brightest case and the lowest in glare potential.

Generally, we can conclude that reducing the slat width can have a positive influence on daylighting performance, better illuminance distribution and glare reduction, in addition to the benefits of decreasing the system's weight for easy accessibility and increasing the slats' strength. Accordingly, such a system can be reduced as the size as the standard Venetian blinds instead of the large louvre, and simultaneously, maximising its daylighting utilities.

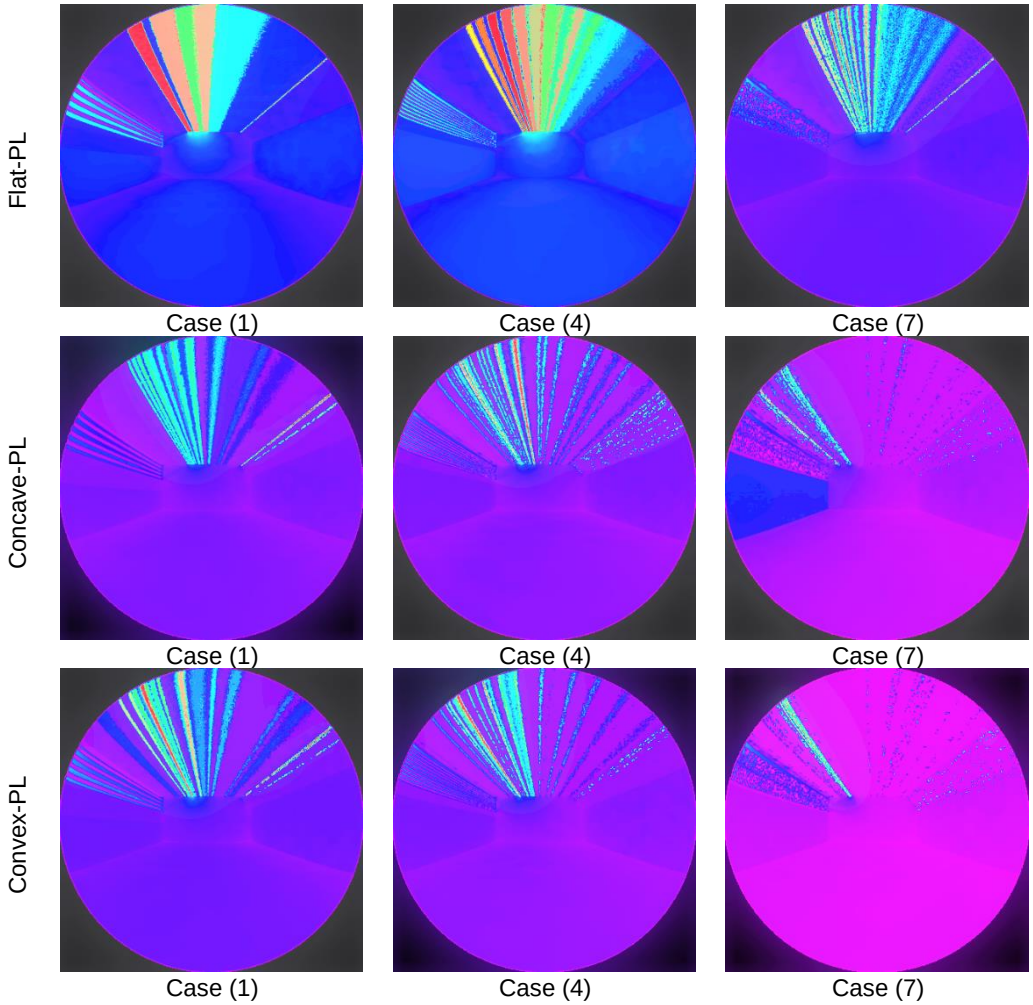


Figure 8-17: HDMI false colour maps for the cases (1), (4) and (7) of the Flat, Concave and Convex-Parametric Louvre, respectively.

8.6 Summary

Practical and feasible aspects are essential to promote any new daylighting system. The proposed Parametric Louvre has been discussed in the previous chapters as a daylighting system, which was initially designated to be installed outdoor over a building's façade, likewise the shading appliances. This chapter investigated using more reliable and practical Parametric Louvre by reducing the slat width and changing the slat shape, which can accordingly reduce their weight, increase their strength and achieve a graceful shape.

The Parametric Louvre performance has been examined after reducing its slats' width gradually from 25 cm to 2.5 cm. The examination performed on flat, concave and convex shapes by investigating their daylight coverage percentage and daylight glare probability for each shape. The results revealed that the reduced slats (slim-slat = 2.5 cm) could achieve better performance in both daylighting coverage and DGP, compared to the bigger ones. Notably, the concave and the convex shapes were resulting in much lower glare than the flat shape.

The slim shapes (SF-PL, SCC-PL and SC-PL) have been examined as well in different dates during the daytime, in June, September and December for more validated results. The results revealed that all shapes almost had similar performance; however, the SCV-PL can be considered as the most promising shape among the other shapes due to its stability performance, especially in June, in addition to its lowest glare probability. In conclusion, SCV-PL can be recommended as a promising daylighting system while it has slim size, lightweight, strength, graceful shape, and simultaneously can provide better daylight performance with low DGP. Such a system can be installed at the upper part of the window inside the

room for more handy control and even can be attached between double glazing due to its slim size. Moreover, this system can provide visual comfort and save energy in addition to its feasible characteristic.

Chapter 9 Conclusion

9.1 Conclusion

In the recent years, in respect of the agile development and new technologies, there has been tendency to move away from analogue to digital, from keyboard to touch screen, from static to dynamic approach, to achieve more accuracy, ease control, flexibility and leisure. Daylighting systems accordingly have been developed from the static state towards automated control, to achieve better performance, energy-saving and utmost visual comfort. Meanwhile, the parametric approach has been widely utilised due to its capability to deal with complex geometries and variable parameters, simultaneously, in addition to its optimisation characteristic. Parametric design has been exploited in this study to control an automated daylighting system to respond parametrically to the sun movement and solar intensity changes, aiming to provide sufficient daylight inside the buildings during the daytime.

Overall, the proposed system succeeded to provide steady and distributed daylight inside a deep-plan room up to 8-meter depth during the daytime, within a recommended illuminance range 300~500 lx.

1. *Provide uniform and distributed daylight*

The proposed louvre system is parametrically tuned to distribute the light over the ceiling uniformly. Two sources of lights provided from the Electrochromic window and the reflected light over the ceiling, work as diffuse light to the room. The diffuse light is highly recommended for occupants in office areas, while it is convenient for desktop reading, office work, workshops and design work.

2. Protect from direct sunlight

The proposed system succeeded to protect from direct sunlight and reduce potential glare.

3. Increase the steadiness of the provided daylight

The proposed system is parametrically tuned to provide daylight within the illuminance range 300~500 lx, to achieve human visual comfort. Thanks to the parametric design, which can retain this range, and simultaneously, keep the reflected light steady inside the room against the continuous movement of sunlight during the daytime.

4. Achieve a more practical and feasible system

Reducing the slats' size of the proposed louvre system and changing their curvature; contributes to better performance, lighter weight and graceful structure, for a more practical and feasible system

9.2 Discussion

The proposed daylighting system has significantly improved the quality and quantity of the daylight inside a deep-plan room for the most of the working hours during the daytime. Compared to other daylighting system in the market, the proposed Integrated Parametric Louvre can achieve up to 90% of daylight coverage with small automation and easy installation, besides its feasible components, which accordingly achieved the aim of this study. Moreover, the system can accurately control the penetration of the daylight inside the building by using simple microcontroller. On the other hand, most daylighting systems are expensive, need regular maintenance and may have size constraints, in addition to their limited efficiency which can reach up to 50% of electrical energy saving at their best performance.

9.3 Recommendations

1. *Recommended elements for best performance:*

In order to obtain the best performance of the proposed system of uniformity and steadiness, it should be used as an integrated system as mentioned in chapter 5 and chapter 8, which consists of; the Slim Convex-Parametric Louvre, Electrochromic window, Thermochromic window and the chamfered ceiling. For high accuracy and full coverage during the day, we may consider the Innovative Parametric Louver in chapter 7. For the best feasibility, the "Slim Convex-Parametric louvre" which investigated in chapter 8, should be considered as a daylighting system.

2. *Recommended territories:*

The system is highly recommended in sunny territories with clear sky conditions. However, such system was even succeeded to provide daylight in the cloudy conditions, due to the aid of the advanced glazing in addition to the mirrored slats, which capable of reflecting the diffuse light emitted from the clouds and skydome.

3. *Recommended orientations:*

The system is highly recommended to orientate to the south and south-west orientations for the Northern Hemisphere part, and vice versa.

4. *Recommended depth:*

The system can efficiently lit a deep-plan room up to 8 m depth with only 80 cm height of a Slim Parametric Louvre, which means that room depth is relative to 1:10 of the system's height. For instance, if the room is 5 m depth, it requires 50 cm height of Slim Parametric Louvre in order to work with full performance.

9.4 Potential outcome

1. Save electrical lighting energy

Daylighting can be a clean alternative solution against artificial lighting. While, 40% of the annual energy consumption of general buildings based on electrical lighting consumption, the current study investigates an innovative daylighting system that can save up to 80% of electric lighting throughout the year. This reduction can help to reduce the emission of CO_2 that dramatically causes global warming.

2. Enhance occupants' health and productivity

Providing natural light inside the building is vital for human circadian rhythm, while, it can increase their efficiency, organise their body clock, improve their creativity, reduce their stress and stimulate their energy levels.

9.5 Limitations of the system

1. Overcast sky condition

The efficiency of the system can be lower than the recommended illuminance level (300 lx) with the overcast sky condition, while the reflective slats are mainly depend on the direct sunlight in order to reflect the incident light. However, even with low daylight condition, the system capable to reflect the diffuse light from the skydome with the help of the translucent window, unless, the Global Horizontal Radiation is lower than 100 Wh/m^2. The contribution of the daylight at this situation is considered extremely low and the horizontal illuminance of the skydome can reach ~5000 lx, while the interior illuminance can be lower than 100 lx.

2. *Maintenance*

The system may have the risk of lower specularity because of potential dust over the slats' surfaces, which probably needs a regular cleaning of the surfaces. This issue can be solved by installing the system between a double layers glazing which can insulate it from poor ambient conditions.

9.6 Future work

1. *Concentrate on executing the system with more accuracy, simple control and the potential application on an existing louvre blinds.*
2. *Investigate the potential application and execution of the Dual-axis and Double-layer louver system.*
3. *Disseminate the findings and outcome of the system to the industry to introduce it to the market for commercial use.*
4. *Work forward to publish two more papers about the new findings of the proposed system.*
5. *Investigate the application of the smart windows via using prototype and experimental test.*
6. *Utilise the machine learning application for optimum performance.*

References

1. Attia, S., M. Hamdy, and S. Ezzeldin, *Twenty-year tracking of lighting savings and power density in the residential sector.* Energy and Buildings, 2017. **154**: p. 113-126.
2. IEA. *SHC Task 50 Advanced Lighting Solutions for Retrofitting Buildings*. 2013; Available from: http://task50.iea-shc.org/.
3. Kim, J.T. and M.S. Todorovic, *Tuning control of buildings glazing's transmittance dependence on the solar radiation wavelength to optimize daylighting and building's energy efficiency.* Energy and Buildings, 2013. **63**: p. 108-118.
4. Boubekri, M., *Daylighting, Architecture and Health*. 2008: Taylor & Francis.
5. A.Vogel. *Avogel*. Biological clock 2017; Available from: https://www.avogel.ca/en/health/sleep/biological-clock.php.
6. Salata, F., et al., *Energy and reliability optimization of a system that combines daylighting and artificial sources. A case study carried out in academic buildings.* Applied Energy, 2016. **169**: p. 250-266.
7. Sadeghi, S.A., et al., *Occupant interactions with shading and lighting systems using different control interfaces: A pilot field study.* Building and Environment, 2016. **97**: p. 177-195.
8. Hammad, F. and B. Abu-Hijleh, *The energy savings potential of using dynamic external louvers in an office building.* Energy and Buildings, 2010. **42**(10): p. 1888-1895.
9. Gong, J., et al., *Potential advantages of a multifunctional complex fenestration system with embedded micro-mirrors in daylighting.* Solar Energy, 2016. **139**: p. 412-425.
10. Busch, J.F., P. Du Pont, and S. Chirarattananon, *Energy-efficient lighting in Thai commercial buildings.* Energy, 1993. **18**(2): p. 197-210.
11. Mardaljevic, J., *Daylight, indoor illumination, and human behavior.* Sustainable built environments, 2012: p. 69-111.
12. Konstantoglou, M. and A. Tsangrassoulis, *Dynamic operation of daylighting and shading systems: A literature review.* Renewable and Sustainable Energy Reviews, 2016. **60**: p. 268-283.
13. Tsangrassoulis, A., *A Review of Innovative Daylighting Systems.* Advances in Building Energy Research, 2008. **2**(1): p. 33-56.
14. Beltran, L., E. Lee, and S. Selkowitz, *Advanced optical daylighting systems: light shelves and light pipes.* Journal of the illuminating engineering society, 1997. **26**(2): p. 91-106.
15. Littlefair, P.J., *Review Paper: Innovative daylighting: Review of systems and evaluation methods.* Lighting Research & Technology, 1990. **22**(1): p. 1-17.
16. Staff, Z., *The lighting handbook.* Austria: Zumtobel, 2004.
17. Serra, R., *Chapter 6—Daylighting.* Renewable and Sustainable Energy Reviews, 1998. **2**(1): p. 115-155.
18. Young, T., *A course of lectures on natural philosophy and the mechanical arts: in two volumes*. Vol. 2. 1807: Johnson.
19. Hub, S.L. *refraction of light in water*. 2012; Available from: https://www.sciencelearn.org.nz/images/49-refraction-of-light-in-water.
20. Rea, M.S., *The IESNA lighting handbook: reference & application*. 2000: Illuminating Engineering Society of North America New York.
21. Henriques, G.C., J.P. Duarte, and V. Leal, *Strategies to control daylight in a responsive skylight system.* Automation in Construction, 2012. **28**: p. 91-105.
22. Petersen, J.F., D. Sack, and R.E. Gabler, *Physical Geography*. 2016: Cengage Learning.

23. Sciencing. *Geographic location*. 2019; Available from: https://sciencing.com/geographic-location-mean-8667.html.
24. Techterms. *Technical Terms : GPS Definition*. 2019; Available from: https://techterms.com/definition/gps.
25. Zhang, F., et al., *What Is the Predictability Limit of Midlatitude Weather?* Journal of the Atmospheric Sciences, 2019. **76**(4): p. 1077-1091.
26. Belcher, S.E., J.N. Hacker, and D.S. Powell, *Constructing design weather data for future climates.* Building services engineering research and technology, 2005. **26**(1): p. 49-61.
27. Chow, D. and G.J. Levermore, *New algorithm for generating hourly temperature values using daily maximum, minimum and average values from climate models.* Building Services Engineering Research and Technology, 2007. **28**(3): p. 237-248.
28. Jentsch, M.F., et al., *Transforming existing weather data for worldwide locations to enable energy and building performance simulation under future climates.* Renewable Energy, 2013. **55**: p. 514-524.
29. Jiang, A., et al., *Hourly weather data projection due to climate change for impact assessment on building and infrastructure.* Sustainable Cities and Society, 2019. **50**: p. 101688.
30. Mardaljevic, J., *Climate-based daylight modelling and its discontents.* 2015.
31. Wang, J., M. Wei, and L. Chen, *Does typical weather data allow accurate predictions of daylight quality and daylight-responsive control system performance.* Energy and Buildings, 2019. **184**: p. 72-87.
32. Wong, I.L., *A review of daylighting design and implementation in buildings.* Renewable and Sustainable Energy Reviews, 2017. **74**(Supplement C): p. 959-968.
33. Fernandes, L.L., E.S. Lee, and G. Ward, *Lighting energy savings potential of split-pane electrochromic windows controlled for daylighting with visual comfort.* Energy and Buildings, 2013. **61**: p. 8-20.
34. Dubois, M.-C., *Impact of shading devices on daylight quality in offices.* Simulations with Radiance, 2001.
35. Andersen, D. and R. Foldbjerg, *Daylight, Energy and Indoor Climate–Basic Book.* Editorial team: Daylight Energy and Indoor Climate (DEIC), VELUX A/S, 2012.
36. Li, D.H.W. and E.K.W. Tsang, *An analysis of daylighting performance for office buildings in Hong Kong.* Building and Environment, 2008. **43**(9): p. 1446-1458.
37. Konstantzos, I. and A. Tzempelikos, *Daylight Glare Probability Measurements And Correlation With Indoor Illuminances In A Full-Scale Office With Dynamic Shading Controls.* 2014.
38. Wienold, J. and J. Christoffersen, *Evaluation methods and development of a new glare prediction model for daylight environments with the use of CCD cameras.* Energy and buildings, 2006. **38**(7): p. 743-757.
39. Cantin, F. and M.-C. Dubois, *Daylighting metrics based on illuminance, distribution, glare and directivity.* Lighting Research & Technology, 2011. **43**(3): p. 291-307.
40. Jakubiec, J.A. and C.F. Reinhart. *Predicting visual comfort conditions in a large daylit space based on long-term occupant evaluations: a field study*. in *13th Conference of International Building Performance Simulation Association*. 2013.
41. Kent, M.G., et al., *Discomfort glare and time of day.* Lighting Research & Technology, 2015. **47**(6): p. 641-657.
42. Mardaljevic, J., L. Heschong, and E. Lee, *Daylight metrics and energy savings.* Lighting Research and Technology, 2009. **41**(3): p. 261-283.
43. Mardaljevic, J. *Examples of climate-based daylight modelling*. in *CIBSE national conference*. 2006.

44. Shameri, M.A., et al., *Daylighting characterstics of existing double-skin façade office buildings.* Energy and Buildings, 2013. **59**: p. 279-286.
45. Nabil, A. and J. Mardaljevic, *Useful daylight illuminances: A replacement for daylight factors.* Energy and Buildings, 2006. **38**(7): p. 905-913.
46. CIBSE, C., *Code for interior lighting.* London: The Chartered Institute of Building Services Engineers, 1994.
47. Berrutto, V., M. Fontoynont, and P. Avouac-Bastie. *Importance of wall luminance on users satisfaction: pilot study on 73 office workers*. in *Proc. of Lux Europa 1997: the 8th European Lighting Conference*. 1997.
48. Begemann, S., G. Van den Beld, and A. Tenner, *Daylight, artificial light and people in an office environment, overview of visual and biological responses.* International Journal of Industrial Ergonomics, 1997. **20**(3): p. 231-239.
49. Kota, S., et al., *Building Information Modeling (BIM)-based daylighting simulation and analysis.* Energy and Buildings, 2014. **81**: p. 391-403.
50. Ruck, N., et al., *Daylight in Buildings-A source book on daylighting systems and components.* Lawrence Berkeley National Laboratory: Washington, DC, USA, 2000.
51. Littlefair, P.J., M.E. Aizlewood, and A.B. Birtles, *The performance of innovative daylighting systems.* Renewable Energy, 1994. **5**(5): p. 920-934.
52. Roche, L., *Summertime performance of an automated lighting and blinds control system.* Lighting Research & Technology, 2002. **34**(1): p. 11-25.
53. Baker, N. and K. Steemers, *Daylight design of buildings: a handbook for architects and engineers*. 2014: Routledge.
54. Littlefair, P., *Designing with innovative daylighting*. 1996: Building Research Establishment Watford.
55. Kunwar, N., K.S. Cetin, and U. Passe, *Dynamic Shading in Buildings: a Review of Testing Methods and Recent Research Findings.* Current Sustainable/Renewable Energy Reports, 2018. **5**(1): p. 93-100.
56. Hashemi, A., *Daylighting and solar shading performances of an innovative automated reflective louvre system.* Energy and Buildings, 2014. **82**: p. 607-620.
57. Yun, G., K.C. Yoon, and K.S. Kim, *The influence of shading control strategies on the visual comfort and energy demand of office buildings.* Energy and Buildings, 2014. **84**: p. 70-85.
58. Galasiu, A.D. and J.A. Veitch, *Occupant preferences and satisfaction with the luminous environment and control systems in daylit offices: a literature review.* Energy and Buildings, 2006. **38**(7): p. 728-742.
59. Vine, E., et al., *Office worker response to an automated Venetian blind and electric lighting system: a pilot study.* Energy and Buildings, 1998. **28**(2): p. 205-218.
60. Kastner, W., et al., *Communication systems for building automation and control.* Proceedings of the IEEE, 2005. **93**(6): p. 1178-1203.
61. Lee, E.S. and S.E. Selkowitz, *The New York Times Headquarters daylighting mockup: Monitored performance of the daylighting control system.* Energy and Buildings, 2006. **38**(7): p. 914-929.
62. Lee, E., *Integrated performance of an automated venetian blind/electric lighting system in a full-scale private office.* 1998.
63. Olbina, S. and J. Hu, *Daylighting and thermal performance of automated split-controlled blinds.* Building and Environment, 2012. **56**(Supplement C): p. 127-138.
64. Selkowitz, S. and E. Lee, *Integrating automated shading and smart glazings with daylight controls.* 2004.
65. Berman, J., et al., *Automated shade control method and system*. 2008, Google Patents.

66. Shen, H. and A. Tzempelikos, *Sensitivity analysis on daylighting and energy performance of perimeter offices with automated shading.* Building and Environment, 2013. **59**: p. 303-314.
67. Shen, H. and A. Tzempelikos, *Daylighting and energy analysis of private offices with automated interior roller shades.* Solar Energy, 2012. **86**(2): p. 681-704.
68. Koo, S.Y., M.S. Yeo, and K.W. Kim, *Automated blind control to maximize the benefits of daylight in buildings.* Building and Environment, 2010. **45**(6): p. 1508-1520.
69. Aghemo, C., L. Blaso, and A. Pellegrino, *Building automation and control systems: A case study to evaluate the energy and environmental performances of a lighting control system in offices.* Automation in Construction, 2014. **43**: p. 10-22.
70. Athienitis, A.K. and A. Tzempelikos, *A methodology for simulation of daylight room illuminance distribution and light dimming for a room with a controlled shading device.* Solar Energy, 2002. **72**(4): p. 271-281.
71. Nielsen, M.V., S. Svendsen, and L.B. Jensen, *Quantifying the potential of automated dynamic solar shading in office buildings through integrated simulations of energy and daylight.* Solar Energy, 2011. **85**(5): p. 757-768.
72. Lee, E.S., et al., *A post-occupancy monitored evaluation of the dimmable lighting, automated shading, and underfloor air distribution system in The New York Times Building.* 2013.
73. Onaygıl, S. and Ö. Güler, *Determination of the energy saving by daylight responsive lighting control systems with an example from Istanbul.* Building and Environment, 2003. **38**(7): p. 973-977.
74. Welle, B., Z. Rogers, and M. Fischer, *BIM-Centric Daylight Profiler for Simulation (BDP4SIM): A methodology for automated product model decomposition and recomposition for climate-based daylighting simulation.* Building and Environment, 2012. **58**: p. 114-134.
75. Mayhoub, M.S., *Innovative daylighting systems' challenges: A critical study.* Energy and Buildings, 2014. **80**: p. 394-405.
76. Selkowitz, S. and E. Lee, *Advanced fenestration systems for improved daylight performance.* 1998.
77. Chaiwiwatworakul, P., S. Chirarattananon, and P. Rakkwamsuk, *Application of automated blind for daylighting in tropical region.* Energy Conversion and Management, 2009. **50**(12): p. 2927-2943.
78. Park, B.-C., et al., *Performance of integrated systems of automated roller shade systems and daylight responsive dimming systems.* Building and Environment, 2011. **46**(3): p. 747-757.
79. Köster, H., *Dynamic daylighting architecture: basics, systems, projects*. 2004: Springer Science & Business Media.
80. Konis, K., *Evaluating daylighting effectiveness and occupant visual comfort in a side-lit open-plan office building in San Francisco, California.* Building and Environment, 2013. **59**: p. 662-677.
81. Gauger, M., et al. *Prototyping sensor-actuator networks for home automation*. in *Proceedings of the workshop on Real-world wireless sensor networks*. 2008. ACM.
82. Colaco, S.G., et al., *Prospective techniques of effective daylight harvesting in commercial buildings by employing window glazing, dynamic shading devices and dimming control—a literature review.* Building Simulation, 2008. **1**(4): p. 279.
83. Popat, P.P., *State-based system for automated shading*. 2011, Google Patents.
84. Wen, Y.-J., J. Granderson, and A.M. Agogino. *Towards embedded wireless-networked intelligent daylighting systems for commercial buildings*. in *null*. 2006. IEEE.
85. Brown, G.Z., et al., *Weather-responsive shade control system*. 2013, Google Patents.

86. Granderson, J., et al., *Field-measured performance evaluation of a digital daylighting system.* Leukos, 2010. **7**(2): p. 85-101.
87. Pang, C., et al. *Virtual smart metering in automation and simulation of energy-efficient lighting system*. in *Emerging Technologies & Factory Automation (ETFA), 2013 IEEE 18th Conference on*. 2013. IEEE.
88. Berman, J., et al., *Automated shade control in connection with electrochromic glass*. 2014, Google Patents.
89. Bakker, L.G., et al., *User satisfaction and interaction with automated dynamic facades: A pilot study.* Building and Environment, 2014. **78**: p. 44-52.
90. Boscarino, G. and M. Moallem, *Daylighting control and simulation for LED-based energy-efficient lighting systems.* IEEE Transactions on Industrial Informatics, 2016. **12**(1): p. 301-309.
91. Berman, J., et al., *Automated shade control reflectance module*. 2012, Google Patents.
92. Atkin, B., *Intelligent buildings: applications of IT and building automation to high technology construction projects*. 1988: Kogan Page.
93. Park, D., et al., *Dynamic daylight control system implementing thin cast arrays of polydimethylsiloxane-based millimeter-scale transparent louvers.* Building and Environment, 2014. **82**: p. 87-96.
94. Hu, J. and S. Olbina, *Illuminance-based slat angle selection model for automated control of split blinds.* Building and Environment, 2011. **46**(3): p. 786-796.
95. Martirano, L., et al., *A fuzzy-based building automation control system: Optimizing the level of energy performance and comfort in an office space by taking advantage of building automation systems and solar energy.* IEEE Industry Applications Magazine, 2016. **22**(2): p. 10-17.
96. Lee, E.S., et al., *Market transformation opportunities for emerging dynamic facade and dimmable lighting control systems.* 2004.
97. Yan, W., et al., *Interfacing BIM with building thermal and daylighting modeling.* 2013.
98. Lagios, K., J. Niemasz, and C.F. Reinhart, *Animated building performance simulation (ABPS)–linking Rhinoceros/Grasshopper with Radiance/Daysim.* Proceedings of SimBuild, 2010. **4**(1): p. 321-327.
99. Olbina, S. and Y. Beliveau, *Developing a transparent shading device as a daylighting system.* Building Research & Information, 2009. **37**(2): p. 148-163.
100. Mettanant, V. and P. Chaiwiwatworakul, *Automated vertical blinds for daylighting in tropical region.* Energy Procedia, 2014. **52**: p. 278-286.
101. Sulaiman, F., A. Ahmad, and A.Z. Ahmed, *Fuzzy logic algorithm for automated dimming control used in passive optical fiber daylighting system for energy savings.* WSEAS Transactions on Electronics, 2005. **2**(4): p. 189-196.
102. Andersen, M., J.M.L. Gagne, and S. Kleindienst, *Interactive expert support for early stage full-year daylighting design: A user's perspective on Lightsolve.* Automation in Construction, 2013. **35**: p. 338-352.
103. Stunder, M.J., et al., *Integration of real-time data into building automation systems*. 2003, Air-Conditioning and Refrigeration Technology Institute (US).
104. Kazanasmaz, T., *Fuzzy logic model to classify effectiveness of daylighting in an office with a movable blind system.* Building and Environment, 2013. **69**: p. 22-34.
105. Katz, D., *Daylight harvesting technologies.* Energy engineering, 2005. **102**(1): p. 40-48.
106. Fernandes, L. and K. Papamichael, *Automating the selection of fenestration systems to best meet daylighting performance goals.* 2003.
107. Kim, J.-H., et al., *An experimental study on the environmental performance of the automated blind in summer.* Building and Environment, 2009. **44**(7): p. 1517-1527.

108. Chen, H., et al. *The design and implementation of a smart building control system*. in *e-Business Engineering, 2009. ICEBE'09. IEEE International Conference on*. 2009. IEEE.
109. Todorovic, M.S. and J.T. Kim, *Beyond the science and art of the healthy buildings daylighting dynamic control's performance prediction and validation.* Energy and Buildings, 2012. **46**: p. 159-166.
110. Leung, T.C., P. Rajagopalan, and R. Fuller, *Performance of a daylight guiding system in an office building.* Solar energy, 2013. **94**: p. 253-265.
111. Sanders, H. and B.D. Greer, *Dynamic façade system consisting of controllable windows, automated shades and dimmable electric lights*. 2014, Google Patents.
112. El Daly, H.M.T., *Automated fenestration allocation as complying with LEED rating system.* Alexandria Engineering Journal, 2014. **53**(4): p. 883-890.
113. Park, C.-S., G. Augenbroe, and T. Messadi. *Daylighting optimization in smart facade systems*. in *Proceedings of the Eighth International IBPSA Conference*. 2003.
114. Wang, J., L.O. Beltrán, and J. Kim. *From static to kinetic: A review of acclimated kinetic building envelopes*. in *World Renewable Energy Forum, WREF 2012, Including World Renewable Energy Congress XII and Colorado Renewable Energy Society (CRES) Annual Conferen*. 2012.
115. Collett, R.W., *Control strategies for automated venetian blinds used in daylighting multistory buildings.* Proc. Annu. Meet.-Am. Sect. Int. Sol. Energy Soc.;(United States), 1983. **6**(CONF-830622-).
116. Gentile, N., M.-C. Dubois, and T. Laike. *Daylight harvesting control systems design recommendations based on a literature review*. in *Environment and Electrical Engineering (EEEIC), 2015 IEEE 15th International Conference on*. 2015. IEEE.
117. Gagne, J.M. and M. Andersen, *Multi-objective facade optimization for daylighting design using a genetic algorithm.* Proceedings of SimBuild, 2010. **4**(1): p. 110-117.
118. Shen, E., J. Hu, and M. Patel, *Energy and visual comfort analysis of lighting and daylight control strategies.* Building and Environment, 2014. **78**: p. 155-170.
119. Morrow, W.L., *Self calibrating, adaptive setpoint daylighting*. 2015, Google Patents.
120. Meerbeek, B., et al., *Building automation and perceived control: a field study on motorized exterior blinds in Dutch offices.* Building and Environment, 2014. **79**: p. 66-77.
121. Bhavani, R.G. and M. Khan. *An intelligent simulation model for blind position control in daylighting schemes in buildings*. in *Building Simulation*. 2009. Springer.
122. O'Neill, B., A. Tzempelikos, and A. Athienitis. *Daylight and luminaire control in a perimeter zone using an automated Venetian blind*. in *2nd Canadian Solar Buildings Conference*. 2007. Citeseer.
123. Eltaweel, A. and Y. Su, *Parametric design and daylighting: A literature review.* Renewable and Sustainable Energy Reviews, 2017. **73**: p. 1086-1103.
124. Golasangimath, D.V., *Thermal and daylighting performance of automated split-controlled blinds*. 2009, University of Florida.
125. Yun, G. and K.S. Kim, *An empirical validation of lighting energy consumption using the integrated simulation method.* Energy and Buildings, 2013. **57**: p. 144-154.
126. Meek, C. and A. John Breshears, *Dynamic Solar Shading and Glare Control for Human Comfort and Energy Efficiency at UCSD: Integrated Design and Simulation Strategies*. 2010, Washington: American Solar Energy Society.
127. Bellia, L., A. Pedace, and F. Fragliasso, *Dynamic daylight simulations: Impact of weather file's choice.* Solar Energy, 2015. **117**: p. 224-235.
128. Wigginton, M. and J. Harris, *Intelligent skins*. 2013: Routledge.
129. Habibi, S., *Micro-climatization and real-time digitalization effects on energy efficiency based on user behavior.* Building and Environment, 2017. **114**: p. 410-428.

130. Dogan, T. and P. Stec, *Prototyping a façade-mounted, dynamic, dual-axis daylight redirection system.* Lighting Research & Technology. **0**(0): p. 1477153516675392.
131. Lee, E.S., D.L. DiBartolomeo, and S.E. Selkowitz, *Thermal and daylighting performance of an automated venetian blind and lighting system in a full-scale private office.* Energy and Buildings, 1998. **29**(1): p. 47-63.
132. Oh, M.H., K.H. Lee, and J.H. Yoon, *Automated control strategies of inside slat-type blind considering visual comfort and building energy performance.* Energy and Buildings, 2012. **55**: p. 728-737.
133. El Sheikh, M. and K. Kensek. *Intelligent skins: Daylight harvesting through dynamic light-deflection in office spaces*. in *En ARCC 2011 Conference proceedings*. 2011.
134. Reinhart, C.F., *Lightswitch-2002: a model for manual and automated control of electric lighting and blinds.* Solar Energy, 2004. **77**(1): p. 15-28.
135. Mayhoub, M.S., *Fifty years of building core sunlighting systems – Eight lessons learned.* Solar Energy, 2019. **184**: p. 440-453.
136. Kontadakis, A., et al., *An active sunlight redirection system for daylight enhancement beyond the perimeter zone.* Building and Environment, 2017. **113**(Supplement C): p. 267-279.
137. Konis, K. and E.S. Lee, *Measured daylighting potential of a static optical louver system under real sun and sky conditions.* Building and Environment, 2015. **92**: p. 347-359.
138. Tsangrassoulis, A., M. Kostantoglou, and A. Kontadakis, *Lighting energy savings due to the use of a sun tracking mirrored lightself in office buildings.* ASHRAE hellenic, 2014.
139. Xue, P., C.M. Mak, and H.D. Cheung, *New static lightshelf system design of clerestory windows for Hong Kong.* Building and Environment, 2014. **72**(Supplement C): p. 368-376.
140. Freewan, A.A., *Maximizing the lightshelf performance by interaction between lightshelf geometries and a curved ceiling.* Energy Conversion and Management, 2010. **51**(8): p. 1600-1604.
141. *Bright Shelf*. 2015; Available from: http://www.brightshelf.com/light_shelf_design.html.
142. METALS, H.H. *Light shelf daylighting system*. Available from: http://h-hmetals.com/products_and_services-item/light-shelf-brightshelf/.
143. Whitehead, L., E. Lee, and A. Kotlicki, *New efficient tubular daylighting system for multi-floor buildings.* PUBLICATIONS-COMMISSION INTERNATIONALE DE L ECLAIRAGE CIE, 2003. **152**: p. D3-76.
144. Kennedy, D.M. and F. O'Rourke, *Experimental analysis of a scaled, multi-aperture, light-pipe, daylighting system.* Solar Energy, 2015. **122**: p. 181-190.
145. Senior, J.M. and M.Y. Jamro, *Optical fiber communications: principles and practice*. 2009: Pearson Education.
146. Nave, R. *Fibre Optic Applications*. HyperPhysics 2000; Available from: http://hyperphysics.phy-astr.gsu.edu/hbase/optmod/fibopt.html.
147. Feuermann, D. and J.M. Gordon, *SOLAR FIBER-OPTIC MINI-DISHES: A NEW APPROACH TO THE EFFICIENT COLLECTION OF SUNLIGHT.* Solar Energy, 1999. **65**(3): p. 159-170.
148. Ullah, I. and S. Shin, *Highly concentrated optical fiber-based daylighting systems for multi-floor office buildings.* Energy and Buildings, 2014. **72**: p. 246-261.
149. Xie, W.T., et al., *Concentrated solar energy applications using Fresnel lenses: A review.* Renewable and Sustainable Energy Reviews, 2011. **15**(6): p. 2588-2606.
150. Mayhoub, M. and D. Carter, *Hybrid lighting systems: Performance and design.* Lighting Research & Technology, 2012. **44**(3): p. 261-276.

151. Pohl, W. and C. Anselm, *Review of existing heliostats.* Bartenbach LichtLabor GmbH, Rinner Straße, 2000. **14**.
152. Faizi, M., F.M. Seraj, and M.G. Gashniani, *Review of the innovative strategies to improve daylight penetration in building.* Journal of Fundamental and Applied Sciences, 2016. **8**: p. 1428-1447.
153. Mashaly, I.A., et al., *A prismatic daylight redirecting fenestration system for southern skies.* Renewable Energy, 2017. **109**: p. 202-212.
154. McNeil, A., E.S. Lee, and J.C. Jonsson, *Daylight performance of a microstructured prismatic window film in deep open plan offices.* Building and Environment, 2017. **113**: p. 280-297.
155. Vlachokostas, A. and N. Madamopoulos, *Liquid filled prismatic louver façade for enhanced daylighting in high-rise commercial buildings.* Optics Express, 2015. **23**(15): p. A805-A818.
156. Salazar Trujillo, J.H., *Calculation of the shadow-penumbra relation and its application on efficient architectural design.* Solar Energy, 2014. **110**: p. 139-150.
157. Ghaffarianhoseini, A., et al., *Exploring the advantages and challenges of double-skin façades (DSFs).* Renewable and Sustainable Energy Reviews, 2016. **60**: p. 1052-1065.
158. Taveres-Cachat, E., et al., *Advanced transparent facades: market available products and associated challenges in building performance simulation.* Energy Procedia, 2017. **132**: p. 496-501.
159. Baetens, R., B.P. Jelle, and A. Gustavsen, *Properties, requirements and possibilities of smart windows for dynamic daylight and solar energy control in buildings: A state-of-the-art review.* Solar energy materials and solar cells, 2010. **94**(2): p. 87-105.
160. Belzer, D.B., *An exploratory energy analysis of electrochromic windows in small and medium office buildings-simulated results using EnergyPlus*. 2010, Pacific Northwest National Lab.(PNNL), Richland, WA (United States).
161. Midtdal, K. and B.P. Jelle, *Self-cleaning glazing products: A state-of-the-art review and future research pathways.* Solar Energy Materials and Solar Cells, 2013. **109**: p. 126-141.
162. Keranen, J., *Self-cleaning glass-Nano-structured self-cleaning coated glasses: Modelling and laboratory tests for fundamental knowledge on thin film coatings, EC normalisation and customer benefits.* 36M publishable executive summary, NMP3-CT-2003-505952, Self-Cleaning Glass Consortium, 2007.
163. Mellott, N., et al., *Commercial and laboratory prepared titanium dioxide thin films for self-cleaning glasses: Photocatalytic performance and chemical durability.* Thin Solid Films, 2006. **502**(1-2): p. 112-120.
164. Barthlott, W. and C. Neinhuis, *Purity of the sacred lotus, or escape from contamination in biological surfaces.* Planta, 1997. **202**(1): p. 1-8.
165. You, Z., et al., *A black near-infrared reflective coating based on nano-technology.* Energy and Buildings, 2019. **205**: p. 109523.
166. Jeevanandam, P., et al., *Near Infrared Reflectance Properties of Metal Oxide Nanoparticles.* The Journal of Physical Chemistry C, 2007. **111**(5): p. 1912-1918.
167. Baneshi, M., et al., *A new approach to optimizing pigmented coatings considering both thermal and aesthetic effects.* Journal of Quantitative Spectroscopy and Radiative Transfer, 2009. **110**(3): p. 192-204.
168. Wurm, J. *Photobioreactors as adaptive shading devices*. http://smartgeometry.org/?option=com_content&view=article&id=154Photobioreactors 2012.
169. Yang, S. and J. Aizenberg, *Porous Biomimetic Microlens Arrays as Multifunctional Optical Structures.* 2005.

170. Ruthrauff, H. *Biomimetic and Architecture*. HygroScope – Centre Pompidou Paris 2012 APRIL 26, 2012; Available from: http://www.biomimetic-architecture.com/2012/hygroscope-centre-pompidou-paris/.
171. Suyoto, W., A. Indraprastha, and H.W. Purbo, *Parametric Approach as a Tool for Decision-making in Planning and Design Process. Case study: Office Tower in Kebayoran Lama.* Procedia - Social and Behavioral Sciences, 2015. **184**: p. 328-337.
172. Davis, D., *A History of Parametric.* Available at: h ttp://www. danieldavis. com/d/history, 2013.
173. Gerber, D.J., *Parametric practices: Models for design exploration in architecture*. 2007: Harvard University.
174. de Ruiter, M.M., *Advances in computer graphics III*. 1988: Springer Science & Business Media.
175. Reddy, E.J., C. Sridhar, and V.P. Rangadu, *Knowledge Based Engineering: Notion, Approaches and Future Trends.* American Journal of Intelligent Systems, 2015. **5**(1): p. 1-17.
176. Ahamed, S.N., J.V. Kumar, and P. Sravani, *Weight Optimization Of Empennage Of Light Weight Aircraft.* International Journal of Technology Enhancements and Emerging Engineering Research, 2014. **3**(4): p. 40-57.
177. Hillyard, R.C. and I.C. Braid, *Analysis of dimensions and tolerances in computer-aided mechanical design.* Computer-Aided Design, 1978. **10**(3): p. 161-166.
178. Moretti, L., F. Bucci, and M. Mulazzani, *Luigi Moretti: opere e scritti*. 2000: Electa.
179. Davis, D., *Modelled on software engineering: Flexible parametric models in the practice of architecture*. 2013, RMIT University.
180. Dana, J.D., *On the drawing of figures of crystals*. 1888: publisher not identified.
181. Frazer, J., *Parametric Computation: History and Future.* Architectural Design, 2016. **86**(2): p. 18-23.
182. Woods, L., *Drawn into Space: Zaha Hadid.* Architectural design, 2008. **78**(4): p. 28-35.
183. Monedero, J., *Parametric design: a review and some experiences.* Automation in Construction, 2000. **9**(4): p. 369-377.
184. Rogler, K., *Energy Modeling and Implementation of Complex Building Systems.* 2014.
185. Yu, X. and Y. Su, *Daylight availability assessment and its potential energy saving estimation –A literature review.* Renewable and Sustainable Energy Reviews, 2015. **52**: p. 494-503.
186. Erlendsson, Ö., *Daylight Optimization-A Parametric Study of Atrium Design: Early Stage Design Guidelines of Atria for Optimization of Daylight Autonomy.* 2014.
187. Pratt, K.B. and D.E. Bosworth. *A method for the design and analysis of parametric building energy models*. in *Proceedings of Building Simulation 2011: 12th Conference of International Building Performance Association, Sydney, Australia*. 2011.
188. Hanan, I.I.H., et al., *REFLECTIONS ON CREATIVITY: PUBLIC ENGAGEMENT AND THE MAKING OF PLACEParametric Approach as a Tool for Decision-making in Planning and Design Process. Case study: Office Tower in Kebayoran Lama.* Procedia - Social and Behavioral Sciences, 2015. **184**: p. 328-337.
189. Saleh, M.M. and K.S. Al-Hagla. *Parametric Urban Comfort Envelope An Approach toward a Responsive Sustainable Urban Morphology*. in *Proceedings of World Academy of Science, Engineering and Technology*. 2012. World Academy of Science, Engineering and Technology (WASET).
190. Hudson, R., *Strategies for parametric design in architecture: an application of practice led research*. 2010, University of Bath.
191. Zarei, Y., *The Challenges of Parametric Design in Architecture Today: Mapping the Design Practice.* 2012.

192. Davidson, S. *Grasshopper*. Sonic 2016 [cited 2016 29/7/2016]; Available from: http://www.grasshopper3d.com/group/sonic.
193. Hanan, I.I.H., et al., *Parametric Approach as a Tool for Decision-making in Planning and Design Process. Case study: Office Tower in Kebayoran Lama.* Procedia - Social and Behavioral Sciences, 2015. **184**: p. 328-337.
194. Boake, T.M., *Diagrid Structures: Systems, Connections, Details*. 2014: Birkhäuser.
195. Wagdy, A. and F. Fathy, *A parametric approach for achieving optimum daylighting performance through solar screens in desert climates.* Journal of Building Engineering, 2015. **3**: p. 155-170.
196. Banihashemi, S., et al., *Climatic, parametric and non-parametric analysis of energy performance of double-glazed windows in different climates.* International Journal of Sustainable Built Environment, 2015. **4**(2): p. 307-322.
197. pinterest. [cited 2016 19/12/2016]; Available from: https://www.pinterest.com/source/grasshopper3d.com.
198. Ali, M. 2012 2016 [cited 2016 19/12/2016]; Available from: http://www.grasshopper3d.com/photo/dsc-0158?context=latest.
199. Levin, G. *Interactive Art & Computational Design*. 2015 24/3/2015 [cited 2016 19/12/2016]; Available from: http://golancourses.net/2015/jackkoo/03/24/looking-outward-6/.
200. Sood, G. *Biomimicry shoe that mimics bird's cranium is created using 3D printing*. 2012 2016 [cited 2016 19/12/2016]; Available from: http://www.atcrux.com/2012/07/20/3534/biomimicry-shoe-that-mimics-birds-cranium-is-created-using-3d-printing.html.
201. arch2o. *Shoes - Tea Petrovic*. 2015 [cited 2016 19/12/2016]; Available from: http://www.arch2o.com/shoes-tea-petrovic/.
202. Pinterest. 2009 2016 [cited 2016; Available from: https://www.pinterest.com/milleychin/grasshopper_kangaroo/.
203. inhabitat. *Twisted ContemPLAY Pavilion*. 2012 [cited 2016; Available from: http://inhabitat.com/mcgill-university-students-build-twisted-contemplay-pavilion-out-of-locally-sourced-materials/contemplay-pavilion-1/.
204. Konis, K., A. Gamas, and K. Kensek, *Passive performance and building form: An optimization framework for early-stage design support.* Solar Energy, 2016. **125**: p. 161-179.
205. Turrin, M., et al., *Performative skins for passive climatic comfort: A parametric design process.* Automation in Construction, 2012. **22**: p. 36-50.
206. Ramzy, N. and H. Fayed, *Kinetic systems in architecture: New approach for environmental control systems and context-sensitive buildings.* Sustainable Cities and Society, 2011. **1**(3): p. 170-177.
207. Choi, J., et al., *Parametric Louver Design System Based On Direct Solar Radiation Control Performance.* Journal of Asian Architecture and Building Engineering, 2014. **13**(1): p. 57-62.
208. Larson, G.W. and R. Shakespeare, *Rendering with Radiance: The Art and Science of Lighting Visualization*. 1998: Morgan Kaufmann.
209. El-Sheikh, M. and D. Gerber. *Building Skin Intelligence*. in *Proceedings of ACADIA*. 2011.
210. Sjarifudin, F.U. and L. Justina. *Daylight Adaptive Shading Using Parametric Camshaft Mechanism for SOHO in Jakarta*. in *EPJ Web of Conferences*. 2014. EDP Sciences.
211. Henriques, G.C., *TetraScript: A Responsive Pavilion, From Generative Design to Automation.* International Journal of Architectural Computing, 2012. **10**(1): p. 87-104.

212. Tabadkani, A., S. Banihashemi, and M.R. Hosseini, *Daylighting and visual comfort of oriental sun responsive skins: A parametric analysis.* Building Simulation, 2018. **11**(4): p. 663-676.
213. Turrin, M., P. Von Buelow, and R. Stouffs, *Design explorations of performance driven geometry in architectural design using parametric modeling and genetic algorithms.* Advanced Engineering Informatics, 2011. **25**(4): p. 656-675.
214. Nicol, F. and S. Roaf, *Progress on passive cooling: adaptive thermal comfort and passive architecture.* Advances in Passive Cooling, Earthscan, London, UK, 2007: p. 1-29.
215. Turrin, M., et al., *Integrated design of a large span roof: a parametric investigation on structural morphology, thermal comfort and daylight.* Proceedings of ICCCBE, 2010.
216. Flor, J.-F., et al., *Optical aspects and energy performance of switchable ethylene-tetrafluoroethylene (ETFE) foil cushions.* Applied energy, 2018. **229**: p. 335-351.
217. Flor, J.-F., et al. *Dynamic environmental control mechanisms for pneumatic foil constructions*. in *E3S Web of Conferences*. 2017. EDP Sciences.
218. Cunningham, P., Zaferiou, P. & Lagios, Kera, *A Case Study in Reflective Daylighting.* Perkins+Will Research Journal, 2014. **Vol. 6, No. 1, pp 30-53**.
219. Park, J.J. and B. Dave. *Bio-inspired Parametric Design for Adaptive Stadium Façades*. in *Australasian Journal of Construction Economics and Building-Conference Series*. 2014.
220. Land, M.F., *Eyes with mirror optics.* Journal of Optics A: Pure and Applied Optics, 2000. **2**(6): p. R44.
221. Land, M.F., *Superposition images are formed by reflection in the eyes of some oceanic decapod Crustacea.* 1976.
222. Sarvani, V. and O. Kontovourkis, *Parametric Design of a High-Rise Habitation Unit System through Lighting and Solar Energy Performances.* Journal of Sustainable Architecture and Civil Engineering, 2013. **3**(4): p. 9-18.
223. Chronis, A. and K.A. Liapi. *Parametric Approach to the Bioclimatic Design of a Student Housing Building in Patras, Greece*. in *Proceedings of the eCAADe 2010 Conference*. 2010.
224. USGBC, L., *For new construction and major renovations.* US Green Building Council, Version, 2009. **2**: p. 24-28.
225. Ercan, B. and S.T. Elias-Ozkan, *Performance-based parametric design explorations: A method for generating appropriate building components.* Design Studies, 2015. **38**: p. 33-53.
226. Lauridsen, P.K.B. and S. Petersen. *Integrating Indoor Climate, Daylight and Energy Simulations in Parametric Models and Performance-Based Design*. in *Proceedings of the Third International Workshop on Design in Civil and Environmental Engineering*. 2014.
227. Qingsong, M. and H. Fukuda, *Parametric Office Building for Daylight and Energy Analysis in the Early Design Stages.* Procedia - Social and Behavioral Sciences, 2016. **216**: p. 818-828.
228. Aedas. *Al Bahr Towers in Abu Dhabi*. 2012 2016 [cited 2016 20/12/2016]; Available from: http://www.designboom.com/architecture/aedas-al-bahar-towers/.
229. Drozdowski, Z. and S. Gupta. *Adaptive fritting as case exploration for adaptivity in architecture*. in *ACADIA 09: reForm ()-Building a Better Tomorrow [Proceedings of the 29th Annual Conference of the Association for Computer Aided Design in Architecture (ACADIA)*. 2009.
230. Narangerel, A., J.-H. Lee, and R. Stouffs, *Daylighting Based Parametric Design Exploration of 3D Facade Patterns.*

231. Glassman, E.J. and C. Reinhart, *FACADE OPTIMIZATION USING PARAMETRIC DESIGN AND FUTURE CLIMATE SCENARIOS.*
232. Mahmoud, A.H.A. and Y. Elghazi, *Parametric-based designs for kinetic facades to optimize daylight performance: Comparing rotation and translation kinetic motion for hexagonal facade patterns.* Solar Energy, 2016. **126**: p. 111-127.
233. Barozzi, M., et al., *The Sustainability of Adaptive Envelopes: Developments of Kinetic Architecture.* Procedia Engineering, 2016. **155**: p. 275-284.
234. Elghazi, Y., et al. *Daylighting driven design: optimizing kaleidocycle facade for hot arid climate*. in *Aachen: Fifth German-Austrian IBPSA Conference, RWTH Aachen University*. 2014.
235. USGBC, L., *Reference Guide for Building Design and Construction v4.* US Green Building Council, 2014.
236. Ward, G.J. *The RADIANCE lighting simulation and rendering system*. in *Proceedings of the 21st annual conference on Computer graphics and interactive techniques*. 1994. ACM.
237. Gao, W. and K. Ramani, *Kaleidogami™: Multi-Primitive Reconfigurable Artistic Structures.* School of Mechanical Engineering School, Electrical and Computer Engineering, Purdue University: by Courtesy.
238. Fowler, P. and S. Guest. *A symmetry analysis of mechanisms in rotating rings of tetrahedra*. in *Proceedings of the Royal Society of London A: Mathematical, Physical and Engineering Sciences*. 2005. The Royal Society.
239. Vergauwen, A., et al. *Parametric design of adaptive shading elements based on Curved-line Folding*. in *Proceedings of the First Conference Transformables 2013*. 2013.
240. Schleicher, S., et al. *Adaptive façade shading systems inspired by natural elastic kinematics*. in *Proceedings of the International Conference on Adaptive Architecture*. 2011.
241. Mohamed Gomaa, W.J., *Evaluating Daylighting Analysis of Complex Parametric Facades*, in *eCAADe*. 2016.
242. Ibrahim, H., et al., *Applicability of flexible photovoltaic modules onto membrane structures using grasshopper integrative model.* Procedia Engineering, 2016. **155**: p. 379-387.
243. Li, D.H.W., *A review of daylight illuminance determinations and energy implications.* Applied Energy, 2010. **87**(7): p. 2109-2118.
244. Julian, W.G., *Daylighting, Architecture and Health: Building Design Strategies*. 2010, EARTHSCAN 14A ST CROSS STREET, LONDON, EC1N 8XA, ENGLAND.
245. Tian, C., T. Chen, and T.-m. Chung, *Experimental and simulating examination of computer tools, Radlink and DOE2, for daylighting and energy simulation with venetian blinds.* Applied Energy, 2014. **124**: p. 130-139.
246. Moretti, E. and E. Belloni, *Evaluation of energy, thermal, and daylighting performance of solar control films for a case study in moderate climate.* Building and Environment, 2015. **94, Part 1**: p. 183-195.
247. Eltaweel, A. and Y. Su, *Controlling venetian blinds based on parametric design; via implementing Grasshopper's plugins: A case study of an office building in Cairo.* Energy and Buildings, 2017. **139**: p. 31-43.
248. Meresi, A., *Evaluating daylight performance of light shelves combined with external blinds in south-facing classrooms in Athens, Greece.* Energy and Buildings, 2016. **116**: p. 190-205.
249. Cho, J., C. Yoo, and Y. Kim, *Viability of exterior shading devices for high-rise residential buildings: Case study for cooling energy saving and economic feasibility analysis.* Energy and Buildings, 2014. **82**: p. 771-785.

250. Tzempelikos, A. and H. Shen, *Comparative control strategies for roller shades with respect to daylighting and energy performance.* Building and Environment, 2013. **67**: p. 179-192.
251. Bueno, B., et al., *Fener: A Radiance-based modelling approach to assess the thermal and daylighting performance of complex fenestration systems in office spaces.* Energy and Buildings, 2015. **94**: p. 10-20.
252. Li, Z., J. Ju, and W. Xu, *Daylighting Control Performance and Subject Responses to Electrochromic Windows in a Meeting Room.* Procedia Engineering, 2015. **121**: p. 27-32.
253. Yao, J. and N. Zhu, *Evaluation of indoor thermal environmental, energy and daylighting performance of thermotropic windows.* Building and Environment, 2012. **49**: p. 283-290.
254. Labib, R., *Improving daylighting in existing classrooms using laser cut panels.* Lighting Research & Technology, 2013. **45**(5): p. 585-598.
255. Yu, X., et al., *A study on use of miniature dielectric compound parabolic concentrator (dCPC) for daylighting control application.* Building and Environment, 2014. **74**: p. 75-85.
256. Vázquez-Moliní, D., et al., *Horizontal daylighting system for office buildings.* Energy and Buildings, 2013. **67**: p. 525-530.
257. Ihara, T., A. Gustavsen, and B.P. Jelle, *Effect of facade components on energy efficiency in office buildings.* Applied Energy, 2015. **158**: p. 422-432.
258. Yun, G.Y., H. Kim, and J.T. Kim, *Effects of occupancy and lighting use patterns on lighting energy consumption.* Energy and Buildings, 2012. **46**: p. 152-158.
259. Yun, G.Y., T. Hwang, and J.T. Kim, *Performance prediction by modelling of a light-pipe system used under the climate conditions of Korea.* Indoor and Built Environment, 2010. **19**(1): p. 137-144.
260. Warrant, E.J., *Seeing in the dark: vision and visual behaviour in nocturnal bees and wasps.* Journal of Experimental Biology, 2008. **211**(11): p. 1737-1746.
261. anatomy.co.uk. *Saddle Joint*. 2019; Available from: https://anatomy.co.uk/saddle-joint/#.
262. Associates, R.M. *Rhinoceros*. Rhino 5 2017; 5:[Available from: https://www.rhino3d.com/.
263. Davidson, S. *Grasshopper*. ALGORITHMIC MODELING FOR RHINO [Modelling software] 2017; 2017:[ALGORITHMIC MODELING FOR RHINO]. Available from: http://www.grasshopper3d.com/.
264. Europe, M. *food4Rhino*. Apps for Rhino and Grasshopper]. Available from: http://www.food4rhino.com/.
265. Schregle, R., *The RADIANCE Photon Map Extension User Manual.* 2016.
266. Sbar, N.L., et al., *Electrochromic dynamic windows for office buildings.* International Journal of Sustainable Built Environment, 2012. **1**(1): p. 125-139.
267. Lampert, C.M., *Electrochromic materials and devices for energy efficient windows.* Solar Energy Materials, 1984. **11**(1-2): p. 1-27.
268. Svensson, J.S.E.M. and C.G. Granqvist, *Electrochromic tungsten oxide films for energy efficient windows.* Solar Energy Materials, 1984. **11**(1): p. 29-34.
269. Caster, K.C., *2.16 - Arsoles, Stiboles, and Bismoles*, in *Comprehensive Heterocyclic Chemistry II*, A.R. Katritzky, C.W. Rees, and E.F.V. Scriven, Editors. 1996, Pergamon: Oxford. p. 857-902.
270. Granqvist, C.G., *Recent progress in thermochromics and electrochromics: A brief survey.* Thin Solid Films, 2016. **614**: p. 90-96.
271. Jorgenson, G. and J. Lee, *Doped vanadium oxide for optical switching films.* Solar Energy Materials, 1986. **14**(3-5): p. 205-214.

272. Babulanam, S., et al., *Thermochromic VO2 films for energy-efficient windows.* Solar energy materials, 1987. **16**(5): p. 347-363.
273. Eltaweel, A. and S. Yuehong, *Using integrated parametric control to achieve better daylighting uniformity in an office room: A multi-Step comparison study.* Energy and Buildings, 2017. **152**: p. 137-148.
274. Chan, Y.-C. and A. Tzempelikos, *Efficient venetian blind control strategies considering daylight utilization and glare protection.* Solar Energy, 2013. **98**: p. 241-254.
275. Niu, J., *Some significant environmental issues in high-rise residential building design in urban areas.* Energy and Buildings, 2004. **36**(12): p. 1259-1263.
276. Wilson, R., *10 Key question about exterior shading*, in *The Construction Specifier*. 2019, Kenilworth Media: US.
277. Hee, W.J., et al., *The role of window glazing on daylighting and energy saving in buildings.* Renewable and Sustainable Energy Reviews, 2015. **42**: p. 323-343.
278. Christoffersen, J. and K. Johnsen. *An experimental evaluation of daylight systems and lighting control*. in *Proceedings of Right Light 4, 4th European Conference on Energy-efficient Lighting*. 1997.
279. Eltaweel, A. and Y. Su, *Evaluation of Suitability of a Parametrically Controlled Louvers for Various Orientations throughout a Year Comparing to an Existing Case.* Buildings, 2017. **7**(4): p. 109.
280. Barbón, A., et al., *New daylight fluctuation control in an optical fiber-based daylighting system.* Building and Environment, 2019. **153**: p. 35-45.
281. Ali, A.S., et al., *Open Source Building Science Sensors (OSBSS): A low-cost Arduino-based platform for long-term indoor environmental data collection.* Building and Environment, 2016. **100**: p. 114-126.
282. Karami, M., G.V. McMorrow, and L. Wang, *Continuous monitoring of indoor environmental quality using an Arduino-based data acquisition system.* Journal of Building Engineering, 2018. **19**: p. 412-419.
283. Arduino. *Arduino Mega ADK*. 2018; Available from: https://www.arduino.cc/en/Main/ArduinoBoardMegaADK?from=Main.ArduinoBoardADK.
284. Combet, M., H. Van Zonneveld, and L. Verbeek, *Computation of the base two logarithm of binary numbers.* IEEE Transactions on Electronic Computers, 1965(6): p. 863-867.
285. food4Rhino. *Firefly*. Firefly download 2018; Apps for Rhino and Grasshopper]. Available from: https://www.food4rhino.com/app/firefly.
286. *The Firefly User's Guide*. Firefly 2018; Available from: http://www.fireflyexperiments.com/resources/.
287. Lam, K., et al., *Evaluation of six sky luminance prediction models using measured data from Singapore.* International journal of lighting research and technology, 1999. **31**(1): p. 13-17.
288. Darula, S. and R. Kittler, *CIE general sky standard defining luminance distributions.* Proceedings eSim, 2002: p. 11-13.
289. Nasrollahi, N. and E. Shokri, *Daylight illuminance in urban environments for visual comfort and energy performance.* Renewable and Sustainable Energy Reviews, 2016. **66**: p. 861-874.
290. Peel, M.C., B.L. Finlayson, and T.A. McMahon, *Updated world map of the Köppen-Geiger climate classification.* Hydrology and earth system sciences discussions, 2007. **4**(2): p. 439-473.
291. Berger, T., et al., *Impacts of external insulation and reduced internal heat loads upon energy demand of offices in the context of climate change in Vienna, Austria.* Journal of Building Engineering, 2016. **5**: p. 86-95.

292. Doulos, L., A. Tsangrassoulis, and F. Topalis, *Quantifying energy savings in daylight responsive systems: The role of dimming electronic ballasts.* Energy and Buildings, 2008. **40**(1): p. 36-50.
293. Van Den Wymelenberg, K., *Patterns of occupant interaction with window blinds: A literature review.* Energy and Buildings, 2012. **51**: p. 165-176.
294. Lee, E.S., et al., *Advancement of electrochromic windows.* Lawrence Berkeley National Laboratory, 2006.
295. Mäkitalo, J., *Simulating control strategies of electrochromic windows: Impacts on indoor climate and energy use in an office building*. 2013.
296. Hernández, F.F., et al., *Effects of louvers shading devices on visual comfort and energy demand of an office building. A case of study.* Energy Procedia, 2017. **140**: p. 207-216.
297. Al-Obaidi, K.M., et al., *Designing an integrated daylighting system for deep-plan spaces in Malaysian low-rise buildings.* Solar Energy, 2017. **149**: p. 85-101.
298. Piccolo, A. and F. Simone, *Performance requirements for electrochromic smart window.* Journal of Building Engineering, 2015. **3**: p. 94-103.
299. Lee, E.S., et al., *A design guide for early-market electrochromic windows.* Lawrence Berkeley National Laboratory, 2006.
300. Mead, D. *Trans Materials Modeling and Specifying a Next Generation*. 2017; Available from: https://radiance-online.org//community/workshops/2010-freiburg/PDF/DavidMead.pdf.
301. Granqvist, C.G., et al., *Electrochromic materials and devices for energy efficiency and human comfort in buildings: A critical review.* Electrochimica Acta, 2018. **259**: p. 1170-1182.
302. Neufert, E., P. Neufert, and J. Kister, *Architects' data*. 2012: John Wiley & Sons.
303. *KELLWOOD LED LIGHTING*. 2017; Available from: https://www.kellwood.co.uk/led-lighting/technical/cibse-recommended-lux-levels.
304. Singh, R., I.J. Lazarus, and V. Kishore, *Uncertainty and sensitivity analyses of energy and visual performances of office building with external venetian blind shading in hot-dry climate.* Applied energy, 2016. **184**: p. 155-170.
305. Moretti, E. and E. Belloni, *Evaluation of energy, thermal, and daylighting performance of solar control films for a case study in moderate climate.* Building and Environment, 2015. **94**: p. 183-195.
306. Lee, K., K. Han, and J. Lee, *The Impact of Shading Type and Azimuth Orientation on the Daylighting in a Classroom–Focusing on Effectiveness of Façade Shading, Comparing the Results of DA and UDI.* Energies, 2017. **10**(5): p. 635.
307. Jackson, A., D. Pitcher, and H.J. Gerritsen, *A portable alt‐azimuth solar simulator for evaluation of daylighting devices.* Review of scientific instruments, 1991. **62**(3): p. 821-824.
308. Rahimzadeh, S.D., *Use of parametric modelling and climate-based metrics for the efficient design of daylight strategies in buildings with complex geometries*. 2015, Queensland University of Technology.
309. Parkin, I.P., et al. *Thermochromic coatings for intelligent architectural glazing*. in *Journal of Nano research*. 2008. Trans Tech Publ.
310. Uribe, D., et al., *Impact of different control strategies of perforated curved louvers on the visual comfort and energy consumption of office buildings in different climates.* Solar Energy, 2019. **190**: p. 495-510.
311. Kazanasmaz, T., et al., *Three approaches to optimize optical properties and size of a South-facing window for spatial Daylight Autonomy.* Building and Environment, 2016. **102**: p. 243-256.

312. Mainini, A.G., et al., *Daylighting performance of three-dimensional textiles.* Energy and Buildings, 2019. **190**: p. 202-215.
313. Kent, M.G., et al., *Temporal effects on glare response from daylight.* Building and Environment, 2017. **113**: p. 49-64.

Appendix

Appendix A: List of journal publications

1. *Eltaweel, A. and Y. Su, Parametric design and daylighting: A literature review. Renewable and Sustainable Energy Reviews, 2017.* ***73****: p. 1086-1103.*
2. *Eltaweel, A. and Y. Su, Controlling Venetian blinds based on parametric design; via implementing Grasshopper's plugins: A case study of an office building in Cairo. Energy and Buildings, 2017.* ***139****: p. 31-43.*
3. *Eltaweel, A. and S. Yuehong, Using integrated parametric control to achieve better daylighting uniformity in an office room: A multi-Step comparison study. Energy and Buildings, 2017.* ***152****: p. 137-148.*
4. *Eltaweel, A. and Y. Su, Evaluation of Suitability of a Parametrically Controlled Louvers for Various Orientations throughout a Year Comparing to an Existing Case. Buildings, 2017.* ***7****(4): p. 109.*

Appendix B: Submitted for Review

5. *Eltaweel, A. and Y. Su, Prototyping and Validation of an Automated Louver with Individually-angled Mirrored Slats via Using Grasshopper within Arduino board. Solar Energy, 2019.*
6. *Rana Rizi and A. Eltaweel, A User Detective Adaptive Skin towards Improving Visual and Thermal Comfort. Sustainable Cities and Society, 2019.*

Appendix C: Grasshopper's formula